UNIVERSITY OF SOUTHAMPTON

Faculty of Engineering, Science & Mathematics

School of Chemistry

Early Transition Metal Complexes of Carbene Donors Linked to Cyclopentadienyl Ring Analogues or Amidine/Amidinate Moieties

by

Susana Conde Guadaño

Thesis for the Degree of Doctor of Philosophy

September 2010

UNIVERSITY OF SOUTHAMPTON

ABSTRACT

FACULTY OF ENGINEERING, SCIENCE & MATHEMATICS

SCHOOL OF CHEMISTRY

Doctor of Philosophy

EARLY TRANSITION METAL COMPLEXES OF CARBENE DONORS LINKED TO CYCLOPENTADIENYL RING ANALOGUES OR AMIDINE/AMIDINATE MOIETIES

by Susana Conde Guadaño

The new indenyl-functionalised NHC potassium salt, 1-[3-(4, 7-dimethylindenylpropyl]-3-(2,6-diisopropylphenyl)imidazol-2-ylidenepotassium, has been synthesised. Complexes of titanium, zirconium and chromium containing this ligand and the two carbon bridge analogue, 1-[2-(4,7-dimethylindenyl)ethyl]-3-(2,6-diisopropylphenyl)imidazol-2 ylidene potassium, have been synthesised and characterised by X-ray crystallographic techniques. The following complexes were tested as catalysts for the oligomerisation of ethylene in the presence of MAO: 3-(2,6-diisopropylphenyl)-1-[2-(4,7-dimethylindenyl)ethyl]-imidazol-2-ylidene(tert-butylimido)titanium chloride, 3-(2,6-diisopropylphenyl)-1-[3-(4,7-dimethylindenyl)propyl]imidazol-2-ylidene(tert-butylimido)titanium chloride, 3-(2,6-diisopropylphenyl)-1-[3-(4,7-dimethylindenyl)propyl]imidazol-2-ylidenezirconium trichloride, 3-(2,6-diisopropylphenyl)-1-[2-(4,7-dimethylindenyl)ethyl]imidazol-2-ylidenezirconium trichloride, 3-(2,6-Diisopropylphenyl)-1-[2-(4,7-dimethylindenyl)ethyl]-imidazol-2-ylidenechromium dichloride, 3-(2,6-diisopropylphenyl)-1-[3-(4,7-(dimethylindenyl)propyl]imidazol-2-ylidene chromium dichloride, 3-(2,6-diisopropylphenyl)-1-[3-(4,7-dimethylindenyl)propyl]-imidazol-2-ylidene chromium methyl chloride and 3-(2,6-diisopropylphenyl)-1-[2-(4,7-dimethylindenyl)ethyl]-imidazol-2-ylidenevanadium dichloride.

The following alkyl chromium complexes containing 1-[2-(4,7-dimethylindenyl)ethyl]-3-(2,6-diisopropylphenyl)imidazol-2 ylidene potassium have also been synthesised: 3-(2,6-diisopropylphenyl)-1-[2-(4,7-dimethylindenyl)ethyl]-imidazol-2-ylidene chromium phenyl chloride and 3-(2,6-diisopropyl-phenyl)-1-[2-(4, 7-dimethylindenyl)ethyl]-imidazol-2-ylidene chromium dibenzyl. Chromium cations have been synthesised using as starting materials the chromium alkyl complexes. The Cr(II) complex 3-(2,6-diisopropyl-phenyl)-1-[2-(4, 7-dimethylindenyl)ethyl]-imidazol-2-ylidene chromium monochloride and a partially oxidised dimerised product were also isolated. 5-(2-chloroethyl)- 1, 2, 3, 4-tetramethylcyclopentadiene and 5-(3-chloropropyl) 1, 2, 3, 4-tetramethylcyclopentadiene were synthesised and isolated as geminal isomers for the first time.

The trialkyl chromium complex, tribenzyl chromium *tris*(tetrahydrofuran) was synthesised and also it was used as starting material for the complexes di(benzyl)chromium bis(1, 3-diisopropylimidazol-2-ylindene) and tri(benzyl)chromium TACN. All complexes were characterised by X-ray crystallography.

The imidazolium salt 3-(2.6-diisopropylphenyl)-1-[*N, N-bis*(2,6-diisopropylphenyl)acetamidyl] imidazolium chloride was synthesised and used as a precursor for the synthesis of amidinate-functionalised NHC zirconium and amidine-functionalised NHC silver complexes. Double deprotonation of 3-(2,6-diisopropylphenyl)-1-[*N, N'-bis*(2,6-diisopropylphenyl)acetamidyl] imidazolium chloride gave the amidinate-functionalised NHC ligand, 3-(2.6-diisopropylphenyl)-1-[2-*N, N'bis*(2,6 diisopropylphenylamidinate)ethyl]imidazol-2-ylidenepotassium. Titanium, zirconium and chromium complexes containing this ligand were synthesised and characterised by X-ray crystallographic techniques. Transmetallation of the amidine-functionalised NHC silver complex with [Rh(COD)Cl]$_2$ and [Ir(COD)Cl]$_2$ gave the corresponding species. Rh(amidine-functionalised NHC)(COD)Cl reacted with Na(BAr)$_4$ (Ar = 3,5-CF$_3$C$_6$H$_3$) to give the cation Rh(amidine-functionalised NHC)(COD)]$^+$[BAr$_4$]$^-$. These species were also characterised by X-ray diffraction techniques.

Table of Contents

Index of Schemes

Index of Tables

x

Index of Figures

DECLARATION OF AUTHORSHIP

I, Susana Conde Guadaño, declare that the thesis entitled:

"Early Transition Metal Complexes of Carbene Donors Linked to Cyclopentadienyl Ring Analogues or Amidine/Amidinate Moieties"

and the work presented in the thesis are both my own, and have been generated by me as the result of my own original research. I confirm that:

- This work was done wholly or mainly while in candidature for a research degree at this University;

- Where any part of this thesis has previously been submitted for a degree or any other qualification at this University or any other institution, this has been clearly stated;

- Where I have consulted the published work of others, this is always clearly attributed;

- Where I have quoted from the work of others, the source is always given. With the exception of such quotations, this thesis is entirely my own work;

- I have acknowledged all main sources of help;

- Where the thesis is based on work done by myself jointly with others, I have made clear exactly what was done by others and what I have contributed myself;

Some of this work has been published before submission: *"Downing, S. P.; Conde-Guadaño, S.; Pugh, D.; Danopoulos, A. A.; Bellabarba, R. M.; Hanton, M.;Smith, D. and. Tooze, R. P. Organometallics, 2007, 26, 3762."*

Signed:

Date: 14 September 2010

Acknowledgements

List of Abbreviations

Ar = aromatic group

^{t}Bu = *tert*butyl group

Bz = benzyl group

COD = 1,5-cyclooctadiene

Cp = cyclopentadienyl

Cp* = 1, 2, 3, 4-tetramethylcyclopentadienyl

DCE = 1,2-dichloroethane

DCM = dichloromethane

DiPP = diisopropylphenyl group

Exc = excess

HMPA = hexamethylphosphine oxide amine

KHMDS = potassium hexamethyldisilazide

KOBu^{t} = potassium *tert*butyl oxide

LDA = lithium diisopropylamide

L'K = 3-(2,6-diisopropylphenyl)-1-[2-N, N'[*bis*(2,6
     diisopropylphenylamidinate)]ethyl]imidazol-2-ylidene potassium

L(2C)K = 1-[2-(4,7-dimethyl)indenyl)ethyl]-3-(2,6-diisopropylphenyl)imidazol-2
     ylidene potassium

L(3C)K = 1-[3-(4,7-dimethylindenyl)propyl]-3-(2,6-diisopropylphenyl)imidazol-2-
     ylidene potassium

Me = methyl group

Mes = mesityl group

MMAO-3A = modified methyl aluminoxane

NaH = sodium hydride

NHC = *N*-heterocyclic carbene

Ph = phenyl group

^{i}Pr = isopropyl group

Py = pyridine

R = either alkyl or aryl group

TACN = 1, 4, 7-triazacyclononane

THF = tetrahydrofuran

TMEDA = tetramethylethylenediamine

THF = tetrahydrofuran

Chapter 1

Introduction: Organometallic Chemistry of *N*-Heterocyclic Carbenes, Cyclopentadienyl Ring Analogues and Amidine/Amidinate Ligands

1.1 Carbenes

1.1.1 What is a Carbene?

A carbene is a molecule comprising a divalent carbon atom with 6 valence electrons and no formal charge. The general formula for a carbene is RR'C:. [1] Carbenes are generally highly unstable species and quite difficult to isolate. There are two different types of carbene depending on the electron valence arrangement around the carbon atom:

- Singlet carbenes are spin-paired (S=0). In terms of valence bond theory they adopt sp^2 hybridisation at the carbon atom and the two electrons occupy a sp^2 orbital leaving an empty p orbital perpendicular to the planar carbon atom (Figure 1.1).

- Triplet carbenes (S=1) have two unpaired electrons. Although most triplet carbenes have very short life times, some have been isolated and characterised. [2]

Stability depends mainly on the ground state spin multiplicity of the carbene. However, steric and electronic factors of the groups around the carbene carbon atom are also extremely important in determining stability.

The ground state (triplet *vs.* singlet, Figure 1.1) depends on the difference of energy between σ and p_π orbitals. Large σ-p_π separation favours singlet ground states whilst, if σ and p_π orbitals are very close in energy, triplet ground states are more likely. Hoffmann determined that a value of at least 2 eV is necessary to impose a singlet ground state, whereas a value below 1.5 eV leads to a triplet ground state. [3]
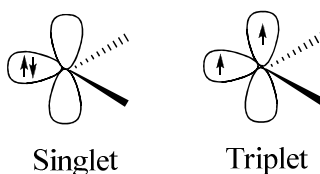
Singlet   Triplet

Figure 1.1: Schematic diagram of the σ and p_π orbitals in the singlet and triplet ground states.

The substituents of the carbene carbon atom play an important role in modifying the energy gap between σ and p_π orbitals. Also the steric hindrance offered by the

substituents in the carbene carbon is very important. A very bulky substituent could block the reactive site at the carbene carbon.

Electronic effects are exerted inductively and mesomerically.

In terms of inductive effects it is known that σ-electron-withdrawing substituents favour the singlet versus the triplet state. Harrison [4] showed by computational methods that the ground state goes from triplet to singlet as substituents electronegativity increased (from lithium to fluorine).

Mesomeric effects can play a more significant role than inductive effects. [5,6] They consist of an interaction caused by interaction between the p_π orbital of the carbene and the π-orbitals of the adjacent heteroatoms (N, S, O, etc...). In singlet carbenes with two π-donating groups in α- position to the carbene carbon (OR, SR, NR_2, PR_2, *etc.*) the energy of the vacant p_π orbital is increased and the energy of the σ-orbital does not change, therefore σ-p_π separation increases, stabilizing the singlet state. The electron pair on the π-donating group interacts with the empty p_π on the carbene carbon atom, giving to the carbene carbon atom certain negative character. Due to the three atoms sharing four electrons delocalised in the p_π system the carbene carbon atom and the α-heteroatom or α-substituent bonding also has multiple-bond character (Figure 1.2). Therefore carbenes have ambiphilic character: they can donate electrons from their lone pair, and they can also accept electrons into the formerly empty p_π orbital. They are normally prevented from acting as electrophiles by intramolecular electron donation from the hetero-atoms flanking the carbene to the empty p_π orbital on the carbene.
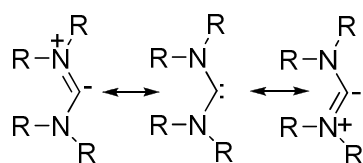
Figure 1.2: Electron delocalisation in a generic system with NR_2 flanking the carbene carbon.

In general, bulky substituents stabilise all types of carbene and they can also dictate the ground-state spin multiplicity. [7] Although is extremely difficult to isolate a triplet carbene, it is possible to favour the triplet state by flanking the divalent carbon with bulky substituents. This makes the carbene bond angle wider towards sp

4

hybridisation, stabilizing the triplet state. In 1996 Tomioka [8] reported the most stable triplet carbene (Figure 1.3). It has a half-life of sixteen seconds in solution but is indefinitely stable when frozen in a THF glass. No triplet carbenes have ever been isolated in the crystalline state.
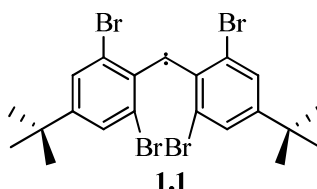
Figure 1.3: The most stable triplet carbene ever prepared.

1.1.2 Fischer and Schrock Carbene Complexes

When a carbene is bonded to a metal centre to form a complex, it is possible to have two types of carbene complexes, Fischer or Schrock, depending on the substituents around the carbene carbon, the metal oxidation state and other co-ligands.

Fischer Carbene Complexes

Fischer carbene complexes are singlet carbenes found with low oxidation transition metals. The bonding can be explained by donation of the lone electron pair from the carbene carbon to an empty orbital of the metal and back-donation from the metal from the d orbital to the empty p_π orbital (π-backbonding). The first Fischer type carbene complex is shown in Figure 1.4 below. [9]
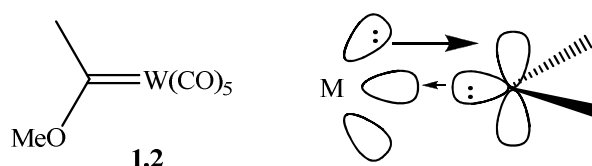
Figure 1.4: First Fischer carbene complex (left) and representation of the electron donation in a Fischer carbene complex (right).

Schrock Carbene Complexes

Schrock carbene complexes involve triplet carbenes coordinated to metals which are typically found in a high oxidation state, bearing no π-donor ligands. Bonding in these types of complex can be described as a bonding between a triplet state of the metal with a triplet state of the ligand (Figure 1.5). Schrock synthesised the first alkylidene complex in 1974 and it is shown in Figure 1.5. [10]

1.3
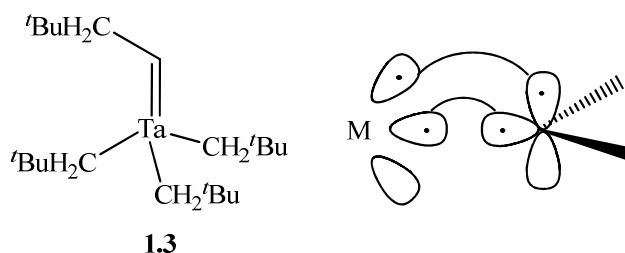
Figure 1.5: Alkylidene Schrock carbene complex of Ta (left) and a generic representation of orbitals and electrons in a Schrock carbene complex (right).

1.1.3 *N*-Heterocyclic Carbenes

The majority of the stable carbenes reported to date are N-heterocyclic carbenes (NHCs), also known as persistent carbenes. These species are extremely reactive and in order to prepare them it is important to work, in most cases, in an inert moisture-free atmosphere. Since carbenes are quite basic compounds (*pKa* = 24 of imidazolium) [11] it is important to avoid protic solvents or acidic species in the reaction mixture.

Some generic structures of NHC and some non-cyclic structures are shown below in Figure 1.6. These carbenes are stabilised by π-donating substituents. Most NHCs are diamino-type, where the nitrogen atom bonded to the divalent carbon offers the best combination of electronic and mesomeric effects to stabilise the carbene. [5, 6]
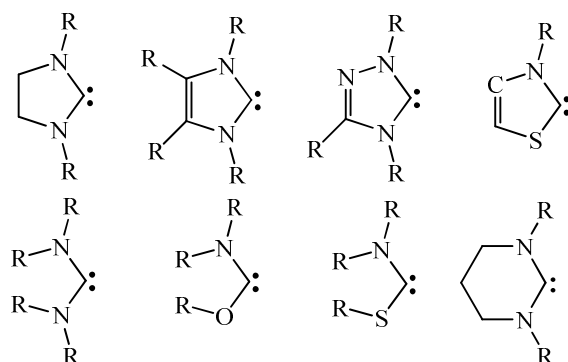
Figure 1.6: Different NHC structures and non-cyclic heteroatom-substituted carbene ligands.

Persistent carbenes were first postulated by Breslow in 1957. [12, 13] In 1960 Wanzlick and co-workers attempted to synthesise 1,3-diphenylimidazolidin-2-ylidene **1.5** by thermal elimination of chloroform (Scheme 1.1). [14] The equilibrium, shown below,

6

involves dimerisation of the NHC to the electron rich olefin **1.6** which inhibit the isolation of **1.5**. This equilibrium was probed two decades later by Wanzlick.
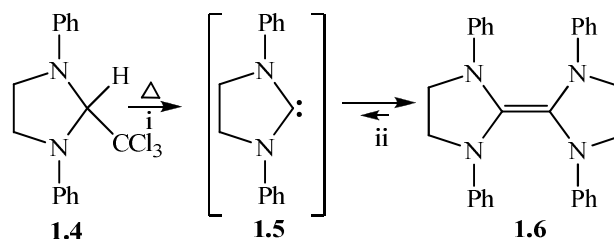
Scheme 1.1: Attempted synthesis of 1,3-diphenylimidazolidin-2-ylidene by Wanzlick.

Neighbouring π systems in conjugation to the heteroatoms adjacent to the carbene carbon atom result in NHC structures where the equilibrium is shifted to the free NHC, for example, by using unsaturated imidazol instead of saturated imidazoline-type rings. This understanding was key to isolating sterically unhindered free singlet carbenes. In 1970 Wanzlick and co-workers demonstrated that imidazolium salts could be deprotonated by potassium *tert*-butoxide to afford the corresponding imidazol-2-yildenes. [15]

But it was not until 1991 that Arduengo not only isolated a carbene for the first time, but also acquired its X-ray structure (Figure 1.7). [16] This carbene was formed by deprotonation of the imidazolium salt with NaH in THF at room temperature.

The carbene compound **1.7** was found to be indefinitely stable at room temperature under inert atmosphere. The $^{13}C\{^{1}H\}$-NMR spectrum showed the resonance of the carbene carbon atom to be 211 ppm which indicates that it is very unshielded in comparison with regular carbon atoms. The crystal structure showed longer N-C(carbene) bond length than in the imidazolium precursor, implying less than double bond character.
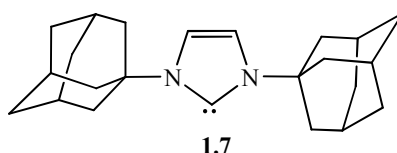
Figure 1.7: First crystalline carbene prepared by Arduengo.

Initially it was believed that the carbene isolated by Arduengo was extremely stable due to the bulky substituents. However, this view was disproved when the adamantyl groups were substituted by small methyl groups. [17]

7

In 1995 the saturated system 1,3-di-1-mesitylimidazolin-2-ylidene was also isolated by Arduengo,[18] showing that the double bond between C4 and C5 was not critical for the isolation of the carbene.

Most of the stable singlet carbenes are based in the substitution of the divalent carbon, being part of a cyclic system, with two nitrogen atoms to give imidazol-2-ylidene or imidazolin-2-ylidene. However, there are also examples where one of the amino substituents is replaced by a different heteroatom (Figure 1.6).[19] Although, the stability of singlet carbenes mainly results from electronic effects (mesomeric and inductive effects), steric hindrance plays also an important contribution, especially in saturated systems. Studies based on inner-shell electron energy loss spectroscopy[20] have confirmed that cyclic electron delocalization occurs in the imidazol-2-ylidenes. Although this aromatic character is less pronounced than in the imidazolium salt precursors, it brings an additional stabilization.

In 1996 the first acyclic carbene was isolated by Alder and the structure was elucidated by X-ray diffraction techniques.[21] As in the saturated version of cyclic diaminocarbenes the species with no-bulky substituents tend to dimerise.

It was believed that carbenes were only stable under inert conditions until, in 1997, Arduengo prepared an air-stable carbene for the first time (Figure 1.8).[22]
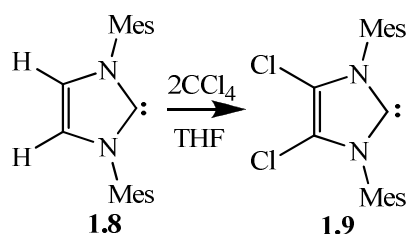
Figure 1.8: The first air-stable carbene isolated by Arduengo.

N-Heterocyclic carbenes are interesting species in themselves but they are even more so when forming complexes with metals.

NHCs and trialkylphosphines are quite similar in terms of the ligand properties and metal complex synthesis. N-heterocyclic carbene ligands are σ-electron donors with little π-accepting ability. They form strong bonds to late transition metal centres, with little tendency for dissociation. The chemistry of NHCs with early transition metals is less studied. For group 4 and 5 metals the NHC bond to the metal centre is more likely to dissociate than for late transition metals.

Recently it has been reported that f-block metal NHC bonds are very labile. Although, in general, metal-NHC bonds are considered as inert, they can show reactivity under certain conditions, which has clear implications for complex synthesis and catalysis. Metal-to-metal transfer reactions, alkyl-carbene elimination or insertion to metal-carbene bonds are some examples of metal-NHC reactivity. The chemistry of NHC complexes with late transition metals has been widely studied whereas the chemistry of NHC complexes with early metals (especially group 4 and 5 metals), is a more novel area of research.

1.1.4 Synthetic Routes for *N*-Heterocyclic Carbene Complexes

N-heterocyclic carbenes form complexes with almost all metals of the periodic table. There are four main methods for the preparation of *N*-heterocyclic carbene complexes: (i) complexation of the previously prepared free carbene ligand with a metal precursor; (ii) *in situ* complexation of imidazolium salts by metal precursors bearing basic groups (this method involves *in situ* deprotonation of the imidazolium salt produced by the basic group on the metal precursor); (iii) cleavage of electron-rich olefins in the presence of low oxidation state metals, and (iv) NHC transmetallation reactions, usually from silver complexes. Examples of these routes to synthesised NHC complexes are discussed below:

Complexation of Preformed NHC Ligands with a Metal Precursor

This method consists of the complexation of the previously prepared free carbene ligand with a readily available metal precursor. The main advantage of this method is that the presence of a basic reagent or a basic substituent on the metal centre is not required because the deprotonation of the NHC precursor takes place in a separated step. Once the NHC ligand has been prepared it is reacted with the metal precursor to give the desired complex.

There are different methods to obtain imidazol 2-ylidene ligands and three generic examples are shown in Scheme 1.2 below.
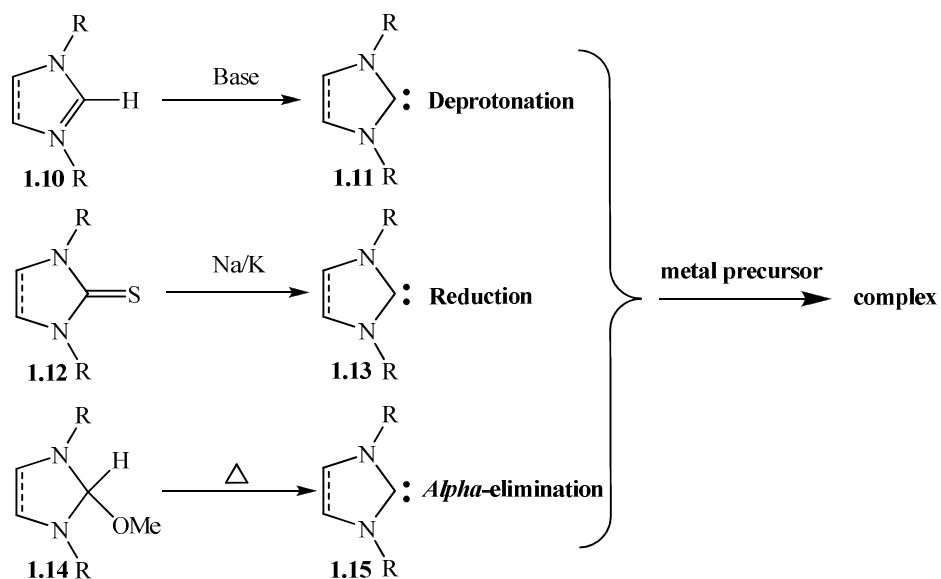
Scheme 1.2: Different methods to form NHC ligands suitable for complexation with metal precursors.

Strong bases such as NaH [16] and KO^{t}Bu in THF can be used. Liquid ammonia can be used as a solvent in combination with NaH improving the yield in some cases. [23, 24] Bases with bulky anions such as KN(SiMe$_3$)$_2$ [25] and lithium diisopropyl amide [26] can also be successfully used.

Cyclic thioureas can react with sodium or potassium metal to give the free carbene which can be isolated after filtration. [27]

Thermal elimination of molecules such as methanol [28] or chloroform [14] have also been used in the preparation of NHC ligands.

Once the free carbene is formed it can react with a great number of readily available metal precursors to form the desired complex. Examples include substitution of a simple neutral molecule such as CO by the preformed NHC on the metal precursor, [29] cleavage of late transition metal dimer precursors [MCl(COD)]$_2$ (M=Rh or Ir), [29] exchange of larger ligand molecules such as phosphines [30] for the preformed NHC on the metal precursor, or substitution of coordinated solvent molecules such as THF. Some of these examples are shown in Scheme 1.3 below.
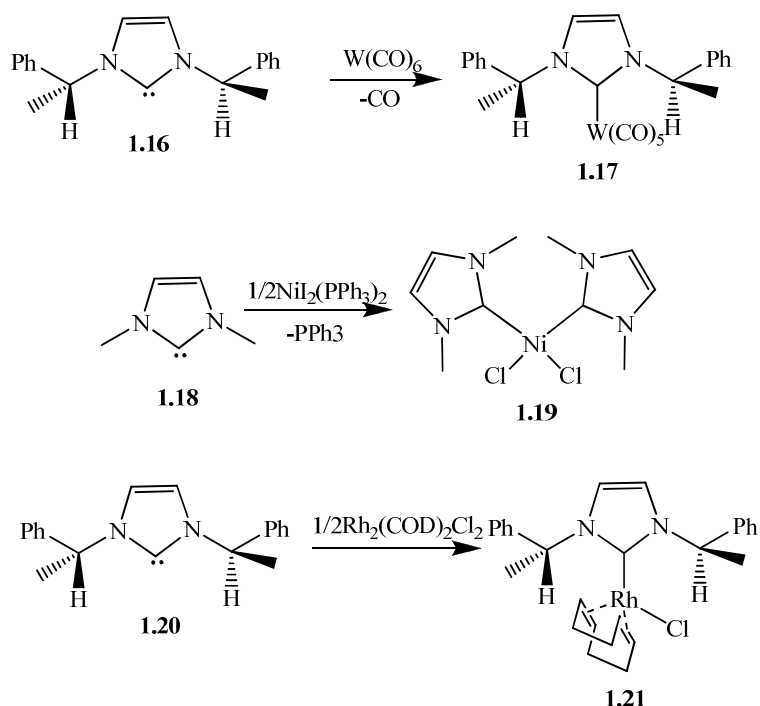
Scheme 1.3: Examples for the complexation of different metal precursors with the preformed NHC.

In Situ **Deprotonation of the Ligand Precursor and Complexation with the Metal Precursor**

The *in situ* complexation of the metal precursor with the NHC ligand precursor, as it is shown in Scheme 1.4, has the advantage that it is not necessary to isolate the free carbene, which may be difficult to handle.

Öfele prepared the first NHC complex by *in situ* deprotonation of the metal precursor **1.22** by elimination of hydrogen. [31] This method is relatively simple but it requires that the appropriate metal precursor needs to be readily available.
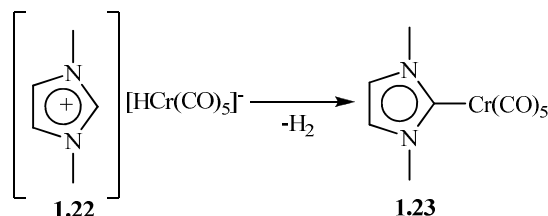
Scheme 1.4: *In situ* complexation to form a pentacarbonyl chromium complex by Oféle.

Deprotonation of the imidazolium ring by basic anions on the metal precursor is also possible. There are several examples in which acetate and alkoxide nickel and

11

palladium salts are frequently used. [32, 33] The counter anion of the imidazolium salt precursor is incorporated in the new complex in this method.

An example of *in situ* complexation of a diimidazolium salt with a palladium metal precursor is shown in the Scheme 1.5. [34] The first imidazolium ring is deprotonated under mild reaction conditions to give the intermediate monocarbenepalladium **1.25** complex. In order to deprotonate the remaining imidazolium pendant arm the intermediate is refluxed in DMSO to yield the chelating dicarbenepalladium dibromide **1.26**.
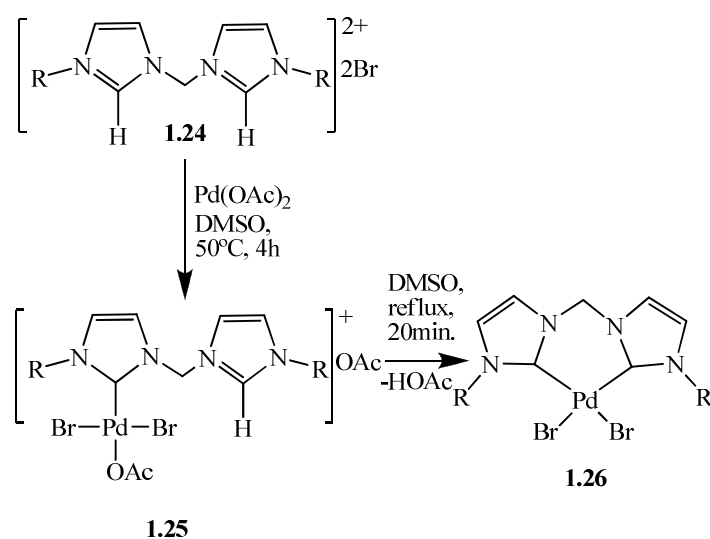
Scheme 1.5: *In situ* deprotonation and complexation of **1.24** with Pd(OAc)$_2$ *via* acetic acid elimination. R= ^{t}Bu.

Cleavage of Electron-rich Olefins

In the early days of carbene chemistry, cleavage of electron rich alkenes using different metal precursors was used to prepare NHC complexes. Some particular examples are shown in the Scheme 1.6. [35] Early transition metal carbene complexes of chromium, molybdenum and tungsten were typically prepared using carbonyl metal precursors. Some late transition metal carbene complexes such as rhodium NHC complexes were obtained from cleavage of electron rich olefins with the dimer [RhCl(COD)]$_2$.
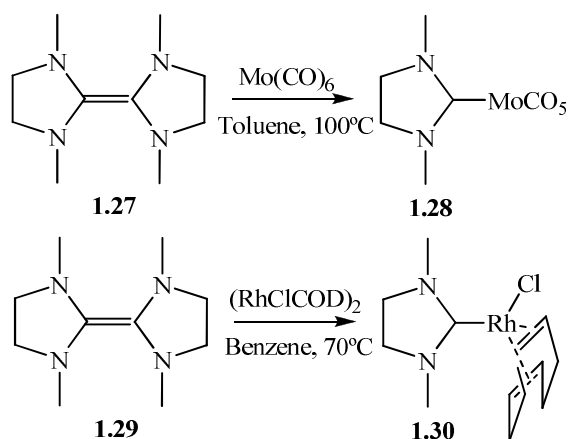
Scheme 1.6: Cleavage of the electron-rich olefin **1.27** and **1.29** with Mo(CO)$_6$ and [RhCl(COD)]$_2$to give NHC complexes **1.28** and **1.30**.

Ligand Transmetallation Reactions

Lin and Wang reported in 1998 that silver NHC complexes are useful as carbene transfer agents. [36] Silver NHC complexes can be reacted with PdCl$_2$(MeCN)$_2$ and Au(SMe$_2$)Cl to form the complexes shown in Scheme 1.7 below.
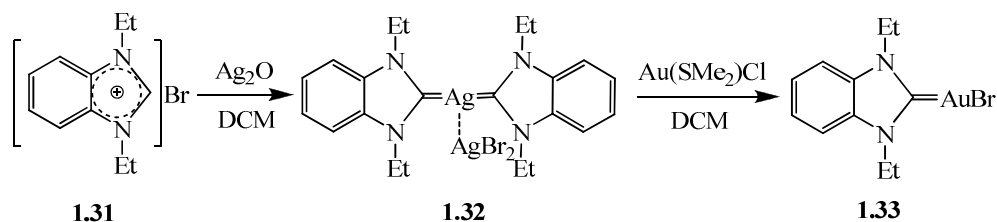
Scheme 1.7: Silver transmetallation reaction by Lin and Wang.

The use of silver NHC complexes provides a convenient way of avoiding the use of strong bases, inert atmospheres and complicated procedures necessary to isolate the free NHC. In many cases transmetallation reactions can be carried out in aerobic conditions. Imidazolium salt reacts with Ag$_2$O to give the mono- or di-NHC silver complex and this can be used *in situ* with the convenient metal complex precursor, usually bearing halide ligands.

Liu reported that carbene ligands can be transferred under mild condition from pentacarbonyl complexes of chromium, molybdenum and tungsten (group 6) to rhodium, platinum, palladium and gold (Scheme 1.8). [37, 38]

13

1.34 → **1.35**
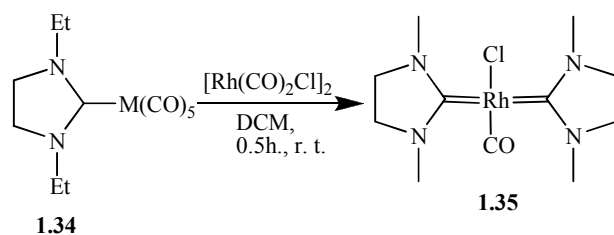
Scheme 1.8: Carbene ligand transfer reaction from diaminocarbene complex (M = Cr, Mo and W) to a Rh complex **1.35**.

The triazolyl-2-ylidene silver(I) carbene complex **1.36** has been used to synthesise the gold (I) complex **1.37** by a transmetallation reaction with Au(SMe$_2$)Cl in a dichloromethane solution (Scheme 1.9). [39]

1.36   **1.37**
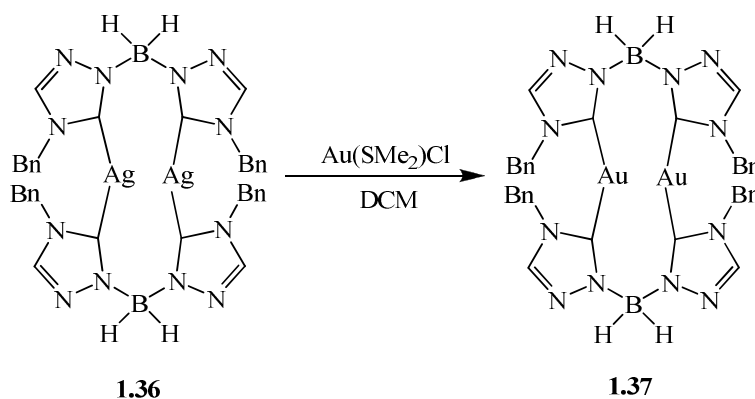
Scheme 1.9: Carbene ligand transfer reaction from an Ag complex to an Au complex.

1.1.5 Importance of NHC Complexes in Catalysis

N-Heterocyclic carbene and phosphine ligands have often been compared in terms of bonding properties and reactivity around the metal centre. Phosphine complexes have been used as catalysts in a vast number of processes but in the last decade NHC compounds have been added to the small group of ligands which are useful in catalysis. [40]

Catalysts based on carbene complexes may have advantages over phosphine based catalysts. *N*-Heterocyclic carbene ligands are more rigid, and the carbene metal bond is stronger (better σ-donor than phosphines) which leads to less catalyst decomposition (less catalyst deactivation). They also are more resistant to oxidation than phosphine ligands. In terms of steric characteristics they are also different since phosphines are considered structurally as cones whilst the NHCs are considered as wedges. Phosphines are typically cone-shaped, so rotation about the M–L bond

should not have major consequences. On the other hand NHC ligands are wedge-shaped so rotation can have electronic and steric effects around the metal centre; monoNHC ligands tend to rotate to minimize any steric clash with other ligands. However, in the case of chelating NHC ligands the orientation of the rings is partially locked within a relatively narrow range by the constraints of the linker.

NHC Complexes of Late Transition Metals in Catalysis

The Heck reaction, the coupling of aryl halides with terminal olefins, is one of the most important palladium-catalysed transformations in organic synthesis for generation of C-C bonds. This reaction is catalysed by organopalladium compounds. The best results have been obtained by using phosphines as ligands. [41, 42] The catalytic mechanism is not limited to terminal olefins. In related reactions, the Sonogashira coupling [43, 44] one of the reactants is an alkyne and in the Suzuki coupling [45, 46] the alkene is replaced by an aryl boronic acid.

N-Heterocyclic palladium complexes have been proved to be excellent catalysts for Heck, Suzuki, Sonagashira [47, 48, 49, 50] and Negisi [51] cross-coupling reactions.

Two active palladium pro-catalysts for the Heck coupling reaction are shown in Figure 1.9 below. Pro-catalyst **1.38** is very active, although it starts showing decomposition above 70 ℃. Since thermal stability of phosphine complexes improves when they are incorporated into a chelating ligand (pincer phosphines), the same strategy was used by Crabtree in the synthesis of complex **1.39**. [52] This results in an active catalyst for the Heck coupling reaction that is stable up to 160 ℃.

| **1.38** | **1.39** |
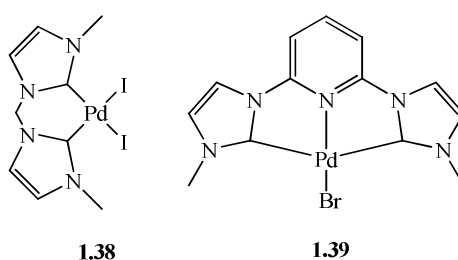
Figure 1.9: Active pro-catalysts for the Heck coupling reaction.

In 1999 Grubbs reported the Second Generation of catalysts for metathesis reactions. [53, 54] In this catalyst system a phosphine ligand in the First Generation pro-catalyst **1.40** is replaced with a NHC ligand, as is shown in Scheme 1.10 below, to give the Second Generation pro-catalyst **1.41**. The saturated NHC ruthenium complex version shows better performance than the unsaturated NHC complex analogue since the

carbene carbon is bonded more strongly to the metal due to its higher basicity. Phosphine dissociation in the Second Generation catalyst facilitates the formation of active species.
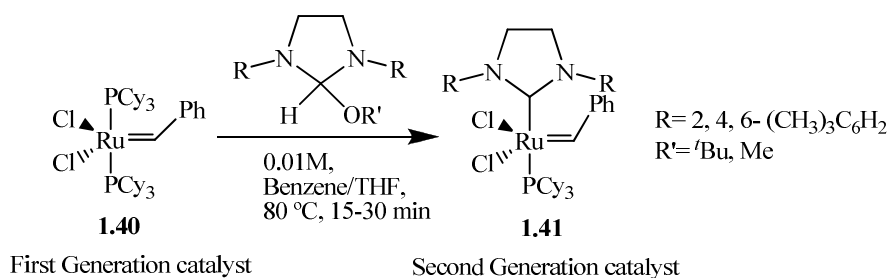
Scheme 1.10: Ruthenium NHC saturated complex **1.41** highly active for metathesis reactions by Grubbs.

Dorta has reported recently [55] that steric modifications of the Second Generation catalyst lead to both higher activity and better stability of catalyst. The substitution of simple aromatic rings with naphthyl ligands on the NHC minimizes the availability of carbon–hydrogen bonds that react with the ruthenium center *via* C–H activation leading to catalyst decomposition.

cis-Chelating diphosphine complexes of palladium were usually used as catalysts for the copolymerisation of ethylene and carbon monoxide. In 1999 Herrmann reported an efficient NHC Pd(II) catalyst for the copolymerisation of carbon monoxide with ethylene under mild conditions, which is shown in Figure 1.10 below. [56]
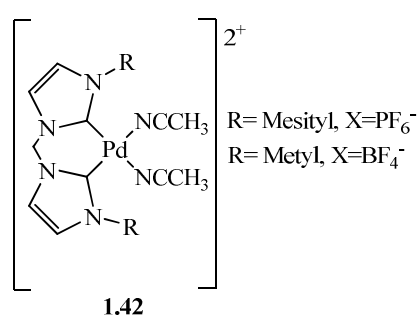
Figure 1.10: NHC palladium complex **1.42** active in the copolymerisation of ethylene with CO.

NHC Complexes of Early Transition Metals in Catalysis

Catalytic activity of NHC complexes of early transition metals has not been studied as much as with late transition metals. One reason is that the carbene metal bond is more labile in complexes with early metals. [57] Therefore, NHC ligands combined with other

16

functionalities may increase the stability of the complexes which might improve their performance in catalysis. The aryl oxide groups in complex **1.43** shown in Figure 1.11 below act as anchors and reduce the tendency for NHC dissociation. [58] This complex was found to be a highly active catalyst in the polymerisation of ethylene when it is activated with MMAO.

1.43
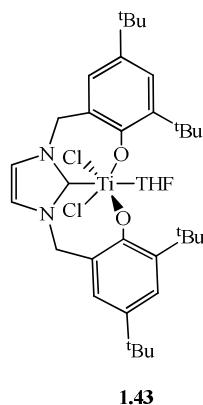
Figure 1.11: NHC titanium complex stabilised by two aryl oxide groups.

Gibson reported *N*-heterocyclic chromium complexes as being highly effective catalysts for ethylene oligomerisation. [59] The chromium complexes shown in Figure 1.12 are air stable, even in solution and give Schulz-Flory distribution of α-olefins when activated with MAO. The chromium complex with ligand L3 produced polyethylene with very little amounts of oligomers: therefore the large substituents have a detrimental effect on the catalytic activity.

Titanium and vanadium complexes are air and moisture sensitive, since L2 provided the most stable and active catalyst for chromium, this ligand was used in the synthesis of titanium and vanadium analogues which were tested with a variety of cocatalysts. The vanadium complex presented better activity than the titanium analogue in polymerization of ethylene. However neither titanium nor vanadium complexes produced oligomerisation.

L1, R=^{i}Propyl
L2, R= 2,6-diisopropylphenyl
L3, R= 1-adamantyl

M= Ti, V and Cr

1.44
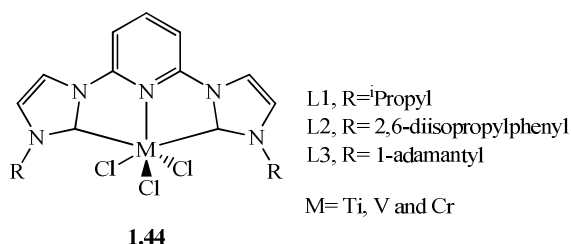
Figure 1.12: Complexes by Gibson suitable for ethylene oligomerisation and polymerisation.

The complexes above and their catalytic performance have also been discussed by Danopoulos, [60, 61] who also reported the synthesis of new Mn(II), Nb(III) and U(IV) halide complexes with this ligand, and the oxidation of V(II) andV(III) complexes by oxo and imido transfer reagents.

1.2 Cyclopentadienyl Analogues Metal Complexes

1.2.1 Metallocene Complexes

In 1951 ferrocene was prepared unintentionally for the first time by Pauson and Kealy. They reacted cyclopentadienyl magnesium bromide and ferric chloride in order to synthesise fulvalene by the oxidative coupling of the diene. Instead, an orange powder of remarkable stability was isolated. [62] This stability is due to the aromatic character of the negative charged cyclopentadienyl rings. Woodward and Wilkinson hypothesised the sandwich structure based on its reactivity. [63]

1.45
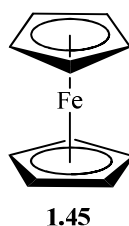
Figure 1.13: Structure of ferrocene.

Fischer, working in parallel, also came to the conclusion of the sandwich structure and synthesized other analogous metallocenes such as nickelocene and cobaltocene. [64]

The structure of ferrocene was confirmed later by X-ray crystallography [65] and then by NMR spectroscopy. [66] The peculiar sandwich structure of the metallocene complexes was found to be of great interest and it was the beginning of the study of the reactivity of d-block metals with hydrocarbons. Therefore it was the starting point for the flourishing of organometallic chemistry.

Fischer, of the Technische Universität München, and Wilkinson, of Imperial College London, shared a Nobel Prize in 1973 for their work in metallocenes and other studies in organometallic chemistry. [67]

In 1953 Wilkinson synthesised the indenyl analogue to ferrocene for the first time, shown in Figure 1.14 below. [68]
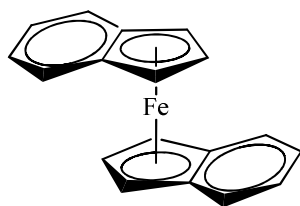
1.46

Figure 1.14: bis-(Indenyl) iron(II).

Indenyl rings can slide from η^5 to η^3 hapticity when they are coordinated to a metal and this behaviour increases the reactivity towards substitution by creating electronically unsaturated metal centres. In the past few decades the indenyl effect has been extensively studied. [69, 70, 71, 72, 73, 74, 75]

1.2.2 Metallocene Complexes and Polymerisation Catalysis

In 1980 Kaminsky and co-workers discovered that group 4 metallocene compounds can be activated by certain co-catalysts to give extremely high activity catalysts for polymerisation of olefins. This fact attracted the interest of industry since they are the homogeneous version of the Ziegler-Natta catalyst. Intermediates in the catalytic process might be isolated helping to understand the polymerisation mechanism.

In addition, the use of chiral metallocenes that have bridged cyclopentadienyl rings has made highly stereoselective polymerization of α-olefins possible. For example, metallocene **1.47** for polymerization of propylene gives atactic polypropylene, while C_2 symmetric metallocene **1.48** and C_s symmetric metallocene **1.49** catalytic systems produce isotactic and syndiotactic macromolecules respectively, (Figure 1.15).

Therefore Kaminsky catalysts have been very attractive from the industrial and academic point of view and their study has been in the direction of improving their activity producing high tacticity and molecular weight polymers.

Despite the improvement of this type of catalyst system, traditional Ziegler-Natta catalysts still dominate the industry for economic reasons.

20

1.47   **1.48**   **1.49**
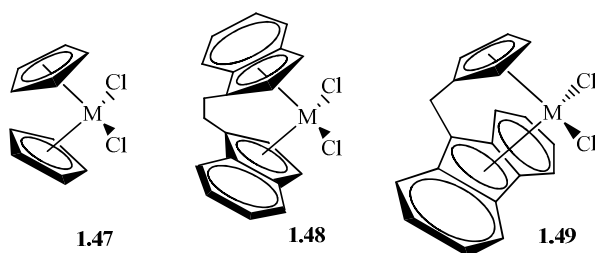
Figure 1.15: Kaminsky type pro-catalysts for homogeneous polymerization of ethylene. M = Zr, Hf.

Jolly and Jensen observed that, whereas chromium played a very important role in the development of heterogeneous catalysts for the polymerization of alkenes, this metal was not studied much in the development of the homogeneous MAO-activated systems. They reported homogeneous MAO-activated chromium catalysis as being highly active for the polymerization of ethylene under mild conditions. [76] Figure 1.16 below shows some examples. However the energy barriers for the ethylene insertion, established by computational methods, are higher in these complexes than in the group 4 analogues.

1.50   **1.51**   **1.52**
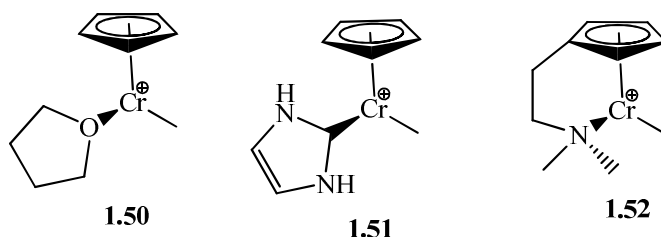
Figure 1.16: Cyclopentadienyl chromium methyl cations active in polymerisation of ethylene reported by Jensen.

The investigations were extended to the related Cp phosphinoalkyl-substituted analogues shown in Figure 1.17 below. A remarkable dependence of the product composition of the reaction with ethylene upon the steric properties of the substituent (R) on the P atom was observed. [77] Complex **1.53** activated with MAO catalyses the formation of 1-butene/1-hexene when R is methyl; it gives a mixture of long-chain oligomers when R is phenyl or isobutyl and polyethylene when R is cyclohexyl.
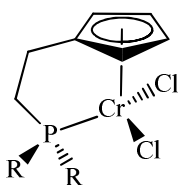
1.53

R= Me, Ph, ^{i}Bu, Cy

Figure 1.17: Phosphinoalkyl-substituted cyclopentadienyl chromium dichloride compounds by Jensen.

Systems where more than one catalyst operates in the same vessel in a tandem fashion have also been used in polymerisation of ethylene to obtain the desired product from simpler starting materials. This type of catalysis is known as *tandem catalysis*.

More than one catalyst operating simultaneously in a one-pot vessel has numerous advantages: for example, it eliminates problems associated with isolation and purification of intermediates in multi-step processes.

The nature of the final product is determined and fine-tuned by the composition of the tandem catalyst mixture in the reaction vessel.

Bazan and co-workers employed a mixture of nickel and titanium complexes for ethylene polymerisation in order to obtain branched products (Figure 1.18). [78] In this triple tandem catalyst mixture the activated Ni complex **1.55** dimerises ethylene into α-butylene. Then the Ti catalyst **1.54** incorporates the α-butene produced in the first step into a growing polyethylene chain. Compound **1.56** generates a Schultz-Flory distribution of 1-alkenes, which are also incorporated into the polyethylene growing chain at catalyst **1.54**.

Different concentrations of catalyst **1.54**, **1.55**, and **1.56** in the reaction vessel provides polymers with different ratios of ethyl branches and longer branches, modifying the properties of the final polymer in a reproducible manner.

1.54　　　**1.55**

1.56
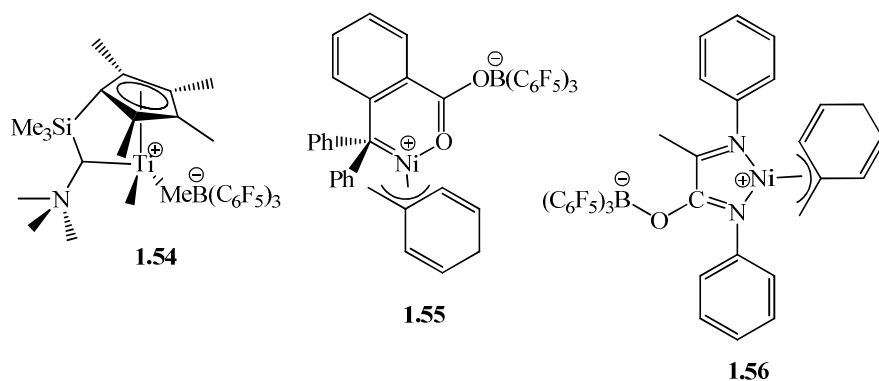
Figure 1.18: Tandem catalyst system for the polymerisation of ethylene reported by Bazan.

The concept of tandem catalysis evolved to molecular levels. Bimetallic early-late transition metal complexes bearing Cp ligands on one of the metal centres have been reported for ethylene polymerisation: an example is shown in Figure 1.19.[79]

The dinuclear Zr-Ni complex **1.57** allows the formation of a branched oligomer at the nickel centre whilst the polymer growth takes place at the zirconium centre. This concept is similar to the tandem catalysis but bimetallic complexes are used instead of a mixture of catalysts.

The polyethylenes produced by using bimetallic complexes have different structures and properties depending on the late transition metal chosen.

1.57

$MX_2 = PdCl_2, CoCl_2, NiBr_2(H_2O)$
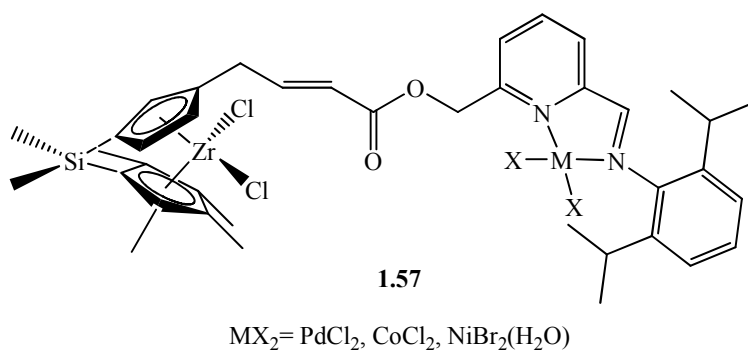
Figure 1.19: Bimetallic complex reported by Osakada for ethylene polymerisation.

1.3 Non-metallocene Complexes and Catalysis

A significant amount of effort has been made over the past decade to modify the reactivity of the metallocene framework. This has led to the design of new non-metallocene complexes that perform as single-site olefin polymerization catalysts.[80]

As has been discussed previously, soluble early transition metal metallocene-based catalysts have been used for polymerization of ethylene and α-olefins. These have served as mechanistic models for traditional Ziegler-Natta catalysts and structural variations in these homogeneous catalysts allow control of polymer microstructures and molecular weights. In contrast to early metal systems, late metal catalysts mostly dimerise or oligomerise olefins due to competing β-hydride elimination. [81]

Brookhart reported for the first time a late metal system capable of converting α-olefins to high molecular weight polymers. [82] This catalytic system, shown in the Figure 1.20 below, uses bulky diimine complexes of Ni and Pd and exhibits extremely high activity, which made them comparable to the metallocene type catalysts.

The metal center is efficiently shielded from associative displacement by bulky substituents on the diimine ligands. Variations in temperature and pressure during the catalysis give different branching and crystallinity levels in the final product.

Brookhart reported two types of precursors. The nickel and palladium dimethylated complexes **1.59** use $H(Et_2O)_2BAr_4$ (Ar = $3,5-C_6H_3(CF_3)_2$) as an activator, methane is released and the metal ether adducts are formed. When these activated species are exposed to ethylene propylene, or 1-hexene, formation of high molecular weight polymers takes place.

The dibromo nickel precursor **1.58** is activated by MAO in toluene. The polyethylene produced by this Ni(II) catalyst ranges from highly linear to moderately branched, with methyl branches predominating.

1.58   **1.59**

M= Ni, Pd
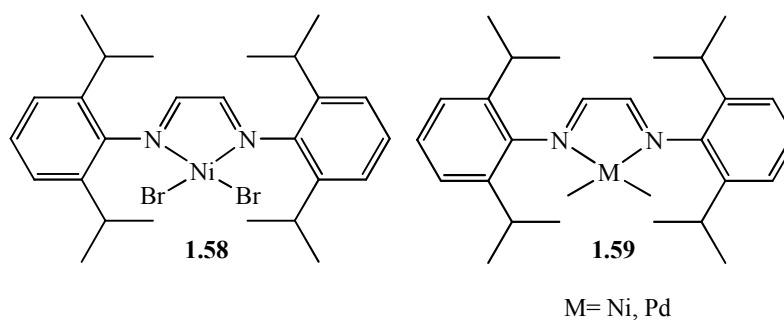
Figure 1.20: Pro-catalysts for the polymerisation of ethylene and α-olefines by Brookhart. M = Ni or Pd.

The technology was further developed in the laboratories of DuPont's Central Research and they are known as DuPont's Versipol olefin polymerization system. [83] The catalysts are able to polymerize ethylene to a variety of products depending on the conditions of the process and the bulk of the diimine used through the "chain-walking" mechanism. As opposed to metallocenes, they can also copolymerize ethylene with polar co-monomers such as methyl acrylate.

Gibson [84] and Brookhart [85, 86] extended the concept of bulky diimine complex incorporating a pyridine ligand between the imine groups creating tridentate ligands, an example is shown in Figure 1.21 below. These catalysts were remarkably active and robust. No chain-walking is observed in these systems so these catalysts gave linear high density polyethylene. When the steric bulk is removed, they are very active catalysts for ethylene oligomerisation to linear α-olefins. [87]

1.60
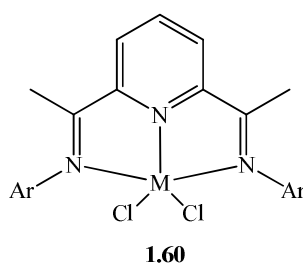
Figure 1.21: Catalyst for the polymerisation of ethylene by Brookhart. M = Fe or Co, Ar = DiPP.

Amidinate complexes of early transition metals have also shown potential in olefin polymerisation catalysis. Titanium and zirconium benzamidinate complexes have been the most studied species. [88] However these organometallic species have shown

25

generally lower activities than the traditional metallocene pro-catalysts Cp_2MR_2 (R= Halide or Alkyl).

The *N,N'-bis*(Trimethylsilyl)benzamidinate system shown in Figure 1.22 below has been particularly widely studied with titanium and zirconium. The activity of the catalyst strongly increases with temperature and pressure. However the activity decreases with the MAO/catalyst ratio and this behaviour is opposite to early transition metallocene catalyst.

1.61

M= Ti, Zr
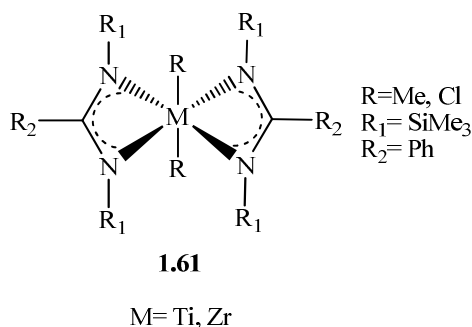
Figure 1.22: bis-(Amidinate) Zr and Ti complexes for polymerisation of ethylene.

Grubbs [89] at Caltech and Johnson at DuPont [90] discovered other types of catalyst based on Ni bearing mono-anionic bidentate ligands. A nickel salicylaldiminato complex is shown in Figure 1.23. Bulky substituents in the 3-position of the salicylaldiminato ring enhance the activity of the catalyst and lower the number of branches in the resulting polyethylene and, as it has been observed in other late metal systems, branching can also be controlled by variation of both temperature and pressure in the catalytic process. An electron-withdrawing group in the 5-position of the salicylaldiminato ring also increases catalyst activity. With these systems, moderately high molecular weight polymers can be obtained.

1.62
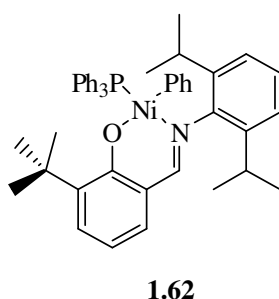
Figure 1.23: Catalyst for the polymerisation of ethylene by Grubbs.

Fujita believed that salicylaldiminato ligands could also be active in catalysis with early transition metals. He synthesized a *bis*-(salicylaldiminato) titanium catalyst **1.63**, shown in Figure 1.24 below, which is extremely active for ethylene polymerization. [91] This pre-catalyst has two available *cis* located sites that can be activated with MAO, needed for the polymerization of ethylene.

1.63
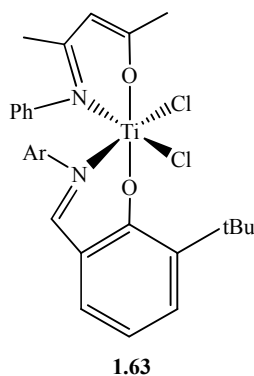
Figure 1.24: Ti catalyst for the polymerization of ethylene by Fujita. Ar = C_6H_5, 2, 4, 6-$Me_3C_6H_2$ or C_6F_5.

Although a lot of effort has been spent developing these systems, very few have been successfully implanted in industry due to the presence of established technologies.

1.4 Metallic Complexes Containing Both NHC Functionalities and Cp Ring Analogues

Both NHC- and Cp-type ligands are very common in organometallic chemistry as has been discussed previously, and it is possible to find examples in which both functionalities are present in the same metallic complex.

Jolly reported in 2001 the synthesis of a NHC cyclopentadienyl chromium complex for the polymerisation of ethylene (see Figure 1.16 above). [76(a)]

Erker reported in 2002 the first example of complexes based on NHC of titanocene and zirconocene cations. [92] The most used stabilizing ligand for metallocene cations is THF. Since Arduengo carbenes are strong σ-donor ligands they have been used to substitute the THF ligand in this species, the reaction is shown in Scheme 1.11 below.

1.64   **1.65**
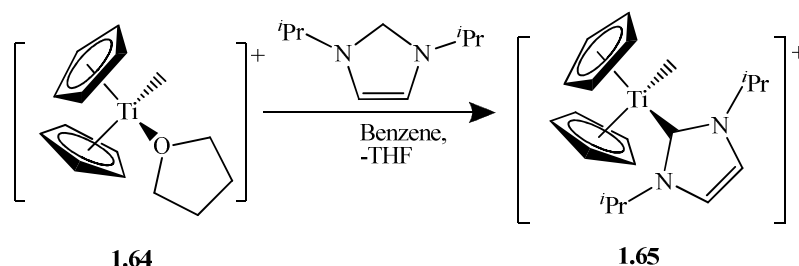
Scheme 1.11: Cationic NHC complex of titanocene reported by Erker.

Anionic groups tethered to N-heterocyclic carbene ligands have been of increasing interest in recent years because of their ability to stabilize a wide range of metal fragments. [93] Therefore it was thought that tethering Cp ring analogues to NHC functionalities would also produce potentially effective chelating species. This asymmetric ligand design would offer a superior level of organization by restricting M-Cp and M-C(NHC) rotation.

In 2006 Danopoulos synthesized for the first time bidentate ligands in which the NHC is tethered to indenyl and fluorenyl functionalities. [94, 95] The imidazolium salts precursors are consecutively double deprotonated by $KN(SiMe_3)_2$ in benzene to give the corresponding potassium salts **1.67** and **1.71**, which can react as bidentate ligands with different early metal precursors as is shown in Schemes 1.12 and 1.13 below.
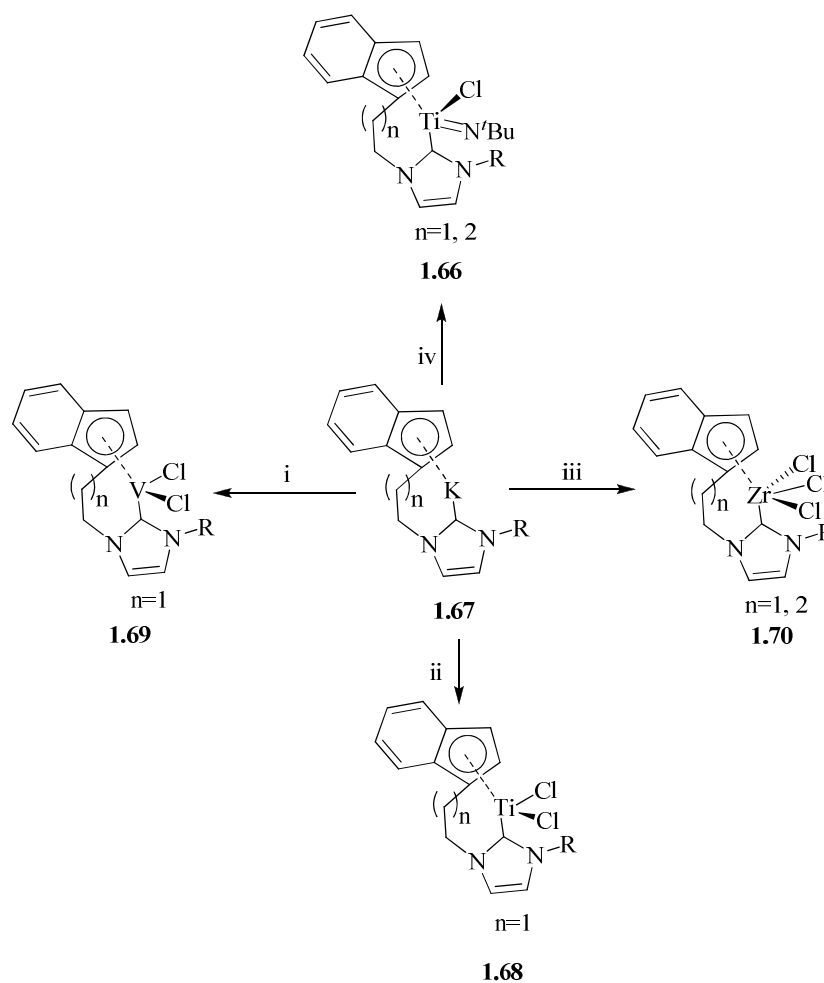
Scheme 1.12: Indenyl-functionalized *N*-heterocyclic carbene complexes of titanium zirconium and vanadium by Danopoulos. R = DiPP; (i): VCl$_3$(THF)$_3$ in THF, addition at -78 °C; (ii): TiCl$_3$(THF) in THF, addition at -78 °C, (iii): ZrCl$_4$(THT)$_2$ in THF, addition at -78 °C, (iv): TiCl$_2$(N^{t}Bu)(py)$_3$ in THF, addition at -78 °C.
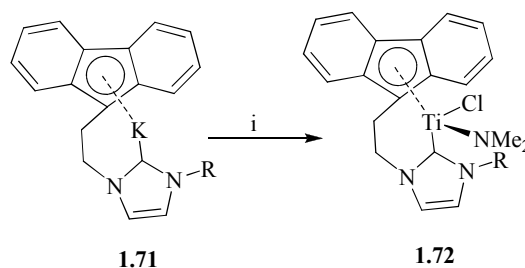
Scheme 1.13: Fluorenyl-functionalized N-heterocyclic carbene complexes of titanium and chromium by Danopoulos. R= DiPP; (i): TiCl$_2$(NMe$_2$)$_2$ in benzene.

In 2007 Shen reported the first indenyl-functionalized N-heterocyclic carbene complex of Ni(II) shown in Figure 1.25 below. [96] This complex is similar to the compounds already reported by our group, which are described later. However, Shen

attempted to synthesise the aryl version of this complex. This complex shows good catalytic activity for the polymerization of styrene in the presence of Na(BPh$_4$).

1.73
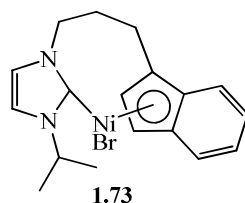
Figure 1.25: Nickel complex by Shen containing an NHC functionalised with an indenyl group.

Peris has recently reported the first pentamethylcyclopentadienyl-functionalized *N*-heterocyclic carbene ligand and its iridium complex shown in Figure below. [97] The ligand has a chiral carbon centre in the linker between the Cp* and the imidazole ring, which makes this ligand of great interest in the design of catalysts for asymmetric catalysis, however only the synthesis of the racemic mixture of all compounds has been reported.

Iridium complex **1.74** appeared to be a versatile catalyst in C-H activation reactions such as transfer hydrogenation, alkylation of secondary alcohols with primary alcohols, and amination of primary alcohols.

1.74
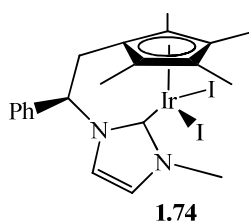
Figure 1.26: Cp*-functionalized N-heterocyclic carbene complex of Ir by Peris.

Most recently Peris has also published Cp, Cp* and Cp^{Bz}- functionalized NHC complexes of Mo(II) shown in Figure 1.27 and the application of these compounds in olefin epoxidation. [98] The chelating effect of this new ligand provides greater stability to the Mo complexes compared to the known CpMo(NHCMes)(CO)$_2$X systems. [99]

Complexes shown in Figure 1.27 are rather slow catalysts, compared to other complexes reported in the literature. However, they are extremely stable under oxidative conditions which allow these complexes to perform for longer reaction times which results in higher conversions to the final products than those provided by other known catalysts. [100]

1.75

1.76

1.77

1.78
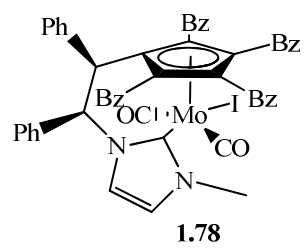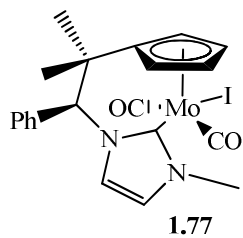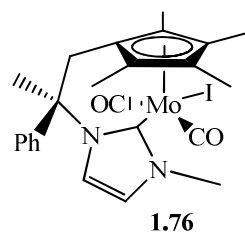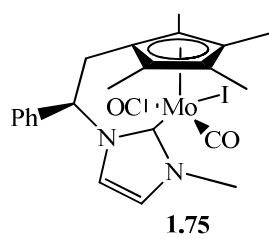
Figure 1.27: Mo(II) complexes by Peris.

1.5 Catalytic Polymerisation and Oligomerisation of Ethylene

In the past few years a large amount of work has been carried out on the oligomerisation [101] and polymerisation of ethylene. [102] Conventional oligomerisation of ethylene to linear α-olefins by transition metal catalysts generally produces a broad range of olefins characterized by either Schulz–Flory or Poisson distributions.

A lot of effort has been put into selective trimerisation and tetramerisation of ethylene to form 1-hexene and 1-octene, respectively. These oligomers play an important role in industry because copolymerization of these α-olefins with ethylene gives different types of low-density polyethylene, depending on the conditions of the polymerisation reaction. From plastic bags and pipes to synthetic lubricants and cables, low-density polyethylene is involved in the manufacture of many everyday products.

1.5.1 Ethylene Trimerisation

The most important process in the trimerisation of ethylene was developed by the Phillips Petroleum Company. Their catalyst system is a product of different pyrroles and chromium salts, $CrCl_2$ and $CrCl_3$, with triethyl aluminium (TEA) and/or diethyl aluminium chloride (DEAC). A solution of this mixture in cyclohexane or toluene is pumped into a reactor where ethylene at 115 °C and 48.5 kg/cm^2 trimerises in a solution phase to produce C_4-C_{10} linear α-olefins. This was the first example of a selective trimerisation catalyst that yielded 1-hexene in greater than 90%. This technology is still the only example of a commercial scale ethylene trimerisation process. [103]

Finally Phillips extended this technology to the co-polymerisation of the trimerisation products with ethylene to produce polyethylene. This process uses a mixture of Phillips trimerisation catalyst on an aluminophosphate support.

Sasol has also developed high activity catalysts for the selective trimerisation of ethylene. [104] The best performance is achieved by using PNP ligands **1.79**, as shown in Scheme 1.14 below.

1.79 → **1.80**

R= phenyl, cyclohexyl or ethyl
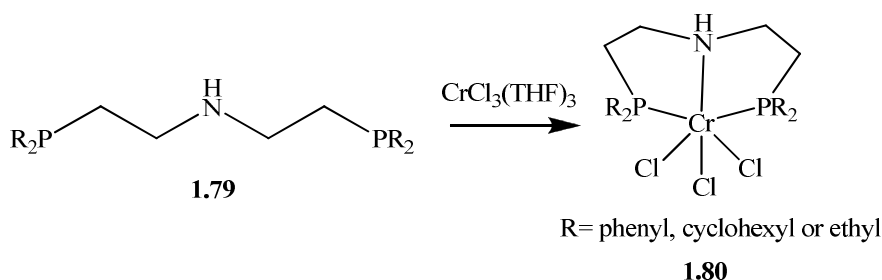
Scheme 1.14: Cr-PNP complexes for trimerisation of ethylene by Sasol.

BP has used systems based in diphosphines [105] for the selective trimerisation of ethylene. The toxicity of the phosphines and their sensitivity towards oxidation makes the use of these systems in industry difficult. [106]

Chromium complexes bearing SNS donor ligands **1.81** (Scheme 1.15) have also been proved efficient in the selective trimerisation of ethylene. Cr(III)-SNS complexes **1.82** have high activity in trimerisation of ethylene in the presence of low amount of co-catalyst MAO.

1.81 → **1.82**

R= methyl, ethyl, *n*-butyl or *n*-decyl
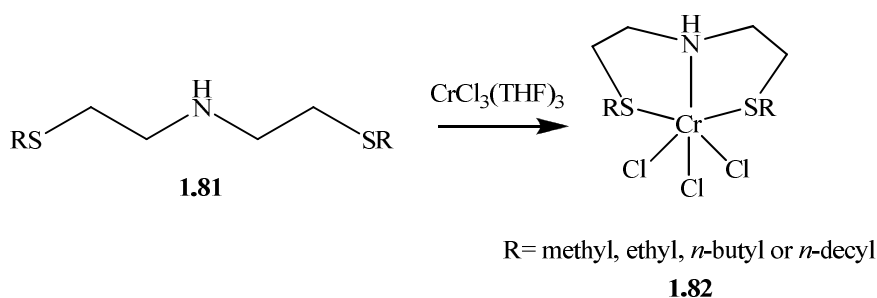
Scheme 1.15: SNS complexes for trimerisation of ethylene.

Mashima has recently reported a new methodology for obtaining Ta(III) species, which are active for the trimerisation of ethylene to obtain 1-hexene under mild conditions. This new system is based on the reduction of $TaCl_5$ with 3,6-*bis*(trimethylsilyl)1,4-cyclohexadiene in the presence of ethylene. [107]

The mechanism proposed for the trimerisation process is shown in the Scheme 1.16 below. $TaCl_3$ is the active specie; two molecules of ethylene simultaneously coordinate to the trivalent metal centre and a rearrangement gives the 5 member-ring metallacycle. The insertion of another molecule of ethylene gives the tantalum cycloheptane which resolves in the formation of 1-hexene and the regeneration of the active specie $TaCl_3$.
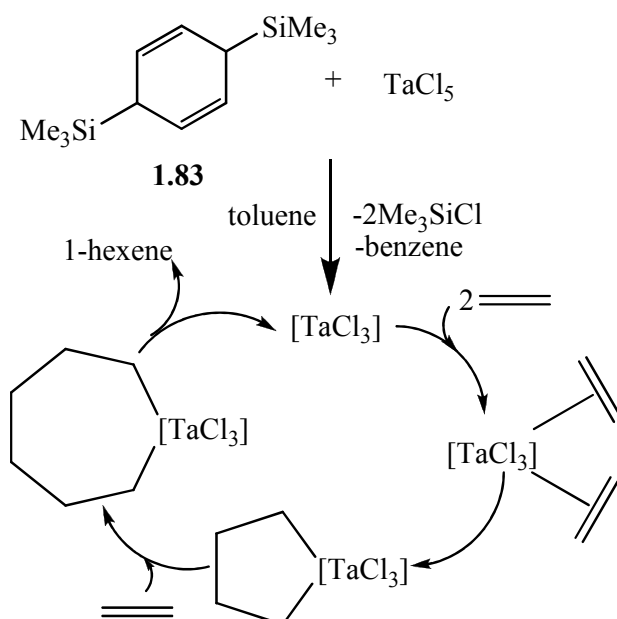
Scheme 1.16: Tantalum ligand-free catalyst system for highly selective trimerisation of ethylene affording 1-hexene.

1.5.2 Ethylene Tetramerisation

Tetramerisation of ethylene is also highly desirable for industry. 1-octene is manufactured by two main routes which are Fischer-Tropsch Synthesis and oligomerisation of ethylene. Fischer-Tropsch Synthesis requires further purification of the product from a mixture of homologues and it is the only commercial process practise by Sasol Ltd. This is employed to produce synthetic fuels at their South Africa plant. A Scheme of the process is shown below. The synthesis gas (CO and H_2) for the production of fuel is derived from coal. Since the product distributions of hydrocarbons formed during this process follows an Anderson-Schulz-Flory distribution, 1-octene represents a small fraction in the mix and it has to be recovered from the fuel stream. The most common catalysts in Fisher-Tropsch Synthesis are based in Fe and Co.

Coal

$$(2n+1)H_2 + nCO \xrightarrow{\text{cat}} C_nH_{(2n+2)} + nH_2O \left.\vphantom{\begin{matrix}a\\b\end{matrix}}\right\} \text{ Fischer-Tropsch Synthesis}$$

Synthesis gas

Mixture of hydrocarbons
in which a fraction is **1-octene**
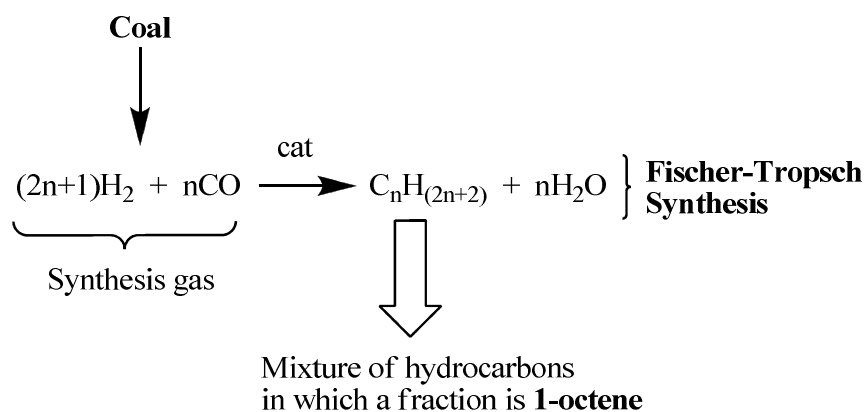
Scheme 1.17: Production of 1-octene by the Fischer-Tropsch Synthesis process.

Sasol published the first system which selectively produces 1-octene in excess of 70% by the oligomerisation of ethylene. [108] This system uses a variety of PNP ligands in combination with Cr(III) compounds, which are activated by aluminoxanes. An example of these ligands **1.84** is shown in Figure 1.28 below. These complexes displayed good activity and selectivity toward 1-octene and 1-hexene during the chromium catalysed ethylene oligomerisation, with the best ligand system having the bulkiest moieties on the N-atom.

1.84
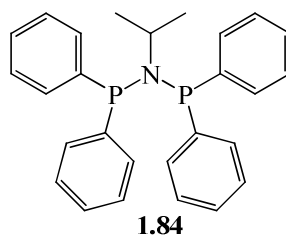
Figure 1.28: Ligand for the synthesis of Cr(III) catalysts for ethylene tetramerisation.

Mechanistic studies on these catalyst systems have demonstrated that the 1-octene is formed by an extension of the classical metallacycle mechanism [109] for 1-hexene production from ethylene. In this mechanism cationic chromium species are implicated in the formation of the active species and Cr(I)Cr(III) redox couples are likely involved. [110]

The production of 1-octene *via* tetramerisation of ethylene is less probable than the analogous trimerisation process (Scheme 1.18). This is because the ethylene tetramerisation proceeds *via* a 9 membered ring metallacycle mechanism, which is less favoured than the 7 membered ring in the trimerisation process.

Cr(acac)$_3$
PNP ligands
MAO

2x

Cr = [Cr]$^+$

PNP ligands
Ph$_2$PN(CH$_3$)PPh$_2$, example for ethylene tetramerisation

PR$_2$(CH$_2$CH$_2$)NH(CH$_2$CH$_2$)PR$_2$, example for ethylene trimerisation
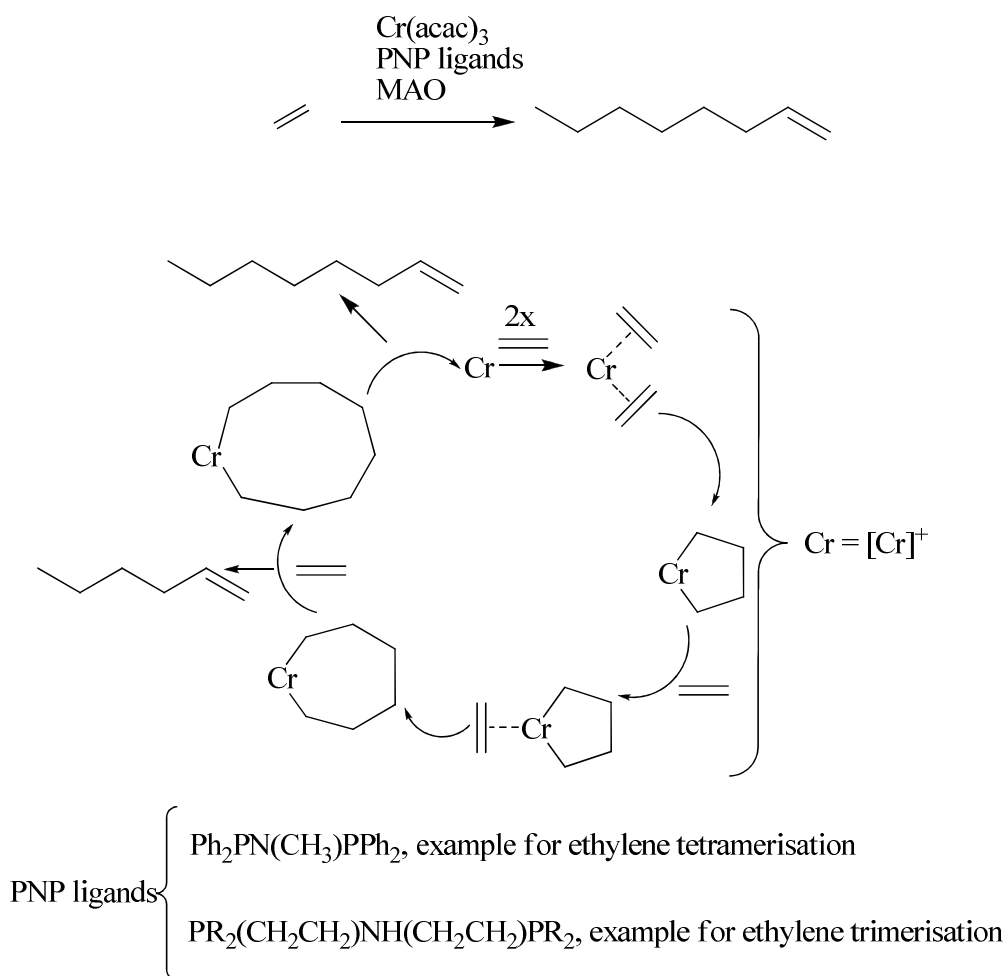
Scheme 1.18: Proposed catalytic cycle for ethylene trimerisation and tetramerisation.

Although constant improvement has been made in developing catalytic techniques for the production of 1-octene, there is not a viable commercial process that selectively produces this tetramer.

In summary the selective production of 1-hexene and 1-octene is highly desirable for the industry and constant progress is being made in this field.

1.6 Aims of This Project

The aims of this project are to synthesise and characterise new early transition metal complexes capable of acting as selective homogeneous catalysts for trimerisation and tetramerisation of ethylene.

Two types of ligands, indenyl-functionalised *N*-heterocyclic carbene and *bis*(dipp-amidinate)-functionalised NHC ligands, have been chosen to prepare new early metal complexes of titanium, zirconium and mainly chromium. These ligands may act as chelating species, giving an asymmetrical environment to the metal centre.

It is well known that early transition metal-carbene bonds are more labile than late-transition metal-carbene bonds. It is thought that in indenyl-functionalised and *bis*(dipp-amidinate)-functionalised NHC complexes the NHC- metal bond might engage and disengage during the catalytic process, resulting in unsaturation of the metal centre, thus facilitating the insertion of ethylene.

One of the most challenging objectives of this project is to synthesise and characterise alkyl cationic complexes of early transition metals, especially alkyl cationic complexes with chromium. They are thought to be the active species in the oligo/polymerisation of ethylene (Scheme 1.18). These cationic species are generated by activation of the pre-catalyst with MAO. Typically a chloride complex is firstly alkylated by MAO and then an alkyl group is abstracted by this activator to generate an ionic couple, the cationic complex and [MAO(alkyl)]⁻. Developing activator free catalyst would be of great interest for industry due to the fact that these materials are expensive and difficult to handle.

Chapter 2

Dimethylindenyl-Functionalised *N*-Heterocyclic Carbene Complexes of Early Transition Metals

2.1 Introduction

The two- and three-carbon-bridged potassium salts L(2C)K and L(3C)K, 1-[2-(4,7-dimethyl)indenyl)ethyl]-3-(2,6-diisopropylphenyl)imidazol-2 ylidene potassium and 1-[3-(4,7-dimethylindenyl)propyl]-3-(2,6-diisopropylphenyl)imidazol-2-ylidene potassium respectively, are excellent compounds to introduce the indenyl-functionalised NHC ligands to a wide range of early transition metal precursors. The different electronic character of the anionic cyclopentadienyl and the neutral N-heterocyclic carbene donor may lead to versatile coordination chemistry with implications in catalysis.

n=2; L(2C)K
n=3; L(3C)K
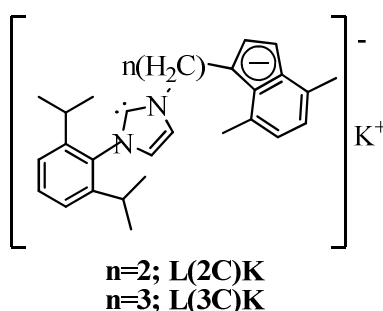
Figure 2.1: Indenyl-functionalised *N*-heterocyclic carbene potassium salts.

A bidentate coordination mode, in which the indenyl-functionalised *N*-heterocyclic carbene ligand acts as chelating specie, is possible. The cyclopentadienyl functionality could provide 2, 4 or 6 electrons, depending on the hapticity of the ring, and two more electrons will be provided by the carbene carbon. Monodentate coordination mode in which one functionality, cyclopentadienyl or NHC, is dangling is also conceivable. A monometallic or bimetallic bridging coordination mode forming polymeric structures might be also possible, as well as discrete bimetallic complexes.

Due to the fact that the postulated mechanism for the oligo/polymerisation of ethylene assumes alkyl cationic complexes as the active species, after activation of the chromium chloride complexes with MAO (Scheme 1.18), one of the objectives of this project is the synthesis of alkyl cationic early metal complexes bearing the indenyl-functionalised *N*-heterocyclic carbene ligands above (Figure 2.1). These new complexes would be tested in the oligo/polymerisation of ethylene in the absence of MAO to corroborate whether they can act as activator-free catalysts. Activators such as MAO are expensive; therefore developing activator-free catalytic systems would be of great economic interest for industry.

2.2 Results and Discussion: Indenyl-functionalised *N*-heterocyclic carbene Ligands and Early Metal Complexes

In this chapter the synthesis and characterisation of new early transition metal complexes (Ti, Zr and mainly Cr) bearing dimethylindenyl tethered to *N*-heterocyclic carbene are discussed.

The synthesis of the dimethylindenyl-functionalised *N*-heterocyclic carbene potassium salt with two carbon bridge L(2C)K (Scheme 2.1), as well as the imidazolium salt precursor L(2C)Br, were both reported for the first time by Danopoulos. [94] They are also included in Stephen Downing thesis.
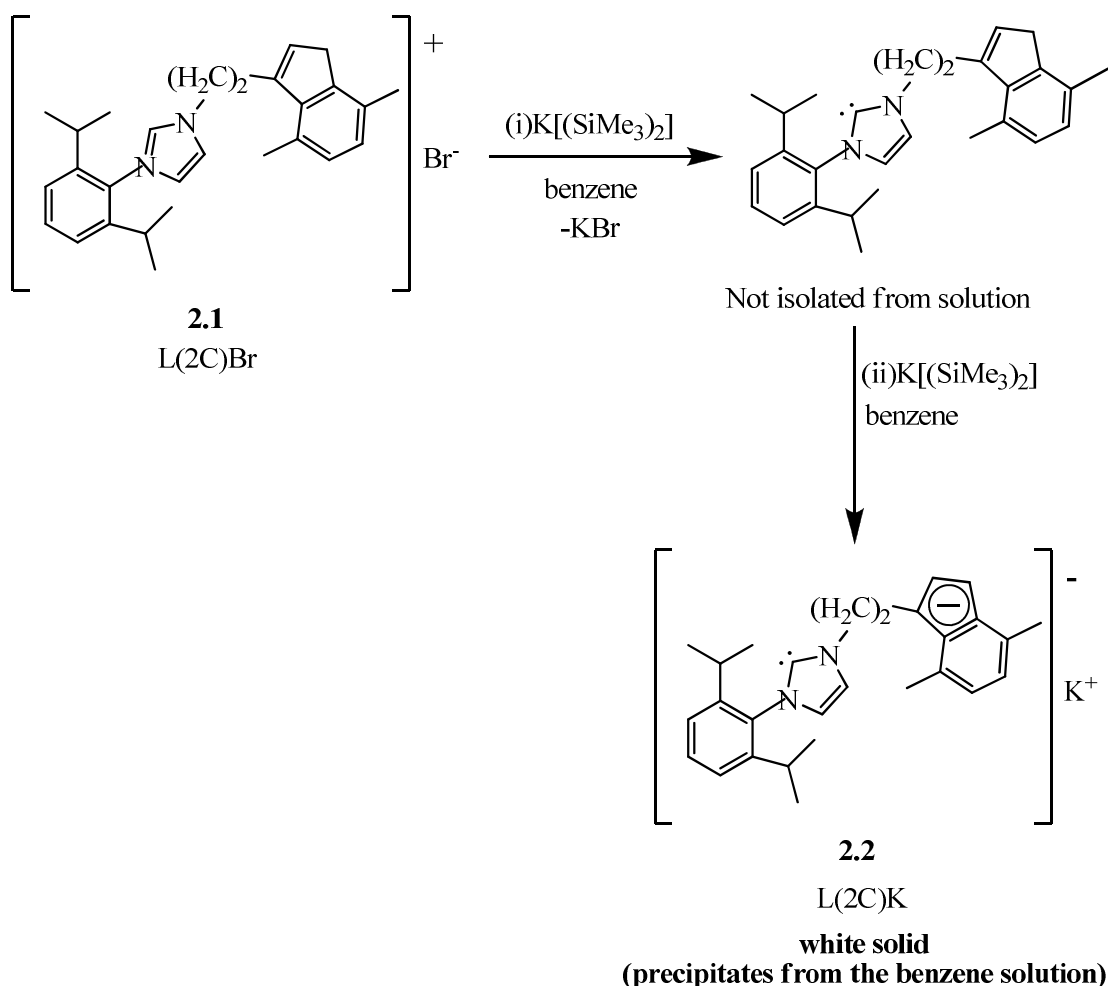
Scheme 2.1: Synthesis of potassium salt **2.2** (L(2C)K).

The new three-carbon bridge imidazolium salt L(3C)Br and potassium salt L(3C)K have been synthesised by using similar procedures as the two-carbon bridge analogues

and they have also been recently reported by our group. [95] Synthesis and characterisation data are discussed in detail below in this chapter.

Double deprotonation of imidazolium salts L(2C)Br and L(3C)Br using two equivalents of $K[N(SiMe_3)_2]$ in two steps in benzene gave the anionic ligand as the potassium salts L(2C)K and L(3C)K, respectively. These salts are capable of reacting with several chloride metal precursors such as $CrCl_3(THF)_3$ $CrCl_2(Me)(THF)_3$, $TiCl_2(N^tBu)(py)_3$ $CrCl_2$ and $ZrCl_4(THT)_2$ to give the desired complex and liberating insoluble KCl.

Zirconium and titanium complexes, as the potassium salts described above, have been fully characterised by NMR spectroscopy (^1H and ^{13}C NMR), elemental analysis (C, H and N) and single crystal X-ray diffraction. Structures of chromium complexes have been elucidated by single crystal X-ray diffraction and elemental analysis.

Some of the new complexes described in this chapter have been tested as catalysts in oligo/polymerisation of ethylene. The autoclave protocol and the catalytic results are described in detail at the end of this chapter.

2.2.1 Pro-ligand and Ligand Synthesis

The three-carbon-bridged L(3C)Br imidazolium salt pro-ligand **2.5** was successfully obtained in high yield by a method analogous to the previously reported for the synthesis of the two carbon bridge analogue, [94] involving quarterisation of 1-(3-bromopropyl)-4,7-dimethylindene with arylimidazole in refluxing dioxane for approximately 1 week.
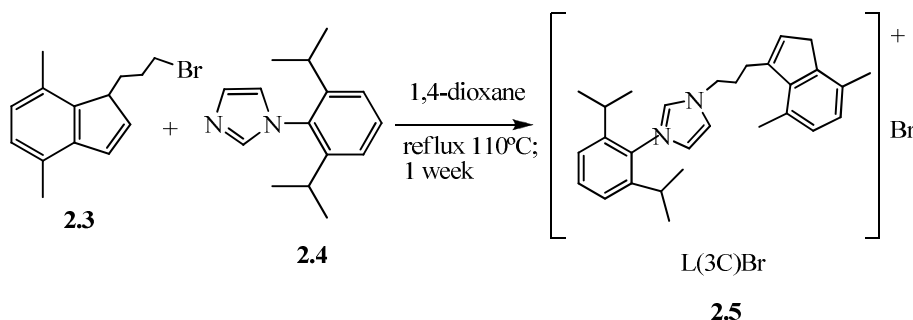
Scheme 2.2: Synthesis of the new three-carbon bridge imidazolium salt L(3C)Br, **2.5.**

Dioxane was removed under reduced pressure and the residue was crystallised from DCM/diethylether, dried azeotropically in toluene, washed with dry diethylether and

dried under vacuum. It was isolated as a white hygroscopic powder and characterized by analytical and spectroscopic methods.

In the ^{1}H- NMR spectrum of **2.5** in DCCl$_3$ the two methyl groups appear as two singlets and the methyl groups in the two isopropyl groups as two doublets.

The structure of the imidazolium salt **2.5** has been determined crystallographically and X-ray data are included at the end of this chapter. Crystal Maker diagram of **2.5** is shown in Figure 2.2. The C(13)-N(1) and C(13)-N(2) bond lengths [1.335(9)Å and 1.331(8) Å respectively] are within the expected range for imidazolium aromatic rings (1.349 Å and 1.326 Å for imidazole). [111]
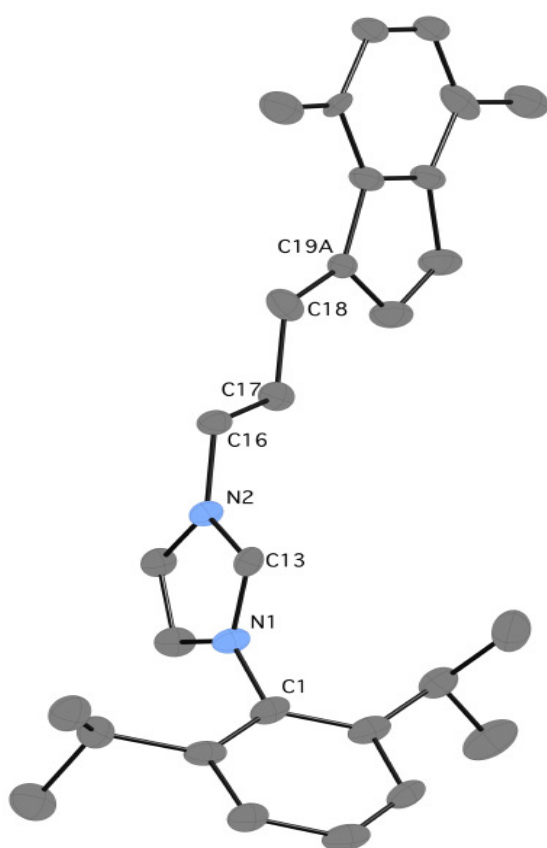
Bond Distances (Å)	
C(1)-N(1)	1.452(8)
C(13)-N(1)	1.335(9)
C(13)-N(2)	1.331(8)
C(16)-N(2)	1.476(8)
C(18)-C(19A)	1.494(8)
Angles (º)	
N(2)-C(13)-N(1)	108.4(6)
C(13)-N(1)-C(1)	123.8(6)
C(13)-N(2)-C(16)	125.6(6)

Figure 2.2: CrystalMaker representation of **2.5**. Counter anion Br⁻ and H atoms have been omitted for clarity. Thermal ellipsoids at 50% probability. Selected bond lengths (Å) and angles (deg) with estimated standard deviations are on the right of the diagram.

The deprotonation of the three-carbon bridge imidazolium salt by K[N(SiMe$_3$)]$_2$ was carried out in two steps in benzene as previously reported for the deprotonation of the

two-carbon bridge analogue L(2C)K.[94] This method gave good yield (70% overall) of the potassium salt L(3C)K . The two deprotonation steps are shown in Scheme 2.3.
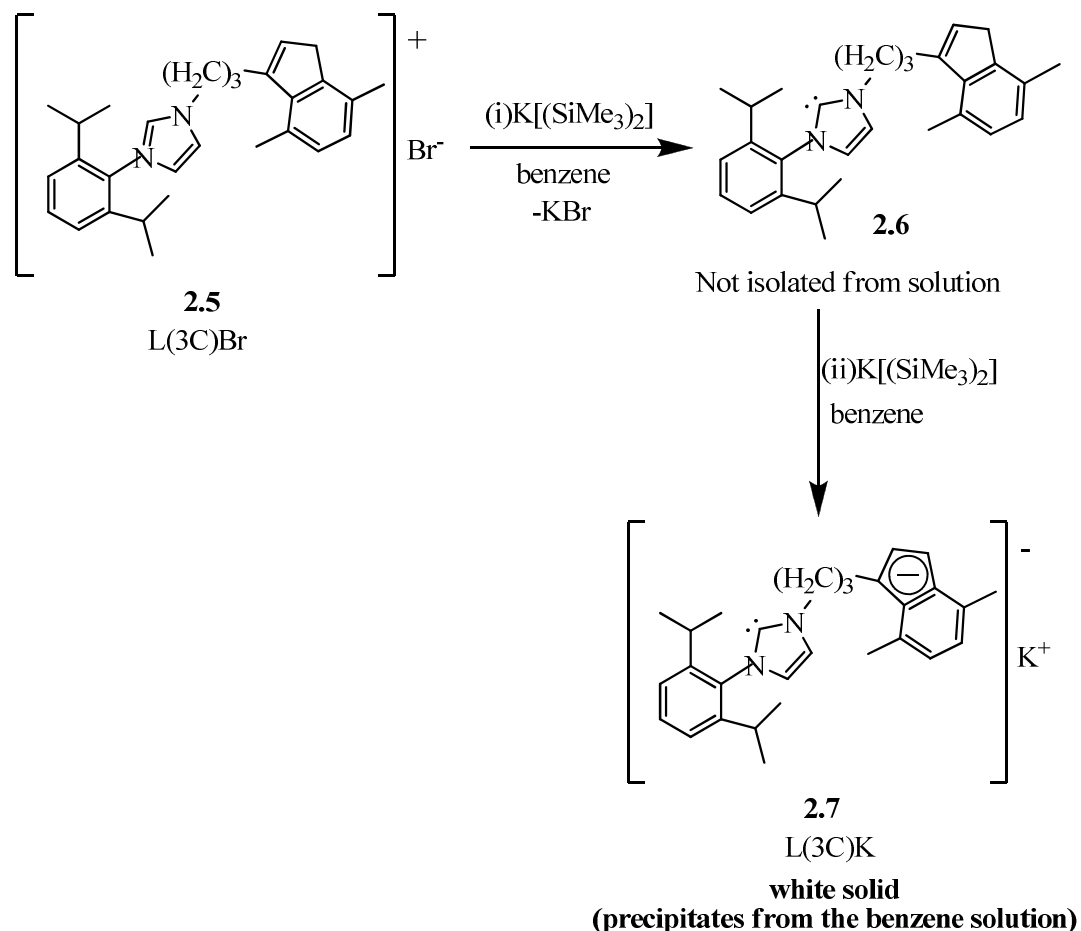
Scheme 2.3: Synthesis of potassium salt L(3C)K **2.7**.

The first equivalent of base removes exclusively the imidazolium proton, producing the neutral, benzene-soluble indenylpropyl-functionalized *N*-heterocyclic carbene. Separation of the insoluble potassium halides from the crude reaction mixtures was followed by treatment with a second equivalent of $KN(SiMe_3)_2$ to give the benzene-insoluble potassium indenylpropyl-NHC after deprotonation of the five-membered ring of the indene system. The potassium salt L(3C)K was isolated by filtration as an analytically pure, extremely air-sensitive powder, soluble in polar non-protic solvents such as pyridine and THF. The observed order of deprotonation of the two C-H acidic sites (imidazolium proton and 5-membered ring of the indene system) is the reverse of the expected order based on the known thermodynamic pKa of the C-H acids involved (Bordwell pKa values for methylindene and dialkylimidazolium salts in DMSO are 22.4 and 24.0, respectively).[112] This may be due to the kinetic nature of the products formed under the employed deprotonation conditions.

45

As was the case in the imidazolium bromide precursor **2.5**, the two methyl groups appeared as two singlets and the methyl groups in the two isopropyl groups as two doublets. The carbene carbon signal appears in the $^{13}C\{^1H\}$ NMR spectrum at 212.5 ppm which indicates that the carbon atom is quite unshielded in comparison with the equivalent carbon atom in imidazolium salts.

2.2.2 Indenyl-Functionalised *N*-Heterocyclic Carbene Titanium and Zirconium Complexes

The potassium salts **2.2** and **2.7** serve as convenient reagents for the introduction of the ligand to a variety of early transition metals. For example, reaction of L(2C)K and L(3C)K and with Ti(NBut)Cl$_2$(py)$_3$ in THF gave good yields of the titanium complexes **2.8** and **2.9**, respectively, which were characterized by spectroscopic, analytical, and diffraction methods.

n=2, **2.2**
n=3, **2.7**

n=2, **2.8**
n=3, **2.9**

Scheme 2.4: Synthesis of the new two- and three-carbon-bridged Ti (IV) complexes **2.8** and **2.9**.

The low molecular symmetry of the titanium complexes **2.8** and **2.9** was shown in the ^{1}H-NMR spectra of both complexes. The methyl groups of the isopropyl and indenyl groups are diastereotopic, as well as the methylene protons of the bridge.

The carbene carbon NHC signal in the $^{13}C\{^1H\}$ NMR spectrum was observed at 196.7 ppm for the two-carbon bridge **2.8**, slightly shielded relative to the potassium salt **2.2**. In contrast, the carbene carbon NHC signal for the three carbon bridge complex **2.9** could not be observed due to the limited solubility of the complex in C$_6$D$_6$, in which it is inert. There is no NMR evidence of dissociation of the NHC in hydrocarbon solvents.

Complexes **2.8** and **2.9** were crystallised by cooling petrol and toluene solutions, respectively. CrystalMaker representations of **2.8** and **2.9** are shown in Figures 2.3

and 2.4, respectively. The complexes adopt a distorted tetrahedral geometry with the indenyl centroid occupying one coordination site. The Ti-C(NHC) bond lengths [2.227(4) Å in **2.8** and 2.226(2) Å in **2.9**] are slightly shorter than the observed for other NHC titanium(IV) imido complexes [2.290(6) Å and 2.297(3) Å]. [113]

The difference between the endocyclic angle N(2)-C(13)- Ti and exocyclic angle N(1)-C(13)-Ti is 10° for **2.8** and 6.8° for **2.9**. The smallest value is in agreement with the reduced strain in the bridge imposed by the 3 carbon bridge tethered functionality in complex **2.9**.

The *tert*-butyl imido group is deviating slightly from linearity in both complexes and leads to a distortion of the bonding of the indenyl system to the Ti, with the C atoms opposite the imido group being more distant from the metal [(C(18), C(21) and C(22) in **2.8** and C(19), C(20) and C(23) in **2.9**]. However, the hapticity of the five-membered rings in both complexes is still best described as 5.

The Ti=N bond lengths [1.705(3) Å for **2.8** and 1.703(2) Å for **2.9**] are similar to the Ti=N bond length in the starting material Ti(=N^{t}Bu)Cl$_2$Py$_3$ [1.705(3) Å] and other imido compounds such as Ti(=NPh)Cl$_2$Py$_3$ [1.714(2) Å] and Ti(=Np-Tol)Cl$_2$Py$_3$ [1.705(4) Å]. [114]
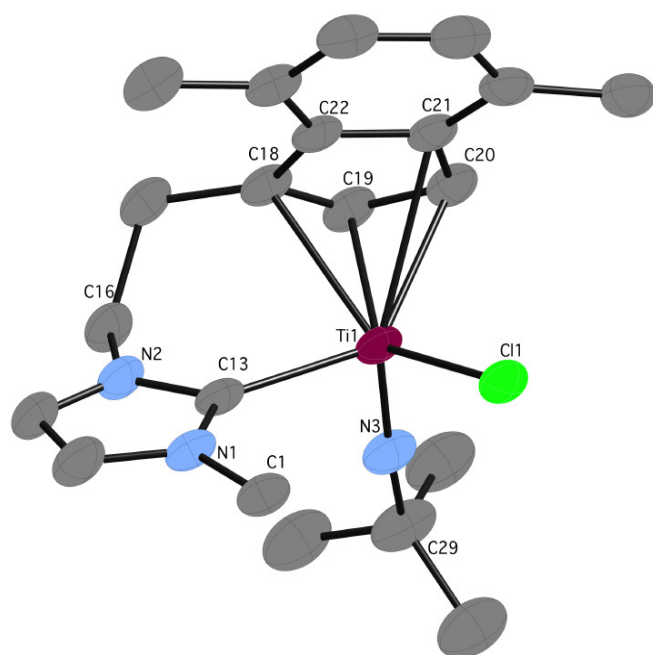
Bond Distances (Å)	
Cl(1)-Ti(1)	2.3209(10)
N(3)-Ti(1)	1.705(3)
C(13)-Ti(1)	2.227(4)
C(13)-N(1)	1.362(4)
C(13)-N(2)	1.365(4)
C(18)-Ti(1)	2.439(3)
C(19)-Ti(1)	2.360(3)
C(20)-Ti(1)	2.353(4)
C(21)-Ti(1)	2.538(3)
C(22)- Ti(1)	2.572(3)
Angles (º)	
C(29)-N(3)-Ti(1)	169.0(3)
C(13)-Ti(1)-N(3)	98.39(14)
C(13)-Ti(1)-Cl(1)	103.14(9)
Ti(1)-C(13)-N(1)	133.8(2)
Ti(1)-C(13)-N(2)	123.9(2)

Figure 2.3: CrystalMaker representation of the structure of **2.8**. Thermal ellipsoids at 50% probability. Hydrogen atoms and 2, 6-DiPP on N1, except the *ipso* carbon atom, have been omitted for clarity. Selected bond lengths (Å) and angles (deg) with estimated standard deviations on the right of the diagram.

Bond Distances (Å)	
Cl(1)-Ti(1)	2.3168(7)
N(3)-Ti(1)	1.703(2)
C(13)-Ti(1)	2.226(2)
C(13)-N(1)	1.367(3)
C(13)-N(2)	1.353(3)
C(19)-Ti(1)	2.439(3)
C(20)-Ti(1)	2.497(2)
C(21)-Ti(1)	2.353(2)
C(22)-Ti(1)	2.323(2)
C(23)- Ti(1)	2.520(2)
Angles (º)	
C(30)-N(3)-Ti(1)	171.07(18)
C(13)-Ti(1)-N(3)	95.88(9)
C(13)-Ti(1)-Cl(1)	102.22(6)
Ti(1)-C(13)-N(1)	131.54(17)
Ti(1)-C(13)-N(2)	124.60(16)

Figure 2.4: CrystalMaker representation of the structure of **2.9**. Thermal ellipsoids at 50% probability. Hydrogen atoms and 2, 6-DiPP on N1, except the *ipso* atom, have been omitted for clarity. Selected bond lengths (Å) and angles (deg) with estimated standard deviations on the right of the diagram.

Reaction of the L(3C)K with $ZrCl_4(THT)_2$ (THT = tetrahydrothiophen) in THF gave complex **2.10** in good yield; it was isolated as a yellow air-sensitive analytically pure material by extraction wit DCM and filtration of the solution through Celite.

Complex **2.10** is soluble in THF and DCM and insoluble in toluene, diethyl ether and petrol. Attempts at the crystallisation of **2.10** were made by layering DCM and THF solutions with diethyl ether and petrol, respectively, but no crystals were isolated.
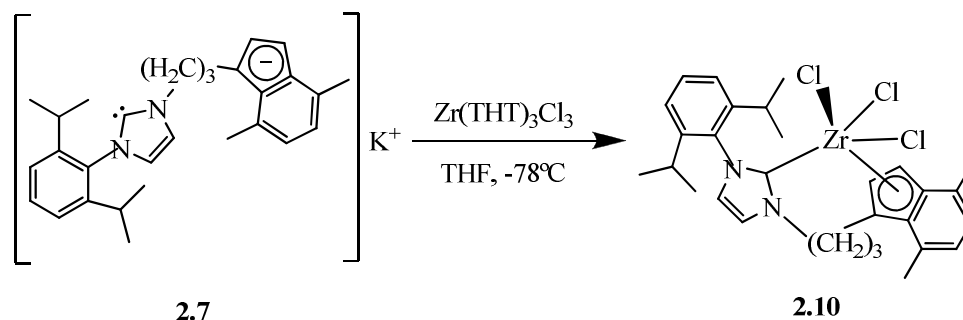
Scheme 2.5: Synthesis of the Zr(IV) complex **2.10**.

Although purification of **2.10** was carried out by extraction into dichloromethane, long exposure times should be avoided (>1 day) with this solvent due to partial decomposition.

Complex **2.10** exhibits complicated ^{1}H NMR spectra in polar non-coordinating solvents (CD$_2$Cl$_2$, C$_6$D$_5$Cl) due to the low molecular symmetry in solution. The ^{1}H NMR spectra of **2.10** in CD$_2$Cl$_2$ and C$_6$D$_5$Cl show the methyl groups on the isopropyl and indenyl groups appearing as four doublets and two singlets, respectively. Bridge methylene protons are also inequivalent.

In the ^{13}C{^{1}H} NMR spectrum of **2.10** all backbone carbons are inequivalent. The signal due to the coordinated carbene carbon NHC is observed only in C$_6$D$_5$Cl at 190.1 ppm (free carbene is observed at 211 ppm for L(2C)K), supporting coordination of the Zr-C(carbene) under these conditions. There is no evidence of fluxionality in solution in CD$_2$Cl$_2$.

When complex **2.10** is dissolved in carefully dried pyridine, a rapid decomposition takes place. The final product could be identified spectroscopically as the imidazolium salt **2.5**. It is unclear what the origin of the proton is in this transformation, and monitoring of the reactions by NMR does not reveal the presence of any intermediates.

2.2.3 Indenyl-Functionalised *N*-Heterocyclic Carbene Chromium Complexes

Indenyl-Functionalised *N*-Heterocyclic Carbene Chromium(III) Dichloride Complexes

Reaction of the two- and three-carbon-bridged potassium salts **2.2** and **2.7** with CrCl$_3$(THF)$_3$ in THF gave in good yields the paramagnetic Cr(III) complexes **2.11** and **2.12** as air-sensitive, intense green powders.
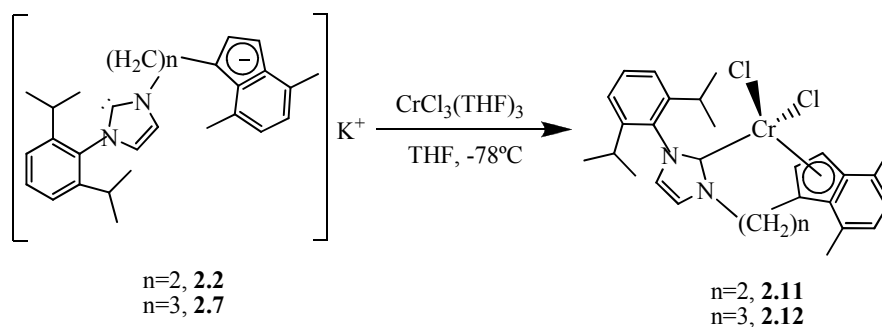
Scheme 2.6: Synthesis of the Cr(III) two- and three-carbon-bridge complexes **2.11** and **2.12**.

These chromium complexes were obtained analytically pure after extraction in DCM, filtration through Celite to remove the insoluble KCl and removal of the volatile components under reduced pressure.

Complexes **2.11** and **2.12** are both insoluble in diethyl ether and non-polar hydrocarbon solvents such as petrol and toluene. They have limited solubility in tetrahydrofuran and good solubility in dichlorometane.

Complexes **2.11** and **2.12** were both characterised by crystallographic techniques and the structures can be seen in Figures 2.5 and 2.6, below. They both adopt a distorted tetrahedral geometry. Cr-C(Indenyl) bond lengths, [between 2.227(2) Å and 2.326(2) Å] in **2.11** and [between 2.242(4) Å and 2.355(4)] Å in **2.12**, are similar to other dichloride cyclopentadienyl chromium(III) complexes in the literature.[115] Therefore the hapticity of the five-membered rings in both complexes is still best described as 5, with the indenyl centroid occupying one coordination site.

The Cr-C(NHC) bond lengths are 2.154(2) Å and 2.089(4) Å for **2.11** and **2.12** respectively which are within the observed range for other reported Cr-NHC complexes.[116]

The difference between the endocyclic and exocyclic angle is 6.16° and 5.9° for **2.11** and **2.12** respectively. These values agree with the reduced strain in the bridge imposed by the 3 carbon bridged tethered functionality in complex **2.12**, Although the difference is not as significant as in the titanium complexes **2.8** and **2.9** discussed above, possible due to larger size of Cr(III) compared to Ti(IV).

Bond Distances (Å)	
C(14)-Cr(1)	2.154(2)
Cl(2)-Cr(1)	2.2436(6)
Cl(3)-Cr(1)	2.3074(6)
C(14)-N(2)	1.303(3)
C(14)-N(1)	1.396(3)
Cr(1)-C(5)	2.326(2)
Cr(1)-C(6)	2.268(2)
Cr(1)-C(9)	2.286(2)
Cr(1)-C(10)	2.271(2)
Cr(1)-C(11)	2.227(2)
Angles (º)	
N(1)-C(14)-Cr(1)	126.994
N(2)-C(14)-Cr(1)	133.153
C(14)-Cr(1)Cl(2)	91.63(5)
C(14)-Cr(1)-Cl(3)	110.53(6)

Figure 2.5: CrystalMaker representation of complex **2.11**. Thermal ellipsoids at 50% probability. Hydrogen atoms and the isopropyl substituents of the 2, 6-DiPP group on N2 were omitted for clarity. Selected bond lengths (Å) and angles (deg) with estimated standard deviations on the right of the diagram.

Bond Distances (Å)	
Cr(1)-Cl(1)	2.2765(10)
Cr(1)-Cl(2)	2.3022(11)
Cr(1)-C(12)	2.089(4)
N(1)-C(12)	1.359(5)
N(2)-C(12)	1.367(5)
Cr(1)-C(6)	2.242(4)
Cr(1)-C(5)	2.249(4)
Cr(1)-C(4)	2.355(4)
Cr(1)-C(7)	2.243(4)
Cr(1)-C(8)	2.350(4)
Angles (º)	
Cr(1)-C(12)-N(1)	124.8(3)
Cl(2)-Cr(1)-C(12)	95.14(11)
Cl(1)-Cr(1)-C(12)	102.37(10)
Cr(1)-C(12)-N(2)	130.7(3)
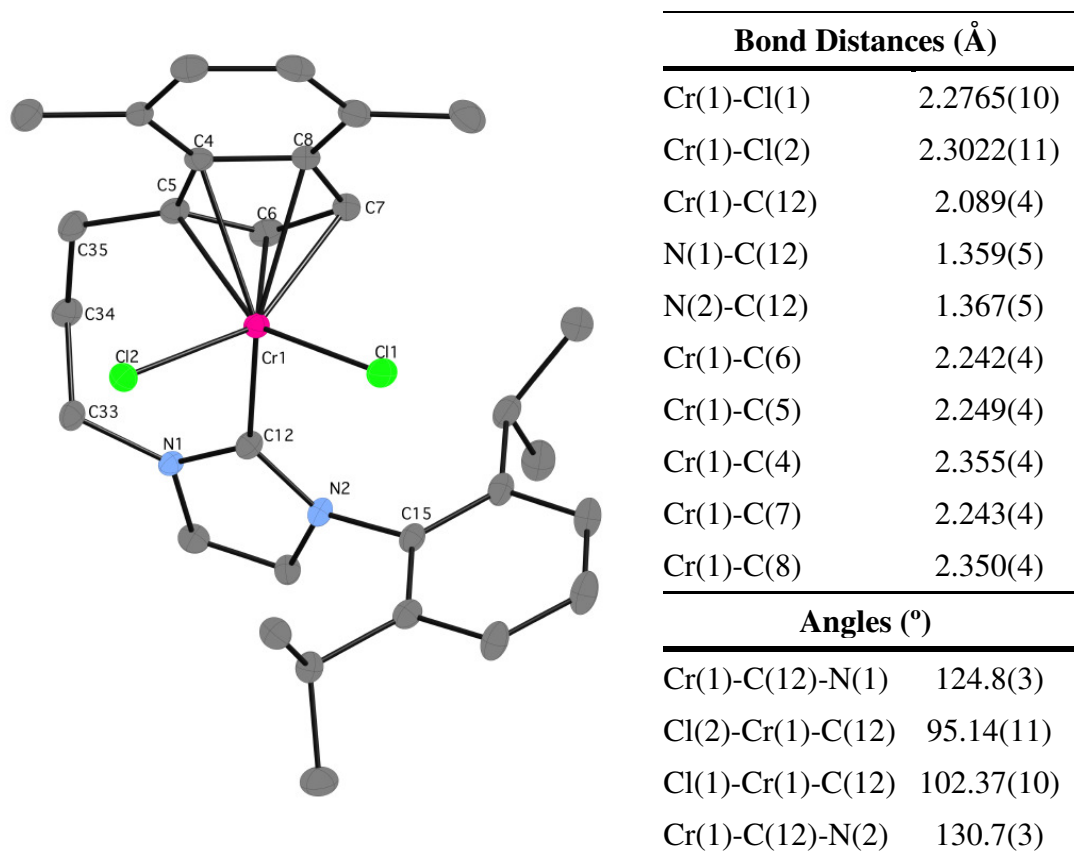
Figure 2.6: CrystalMaker representation of complex **2.12**. Thermal ellipsoids at 50% probability. Hydrogen atoms were omitted for clarity. Selected bond lengths (Å) and angles (deg) with estimated standard deviations on the right of the diagram.

Indenyl-Functionalised *N*-Heterocyclic Carbene Chromium (III) Alkyl Complexes

Chromium alkyl complexes are interesting since they can be the precursors of alkyl chromium cations. These species can act as the homogeneous analogues of chromium-based heterogeneous catalysts, which are used commercially, such as the Phillips [117] and the Union Carbide catalyst. [118]

In 1991 Theopold reported a class of cationic alkyl complexes of chromium (III) which catalysed the polymerization of ethylene and thus serve as homogeneous model compounds for commercial catalysts based on chromium. An example is shown in Figure 2.7. [119]

2.13
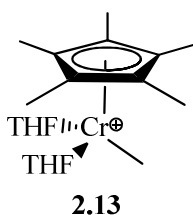
Figure 2.7: Alkyl chromium cation by Theopold catalytically active for the polymerisation of ethylene.

Some alkyl chromium(III), neutral and cationic, compounds have been synthesised bearing indenyl-functionalised NHC ligand and the results are discussed below. Alkyl cationic complexes, which can be synthesised from alkyl neutral complexes, are considered of great interest for this project due to the fact that they might act as activator-free catalyst in the oligo/polymerisation of ethylene.

The reaction of chromium dichloride complex **2.11** with diphenyl magnesium was carried out in cold tetrahydrofuran. Extraction with cold dichloromethane, filtration trough Celite to remove the magnesium salts and removal of the volatile components under reduced pressure gave the analytically pure complex **2.14** as an air sensitive purple powder in good yield.
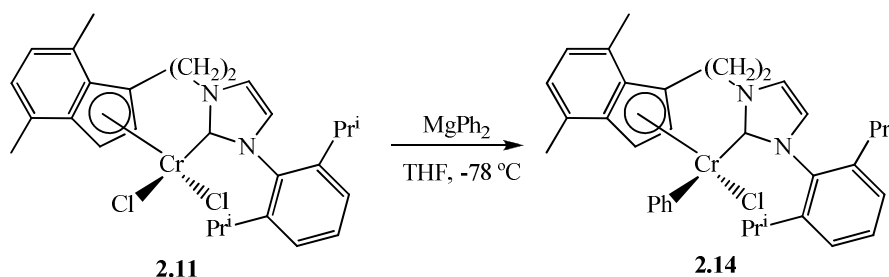
Scheme 2.7: Synthesis of the Cr(III) complex **2.14**.

A concentrated solution in toluene was cooled at -30 ℃ for 1 week to afford red-purple crystals of **2.14**. This complex was insoluble in diethyl ether and petrol, but soluble in toluene and very soluble in dichloromethane, although prolonged exposure time (>1 day) to the latter led to decomposition. Complex **2.14** was stored at -30 ℃ for to avoid decomposition although it is fairly stable at room temperature for short periods of time. It was characterised by X-ray crystallographic techniques and the structure can be seen in Figure 2.8.

Complex **2.14** adopts distorted tetrahedral geometry with the indenyl 5-membered ring centroid occupying one position. The Cr-C(indenyl) bond lengths [between

54

2.214(6) Å and 2.386(6) Å] are within the expected values for chromium compounds in the literature; [115] thus the hapticity of the five-membered ring is still better described as 5.

The Cr-C(NHC) [2.100(5)Å] and the Cr-C(Ph) [2.050(6) Å] bond lengths are within the observed range for other Cr-C(NHC) [116] and Cr-C(Ph) [120] complexes reported in the literature.

Bond Distances (Å)	
Cr(1)-Cl(2)	2.2840(19)
Cr(1)-C(29)	2.050(6)
Cr(1)-C(1)	2.100(5)
C(1)-N(1)	1.373(6)
C(1)-N(2)	1.331(7)
Cr(1)-C(6)	2.266(6)
Cr(1)-C(7)	2.214(6)
Cr(1)-C(8)	2.264(6)
Cr(1)-C(9)	2.382(5)
Cr(1)-C(14)	2.386(6)
Angles (º)	
Cl(2)-Cr(1)-C(1)	103.48(16)
C(1)-Cr(1)-C(29)	94.9(2)
C(1)-N(1)-C(17)	129.2(4)
C(1)-N(2)-C(4)	125.4(5)

Figure 2.8: CrystalMaker representation of complex **2.14**. Thermal ellipsoids at 50% probability. Hydrogen atoms and the isopropyl substituents of the 2, 6-DiPP group on N1 were omitted for clarity. Selected bond lengths (Å) and angles (deg) with estimated standard deviations on the right of the diagram.

Attempts to synthesise the indenyl-functionalised *N*-heterocyclic carbene chromium diphenyl complex were made. Using two equivalents of MgPh$_2$ gave only the indenyl-functionalised *N*-heterocyclic carbene chromium chloride phenyl complex **2.14** described above, leaving the remaining diphenyl magnesium unreacted. This could be due to steric factors.

The reaction of two- and three-carbon bridge potassium salts **2.2** and **2.7** with Cr Cl$_2$(Me)(THF)$_3$ was carried out in THF at low temperature due to chromium alkyls are known to be thermally unstable, [132] specially in solution. Extraction with cold toluene, filtration through Celite and removal of the volatile components under reduced pressure gave the analytically pure complexes as air sensitive deep purple powders.

Scheme 2.8: Synthesis of two- and three-carbon bridge chromium complexes **2.15** and **2.16**.

Complexes **2.15** and **2.16** were both insoluble in petrol and diethyl ether but soluble in THF, toluene and dichloromethane, although long exposure to the latter (>1 day) resulted in decomposition. The solids were kept at -30 ℃ due to slow decomposition at room temperature.

The structure of the two-carbon-bridged analogue **2.15** was determined crystallographically and is shown in Figure 2.9. Complex **2.15** adopts distorted tetrahedral geometry with the indenyl 5 membered ring centroid occupying one position. The Cr-C(indenyl) bond lengths are between 2.273(6) Å and 2.341(7) Å, therefore the hapticity of the five-membered ring is still better described as 5 as other chromium complexes reported in the literature. [115] The Cr-C(carbene) distance [2.070(6) Å] is comparable with literature values, [116] as well as the Cr-C(CH$_3$) bond length [2.150(6) Å]. [76(a), 115, 119]

Bond Distances (Å)	
Cr(1)-C(29)	2.150(6)
Cr(1)-Cl(2)	2.287(2)
Cr(1)-C(1)	2.070(6)
C(1)-N(1)	1.354(8)
C(1)-N(2)	1.378(8)
Cr(1)-C(6)	2.273(6)
Cr(1)-C(7)	2.341(7)
Cr(1)-C(12)	2.320(6)
Cr(1)-C(13)	2.292(7)
C(1)-N(14)	2.292(7)
Angles (º)	
C(1)-Cr(1)-Cl(2)	103.88(17)
C(1)-Cr(1)-C(29)	94.2(2)
Cr(1)-C(1)-N(1)	134.3(4)
Cr(1)-C(1)-N(2)	122.5(4)

Figure 2.9: CrystalMaker representation of complex **2.15**. Thermal ellipsoids 50% probability. Hydrogen atoms omitted for clarity. 2, 6-DiPP group on N1 (diisopropyl groups have been omitted for clarity). Selected bond lengths (Å) and angles (deg) with estimated standard deviations on the right.

Chloride methyl complexes **2.15** and **2.16** were thought to be especially interesting as precursors to methyl chromium cations, which are believed they might act as activator free-catalysts in the oligomerisation of ethylene, since alkyl cationic chromium complexes are postulated to be the active species in this catalytic process.

Attempts to abstract the chloride to form these interesting species were made by using $B(C_6F_5)_3$ $[B[(3,5-(CF_3)_2-C_6H_3)]_3]$. No reaction took place, even upon stirring the reaction mixture for several days at room temperature.

Alternatively the reaction of complexes **2.15** and **2.16** with $NaB[(3,5-(CF_3)_2-C_6H_3)]_4$ in dichloromethane/tetrahydrofuran was completed after three days at room temperature, when the purple solution turned dark green. The solution was filtered through Celite, concentrated under vacuum and layered with petrol to afford green

needles. X-ray diffraction methods and elemental analysis confirmed that, surprisingly, the methyl group was abstracted from the metal instead of the chloride.
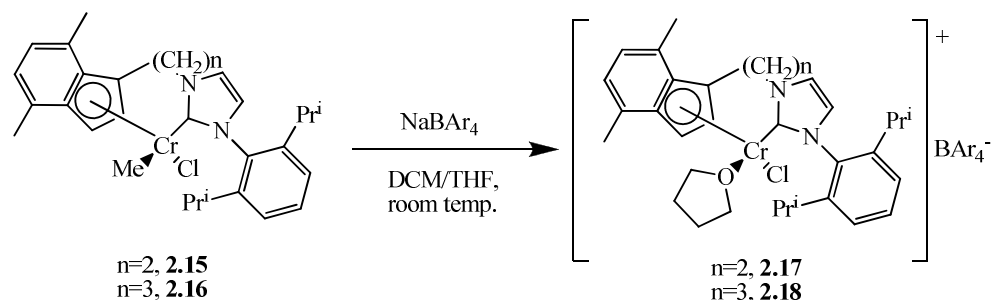
Scheme 2.9: Two- and three-carbon bridge chloride cations **2.17** and **2.18**. R= 3,5-$(CF_3)_2$-C_6H_3.

Analytically pure green powders of chloride cations **2.17** and **2.18** were isolated in good yields, 60% and 50% respectively, after filtration of the solution thought Celite and removal of the volatile components under reduced pressure.

The reason why chloride cations are formed instead of methyl cations is not clear. Methyl cations are known to be very reactive species; they might be formed in the first place and react quickly with DCM to form the more stable cations **2.17** and **2.18**.

A likely reaction that also may have formed cations **2.17** and **2.18** is shown in scheme 2.10.
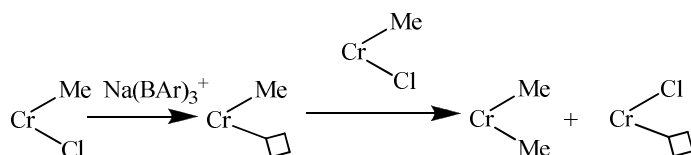
Scheme 2.10: Proposed route for the formation of **2.17** and **2.18**.

Isolation of intermediates to corroborate this hypothesis was attempted; the reaction was stopped before the solution turned green, filtrated through Celite concentrated and layered with petrol, but no crystals were obtained.

The cations **2.17** and **2.18** are both insoluble in petrol, toluene and diethyl ether and soluble in dichloromethane and tetrahydrofuran. The structure of the three carbon bridge cation **2.18** was determined crystallographically and is shown in Figure 2.10.

Cation **2.18** adopts distorted tetrahedral geometry with the indenyl 5 membered ring centroid occupying one position. The Cr-C(indenyl) [between 2.199(8) Å and 2.386(10) Å] and the Cr-O(THF) [2.060(6) Å] bond lengths are similar to the

58

corresponding distances for Cr(III) cations reported by Theopold.[119] Therefore the hapticity of the five-membered ring is still better described as 5. Although this geometry is slightly more distorted that in the complexes discussed above.

The Cr-C(carbene) distance is 2.062(10) Å which is within the observed range in the literature. [116] The Cr-Cl bond length [2.260(3) Å] is slightly shorter than in the dichloride chromium complexes **2.11** and **2.12** which might be for the cationic nature of **2.18.** The tetrarylborate counter ion exhibits no close contacts to the chromium complex, and its bond distances and angles are not exceptional.

Bond Distances (Å)	
Cr(1)-O(1)	2.060(6)
Cr(1)-C(33)	2.062(10)
Cr(1)-Cl(1)	2.260(3)
Cr(1)-C(51)	2.199(8)
Cr(1)-C(52)	2.300(9)
Cr(1)-C(57)	2.386(10)
Cr(1)-C(58)	2.295(10)
Cr(1)-C(59)	2.272(9)
C(33)-N(1)	1.347(11)
C(33)-N(2)	1.386(11)
Angles (º)	
C(33)-Cr(1)-O(1)	106.7(3)
C(33)Cr(1)-Cl(1)	92.6(3)
Cr(1)-C(33)-N(1)	133.7(6)
Cr(1)-C(33)-N(2)	123.9(6)
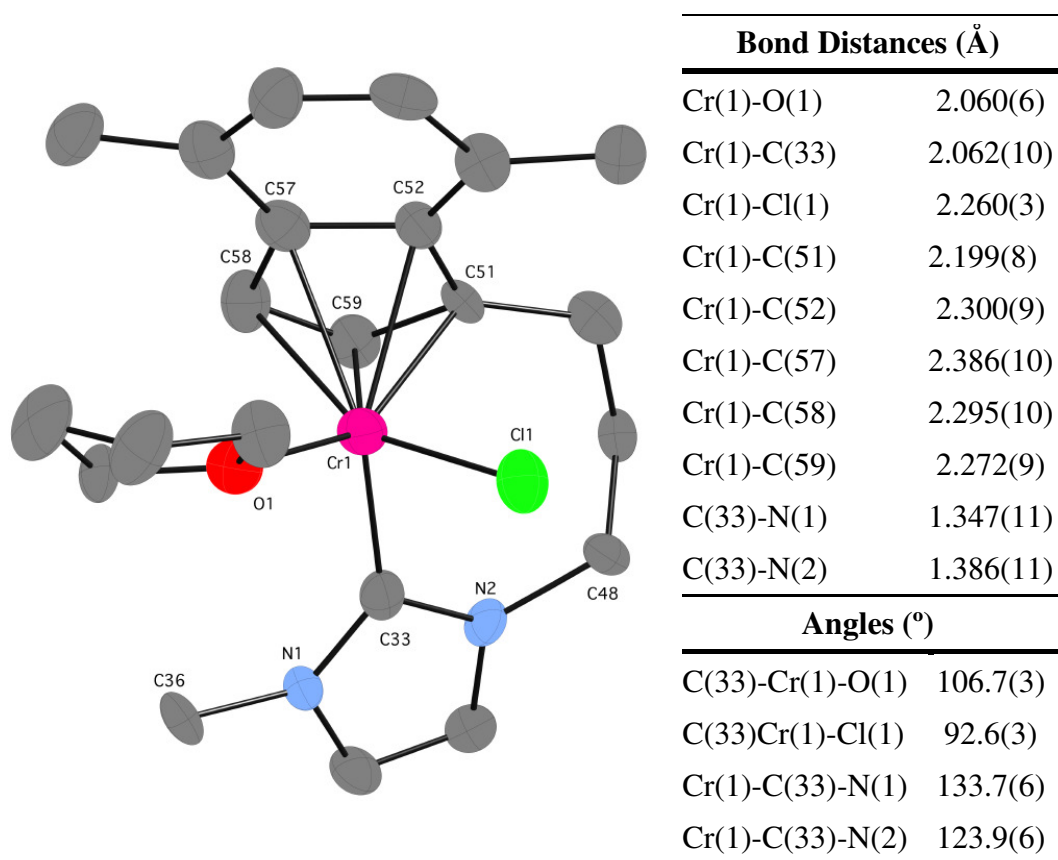
Figure 2.10: CrystalMaker representation of complex **2.18**. Thermal ellipsoids at 50% probability. Hydrogen atoms, Counter anion [B[(3,5-(CF$_3$)$_2$-C$_6$H$_3$)]$_4$] and 2, 6-DiPP group, except the *ipso* carbon atom, on N1 have been omitted for clarity. Selected bond lengths (Å) and angles (deg) with estimated standard deviations on the right of the diagram.

Another interesting aspect of the synthesis of **2.17** and **2.18** is that a small amount of THF is necessary for the cation formation. The hard THF ligand coordinates to the chromium stabilizing the complex.

The reaction of **2.15** and NaB[(3,5-(CF$_3$)$_2$-C$_6$H$_3$)]$_4$ under the same conditions as those used to isolate **2.17** and **2.18**, but in the absence of THF, gave the dichloride complex **2.11** co-crystallised with NaB[(3,5-(CF$_3$)$_2$-C$_6$H$_3$)]$_4$ shown in Figure 2.11 below. This fact help to corroborate that methyl groups can be substitute by chloride groups by long exposure times of methyl chromium complexes with DCM. Comproportionation could be another possible route to form **2.11** and indenyl-functionalised *N*-heterocyclic carbene chromium dimethyl complex.
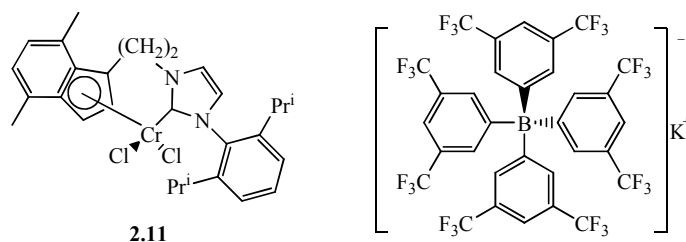
Figure 2.11: Complex **2.11** and NaB[(3,5-(CF$_3$)$_2$-C$_6$H$_3$)]$_4$.

Attempts to isolate indenyl-functionalised *N*-heterocyclic carbene chromium methyl cations by carrying out the reaction of **2.15** and **2.16** with NaB[(3,5-(CF$_3$)$_2$-C$_6$H$_3$)]$_4$ in an inert solvent such as toluene were made. Starting materials and decomposition products were isolated showing no reaction after a few days stirring at room temperature.

The dibenzyl chromium complex **2.19** was prepared by reaction of the dichloride chromium complex **2.11** with freshly prepared dibenzyl magnesium solution in diethyl ether. [133] The reaction was carried out at low temperature in THF.
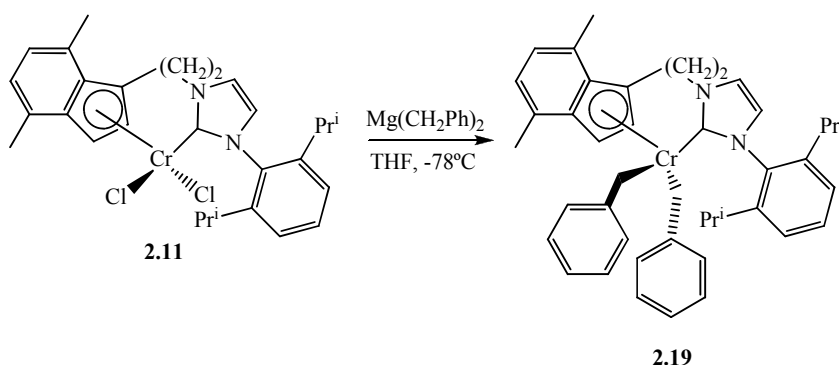
Scheme 2.11: Synthesis of the dibenzyl chromium complex **2.19**.

The green solution turned violet following the addition of the Grignard and it was kept at -25 ºC for two days to complete the reaction. Removal of the volatile components under reduced pressure, extraction of the residue in cold toluene,

filtration of the violet solution through Celite gave a clear solution which was dried under vacuum. The purple residue was washed with cold petrol and the dibenzyl chromium complex **2.19** was isolated as a purple, analytically pure powder after drying under vacuum. This compound was kept at -30 ºC because it decomposes at room temperature. Complex **2.19** is insoluble in petrol, diethyl ether and soluble in toluene and THF. It was characterised by X-ray crystallographic techniques and the structure is depicted in Figure 2.12.

Complex **2.19** adopts a distorted tetrahedral geometry with the indenyl 5-membered ring centroid occupying one position. The Cr-C(indenyl) [between 2.274(5) Å and 2.415(5) Å] bond lengths are comparable with the complexes that have been discussed above and in the literature.[115] Therefore the hapticity of the five-membered ring is still better described as 5. The Cr-C(carbene) distance is 2.119(5) Å which is within the observed range in the literature. [116] The distance between the metal atom and the carbon atoms of the benzyl groups [2.164(4) Å and 2.113(5) Å] are characteristic of carbon-chromium σ-bonds and they are within the observed range for several chromium complexes in the literature. [76(a), 119, 115]
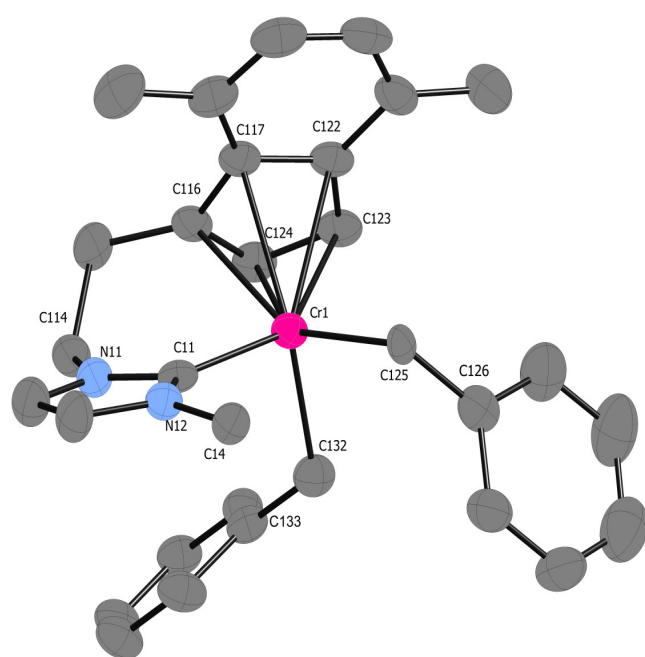
Bond Distances (Å)	
Cr(1)-C(11)	2.119(5)
Cr(1)-C(125)	2.164(4)
Cr(1)-C(132)	2.113(5)
Cr(1)- C(116)	2.299(5)
Cr(1)-C(117)	2.385(5)
Cr(1)-C(122)	2.415(5)
Cr(1)-C(123)	2.290(5)
Cr(1)-C(124)	2.274(5)
C(11)-N(11)	1.357(6)
C(11)-N(12)	1.377(6)
Angles (º)	
C(11)-Cr(1)-C(132)	95.8(2)
C(11)-Cr(1)-C(125)	104.66(18)
Cr(1)-C(11)-N(11)	121.7(3)
Cr(1)-C(11)-N(12)	135.0(4)
Cr(1)-C(132)C-(133)	120.43(4)
Cr(1)-C(125)C(126)	114.88(4)

Figure 2.12: CrystalMaker representation of complex **2.19**. Thermal ellipsoids at 50% probability. Hydrogen atoms and 2, 6-DiPP group, except the *ipso* carbon atom, on N12 were omitted for clarity. Selected bond lengths (Å) and angles (deg) with estimated standard deviations on the right of the diagram.
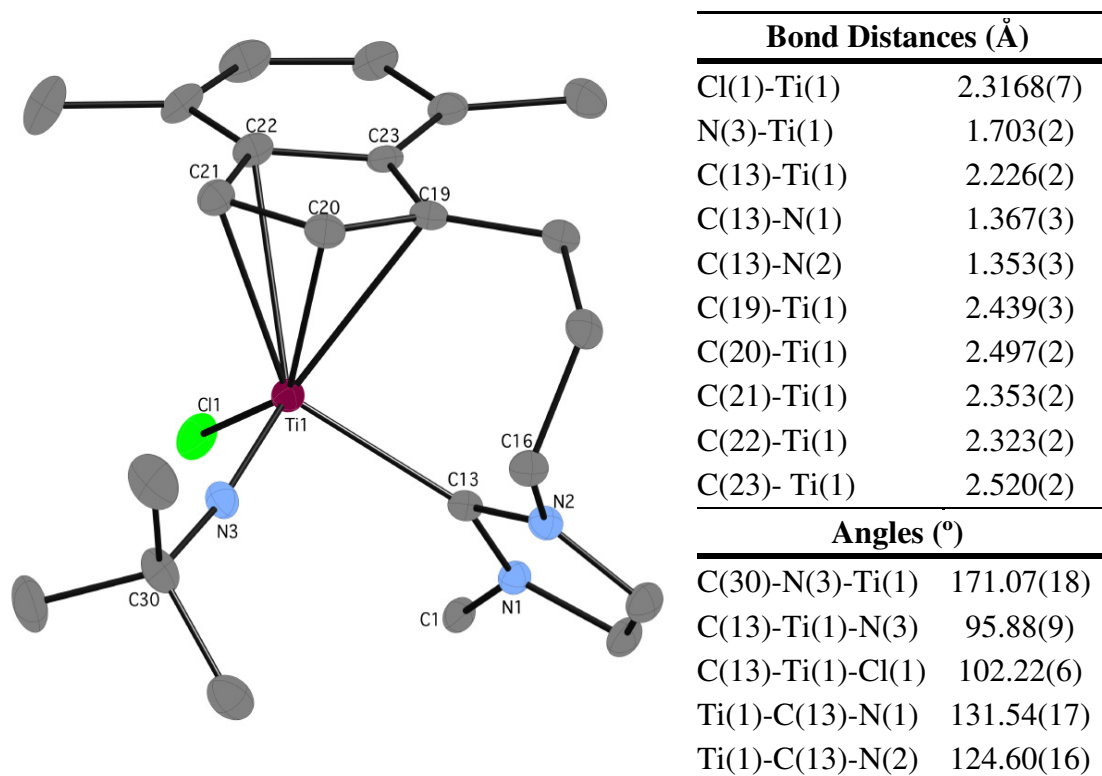
As was discussed above in the introduction of this chapter (section 2.1), the formation of alkyl chromium cations complexes is of great interest. Dibenzyl chromium complex **2.19** was reacted with $H(Et_2O)_2BAr_4$ ($B[(3,5-(CF_3)_2-C_6H_3)]_4$)134 at -78 ºC in tetrahydrofuran. The reaction mixture turned immediately from violet to orange.
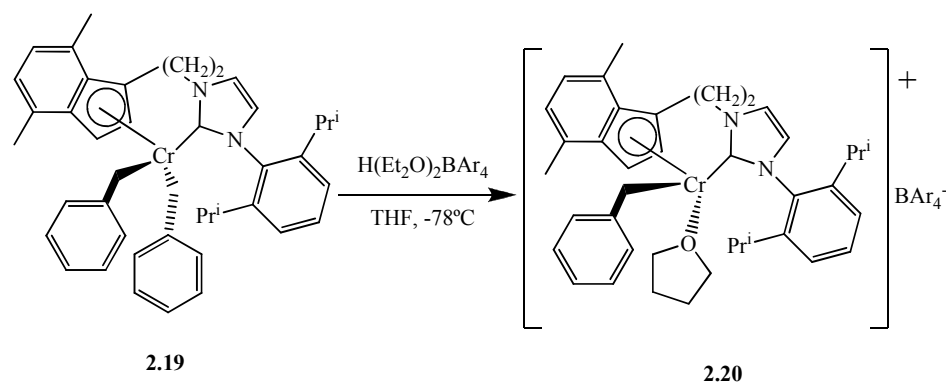
Scheme 2.12: Synthesis of the benzyl chromium cation **2.20**.

Volatile components were removed under reduced pressure and the residue washed with cold petrol. The benzyl cation **2.20** was isolated as fine orange needles after crystallisation of a very concentrated solution in diethylether at low temperature (-30 °C). This complex is extremely thermally unstable and all the steps, including crystal selection, for X-ray single crystal data collection were carried out at low temperature.

This data set is not very good due to partial decomposition during the data collection. However it provides unequivocal identity and approximate metrical data for the cation **2.20**. The diffraction pattern showed a lot of background diffuse scattering probably from disordered solvent, and the Bragg reflections were very broad. As a result the structure, especially the thermal parameters, is of low quality.

Complex **2.20** adopts a distorted tetrahedral geometry as was the case for all the chromium complexes discussed above. The Cr-C(NHC) distance [2.130(5) Å] is within the observed range in the literature. [116] The Cr-C(indenyl) [between 2.214(3) Å and 2.3755(18) Å] and the Cr-O(THF) [2.070(2) Å] bond lengths are similar to the corresponding distances for the Cr(III) cations reported by Theopold. [119] Cr-C(benzyl) bond length [2.111(4) Å] is similar to the starting material so it also comparable with the values found in the literature for Cr-C σ-bonds. [76(a), 119, 115]

THF is coordinated to the Cr as in the cation **2.18** discussed above. Therefore the coordination of this solvent might play an important role stabilizing chromium (III) cation complexes with this ligand system.

It would have been very interesting to test the cation **2.20** in catalysis for oligo/polymerisation of ethylene as free activator catalyst. However it is extremely

thermally unstable, which makes it impossible to handle without immediate decomposition at the conditions of the polymerisation studies.

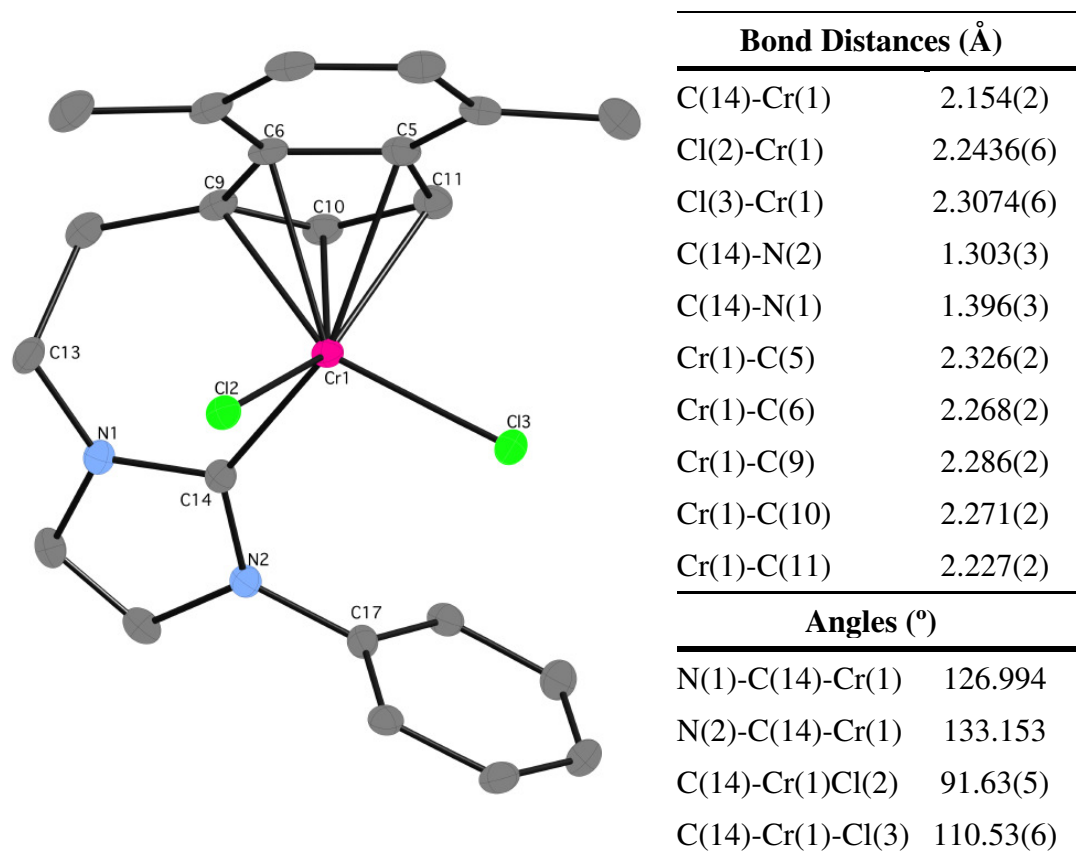| Bond Distances (Å)	
Cr(1)-C(16)	2.130(5)
Cr(1)-C(29)	2.111(4)
Cr(1)-O(1)	2.070(2)
Cr(1)-C(1)	2.3755(18)
Cr(1)-C(6)	2.362(2)
Cr(1)-C(7)	2.261(4)
Cr(1)-C(8)	2.214(3)
Cr(1)-C(9)	2.245(3)
C(16)-N(1)	1.364(5)
C(16)-N(2)	1.350(5)
Angles (º)	
C(16)-Cr(1)-O(1)	104.33(12)
C(16)-Cr(1)-C(29)	96.02(17)
Cr(1)-C(16)-N(1)	118.4(3)
Cr(1)-C(16)-N(2)	135.2(3)
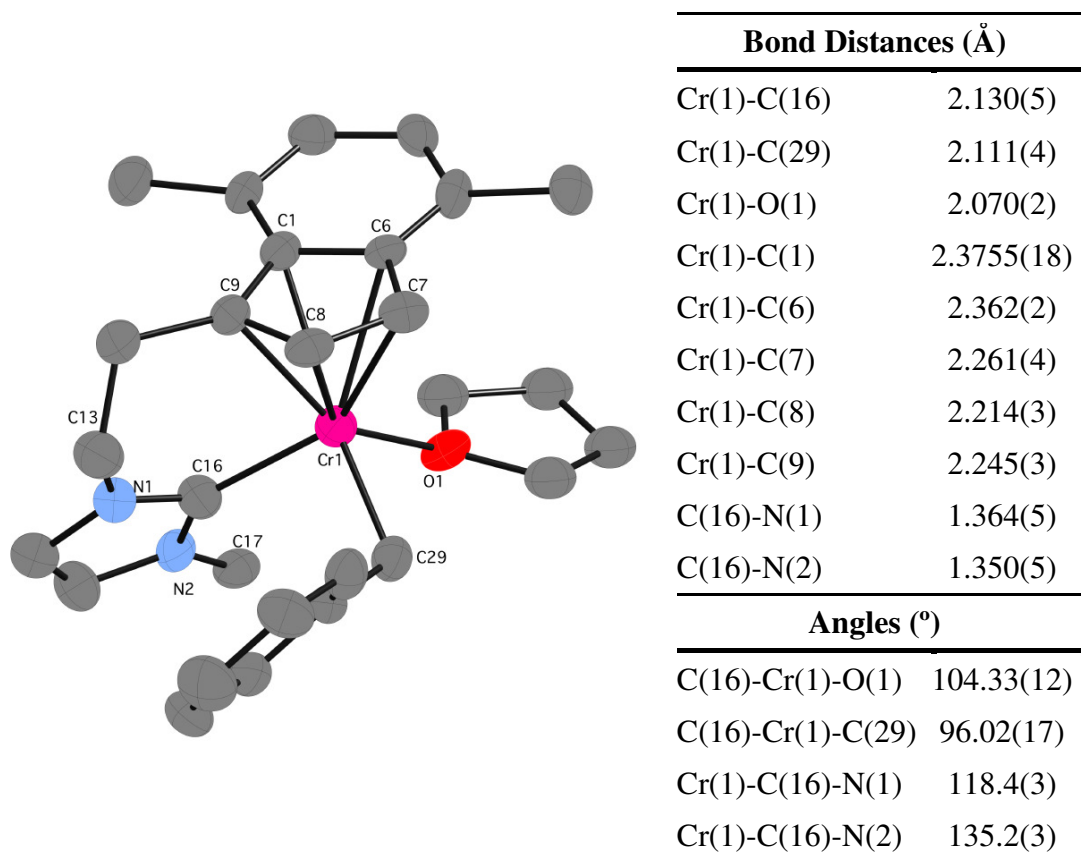
Figure 2.13: CrystalMaker representation of complex **2.20**. Thermal ellipsoids at 50% probability. Hydrogen atoms and 2, 6-DiPP group, except the *ipso* carbon atom, on N2 were omitted for clarity. Selected bond lengths (Å) and angles (deg) with estimated standard deviations on the right of the diagram.

Indenyl-Functionalised *N*-Heterocyclic Carbene Chromium(II) Complexes

A brief exploration to Cr(II) chemistry using the two carbon bridge indenyl-N-heterocyclic carbene ligand was made. $CrCl_2$ was reacted with the potassium salt L(2C)K **2.2** in cold tetrahydrofuran. The lime coloured suspension turned into olive green. This solution was concentrated and cooled at -30 ºC for one week to afford a good crop of light brown crystals of complex **2.21**. This compound was insoluble in petrol, diethyl ether and toluene; it was slightly soluble in tetrahydrofuran and unstable in dichloromethane. Complex **2.21** is extremely air- and moisture-sensitive and it reacted over long periods of time (>2 days) in tetrahydrofuran at room temperature to give the dimerised compound **2.22** in which an oxygen atom acts as a bridge. Complexes **2.21** and **2.22** are shown is Scheme 2.13 below.

Complex **2.22** was crystallised by slow vapour diffusion of petrol into a concentrated solution of **2.21** in THF.
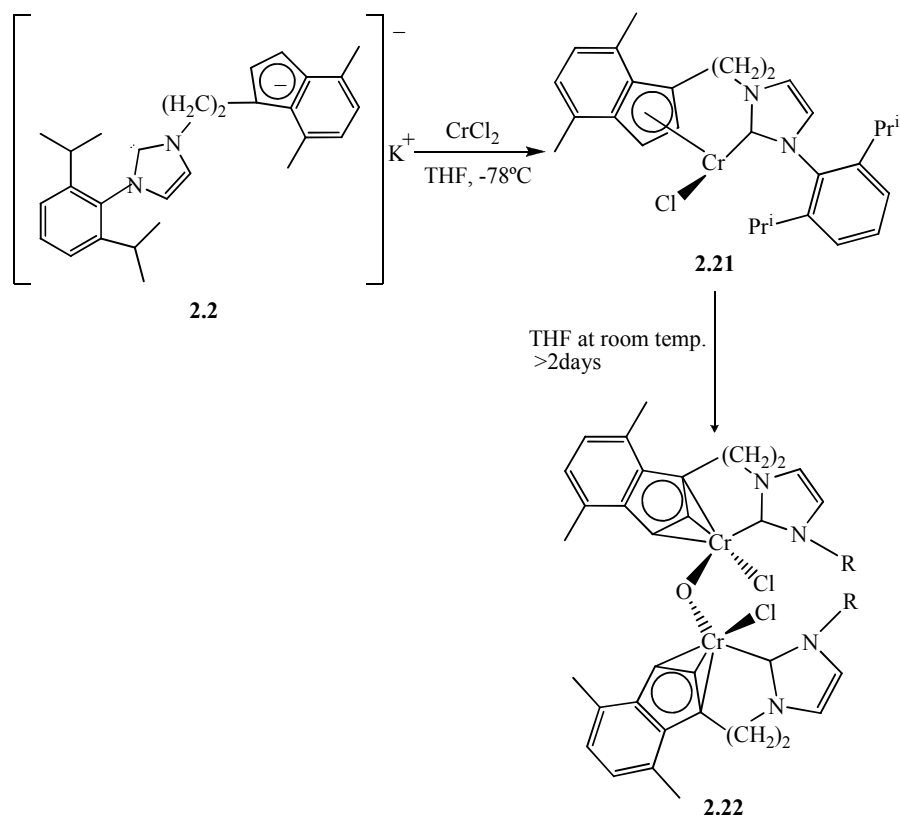
Scheme 2.13: Synthesis of the Cr(II) complexes **2.21** and **2.22**.

Cr(II) complexes **2.21** and **2.22** were both characterised by X-ray diffraction techniques and they are shown in Figures 2.14 and 2.15.

Complex **2.21** adopts a distorted triangular planar structure. The indenyl 5-membered ring centroid occupies one coordination site in complex **2.21.** The Cr-C(indenyl) bond lengths [between 2.259(4) Å and 2.395(4) Å] are similar to the corresponding distances for the Cr(III) complexes discussed above and also are in the range observed in the literature for Cr(II) complexes.[121] The Cr-C(NHC) distance is 2.085(4) Å, which is within the observed range in the literature. [116] The C-Cl bond length [2.2879(11) Å] is very similar to the Cr-Cl distances [between 2.2436(6) Å -2.3074(6) Å] found in dichloride Cr(III) complexes **2.11** and **2.12** discussed above.

Bond Distances (Å)	
Cr(2)-Cl(2)	2.2879(11)
Cr(2)-C(13)	2.085(4)
Cr(2)-C(2)	2.259(4)
Cr(2)-C(3)	2.395(4)
Cr(2)-C(8)	2.391(4)
Cr(2)-C(9)	2.302(5)
Cr(2)-C(10)	2.286(4)
C(13)-N(3)	1.365(5)
C(13)-N(4)	1.367(5)
Angles (°)	
Cl(2)- Cr(2)-C(13)	103.93(11)
Cr(2)-C(13)-N(3)	134.0(3)
Cr(2)-C(13)-N(4)	123.2(3)
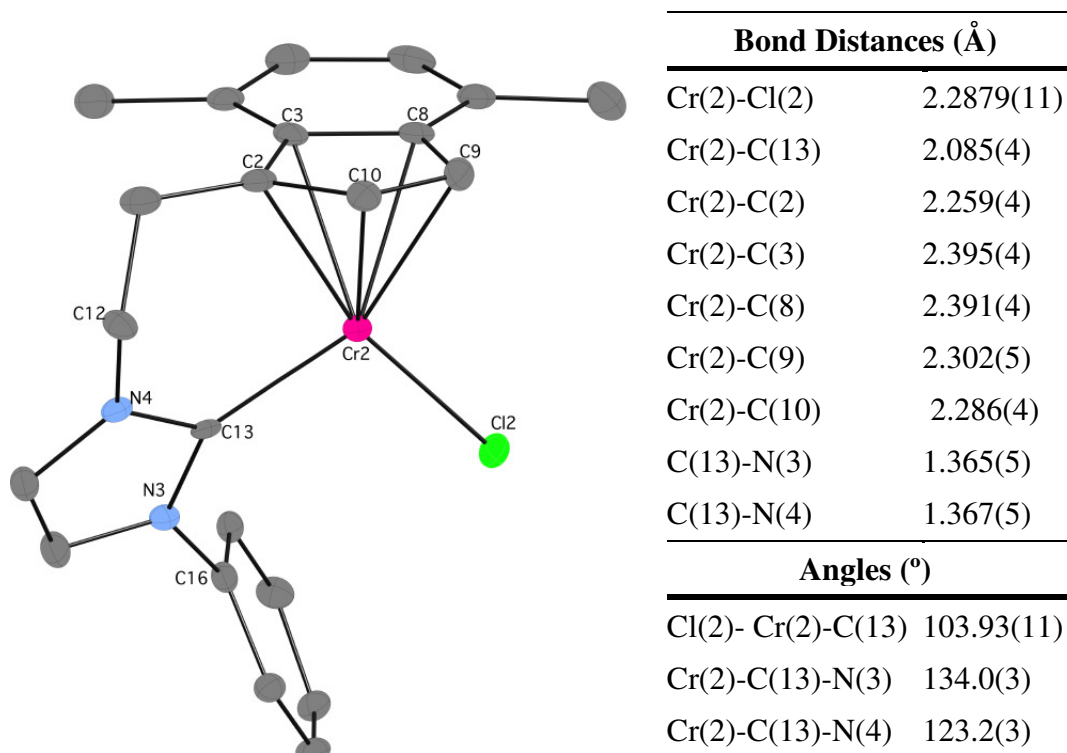
Figure 2.14: CrystalMaker representation of complex **2.21**. Thermal ellipsoids at 50% probability. Hydrogen atoms and diisopropyl substituents of the 2,6- DiPP group on N3 were omitted for clarity. Selected bond lengths (Å) and angles (deg) with estimated standard deviations on the right of the diagram.

Keeping a THF solution of complex **2.21** at room temperature for long periods of time (> 2days) results in the oxidation of **2.21** to give complex **2.22**. The mechanism of this oxidation is unknown, but it is thought that the oxygen atom might come from the THF.

Complex **2.22** adopts a distorted tetrahedral geometry around both equivalent chromium atoms, as all the complexes discussed above with this ligand. The Cr-C(indenyl) bond lengths [2.239(7) Å, 2.278(7) Å and 2.274(7) Å] are similar to the corresponding distances reported for Jolly in the literature for the η^3-indenyl ligand in the complex [(η^5-indenyl)(μ-η^3-indenyl)Cr]$_2$ [2.199(5) Å, 2.221(3) Å and 2.356(5) Å].[121] The distances between the Cr and the non-bonding carbon atoms of the 5 membered indenyl ring are 2.458 Å and 2.444 Å; therefore the hapticity of the five-membered ring is better described as 3 for complex **2.22.** The Cr-C(NHC) bond length [2.100(8) Å] is within the expected value, as well as the Cr-Cl bond distance.[116] An oxidation reaction from Cr(II) to Cr(III) has taken place for both

66

chromium atoms. There are not examples in the literature for organo-chromium compounds with a bridging oxygen between metal centres with this oxidation state, although the angle observed in **2.22** Cr(1)-O(1)-Cr(1)[148.1(7) º] is similar to the corresponding angle for the inorganic complex $(NH_3)_5$-Cr-O-Cr-$(NH_3)_5$ [154 º] reported in the literature. [122]

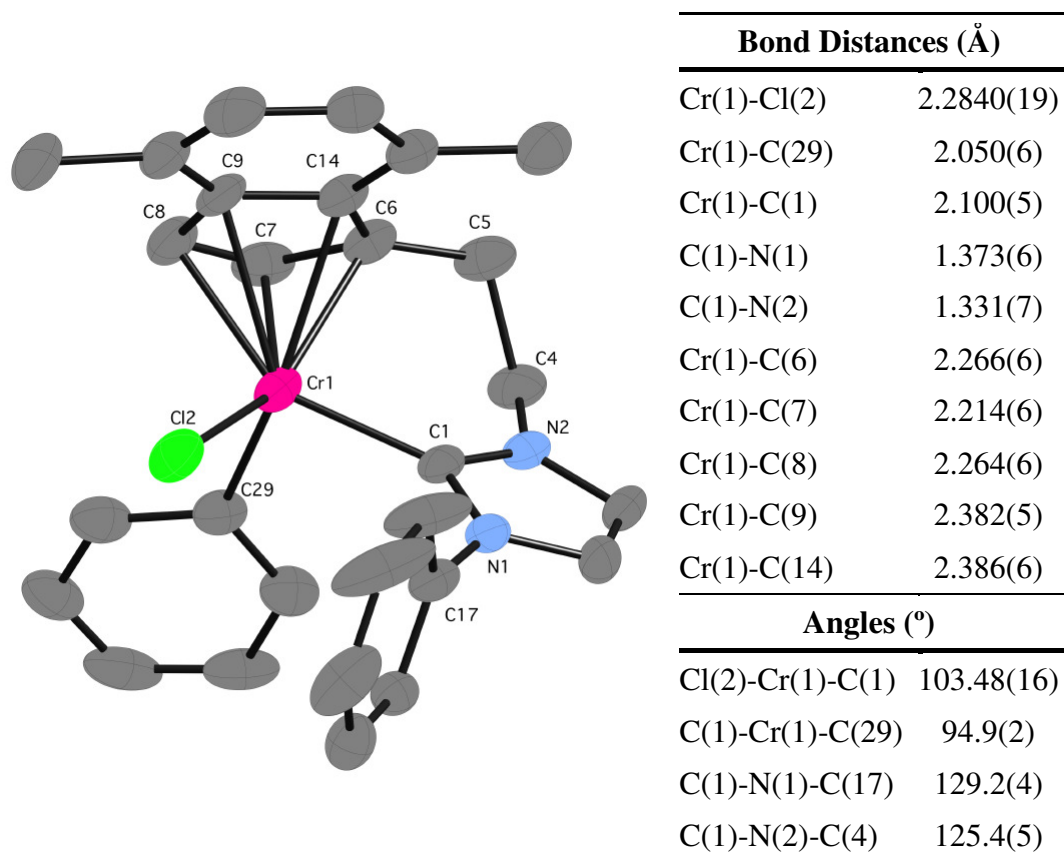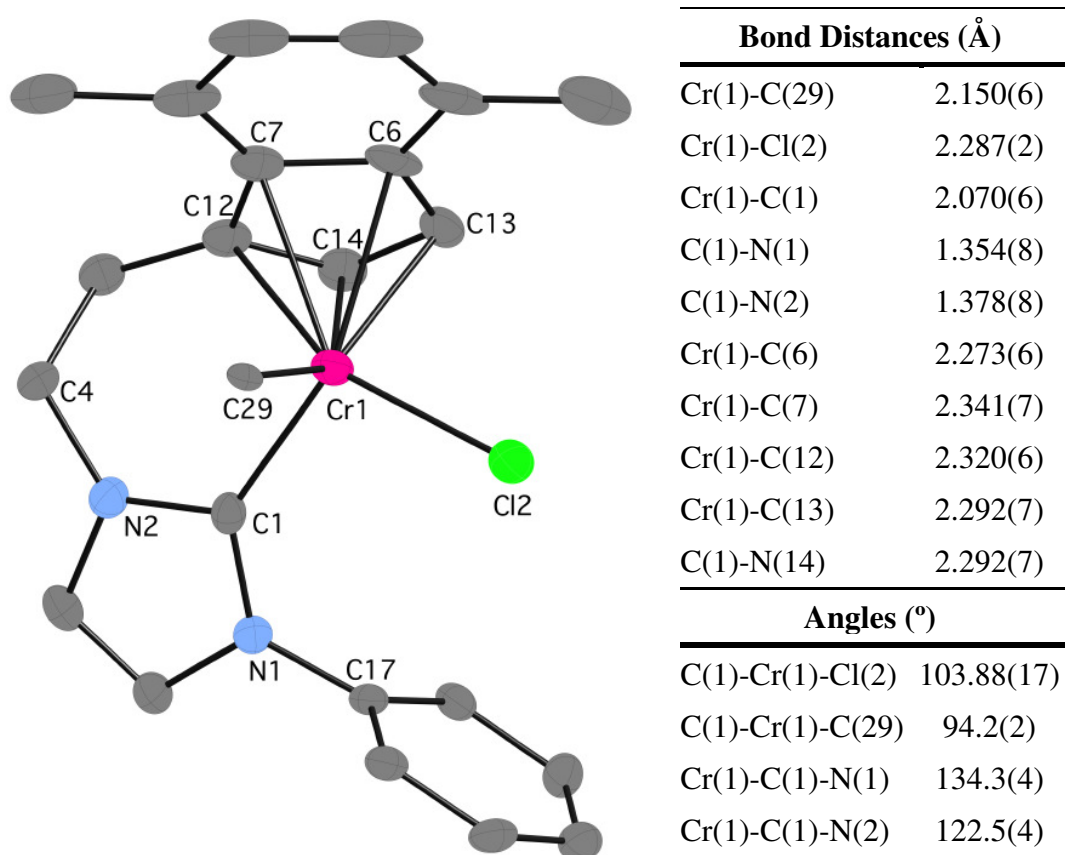| Bond Distances (Å)	
Cr(1)-Cl(1)	2.310(2)
Cr(1)-C(16)	2.100(8)
Cr(1)-C(9)	2.274(7)
Cr(1)-C(10)	2.239(7)
Cr(1)-C(11)	2.278(7)
C(16)N(1)	1.368(9)
C(16)-N(2)	1.358(9)
Cr(1)-O(1)	1.809(2)
Angles (º)	
C(16)-Cr(1)-Cl(1)	102.0(2)
Cr(1)-C(16)-N(1)	136.7(6)
Cr(1)-C(16)-N(2)	119.0(5)
O(1)-Cr(1)-Cl(1)	98.65(7)
O(1)-C(16)-Cr(1)	96.4(3)
Cr(1)-O(1)-Cr(1)	148.1(7)
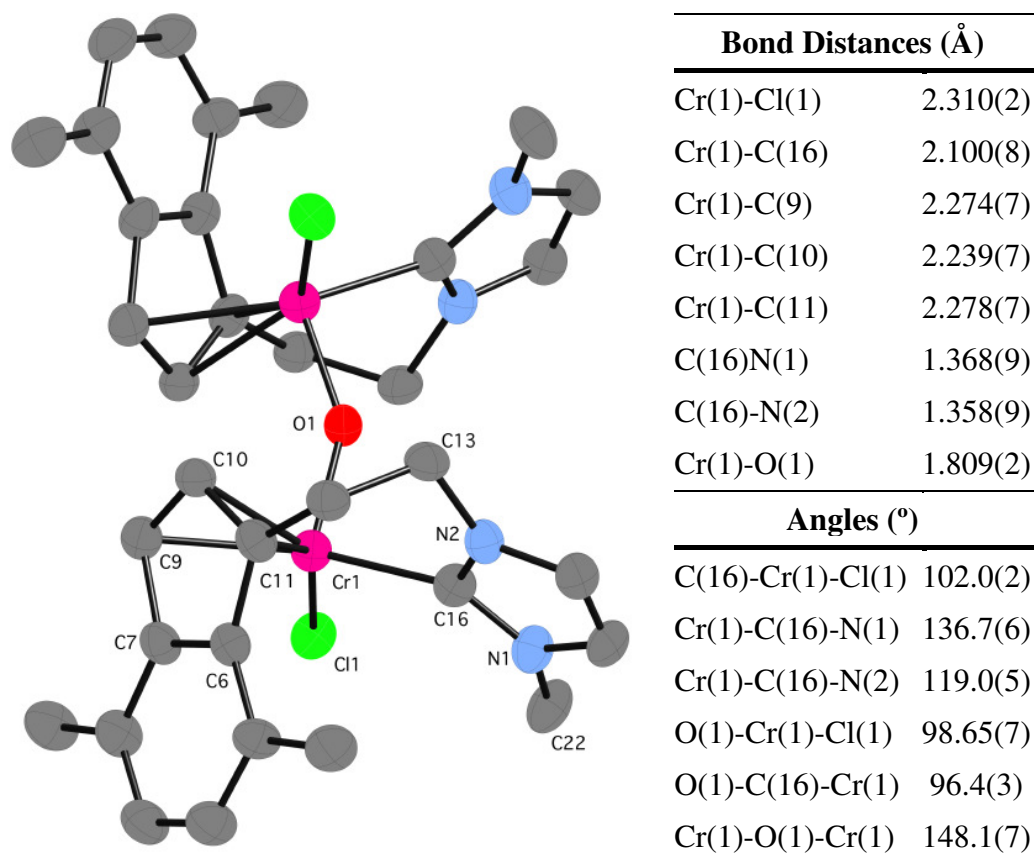
Figure 2.15. CrystalMaker representation of complex **2.22**. Thermal ellipsoids at 50% probability. Hydrogen atoms and 2, 6-DiPP groups, except the *ipso* carbons, on N1 were omitted for clarity. Selected bond lengths (Å) and angles (deg) with estimated standard deviations on the right of the diagram.

2.3 Catalytic Testing of Indenyl-Functionalised NHC Complexes in the Oligo/Polymerisation of Ethylene

The early transition metal complexes shown below in Figure 2.16 have been tested under different conditions in the oligo/polymerisation of ethylene. The results are summarised in Table 2.1 below.
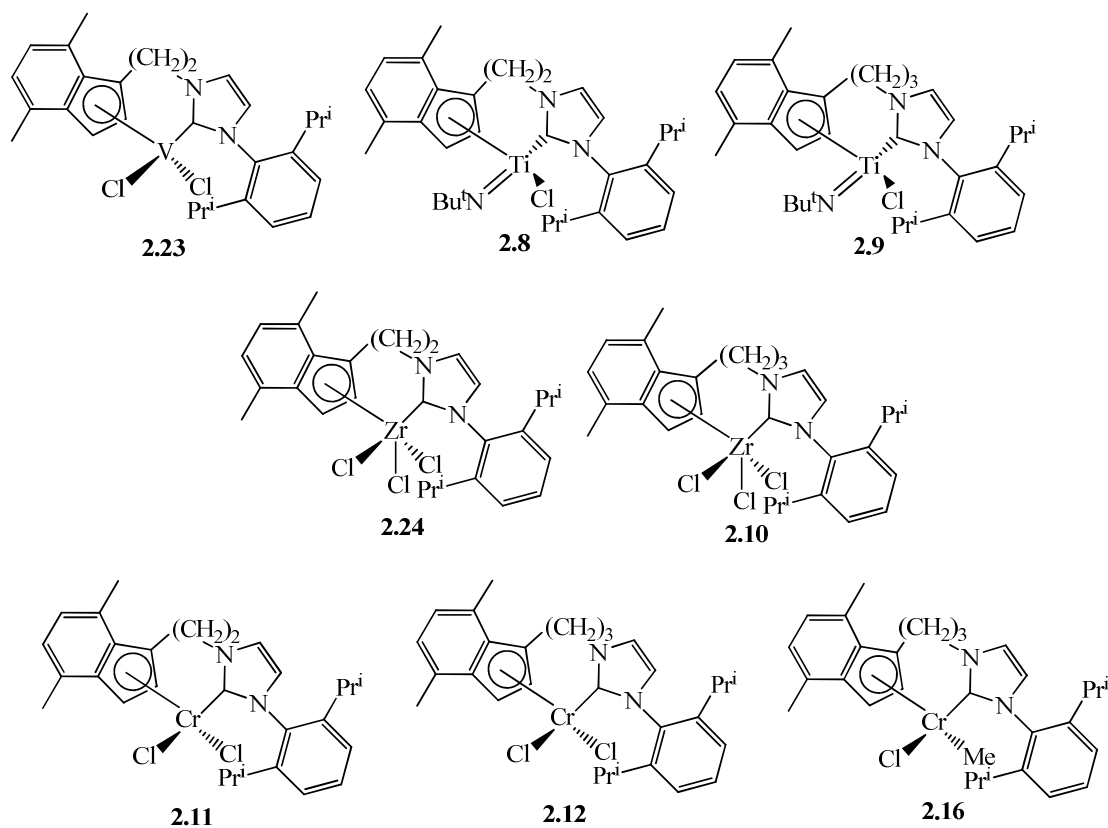
Figure 2.16: Complexes tested in the oligo/polymerisation of ethylene. The synthesis of vanadium complex **2.23** and two carbon bridge zirconium complex **2.24** were both reported by our group [95] and also included in Stephen Downing's thesis.

Pre-catalysts **2.8, 2.9, 2.10** and **2.24** were poorly active for systems based on zirconium and titanium; no obvious gas uptake could be detected in any run after the initial filling of the autoclave. However once the autoclave was opened polymer was recovered in all cases, also trace oligomers were detected in the liquid fraction by gas chromatography (see Table 2.1).

The formation of small oligomers such as butane (C4), hexane (C6) and octane (C8) was more important in the 40 bar test than the 8 bar test, but in both cases only C4

oligomers were formed with the zirconium and titanium pre-catalyst. The oligomerisation observed was Schulz-Flory.

Polymer was formed in all experiments carried out with the zirconium and titanium complexes. At higher pressures polymerisation is more important than oligomerisation as well as the activities of the pre-catalyst.

Pre-catalyst **2.23** was selective towards polymerisation and no trace of liquid products was detected. The activity of **2.23** was very good for a vanadium-based system, although the lifetimes were short. However it is impossible to ensure if the sort lifetime is inherent to the vanadium centre or is a consequence of entrapment of the active centre within the polymer due to all the tests carried out with pre- catalyst **2.23** produced sufficient polymer to stop stirring. One notable observation from all of the tests with this pre-catalyst relates to the nature of polymer formed. Normally polymer formation is random in that polymer adheres to all internal surfaces in a stringy or blocky form depending on the MW, however there is generally no 'order' to the formation. However, with pre-catalyst **2.23**, small, perfectly spherical balls of polymer formed (in addition to the random polymer) in all three tests (Figure 2.17). Dissection of the balls after recovery revealed a small metallic particle at the centre.

Figure 2.17: Spherical ball formed in the polymerisation of ethylene in experiment C4 (see table 12.1 for conditions).

As can be seen from the data in Table 2.1 all of the chromium pre-catalysts tested showed selectivity towards polymerization exclusively, for which the methylchloride chromium complex **2.16** was moderately active. Both dichloride chromium complexes showed higher activities than the methyl chromium analogue **2.16**, especially at high temperature and pressure. Non-liquid fraction was isolated in all the cases and it is suggested that ethylene uptake ceased due to encapsulation of the active

species in the polymer, and in several cases the stirring within the autoclave became inhibited.

Table 2.1: Results for the catalytic tests of the above complexes.

Experiment code/catalyst	t(min)	Activity (mol=)(mol M)-1hr-1	% liquid	% polymer	g polymer
C1/**2.24**	10	53,766	75.1	24.9	0.188
C2/**2.24**	10	32,087	5.4	94.6	2.838
C3/**2.23**	0.8	395,671	0	100	2.960
C4/**2.23**	2.1	480,712	0	100	2.360
C5/**2.23**	4.6	470,760	0	100	10.125
C6/**2.8**	10	32,701	83.8	16.2	0.057
C7/**2.8**	10	39,056	17.5	82.5	0.422
C8/**2.9**	10	28,093	96.0	4.0	0.010
C9/**2.9**	10	15,796	29.6	70.4	0.130
C10/**2.10**	10	12,115	95.9	4.1	0.010
C11/**2.10**	10	5,335	11.2	88.8	0.633
C12/**2.11**	51.1	65,752	0	100	7.850
C13/**2.11**	24.2	749.710	0	100	26.978
C14/**2.12**	18.8	157,916	0	100	9.925
C15/**2.12**	13.8	1,178,737	0	100	38.028
C16/**2.16**	40.9	112,298	0	100	10.738
C17/**2.16**	19.3	599,071	0	100	26.978

2.4 Towards the Synthesis of Pro-ligands with Imidazolium Linked to Cyclopentadiene or Tetramethylcyclopentadiene Moieties

2.4.1 Introduction

As was discussed in section 2.3, indenyl-functionalised *N*-heterocyclic carbene ligands have been proved to be suitable species for the formation of neutral and cationic bidentate complexes with early metals. Indenyl-functionalised *N*-heterocyclic carbene chromium and vanadium complexes showed selectivity towards ethylene polymerisation with moderate activities, and titanium and zirconium complexes are also catalytically active.

The synthesis of cyclopentadiene- and/or tetramethylcyclopentadiene-functionalised *N*-heterocyclic carbene ligands is considered to be of great interest for this project since they are analogues to the indenyl-functionalised *N*-heterocyclic carbene ligands discussed above. Structures and catalytic behaviours of cyclopentadiene- and/or tetramethylcyclopentadiene-functionalised *N*-heterocyclic carbene complexes would be compared with the new complexes reported earlier in this chapter. It would also provide an indication of how the steric hindrance of the Cp ring affects the catalytic behaviour of analogous complexes.

The following sections outline attempts that were made at tethering cyclopentadiene- and/or tetramethylcyclopentadiene-functionalised moieties to NHC functionalities. These proposed routes for the synthesis of cyclopentadiene- and/or tetramethylcyclopentadiene-functionalised *N*-heterocyclic carbene ligands and the methods used for the synthesis of their ligand precursors are described in detail. Although these routes were not proved to be successful some interesting intermediate ligands were synthesised and characterised for the first time.

2.4.2 Attempted Synthesis of 1-[2-(cyclopenta-1,3-diene)ethyl] imidazole *via* opening spiro ring

It was thought that lithium imidazolide could act as a nucleophile, as the lithium phosphide acts in an already known reaction used for the synthesis of **2.26** shown in Scheme 2.14 below. [123]

2.25   **2.26**
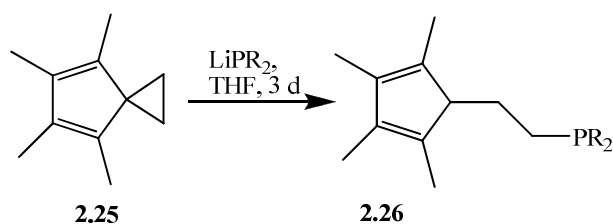
Scheme 2.14: Synthesis of **2.26** by Hamilton. R= Et or Ph.

Lithium imidazolide could attack carbon 3 in spiro(2,4)hepta- 4, 6- diene **2.27** and consequently open the ring, to give the compound **2.28** shown in Scheme 2.15. Spiro(2,4)hepta-4,6-diene **2.27** was reacted with lithium imidazolide under a variety of conditions. [124] The reactions were carried out in an ampoule. TMEDA or HMPA were added to the reaction mixture to reduce the aggregation of the polymeric lithium imidazolide. ^{1}H-NMR spectra in deuterated chloroform showed that starting imidazole was isolated in all cases after hydrolysis of the reaction mixture with water, extraction in pentane, drying over magnesium sulphate and removal of the volatile components under reduced pressure. This implies that the ring opening reaction does not take place.

2.27   **2.28**
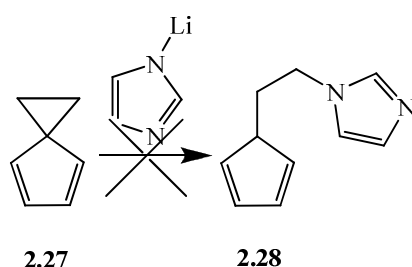
Scheme 2.15: Toluene, reflux overnight; benzene, TMEDA(exc), r.t. over 2 days and toluene, HMPA (2 equiv.), reflux overnight.

2.4.3 Attempted Synthesis of 1-[2-(1,2,3,4-tetrametylcyclopenta-1,3-diene(ethyl)]3-isopropylimidazole -2-ylidene

Scheme 2.16 shows a proposed route to synthesise the tetramethyl cyclopentadienyl analogue **2.32**. The new thiourea **2.30** (R= isopropyl) was prepared for the first time in low yield from a mixture of endocyclic isomers, **2.29** [125] and fully characterised.
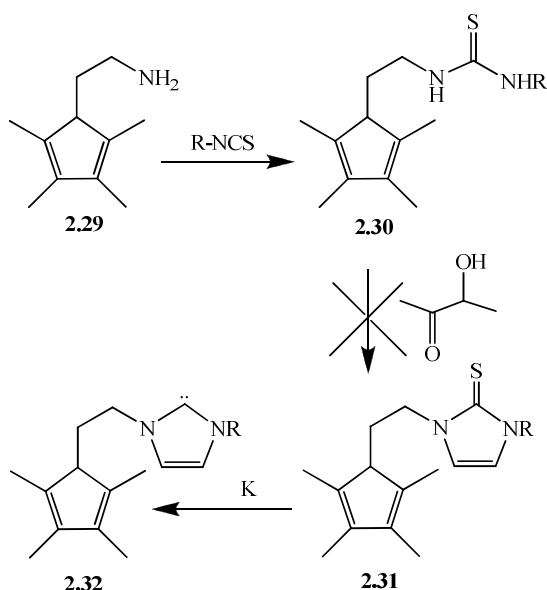
Scheme 2.16: Proposed route to synthesise **2.32**, R= isopropyl.

Attempt for the formation of compound **2.31** was made by refluxing **2.30** and 3-hydroxybutan-2-one in hexanol for 20 hours. Uncharacterisable dark oil was isolated after removal of hexanol under reduced pressure. Attempts to isolate any solid out of this oil were made but were not successful.

2.4.4 Attempted Synthesis of 1-[2-(1,2,3,4-tetramethylcyclopenta-1,3-diene(ethyl)] 3-diisopropylimidazol-2-yildene *via* 5-(2-chloroethyl)- 1, 2, 3, 4-tetramethylcyclopentadiene

A method to synthesize 5-(2-chloroethyl)cyclopenta-1,3-diene is unavailable to date. Any attempt for this synthesis results in the formation of the spiro and the dimerisation compound as can be seen in Scheme 2.17 below.
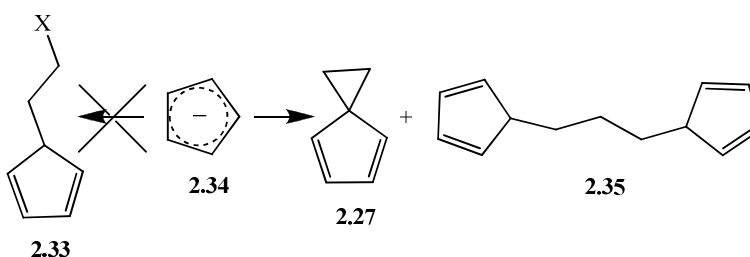
Scheme 2.17: Reaction of cyclopentadienide with 1,2-dihaloethane (X=Br or Cl).

However the tetramethylcyclopentadiene analogue appears to be more stable. The reaction of tetramethylcyclopentadiene with 1,2-dihaloethane has been reported. [123]

73

This reaction performed in diethyl ether has the drawback that a mixture of non-geminal and geminal isomers is produced as is shown in Figure 2.18.

2.36a

Non-geminal isomers

2.36b
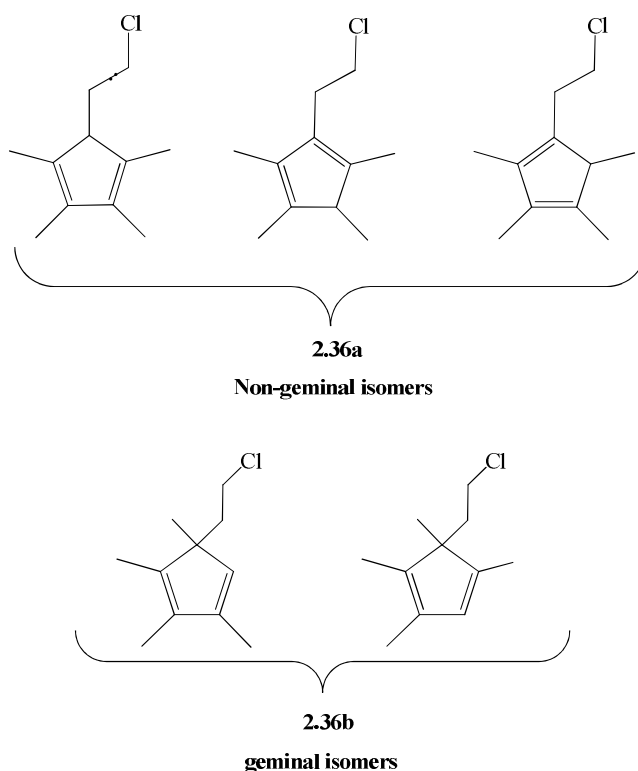
geminal isomers

Figure 2.18: Representation of the geminal **2.36b** and non-geminal isomers **2.36a**.

A mixture of exclusively non-geminal isomers of **2.36a** has been achieved for the first time in good yield by stirring lithium cyclopentadienide and 1-bromo-2-chloroethane in petrol for 1 month at room temperature (Scheme 2.18). Compound **2.36a** (non-geminal isomers) was found quite sensitive and the mixture decomposes overnight in contact with air to give thick oil. Therefore the mixture should be stored in a cold place and under inert conditions.
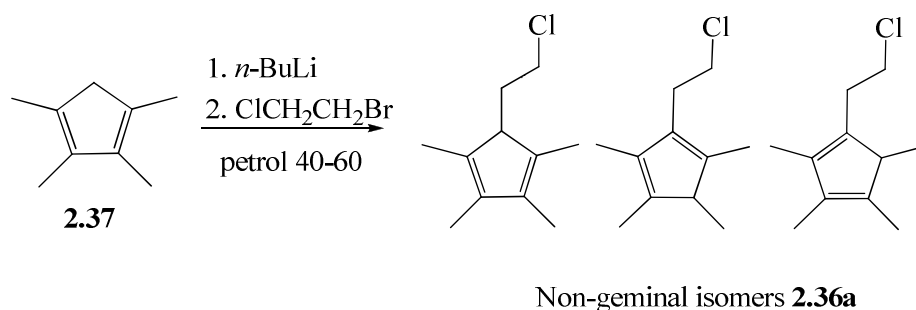
Scheme 2.18: Synthesis of non-geminal isomers **2.36a**.

The polarity of the solvent seems to play a very important role for the synthesis of **2.36a**. The reaction in Scheme 2.18 above was carried out in three different solvents

74

(THF, diethyl ether and petrol) but using the same conditions and starting materials. The three reactions were worked up in the same way; the white precipitates were left to settle and solutions were decanted, washed with water and dried over $MgSO_4$. The three solutions were dried under vacuum to give light yellow oils.

^{1}H-NMR spectroscopy and (EI) mass spectrometry gas chromatography experiments showed that a mixture of geminal isomers **2.36b** is mainly obtained by reaction in THF. Reaction in diethyl ether showed a mixture of geminal and non-geminal isomers as it was reported by Hamilton. [123] However, only a mixture of non-geminal isomers **2.36a** is obtained by carrying out the reaction in petrol. Therefore the use of no-polar hydrocarbon solvents may have an effect on the mechanism of the substitution reaction, favouring the formation of the non-geminal isomers.

A proposed synthetic route to obtain imidazolium salt **2.38** from a mixture of non-geminal isomers is shown in Scheme 2.19. The resulting product would be also a mixture of isomers which would have allylic hydrogen atoms that could be abstracted by reaction with a base to form ligand **2.39**. A second deprotonation could take place to generate the bidentate ligand **2.40** as is shown in Scheme 2.19.
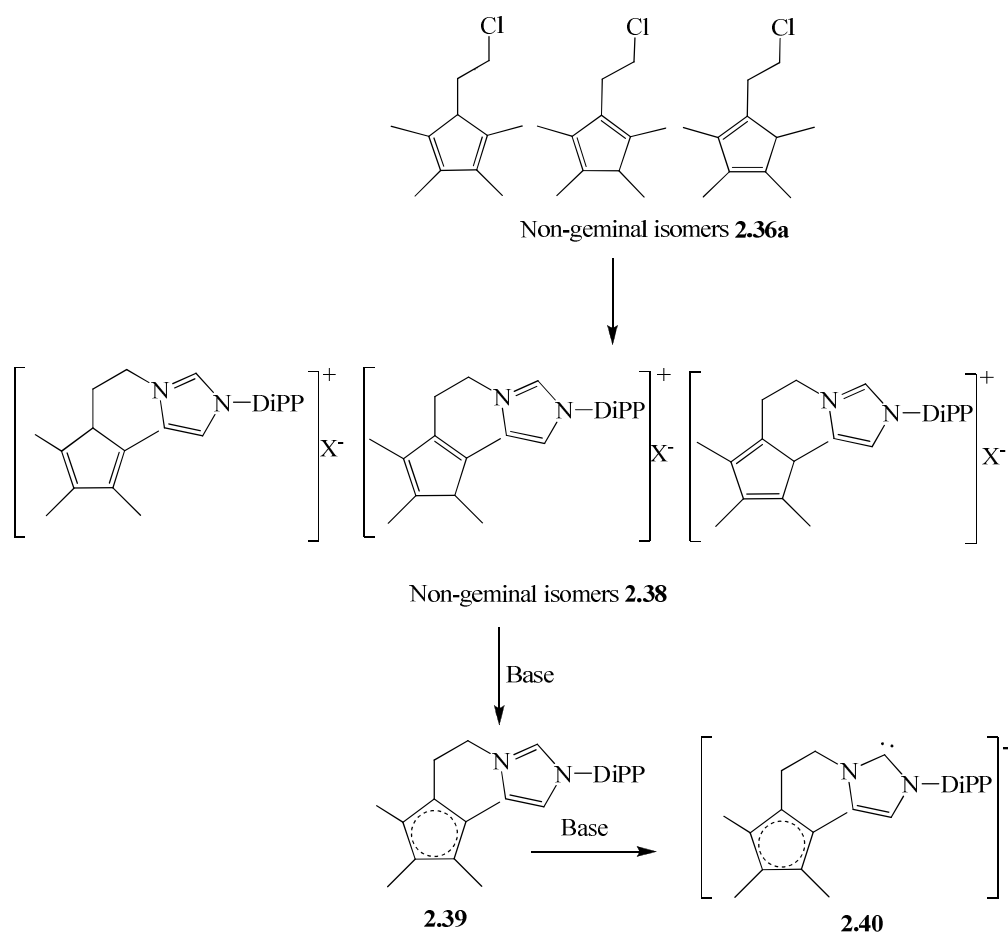
Scheme 2.19: Proposed route for the synthesis of **2.39** and further deprotonation to synthesise bidentate ligand **2.40**.

Attempted synthesis of 1-[2-(1,2,3,4-tetramethylcyclopenta-1,3-diene(ethyl)] 3-diisopropylimidazolium chloride **2.38** was made by using methods 1 and 2 described below. These methods gave the undesired products shown in Scheme 2.20.

Method 1

A mixture of isomers **2.36a** with one equivalent of DiPP-imidazol at 160 ℃ under partial vacuum for several days gave 2,6-diisopropylimidazolium chloride **2.41**, which was characterised by electrospray mass spectrometry in acetonitrile.

Method 2

Non-geminal isomers and potassium imidazolide were both dissolved in THF and combined at -78 ℃. The mixture stirred at room temperature for two hours. The white suspension was filtered through Celite and the solution submitted for gas chromatography electrospray mass spectrometry which show that the main product formed is the spiro **2.42**.
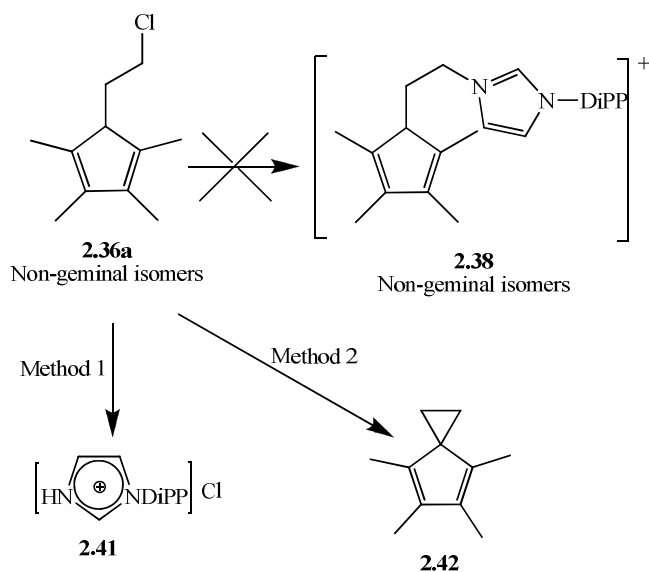
Scheme 2.20: Attempted synthesis of **2.38** by methods 1 and 2.

2.4.5 Attempted Synthesis of 1-[2-(1,2,3,4tetramethylcyclopenta-1,3-diene(propyl)] 3-diisopropylimidazolium chloride

Attempted synthesis of the 2-carbon-bridged species **2.38** gave undesired products as it has been discussed above. It would be also of great interest to be able to isolate the three-carbon bridge imidazolium salts **2.44**. The proposed route is shown below in Scheme 2.21. It was hoped that the reaction to form the spiro compound by elimination of the chloride atom in the three-carbon bridge species would be less favoured than for the two-carbon bridged species.
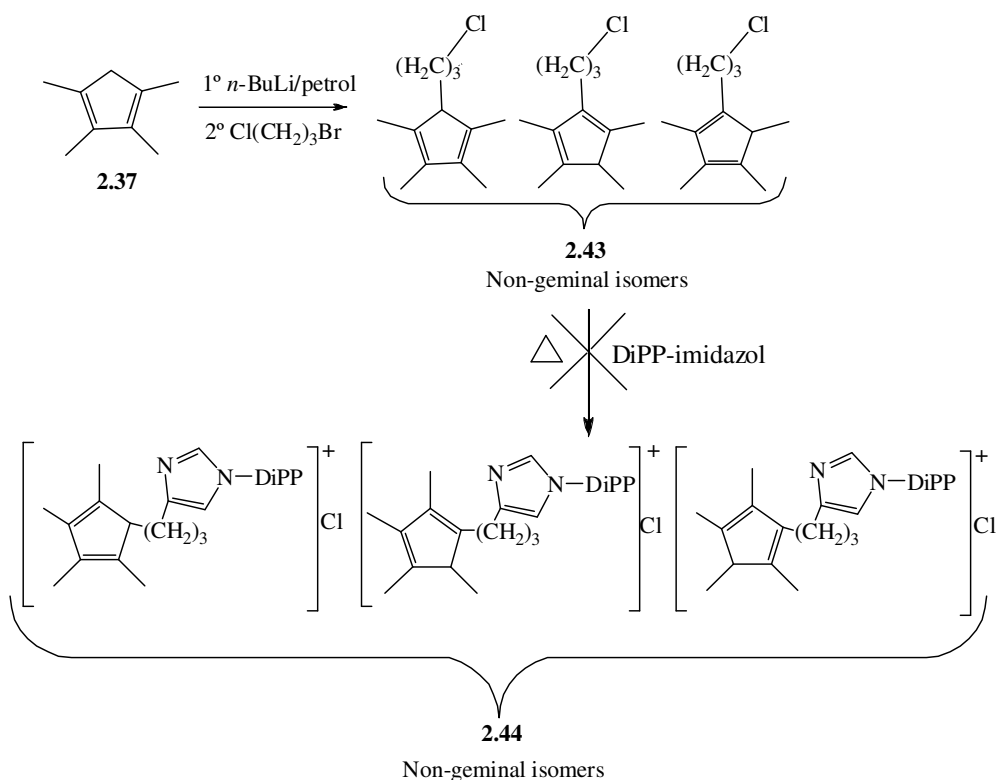
Scheme 2.21: Proposed route for the synthesis of three carbon bridged imidazolium salt ligand **2.44** (non-geminal isomers).

A mixture of non-geminal isomers **2.43** has been successfully synthesised in good yield and characterised by using a similar method as for the 2 carbon bridged analogue. 1, 2, 3, 4-tetramethylcyclopentadiene and 1-bromo-3-chloropropane were stirred in petrol for 1 month at room temperature. A yellow oil was isolated and characterised by NMR spectroscopy. This mixture of non-geminal isomers decomposes slowly in the absence of solvent at room temperature under normal atmosphere. Due to this fact the ligand should be stored refrigerated under inert conditions.

An attempted synthesis of **2.44** was made by heating **2.43** and 2,6-DiPP imidazol at 160 °C under partial vacuum. This method gave an uncharacterisable yellow gummy solid.

In summary, some interesting intermediate ligands such as **2.30**, **2.36a** and **2.43**, necessary for the cyclopentadiene- and/or tetramethylcyclopentadiene-functionalised *N*-heterocyclic carbene ligands proposed synthetic routes, have been synthesised for the first time. However, attempts to obtain the desired bi-functional ligands were unsuccessful.

2.5 Conclusions

The coordination chemistry of NHC ligands with certain early transition metals is not as well-known as with late transition metals. In this project a large amount of effort has been made in order to better understand the chemistry of these important and relatively new ligands with electropositive metals in the periodic table, which are well-known to be active in the oligo/polymerisation of ethylene.

Indenyl-functionalised NHC ligands have been proved to act as suitable bidentate ligands with early transition metal complexes, producing a wide range of new compounds.

The two- and three-carbon-bridged ligands have been introduced to the metals as result of reaction of metalchloride complexes with the potassium salts L(2C)K and L(3C)K. Insoluble potassium chloride is produced as side product and it is believed to be a driving force for the reaction to take place.

Alkyl complexes, as well as cationic complexes, have also been synthesised with the indenyl-functionalised NHCs ligands above.

Catalytic studies in oligo/polymerisation of ethylene using as catalyst some of the new early transition metal complexes described above in this chapter in presence of the activator MMAO-3A, proved that they are active, especially towards polymerisation, presenting in some cases moderate to high activities. Therefore a new research pathway has been opened in organometallic chemistry in which electropositive metals bearing NHC tethered to cyclopentadienyl ring analogues have shown their potential in catalytic processes such as the oligomerisation and polymerisation of ethylene.

2.6 Experimental

2.6.1 General Methods for Synthesis of Ligands and Complexes

Elemental analyses were carried out by the London Metropolitan University micro-analytical laboratory. All manipulations were performed under nitrogen in a Braun glovebox or using standard Schlenk techniques, unless stated otherwise. Solvents were dried using standard methods and distilled under nitrogen prior to use. The light petroleum used throughout had a bp of 40-60 °C. The starting materials bromoethylindene, [126]5,7-dimethylindene, [127] 2,6 diisopropylphenylimidazole, [128] ZrCl$_4$(THT)$_2$, [129] Ti(N^{t}Bu)Cl$_2$(pyridine)$_3$, [130] CrCl$_3$(THF)$_3$, [131] Cr Cl$_2$(Me)(THF)$_3$; [132] dibenzylmagnesium; [133] [H(Et$_2$O)$_2$][BAr$_4$] and NaBAr$_4$ Ar = (B[(3,5-(CF$_3$)$_2$-C$_6$H$_3$)]$_4$) [134] were prepared according to literature procedures. NMR data were recorded on Bruker AV 300 and DPX-400 spectrometers, operating at 300 and 400 MHz (^{1}H), respectively. The spectra were referenced internally using the signal from the residual protio-solvent (^{1}H) or the signals of the solvent (^{13}C). Data for X-ray crystallography is included at the end of this chapter.

2.6.2 Synthesis of Imidazolium Salts

1-(2-Bromoethyl)-4,7-dimethylindene
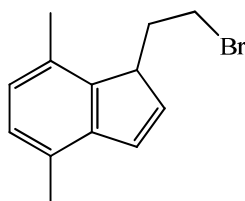
4,7-Dimethylindene (18.00 g, 125 mmol) was treated with 1 equiv. of *n*-BuLi (2.5 M in hexanes, 50 mL, 125 mmol) at -78 °C. After warming to room temperature and stirring for 2 h, the solution was again cooled to -78 °C and 3 equiv. of dibromoethane (69.00 g, 375 mmol) were added. The solution was allowed to warm to room temperature and stirred overnight. After addition of water (200 mL) and phase separation, the organic phase was dried over MgSO$_4$. Evaporation of the volatile components under vacuum left a dark residue, which was distilled under reduced pressure (98-104 °C, 1 Torr) to give a light yellow orange oil (22.90 g, 75%). The product was stored under nitrogen in the freezer.

^{1}H NMR (CDCl$_3$, 400 Hz): 7.10-6.89 (3H, m, Ar-H); 6.60 (1H, d, J= 6 Hz, Ar-H); 3.81-3.78 (1H, m, C2-indenyl); 3.40-3.30 (2H, m, BrCH_2); 2.80- 2.60 (1H, m, BrCH$_2$CH_2); 2.45 (6H, s, 2x CH_3); 2.20-1.98 (1H, m, BrCH$_2$CH_2).

^{13}C{^{1}H} NMR (CDCl$_3$, 100 MHz): 142.2; 141.3; 134.9 128.7; 128.7; 126.7; 126.4; 125.6; 47.6; 31.3; 29.5; 17.2; 16.6.

MS (EI): 250, 252 (M-Br)$^+$.

L(2C)Br, 2.1
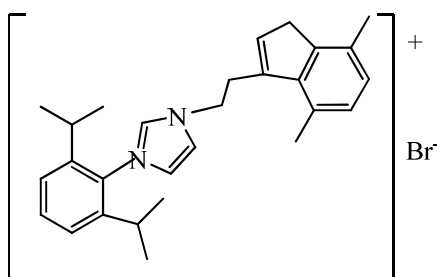
1-(2-Bromoethyl)-4,7-dimethyl- 1H-indene (22.60 g, 90.0 mmol) and 2,6-diisopropylphenylimidazole (21.00 g, 90.0 mmol) were dissolved in dioxane (100 mL) and heated at 110 °C for 1 week. The dioxane was removed under vacuum, and the solid residue was dissolved in dichloromethane and precipitated with ether. Azeotropic drying with toluene gave the product as an off-white powder after removal of the toluene under reduced pressure, washing the residue with petrol, and drying under vacuum .Yield: 26.00 g, 61%.

^{1}H NMR (CDCl$_3$, 300 MHz): 10.34 (1H, s, imidazolium H); 7.68 (1H, s, Ar-H); 7.45 (1H, t, J= 6Hz, Ar-H); 7.23-7.20 (2H, m, Ar-H); 7.00 (1H, s, Ar-H); 6.88 (2H, dd, J= 6 Hz, Ar-H); 6.30 (1H, s, C2-Indenyl); 5.11 (2H, t, J= 6 Hz, CH_2 bridge); 3.47 (2H, bs, CH_2 bridge); 3.06 (2H, s, C9-Indenyl); 2.53 (3H, s, CH_3); 2.18 (3H, s, CH_3); 2.16 (2H, sept, J= 7Hz, CH(CH$_3$)$_2$; 1.15 (6H, d, J= 7 Hz, CH(CH_3)2); 1.04 (6H, d, J= 7 Hz, CH(CH_3)$_2$.

^{13}C{^{1}H} NMR (CDCl$_3$, 75 MHz): 145.3; 143.8; 140.9; 140.6; 138.5; 131.9; 131.8; 131.0; 130.8; 130.1; 129.8; 126.5; 124.7; 123.6; 123.2; 49.8; 36.6; 31.5; 28.7; 24.3; 24.2; 20.2; 18.2.

Elemental Analysis: Calculated (%): C, 70.14; H, 7.36; N, 5.84. Found (%): C, 69.90; H, 7.37; N, 5.77.

MS ES$^+$: 400 (M-Br)$^+$

1-(3-Bromopropyl)-4,7-dimethylindene, 2.3
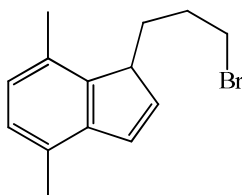
4,7-Dimethylindene (6.50 g, 45.1 mmol) in ether (150 mL) was reacted with 1 equiv. of *n*-butyl lithium (2.5 M, 180 mL) at -78 °C. The mixture was allowed to warm to room temperature and stirred for 2 h. The solution was cooled again to -78 °C, 1,3-dibromopropane (13.8 mL, 135.3 mmol) was added dropwise, and the mixture was stirred at room temperature for 2 days. After addition of water (200 mL), isolation of the ether layer, washing with water (3 x 50 mL), drying over MgSO$_4$, removal of the volatile components under reduced pressure, and distillation of the residue under vacuum (1.2 Torr, 120-124 °C) gave an orange oil. Yield: 4.88g, 41%.

^{1}H NMR (CDCl$_3$, 300 MHz): 6.91-6.79 (3H, m, Ar-H); 6.38 (1H, dd, *J*= 5.6 Hz, Ar-H), 3.26 (2H, dd, *J*= 6.5 Hz, C2-Indenyl); 3.30-3.20 (2H, m, C*H*$_2$-Br bridge); 2.32 (3H, s, C*H*$_3$); 2.31 (3H, s, C*H*$_3$); 2.25-2.05 (2H, m, C*H*$_2$ bridge); 1.45- 1.80 (4H, m, C*H*$_2$ bridge).

^{13}C{^{1}H} NMR (CDCl$_3$, 75 MHz): 144.5; 143.1; 138.0; 130.3; 129.7; 128.0; 127.8; 126.9; 49.3; 34.2; 29.1; 27.6; 18.8; 18.2.

MS ES$^+$: 186.3 (M - Br)$^+$.

L(3C)Br, 2.5
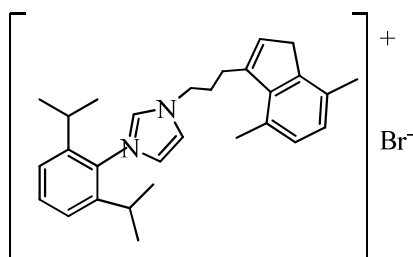
1-(3-Bromopropyl)-4,7-dimethylindene (0.55 g, 2.1 mmol) and 2,6-diisopropylphenylimidazole (0.58 g, 2.54 mmol) were both dissolved in 15 mL of 1,4-dioxane and refluxed for 1 week at 110 °C. After removal of the solvent under vacuum, the resulting solid was dissolved in dichloromethane (25 mL) and precipitated with ether (20 mL). The precipitate was isolated by filtration and dried azeotropically with toluene. The dried white product was washed with ether and dried

under vacuum. Yield: 1.10 g, 97%.

^{1}H NMR (CDCl$_3$, 300 MHz): 10.61 (1H, s, imidazolium H); 7.82 (1H, s, Ar-H); 7.53-7.40 (1H, t, J= 6.5 Hz, Ar-H); 7.25-7.05 (3H, m, Ar-H); 6.90-6.77 (2H, m, NHC backbone); 6.22 (1H, s, C2-Indenyl); 4.90 (2H, t, J = 7.3 Hz, CH_2 bridge); 3.10 (2H, s, C9-Indenyl); 2.82 (2H, t, J = 7.0 Hz, CH_2 bridge); 2.45 (3H, s, CH_3); 2.35-2.22 (4H, m, 2 x CH(CH$_3$)$_2$ and CH_2 bridge); 2.22 (3H, s, CH$_3$), 1.17 (6H, d, J = 6.7 Hz, CH(CH_3)$_2$); 1.07 (6H, d, J = 6.7 Hz, CH(CH_3)$_2$).

^{13}C- {^{1}H} NMR (CDCl$_3$, 75 MHz): 145.3; 143.9; 138.8; 131.9; 130.7; 130.1; 129.5; 129.3; 129.0; 128.2; 126.0; 124.7; 124.1; 122.6; 50.1; 36.5; 29.9; 28.8; 27.1; 24.3; 24.2; 20.0; 18.2.

MS ES$^+$: 413.4 (M - Br)$^+$; C$_{29}$H$_{37}$N$_2$ requires m/z = 413.2951; found m/z = 413.2945.

2.6.3 General Method for the Deprotonation of the Imidazolium Salts

KN(SiMe$_3$)$_2$ (3 mmol) was dissolved in benzene (20 mL), and the resulting solution was added at room temperature to the imidazolium salt (3 mmol) to give a suspension. The mixture was stirred overnight. The precipitated potassium halide was removed by filtration through Celite, giving a solution of the crude neutral indenylethyl- or indenylpropyl-functionalized N-heterocyclic carbene. The crude products can be isolated as air-sensitive powders by removal of benzene under reduced pressure. However, for routine work this is not necessary, and the N-heterocyclic carbene obtained as described above was further deprotonated by adding to the solution 1 equiv. of KN(SiMe$_3$)$_2$ (3 mmol) in benzene (20 mL) at room temperature. The mixture was allowed to stir overnight. The precipitated powders (two and three carbon bridged potassium salts L(2C)K and L(3C)K) were isolated by filtration on a frit, washed with benzene (2 mL) and petrol (3 x 10 mL), and dried under vacuum. The products were extremely air-sensitive, white to beige powders. The yields were around 50-80%.

1-[2-(4,7-Dimethylindenyl)ethyl]-3-(2,6-diisopropylphenyl)imidazol-2 ylidene potassium [94], 2.2

L(2C)K
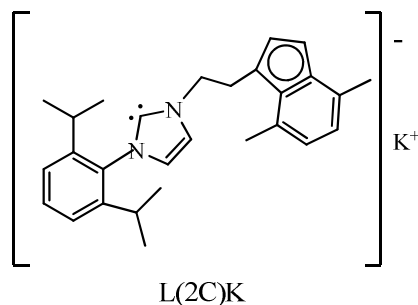
The imidazolium salt 3-(2,6-diisopropylphenyl)-1-[2-(3H-(4,7-dimethyl)inden-1-yl)-ethyl]-2H-imidazolium bromide [94] (1.44 g, 3 mmol) was combined with 1 equiv. of $KN(SiMe_3)_2$ (3 mmol, 0.64 g) in benzene (20 mL), and the orange suspension was stirred overnight. KBr was filtered off through Celite, and the solution of the neutral ligand was subjected to a second deprotonation with 1 equiv. of $KN(SiMe_3)_2$ (3 mmol, 0.64 g) in benzene (20 mL). The red mixture was stirred overnight. The white precipitate formed was isolated on a frit, washed with benzene (2 mL) and petrol (10 mL), and dried under vacuum. Yield: 0.88 g, 70%.

Carrying out the reaction on a larger scale results in lower yields.

Elemental Analysis: Calculated (%): C, 77.01; H, 7.62; N, 6.42. Found (%): C, 76.96; H, 7.71; N, 6.34

^{1}H NMR (d^5-pyridine, 300 MHz): 7.33-7.09 (5H, m, Ar-H); 6.48 (2H, s, Ar-H); 6.45 (1H, s, NHC backbone); 6.28 (1H, s, NHC backbone); 4.33 (2H, t, J = 7.2 Hz, CH_2 bridge); 3.61 (2H, t, J = 7.2 Hz, CH_2 bridge); 2.80 (2H, sept, J= 7.0 Hz, C$H(CH_3)_2$); 2.60 (3H, s, CH_3); 2.45 (3H, s, CH_3); 1.05 (6H, d, J = 7.0 Hz, CH(C$H_3)_2$); 1.00 (6H, d, J = 7.0 Hz, CH(C$H_3)_2$).

^{13}C{^{1}H} NMR (d^5-pyridine, 75 MHz): 209.4; 146.1; 138.3; 129.4; 128.1; 128.1; 123.9; 123.5; 123.4; 123.0; 122.2; 119.2; 119.1; 114.4; 112.1; 105.0; 90.0; 56.3; 32.8; 27.6; 23.9; 23.4; 21.6; 18.9.

1-[3-(4, 7-Dimethylindenylpropyl]-3-(2,6-diisopropylphen-yl)imidazol-2-ylidenepotassium, 2.7

L(3C)K
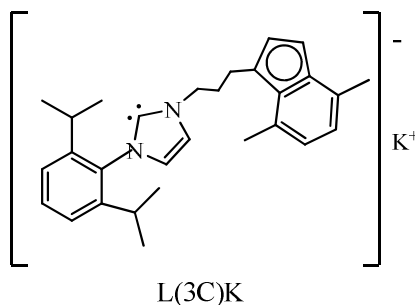
3-(2,6-Diisopropylphenyl)-1-[3-(3H-(4,7-dimethyl)inden-1-yl)-propyl]-2H-imidazolium Bromide (1.48 g, 3 mmol) was combined with 1 equiv. of $KN(SiMe_3)_2$ (3 mmol, 0.64 g) in benzene (20 mL), and the orange suspension was stirred overnight. The precipitated KBr was filtered off through Celite, and the solution of the neutral ligand was subjected to a second deprotonation with another equivalent of $KN(SiMe_3)_2$ (3 mmol, 0.64 g) in benzene (20 mL). The red suspension was stirred overnight. The precipitated product was isolated on a frit washed with benzene (2 mL) and petrol (10 mL) and dried under vacuum. Yield: 0.88 g, 64%.

Elemental Analysis: Calculated (%): C, 77.30; H, 7.78; N, 6.22. Found (%):C, 77.16; H, 5.75; N, 4.38.

^{1}H NMR (d^5-pyridine, 300 MHz): 7.35-7.00 (5H, m, Ar-H); 6.88 (1H, s, Ar-H); 6.48 (2H, dd, J = 5.5 Hz, NHC backbone); 6.39 (1H, d, J = 3.5 Hz, Ar-H); 4.30 (2H, t, J = 6.8 Hz, CH_2 bridge); 3.40 (2H, t, J = 6.8 Hz, CH_2 bridge); 2.70 (3H, s, CH_3); 2.64 (2H, sept, J = 7.5 Hz, CH(CH$_3$)$_2$); 2.52 (3H, s, CH_3); 2.32 (2H, quint, J = 6.8 Hz, CH_2 bridge); 0.94 (6H, d, J = 7 Hz, CH(CH_3)$_2$); 0.88 (6H, d, J = 7 Hz, CH(CH_3)$_2$).

^{13}C{^{1}H} NMR (d^5-pyridine, 75 MHz): 212.5 (C$_{NHC}$); 163.9; 146.9; 139.31; 131.27; 129.46; 129.18; 126.10; 124.93; 120.0; 118.71; 115.59; 115.34; 113.78; 108.49; 91.76; 50.51; 36.14; 28.78; 28.57; 28.48; 27.46; 24.62; 24.06; 23.88; 22.96, 20.57.

2.6.4 Dimethylindenyl-functionalized *N*-Heterocyclic Carbene Complexes of Group 4. Ti(IV) and Zr(IV) Complexes

3-(2,6-Diisopropylphenyl)-1-[2-(4,7-Dimethylindenyl)ethyl]-imidazol-2-ylidene(tert-butylimido)titanium chloride, 2.8
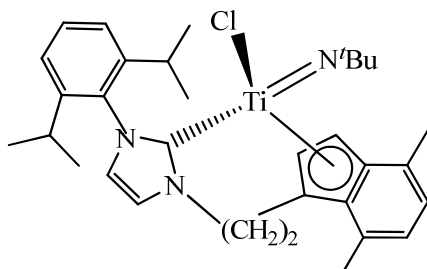
To a stirred solution of Ti(Bu^{t}N)Cl$_2$(pyridine)$_3$ (0.30 g, 0.70 mmol) in THF (30 mL) at -78 °C was added dropwise *via* cannula a precooled suspension of L(2C)K (0.29 g, 0.70 mmol) in the same solvent (30 mL). On completion of the addition the mixture was allowed to reach room temperature within 0.5 h and stirred for 1 h. Evaporation of the volatile components under reduced pressure, extraction of the yellow residue in petrol, filtration of the organic extracts through Celite, concentration, and cooling at 0 °C gave yellow crystals. Yield: 0.16 g, 45%.

Elemental Analysis: Calculated (%): C, 69.62; H, 7.67; N, 7.61. Found (%): C, 69.45; H, 7.55; N, 7.48.

^{1}H NMR (C$_6$D$_6$, 300 MHz): 7.22-6.65(7H, m, Ar-H); 6.45(1H, d, *J*= 0.7 Hz, NHC backbone); 6.26(1H, d, *J*= 0.7 Hz, NHC backbone); 4.22 (1H, d of t, *J* = 6.8 Hz , C*H$_2$* bridge); 3.65 (1H, d of t, *J* = 6.8 Hz , C*H$_2$* bridge); 3.22 (1H, d of t, *J* = 6.8 Hz, C*H$_2$* bridge); 2.82 (1H, d of t, *J* = 6.8 Hz , C*H$_2$* bridge); 2.10 and 2.92 (2H, two septets, *J*= 6 Hz, (CH$_3$)$_2$C*H*); 1.98 and 2.55 (two s, 6H, C*H$_3$*); 0.95, 1.02, 1.18, 1.62 (12H, four d, *J*= 6 Hz, (C*H$_3$*)$_2$CH), 1.32 (9H s, (CH$_3$)$_3$N.

^{13}C{^{1}H} NMR (C$_6$D$_6$ 75 MHz): 196.7 (C$_{NHC}$); 145.8 (Ar); 144.9 (Ar); 136.8 (Ar); 132.4 (Ar); 130.05 (Ar); 129.8 (Ar); 126.1 (Ar); 125.9 (Ar); 125.3 (Ar); 123.9 (Ar); 123.7 (Ar); 122.6 (Ar); 122.3 (Ar); 120.3 (Ar); 115.6 (Ar); 109.1 (Ar); 94.0 (Ar); 68.4; 53.37; 32.6; 28.5; 28.1; 26.0; 25.3; 24.5; 24.3; 23.7; 22.7; 22.4; 21.5; 19.4.

3-(2,6-Diisopropylphenyl)-1-[3-(4,7-dimethylindenyl)propyl]imidazol-2-ylidene(tert-butylimido)titanium chloride, 2.9
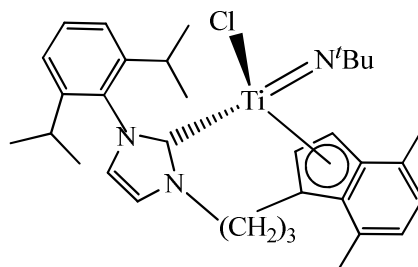
This was prepared by a method analogous to the titanium two carbon bridged complex above; Ti(Bu^{t}N)Cl$_2$(pyridine)$_3$ (0.30 g, 0.70 mmol) and L(3C)K (0.32 g, 0.70 mmol).

After evaporation of the volatile components under reduced pressure, extraction of the yellow-orange residue in toluene, filtration of the organic extracts through Celite, concentration, and cooling at 0 °C gave yellow-orange crystals. Yield: 0.23 g, 60%.

Elemental Analysis: Calculated (%): C, 70.02; H, 7.84; N, 7.42. Found (%): C, 69.80; H, 7.57; N, 7.38.

^{1}H NMR (C$_6$D$_6$, 300 MHz): 7.00-6.45 (7H, m, Ar-H); 6.28 (1H, broad s, NHC backbone); 6.05(1H, broad s, NHC backbone); 4.91-4.82 (1H, m, CH_2 bridge); 3.10-3.20 (1H, m, CH_2 bridge); 2.85-2.60 (3H, m, CH_2 bridge and 2x (CH$_3$)$_2$CH); 2.50-2.40 (1H, m, CH_2 bridge); 2.30 (6H, s, 2x CH$_3$); 1.72-1.45 (2H, m, CH_2 bridge); 1.40, 1.15, 0.9 and 0.75 (12H, four d, J = 6 Hz, (CH_3)$_2$CH), 1.25 (s, 9H, (CH_3)$_3$N).

^{13}C{^{1}H} NMR (C$_6$D$_6$ 100 MHz): 145.8 (Ar); 144.9 (Ar); 136.8 (Ar); 132.4 (Ar); 132.0 (Ar); 129.7 (Ar); 126.1 (Ar); 125.9 (Ar); 125.3 (Ar); 123.9 (Ar); 123.7 (Ar); 122.6 (Ar); 122.3 (Ar); 120.3 (Ar); 115.6 (Ar); 111.9 (Ar); 91.7 (Ar); 68.6; 53.37; 32.1; 28.6; 28.1; 26.1; 26; 25.9; 25.5; 24.1; 23.8; 23.1; 22.2; 21.2.

3-(2,6-Diisopropylphenyl)-1-[3-(4,7-dimethylindenyl)propyl]imidazol-2-ylidenezirconium Trichloride, 2.10
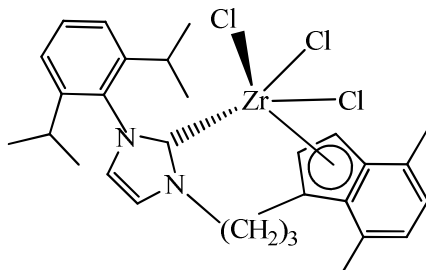
ZrCl$_4$(THT)$_2$ (1 mmol, 0.41 g) and **3.5** (1 mmol, 0.45 g) were dissolved in THF (30 mL) in separate Schlenk tubes, and the two solutions were combined at -78 °C. After stirring for 2 h at this temperature, the yellow reaction mixture was allowed to warm to room temperature and stirred overnight. The volatile components were removed under reduced pressure, and the residue was dissolved in dichloromethane and filtered through Celite. The dichloromethane extracts were dried under vacuum to give the analytically pure product yellow powder. Yield: 0.33 g, 52%.

Elemental Analysis: Calculated (%): C, 57.17; H, 5.75; N, 4.59. Found (%): C, 56.92; H, 5.79; N, 4.38.

^{1}H NMR (CD$_2$Cl$_2$, 400 MHz): 7.22 (2H, t, *J*= 8 Hz, Ar-H); 7.12 (1H, s, Ar-H); 7.03 (2H, t, *J*= 8.0 Hz, Ar-H); 6.84 (1H, s, Ar-H); 6.78-6.65 (3H, m, NHC backbone and Ar-H); 5.61-5.53 (1H, m, C*H*$_2$ bridge); 4.18-4.13(1H, m, C*H*$_2$ bridge); 3.27-3.03 (2H, m, C*H*$_2$ bridge); 2.60-2.05 (3H, m, C*H*$_2$ bridge and 2x C*H*(CH$_3$)$_2$) ; 2.46 (3H, s, CH$_3$); 2.33 (3H, s, CH$_3$); 2.85-2.75(1H, m, C*H*$_2$ bridge); 1.14 (3H, d, *J*= 6.5 Hz, CH(C*H*$_3$)$_2$); 1.11 (3H, d, *J*= 6.5 Hz, CH(C*H*$_3$)$_2$); 1.07 (3H, d, *J*= 6.5 Hz, CH(C*H*$_3$)$_2$), 0.75 (3H, d, *J*= 6.5 Hz, CH(C*H*$_3$)$_2$).

^{13}C{^{1}H} NMR (CD$_2$Cl$_2$, 100 MHz): 130.9(Ar); 128.9 (Ar); 127.2 (Ar) 125.6 (Ar); 1124.9 (Ar); 124.5 (Ar); 124.3 (Ar); 123.7 (Ar); 122.9 (Ar); 122.8 (Ar); 121.4 (Ar); 119.3 (Ar);100.0 (NHC backbone); 48.3(bridge); 46.6 (bridge); 30.8; 28.1; 26.9; 26.4; 25.3; 25.0; 24.8; 24.5; 23.6; 23.4; 23.2; 22.3; 22.0; 21.8; 20.6; 19.6; 17.9; 17.7.

^{1}H NMR (C$_6$D$_5$Cl, 300 MHz): 6.52-6.34 (8H, m, Ar-H); 6.27 (1H, d, *J*= 3.8 Hz, NHC backbone); 5.40-5.28 (1H, m, C*H*$_2$ bridge); 3.48 (1H, d of t, *J*= 7.2 Hz, C*H*$_2$ bridge); 2.70-2.69 (2H, m, C*H*$_2$ bridge and 1x C*H*(CH$_3$)$_2$); 2.37 (1H, ddd, C*H*$_2$ bridge); 2.33 (3H, s, C*H*$_3$); 2.13 (1H, sept, *J*= 6.8, C*H*(CH$_3$)$_2$); 2.04 (3H, s, CH$_3$); 1.39 (1H, ddd, *J*=3.8 Hz, C*H*$_2$ bridge); 1.32 (1H, quint, *J*= 3.0 Hz, C*H*$_2$ bridge); 1.14 (3H, d, *J*= 6.8

Hz, CH(CH_3)$_2$); 1.01 (3H, d, J= 6.8 Hz, CH(CH_3)$_2$); 0.83 (3H, d, J= 6.8 Hz, CH(CH_3)$_2$); 0.54 (3H, d, J= 6.8 Hz, CH(CH_3)$_2$).

^{13}C{^{1}H} NMR (C$_6$D$_5$Cl, 75 MHz): 190.1 (C$_{NHC}$); 145.1; 144.6; 134.5; 126.6; 125.3; 124.4; 124.0; 122.0; 120.0; 100.9; 47.5; 29.2; 28.2; 26.5; 26.3; 24.6; 24.4; 23.7; 21.9; 19.4.

2.6.5 Dimethylindenyl-functionalized N-Heterocyclic Carbene Complexes of Group 6 Cr(III) and Cr(II) Complexes

3-(2,6-Diisopropylphenyl)-1-[2-(4,7-dimethylindenyl)ethyl]-imidazol-2-ylidenechromium dichloride, 2.11
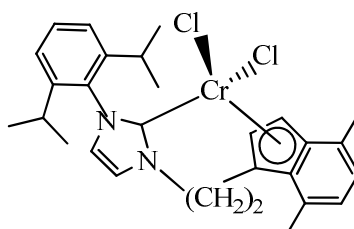
To a stirred solution of CrCl$_3$(THF)$_3$ (0.57 g, 1.5 mmol) in THF (30 mL) at -78 ºC a pre-cooled solution of L(2C)K (0.66 g, 1.5 mmol) in the same solvent (30 mL)was added *via* cannula. On mixing, the reaction mixture changed from purple to dark green. The mixture was allowed to warm to room temperature and stirred overnight. Evaporation of the volatile components under reduced pressure, extraction of the green residue in dichloromethane (3x 30 mL), filtration of the organic extracts through Celite and removal the solvent under reduce pressure gave the analytically pure product as dark green powder. The product was recrystallized from dichlorometane/petrol. Yield: 0.37 g, 47%.

Elemental Analysis: Calculated (%): C, 64.62; H, 6.34; N, 5.38. Found (%): C, 64.70; H, 6.25; N, 5.38.

3-(2,6-Diisopropylphenyl)-1-[3-(4,7-(dimethylindenyl)propyl]imidazol-2-ylidene chromium dichloride, 2.12
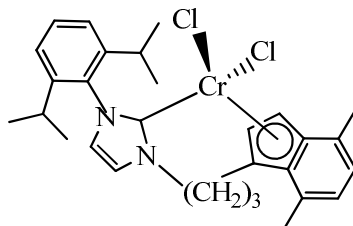
To a stirred solution of CrCl$_3$(THF)$_3$ (0.46 g, 1.2 mmol) in THF (30 mL) at -78 ºC a pre-cooled solution of L(3C)K (0.55 g, 1.2 mmol) in the same solvent (30 mL) was added *via* cannula. On mixing, the reaction mixture changed from purple to dark green. The mixture was allowed to warm to room temperature and stirred overnight. Evaporation of the volatile components under reduced pressure, extraction of the green residue in dichloromethane (3x 30 mL), filtration of the organic extracts through Celite and removal the solvent under reduce pressure gave the analytically pure product as dark green powder. The product was recrystallized from chloromethane/petrol. Yield: 0.36 g, 51%.

Elemental Analysis: Calculated(%): C, 65.17; H, 6.55; N, 5.24. Found (%): C, 65.10; H, 6.54; N, 5.30.

3-(2,6-Diisopropylphenyl)-1-[2-(4,7-dimethylindenyl)ethyl]-imidazol-2-ylidene chromium phenyl chloride, 2.14
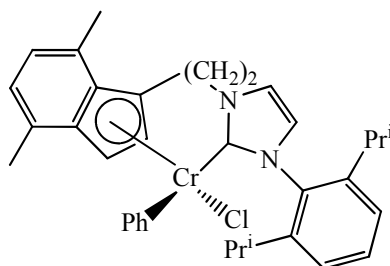
To a stirred solution of **2.11** (0.25 g, 0.5 mmol) in THF (10 mL) at -78 ºC a solution of diphenylmagnesium in THF (0.62 mL, 0.76M) was added. On completion of the addition the green mixture was allowed to warm up at -20 ºC and stirred at this temperature for 2h, the solution turned into dark red and it was stored at -25 ºC for two days. Volatile components were evaporated under reduced pressure. The red residue was extracted in cold dichloromethane (-78 ºC), filtered through Celite and dried under reduced pressure to afford the red analytically pure compound. Yield:

0.12 g, 41%. The solid was dissolved in toluene and kept at -30 ℃ for 1 week to afford red crystals.

Elemental Analysis: Calculated (%): C, 72.73; H, 6.77; N, 4.99. Found (%): C, 72.69; H, 6.83; N, 4.90.

3-(2,6-Diisopropylphenyl)-1-[2-(4,7-dimethylindenyl)ethyl]-imidazol-2-ylidene chromium methyl chloride, 2.15
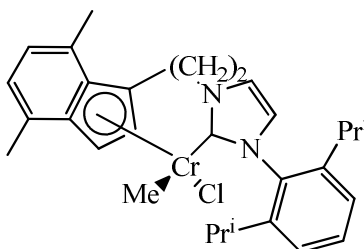
To a stirred solution of CrMeCl$_2$(THF)$_3$ [132] (0.31g, 0.87 mmol) in THF (20 mL) at -78 ℃ a pre-cooled solution of L(2C)K (0.38 g, 0.87 mmol) was added *via* cannula in the same solvent (20 mL). On completion of the addition the green mixture was stirred at this temperature for 1h. It was allowed to warm up at -20 ℃ and stirred for 4 h. The intense red solution was stored overnight at -25 ℃. Evaporation of the volatile components under reduced pressure, extraction of the red residue in cold toluene (3x 20mL, -78 ℃), filtration of the organic extracts through Celite, removal of the solvent under reduced pressure, washing the residue with cold petrol (2x 10 mL, -78 ℃) and drying the residue under vacuum gave the analytically pure product as a brown-red powder. The product was recrystallized by layering a concentrated THF solution with diethyl ether after 1 week at -25 ℃. Yield: 0.20g, *ca.* 60%.

Elemental Analysis: Calculated (%): C, 69.67; H, 7.21; N, 5.60. Found (%): C, 69.59; H, 7.17; N, 5.55.

3-(2,6-Diisopropylphenyl)-1-[3-(4,7-dimethylindenyl)propyl]-imidazol-2-ylidene chromium methyl chloride, 2.16
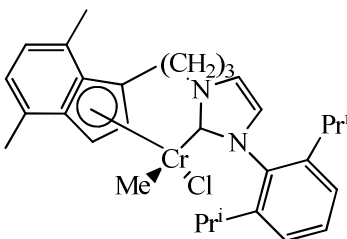
To a stirred solution of CrMeCl$_2$(THF)$_3$[132] (0.18g, 0.5 mmol) in THF (10 mL) at -78 ℃ a pre-cooled solution of L(3C)K (0.22 g, 0.5 mmol) was added *via* cannula in

the same solvent (10 mL). On completion of the addition the green mixture was stirred at this temperature for 1h. It was allowed to warm up at -20 ℃ and stirred for 4 h. The intense red solution was stored overnight at -25 ℃. Evaporation of the volatile components under reduced pressure, extraction of the red residue in toluene (40 mL), filtration of the organic extracts through Celite, removal of the solvent under reduce pressure, washing the residue with petrol (2x 10 mL) and drying the residue under vacuum gave the analytically pure product as a brown-red powder. Yield: 0.18g, 70%. The product was recrystallized by layering a concentrated THF solution with diethyl ether after 1 week at -25 ℃.

Elemental Analysis: Calculated (%): C, 70.10; H, 7.40; N, 5.45. Found (%): C, 69.95; H, 7.34; N, 5.38.

Synthesis of Cr(III) Cation: [L(2C)CrCl]⁺[BAr₄]⁻, 2.17
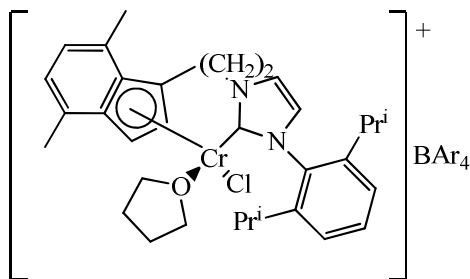
Methyl chloride chromium complex **2.15** (0.20g, 0.52 mmol) was dissolved in DCM/THF (15/0.5mL) and cooled down to -78 ℃. A solution of NaBAr₄ (B[(3,5-(CF₃)₂-C₆H₃)]₄)[134] (0.45g, 0.52 mmol) in DCM (15mL) was added to the purple solution at the same temperature. This mixture was allowed to warm up and it was stirred at room temperature for three days. The mixture turned into dark green. It was filtered through Celite, concentrated up to 5 mL, and layered with petrol (15 mL) to afford dark green crystals. Yield: 0.35g, 60%.

Elemental Analysis: Calculated (%): C, 64.32; H, 4.02; N, 2.50. Found (%): C, 64.22; H, 4.09; N, 2.40 (without THF molecule).

Synthesis of Cr(III) Cation: [L(3C)CrCl]⁺[BAr₄]⁻, 2.18
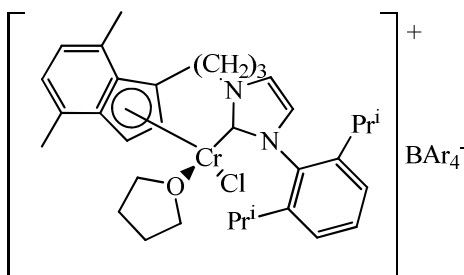
Methyl chloride chromium complex **2.16**, and NaBAr₄ (B[(3,5-(CF₃)₂-C₆H₃)]₄) (0.52g, 0.6 mmol) were both dissolved in DCM/THF (15/0.5mL) and cooled down at 78 ℃. The purple chromium solution was added to the white suspension at this temperature. This mixture was allowed to warm up and it was stirred at room temperature for three days. The mixture turned into dark green. The solution was filtered through Celite and concentrated up to 5 mL, layered with petrol to afford dark green crystals, which were characterised by single crystal X-ray diffraction. Yield: 0.44 g, ca. 54%.

Elemental Analysis: Calculated (%): C, 53.77; H, 3.45; N, 2.05. Found (%): C, 53.65; H, 3.57; N, 1.96 (without THF molecule).

3-(2,6-Diisopropyl-phenyl)-1-[2-(4, 7-dimethylindenyl)ethyl]-imidazol-2-ylidene chromium dibenzyl, 2.19
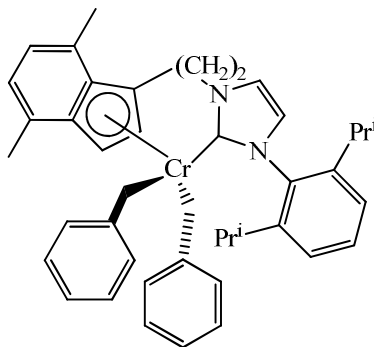
To a stirred solution of **2.11** (0.20 g, 0.38 mmol) in THF (10 mL) at -78 ℃ a solution of freshly made dibenzylmagnesium [133] in ether (6.4 mL, 0.06M) was added dropwise. On completion of the addition the green mixture was allowed to warm up to -30 ℃ and stirred at this temperature for 3h, the solution turned into dark violet and it was stored at -25 ℃ for two days. Volatile components were evaporated under reduced pressure. The violet residue was extracted in toluene (20 mL) and filtered through Celite. Toluene was evaporated under vacuum and the residue washed with petrol and dried under vacuum to give an analytically pure compound. Yield: 0.09g, 37 %. The

violet solid was dissolved in 5 mL of THF and layered with ether (10 mL) to give violet crystals after 1 week at -25 ºC.

Elemental Analysis: Calculated (%): C, 79.87; H, 7.45; N, 4.44. Found (%): C, 79.80; H, 7.52; N, 4.36.

Synthesis of Chromium (III) Cation: [L(2C)Cr(CH₂Ph)]⁺[BAr₄]⁻, 2.21

$$\text{Synthesis of Chromium (III) Cation: } [L(2C)Cr(CH_2Ph)]^+[BAr_4]^-, 2.21$$
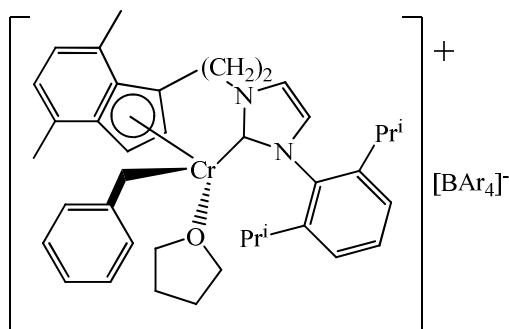
Dibenzyl chromium complex **2.19** (0.20g, 0.3 mmol) and H(Et₂O)₂BAr₄ (B[(3,5-(CF₃)₂-C₆H₃)]₄) [134] (0.33g, 0.3 mmol) were both dissolved in cold THF (20 mL, -78 ºC). Brookhart's acid solution at -78 ºC was added *via* cannula to the violet solution of the chromium starting material at the same temperature. The mixture turned to orange, it was stirred at this temperature for 2 h and kept at -30 ºC overnight. Volatile components were removed under reduced pressure and the brown residue was washed with cold petrol (2x 15 mL, -78 ºC) and dried under vacuum. A good crop of very fine plates was isolated after crystallisation in a concentrated solution in diethyl ether at -30 ºC, (15 mL). The crystals were selected and the data was collected at low temperature (-100 ºC). Unfortunally this data set is not very good due to partial decomposition during the data collection.

3-(2,6-Diisopropyl-phenyl)-1-[2-(4, 7-dimethylindenyl)ethyl]-imidazol-2-ylidene chromium monochloride, 2.21
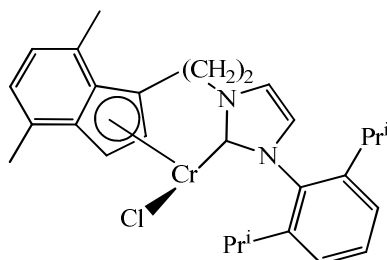
To a stirred suspension of CrCl₂ (0.06g, 0.5 mmol) in THF (10 mL) at -78 ºC a pre-cooled solution of L(2C)K (0.200g, 0.5mmol) was added *via* cannula in the same solvent (20 mL). The yellow suspension was allowed to warm to room temperature

and stirred for 3 hours. The mixture turned into an olive green solution after this period. This solution was concentrated under reduce pressure and cooled down over a week at -30 ºC to afford light brown crystals. Yield: 0.100 g, 42%.

Anal. Calculated (%): C, 69.35; H, 6.81; N, 5.78. Found (%): C, 69.26; H, 6.83; N, 5.69

2.7 Catalysis Experiments

2.7.1 General Considerations

Catalytic testing of complexes **2.8**, **2.9**, **2.10**, **2.11**, **2.12**, **2.16**, **2.23** and **2.24** for the ethylene polymerization was conducted in glass or steel autoclaves (Figure 2.19) for 8 bar or 40 bar experiments respectively. The reactors are equipped with mechanical stirring under a continuous feed of ethylene. MMAO-3A was employed as co-catalyst in all the experiments.

Figure 2.19: Steel autoclave for high-pressure (40 bar) catalytic tests.

2.7.2 Protocol for Autoclave Test

The valve was set at 8 bar and the system was flushed with ethylene for 2 minutes and then with argon for 2 more minutes. Once the system is free of oxygen and moisture, the mechanical stirrer is heated with a heat gun for 5 minutes before the vessel is connected. Once the vessel is on, the system is evacuated and refilled with argon three times. Toluene (70 mL) is added to the autoclave. Positive argon pressure in the reactor is vented out and then a solution of catalyst in toluene is injected *via* syringe through a ball valve equipped with septum. The vessel was then brought to the required reaction temperature and allowed to stabilise at this value, whilst stirring. The reactor is filled with ethylene (10 bar) and stirred for 10 minutes to saturate the catalyst solution with ethylene. The head space was then vented and the required amount of MMAO-3A added. Immediately, thereafter the autoclave was pressurised with ethylene to the required pressure and stirred at 1000 rpm. Cooling/heating was applied as necessary to control any exothermic process and maintain the autoclave at constant temperature throughout the run. Ethylene uptake was monitored *via* mass

96

flow meter and logged to PC. The reaction was allowed to run as long as ethylene uptake was evident, or if no ethylene uptake was evident from the start, the run was continued for 10 minutes. To terminate the run, the ethylene supply was isolated, and the autoclave cooled to 10 ºC as fast as possible. The excess ethylene pressure was then vented and ethanol (10 mL) added to quench the residual pyrophoric materials. Nonane (1 mL) was added *via* electronic pipette as calibration standard for the liquid faction. The liquid faction was then extracted with 10% HCl (aq), and a sample of the organic fraction taken for GC analysis (PONA column). Any polymer produced was recovered, extracted with 1:1:1, 10% HCl (aq): ethanol : toluene, and then collected by filtration, dried and weighed.

2.7.3 Conditions of the Catalyst Tests

Table 2.2: Conditions of the catalytic tests for complexes **2.8**, **2.9**, **2.10**, **2.11**, **2.12**, **2.16**, **2.23** and **2.24** for ethylene polymerization.

Experiment code	Catalyst	Pre-catalyst (μmol)	Solvent (mL)	Equivalents MMAO-3A	T/ºC	P (bar)
C1	**2.24**	20	52	1000	20	8
C2	**2.24**	20	50	500	60	40
C3	**2.23**	5	70	1000	20	8
C4	**2.23**	10	70	500	60	40
C5	**2.23**	20	52	1000	20	8
C6	**2.8**	10	70	1000	20	8
C7	**2.8**	10	70	500	60	40
C8	**2.9**	10	70	1000	20	8
C9	**2.9**	10	70	500	60	40
C10	**2.10**	10	70	1000	20	8
C11	**2.10**	10	70	500	60	40
C12	**2.11**	5	74	500	20	8
C13	**2.11**	5	74	500	60	40
C14	**2.12**	5	74	500	20	8
C15	**2.12**	5	74	500	60	40
C16	**2.16**	5	74	500	20	8
C17	**2.16**	5	74	500	60	40

2.7.4 Towards the Synthesis of Imidazolium linked to Cyclopentadiene or Tetramethylcyclopentadiene Moiety

Thiourea 2.30
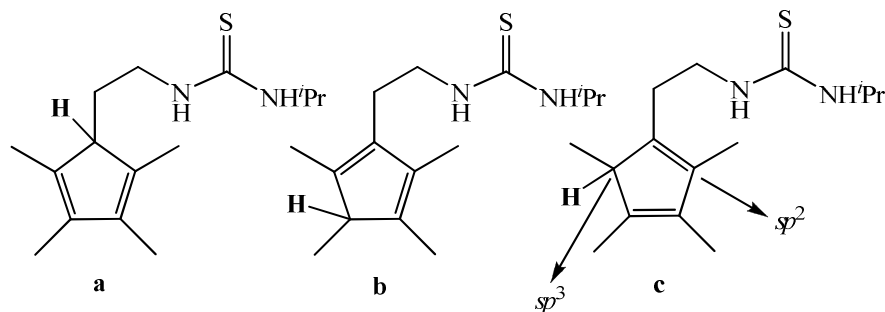
endocyclic isomers

Compound ^{i}PrN=C=S (0.43, 4.3 mmol) and mixture of endocyclic isomers **2.29** (0.70, 4.3 mmol) were both heated at 80 °C for two days in ethanol (20 mL). Ethanol was removed under reduce pressure and the solid was precipitated with petroleum to give white crystals of a mixture of exclusively endocyclic isomers **2.30**. Yield: 0.18g, 15%.

^{1}H-NMR(CDCl$_3$, 300 MHz): 5.33 (d, J=6.0 Hz, N-H); 4.60(d of sept, J= 6.5Hz, CH(CH$_3$)$_2$, a, b, c); 4.22(ddd, J=4.0, CH_2 bridge, b and c); 3.71(1H, dddd, J=7.0, CH_2 bridge, b and c); 2.30(m, H-Cp*, b and c); 2.10(m, H-Cp*, a); 1.93(m, CH_2 bridge, a); 1.75(s, Cp*(sp^2)-CH$_3$); 1.58(m, CH_2 bridge, a); 1.50(s, Cp*(sp^2)-CH$_3$); 1.46(s, Cp*(sp^2)-CH$_3$); 1.20(d, J=6.5Hz, CH(CH_3)$_2$); 1.18(d, J=6.5Hz, CH(CH_3)$_2$); 098(d, J=7.0Hz, Cp*(sp^3)-CH$_3$, b and c).

^{13}C{^{1}H}-NMR (CDCl$_3$, 75 MHz): 181.8; 178.3; 142.9; 131.5; 77.8; 77.4; 77.1; 62.9; 54.7; 47.6; 46.1; 40.5; 26.2; 23.7; 23.3; 22.9; 21.8; 18.5; 13.9; 12.9.

M.S. ES$^+$: 431 (M=Cp*-CH$_2$CH$_2$NH$_2$)$^+$.

5-(2-chloroethyl)- 1, 2, 3, 4-tetramethylcyclopentadiene, 2.36a
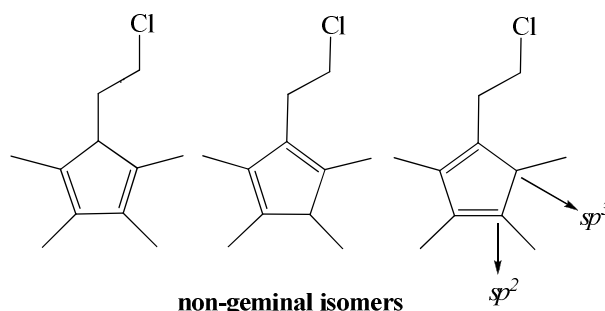
non-geminal isomers

1, 2, 3, 4-Tetramethylcyclopentadiene (4,00g, 32.8 mmol) in petrol (350mL) was reacted with n-BuLi (2.5 M, 13.2mL, 32.8 mmol) at 0 °C. The mixture was stirred at

this temperature for 1 h and allowed warm up until room temperature overnight. 1-bromo- 2-chloroethane (2.73 mL, 32.8 mmol) was added and the mixture stirred at room temperature for 4 weeks. The white suspension was allowed to settle and the petrol solution was decanted *via* cannula, washed with water, dried over $MgSO_4$ and dried under vacuum to afford light yellow oil. The addition of another equivalent of 1-bromo,2-chloroethane (2.73 mL, 32.8 mmol) to the remaining white petrol suspension followed the work up described above gave a second crop of product. Total Yield: 4.80 g, 80%.

^{1}H NMR (C_6D_6, 300 MHz): 2.90(2H, dd, *J*= 7.5Hz, C*H*$_2$ bridge); 2.35 (1H, broad singlet, Cp*-*H*); 2.05-1.95(2H, m, C*H*$_2$ bridge); 1.55(s, Cp*(sp^2)-CH$_3$), 0.80(s, Cp*(sp^3)-CH$_3$); 0.70(s, Cp*(sp^3)-CH$_3$).

^{13}C{^{1}H}-NMR (C_6D_6, 75 MHz)(main isomer): 131.6; 130.2; 53.7; 39.5; 30.8; 10.2; 10.7.

Gas chromatography EI-MS: *m/z* = 184 (M)$^+$; (rt*, % non-geminal isomer): 6.69 min, 10%; 6.80 min, 10%; 7.22min, 80%.

* rt= retention time (min).

5-(3-chloropropyl) 1, 2, 3, 4-tetramethylcyclopentadiene, 2.43
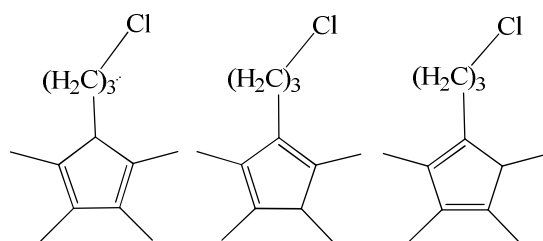
non-geminal isomers

1, 2, 3, 4-tetramethylcyclopentadiene (4.18g, 34.3 mmol) in petrol (150mL) was reacted with *n*-BuLi 2.5 M (13.7mL, 34.3 mmol) at 0°C. The mixture was stirred at this temperature for 1 h and allowed warm up until room temperature overnight. 1-bromo- 3-chloropropane (3.4 mL, 34.3 mmol) was added and the mixture was stirred at room temperature for 4 weeks. The white suspension was allowed to settle and an aliquot of the petrol solution was submitted for gas chromatography mass spectrometry which showed that all 1-bromo, 3-chloropropane was totally consumed therefore the reaction was completed. The petrol solution was decanted, washed with

water and dried over $MgSO_4$. Solvent was removed under reduce pressure to give a yellow oil. Yield: 2.50 g, 37%.

^{1}H NMR (C_6D_6, 300 MHz): 3.27-3.16 (2H, m, CH_2 bridge); 2.57-2.49 (1H, broad m, Cp*-H); 1.88-1.66 (12H, m, Cp*(sp^2)-CH_3); 1.55-1.36 (1H, m, CH_2 bridge)1.27-1.21 (1H, m, CH_2 bridge); 1.06-0.96(2H, ddd, J= 7. 9Hz, CH_2 bridge); 0.39 (<1H, d, J= 2.1, Cp*(sp^3)-CH_3).

Gas chromatography EI-MS: m/z = 198 (M)$^+$; (rt*, % non-geminal isomer): 7.24min, 6.5%; 7.45min, <0.1%; 7.58 min, 93.5 %.

* rt= retention time (min).

2.7.5 Crystallographic Parameters for Compounds in this Chapter

Table 2.3: Crystallographic parameters for complexes **2.8** and **2.9**.

Identification code	2.8	2.9
Empirical formula	$C_{32}H_{42}ClN_3Ti$	$C_{33}H_{44}ClN_3Ti$
Formula weight	552.04	566.06
Temperature	120(2) K	120(2) K
Wavelength	0.6911 Å	0.71073 Å
Crystal system	Monoclinic	Monoclinic
Space group	$P2_1/n$	$P2_1/n$
Unit cell dimensions	a = 10.572(3) Å	a = 10.5872(2) Å
	$\alpha = 90°$	$\alpha = 90°$
	b = 20.095(5) Å	b = 16.7943(4) Å
	$\beta = 106.194(3)°$	$\beta = 96.8550(10)°$
	c = 15.921(4) Å	c = 17.7951(5) Å
	$\gamma = 90°$	$\gamma = 90°$
Volume	3248.1(15) Å^3	3141.43(13) Å^3
Z	4	4
Density (calculated)	1.129 Mg/m^3	1.197 Mg/m^3
Absorption coefficient	0.368 mm^{-1}	0.382 mm^{-1}
F(000)	1176	1208
Crystal size	0.08 x 0.01 x 0.01 mm^3	0.20 x 0.20 x 0.16 mm^3
Theta range for data collection	3.23 to 24.29°	3.08 to 27.57°
Index ranges	-12<=h<=12	-13<=h<=13
	-23<=k<=23	-21<=k<=21
	-18<=l<=18	-23<=l<=23
Reflections collected	23537	36159
Independent reflections	5682 [$R(int)$ = 0.0472]	7204 [$R(int)$ = 0.0550]
Completeness to theta = 24.29°	99.1 %	99.2 %
Absorption correction	Semi-empirical from equivalents	Semi-empirical from equivalents
Max. and min. transmission	0.9963 and 0.9711	0.9433 and 0.9284
Refinement method	Full-matrix least-squares on F^2	Full-matrix least-squares on F^2
Data / restraints / parameters	5682 / 12 / 350	7204 / 0 / 352
Goodness-of-fit on F^2	1.045	1.079
Final R indices [I>2sigma(I)]	$R1$ = 0.0680, $wR2$ = 0.1946	$R1$ = 0.0565, $wR2$ = 0.1039
R indices (all data)	$R1$ = 0.0803, $wR2$ = 0.2051	$R1$ = 0.0802, $wR2$ = 0.1162
Largest diff. peak and hole	0.967 and -0.382 e.Å^{-3}	0.359 and -0.354 e.Å^{-3}

Table 2.4: Crystallographic parameters for complexes **2.11** and **2.12**

Identification code	**2.11**	**2.12**
Empirical formula	$C_{28}H_{32}Cl_2CrN_2$	$C_{29}H_{35}Cl_2CrN_2$
Formula weight	519.46	534.49
Temperature	153(2) K	120(2) K
Wavelength	0.71073 Å	0.71073 Å
Crystal system	Monoclinic	Monoclinic
Space group	$P2_1/c$	$P2_1/c$
Unit cell dimensions	a = 15.5966(2) Å	a = 12.7984(5) Å
	$\alpha = 90°$	$\alpha = 90°$
	b = 10.60350(10) Å	b = 7.4565(3) Å
	$\beta = 109.6820(10)°$	$\beta = 98.134(2)°$
	c = 16.5766(2) Å	c = 28.4004(11) Å
	$\gamma = 90°$	$\gamma = 90°$
Volume	2581.25(5) Å³	2683.02(18) Å³
Z	4	4
Density (calculated)	1.337 Mg/m³	1.323 Mg/m³
Absorption coefficient	0.669 mm⁻¹	0.646 mm⁻¹
$F(000)$	1088	1124
Crystal size	0.16 x 0.04 x 0.02mm³	0.18 x 0.15 x 0.07 mm³
Theta range for data collection	3.10 to 29.38°	2.90 to 27.61°
Index ranges	-19<=h<=21	-16<=h<=16
	-13<=k<=13	-9<=k<=9
	-20<=l<=19	-36<=l<=36
Reflections collected	30438	22543
Independent reflections	5900 [$R(int)$ = 0.0331]	6070 [$R(int)$ = 0.0599]
Completeness to theta = 27.50°	95.5 %	98.1 %
Absorption correction	Semi-empirical from equivalents	
Max. and min. transmission	0.9867 and 0.9005	0.9562 and 0.8926
Refinement method	Full-matrix least-squares on F^2	Full-matrix least-squares on F^2
Data / restraints / parameters	5900 / 0 / 304	6070 / 0 / 313
Goodness-of-fit on F^2	1.079	1.079
Final R indices [I>2sigma(I)]	$R1$ = 0.0412, $wR2$ = 0.0985	$R1$ = 0.0690, $wR2$ = 0.1645
R indices (all data)	$R1$ = 0.0501, $wR2$ = 0.1047	$R1$ = 0.0855, $wR2$ = 0.1781
Largest diff. peak and hole	0.941 and -0.510 e.Å⁻³	0.735 and -0.549 e.Å⁻³

Table 2.5: Crystallographic parameters for complexes **2.14** and **2.15**.

Identification code	2.14	2.15
Empirical formula	$C_{34}H_{38}ClCrN_2$	$C_{31}H_{40}ClCrN_2O_{0.5}$
Formula weight	562.11	536.10
Temperature	120(2) K	153(2)K
Wavelength	0.6939 Å	0.71073 Å
Crystal system	Monoclinic	Orthorhombic
Space group	*P2₁/n*	*Pbcn*
Unit cell dimensions	a = 10.211(2) Å	a = 23.7359(11) Å
	$\alpha = 90°$	$\alpha = 90°$
	b = 21.900(4) Å	b = 16.9318(8) Å
	$\beta = 107.40(3)°$	$\beta = 90°$
	c = 15.640(3) Å	c = 14.8727(6) Å
	$\gamma = 90°$	$\gamma = 90°$
Volume	3337.4(11) Å³	5728.1(5) Å³
Z	4	4
Density (calculated)	1.119 Mg/m³	1.243 Mg/m³
Absorption coefficient	0.445 mm⁻¹	0.516 mm⁻¹
F(000)	1188	2280
Crystal size	0.05 x 0.03 x 0.02 mm³	0.20 x 0.18 x 0.08 mm³
Theta range for data collection	2.97 to 25.03°	2.94 to 25.03°
Index ranges	-12<=*h*<=12	-27<=*h*<=27
	-26<=*k*<=26	-20<=*k*<=20
	-18<=*l*<=18	-17<=*l*<=17
Reflections collected	24219	94641
Independent reflections	5875 [*R(int)* = 0.0619]	5048 [*R(int)* = 0.1598]
Completeness to theta = 25.03°	99.7 %	99.8 %
Absorption correction	Semi-empirical from equivalents	Semi-empirical from equivalents
Max. and min. transmission	0.9956 and 0.9824	0.9599 and 0.9038
Refinement method	Full-matrix least-squares on F^2	Full-matrix least-squares on F^2
Data / restraints / parameters	5875 / 44 / 358	5048 / 6 / 315
Goodness-of-fit on F^2	1.111	1.145
Final *R* indices [I>2sigma(I)]	*R1* = 0.0886, *wR2* = 0.2662	*R1* = 0.1005, *wR2* = 0.2529
R indices (all data)	*R1* = 0.1222, *wR2* = 0.2881	*R1* = 0.1367, *wR2* = 0.2736
Largest diff. peak and hole	1.955 and -0.851 e.Å⁻³	1.276 and -1.078 e.Å⁻³

Table 2.6: Crystallographic parameters for complexes **2.18** and **2.19**.

Identification code	2.18	2.19
Empirical formula	$C_{65}H_{55}BClCrF_{24}N_2O$	$C_{42}H_{46}CrN_2$
Formula weight	1434.37	631.19
Temperature	120(2) K	120(2) K
Wavelength	0.71073 Å	0.6939 Å
Crystal system	Hexagonal	Monoclinic
Space group	*P3(2)*	*P2₁/n*
Unit cell dimensions	a = 12.747 Å	a = 25.109(5) Å
	$\alpha = 90°$	$\alpha = 90°$
	b = 12.747 Å	b = 11.132(2) Å
	$\beta = 90°$	$\beta = 91.81(3)°$
	c = 33.708 Å	c = 25.214(5) Å
	$\gamma = 120°$	$\gamma = 90°$
Volume	4743.3 Å^3	7044(2) Å^3
Z	3	8
Density (calculated)	1.506 Mg/m^3	1.190 Mg/m^3
Absorption coefficient	0.339 mm^{-1}	0.356 mm^{-1}
F(000)	2187	2691
Crystal size	0.2 x 0.2 x 0.2 mm^3	0.16 x 0.08 x 0.04 mm^3
Theta range for data collection	3.04 to 27.48°	2.44 to 25.03°
Index ranges	$-13<=h<=15$	$-29<=h<=29$
	$-16<=k<=16$	$-13<=k<=13$
	$-43<=l<=43$	$-30<=l<=29$
Reflections collected	38964	50503
Independent reflections	14364 [R*(int)* = 0.1422]	12416 [R*(int)* = 0.0800]
Completeness to theta = 27.48°	99.7 %	99.8 %
Absorption correction	Semi-empirical from equivalents	Semi-empirical from equivalents
Max. and min. transmission	0.9966 and 0.9254	0.9965 and 0.9894
Refinement method	Full-matrix least-squares on F^2	Full-matrix least-squares on F^2
Data / restraints / parameters	14364 / 361 / 863	12416 / 12 / 791
Goodness-of-fit on F^2	0.902	0.732
Final *R* indices [I>2sigma(I)]	*R1* = 0.0987, wR2 = 0.2517	*R1* = 0.0619, wR2 = 0.1726
R indices (all data)	*R1* = 0.2183, wR2 = 0.3342	*R1* = 0.0886, wR2 = 0.1973
Absolute structure parameter	0.08(5)	
Largest diff. peak and hole	0.934 and -0.863 e.Å^{-3}	0.608 and -0.559 e.Å^{-3}

Table 2.7: Crystallographic parameters for complexes **2.20** and **2.21**.

Identification code	2.20	2.21
Empirical formula	$C_{76}H_{74}BCrF_{24}N_2O_3$	$C_{56}H_{66}Cl_2Cr_2N_4$
Formula weight	1582.18	970.03
Temperature	120(2) K	393(2) K
Wavelength	0.71073 Å	0.71073 Å
Crystal system	Triclinic	Monoclinic
Space group	$P-1$	$P2_1/c$
Unit cell dimensions	a = 12.6125(14) Å	a = 14.1911(5) Å
	α = 107.063(6)°	α = 90°
	b = 15.1254(13) Å	b = 22.6160(7) Å
	β = 93.236(4)°	β = 89.983(2)°
	c = 21.731(2) Å	c = 15.8258(5) Å
	γ = 97.023(5)°	γ = 90°
Volume	3914.8(7) Å^3	5079.2(3) Å^3
Z	2	4
Density (calculated)	1.342 Mg / m^3	1.269 Mg/m^3
Absorption coefficient	0.249 mm^{-1}	0.573 mm^{-1}
F(000)	1626	2048
Crystal size	$0.13 \times 0.1 \times 0.01$ mm^3	0.22 x 0.20 x 0.20 mm^3
θ range for data collection	2.93 − 25.03°	2.95 to 27.54°
Index ranges	-15<=h<=15	-18<=h<=18
	-18<=k<=18	-27<=k<=29
	-25<=l<=25	-20<=l<=20
Reflections collected	45372	47441
Independent reflections	13462 [$R(int) = 0.1316$]	11578 [$R(int) = 0.0931$]
Completeness to θ = 25.03°	97.5 %	99.1 %
Absorption correction	Semi−empirical from equivalents	Semi-empirical from equivalents
Max. and min. transmission	0.9975 and 0.9583	0.8940 and 0.8842
Refinement method	Full-matrix least-squares on F^2	Full-matrix least-squares on F^2
Data / restraints / parameters	13462 / 956 / 800	11578 / 0 / 590
Goodness-of-fit on F^2	1.022	1.032
Final R indices [$F^2 > 2\sigma(F^2)$]	$R1 = 0.1848$, $wR2 = 0.3875$	$R1 = 0.0615$, $wR2 = 0.1122$
R indices (all data)	$R1 = 0.3364$, $wR2 = 0.4833$	$R1 = 0.1098$, $wR2 = 0.1282$
Largest diff. peak and hole	0.871 and −0.797 e Å^{-3}	0.430 and -0.570 e.Å^{-3}

Table 2.8: Crystallographic parameters for complex **2.22** and compound **2.5**.

Identification code	2.22	2.5 L(3C)Br
Empirical formula	$C_{56}H_{66}Cl_2Cr_2N_4O$	$C_{29}H_{37}BrN_2$
Formula weight	986.03	493.52
Temperature	120(2) K	120(2) K
Wavelength	0.71073 Å	0.71073 Å
Crystal system	Cubic	Monoclinic
Space group	*Ia-3*	*P2$_1$/n*
Unit cell dimensions	a = 31.7161(7) Å	a = 8.2359(4) Å
	$\alpha = 90°$	$\alpha = 90°$
	b = 31.7161(7) Å	b = 29.5962(13) Å
	$\beta = 90°$	$\beta = 91.485(2)°$
	c = 31.7161(7) Å	c = 11.8613(5) Å
	$\gamma = 90°$	$\gamma = 90°$
Volume	31903.6(12) Å^3	2890.2(2) Å^3
Z	24	4
Density (calculated)	1.232 Mg/m^3	1.134 Mg/m^3
Absorption coefficient	0.550 mm^{-1}	1.439 mm^{-1}
F(000)	12480	1040
Crystal size	0.16 x 0.15 x 0.13 mm^3	0.30 x 0.10 x 0.01 mm^3
Theta range for data collection	3.01 to 25.01°	3.05 to 25.03°
Index ranges	0<=*h*<=26	-9<=h<=9
	0<=*k*<=26	-35<=k<=35
	3<=*l*<=37	-14<=l<=14
Reflections collected	4696	21914
Independent reflections	4696 [*R(int)* = 0.0000]	5065 [*R(int)* = 0.0804]
Completeness to theta = 25.01°	99.8 %	99.3 %
Absorption correction	Semi-empirical from equivalents	Semi-empirical from equivalents
Max. and min. transmission	0.9319 and 0.9271	0.9858 and 0.6721
Refinement method	Full-matrix least-squares on F^2	Full-matrix least-squares on F^2
Data / restraints / parameters	4696 / 0 / 300	5065 / 36 / 301
Goodness-of-fit on F^2	1.037	1.121
Final *R* indices [I>2sigma(I)]	*R1* = 0.1150, *wR2* = 0.2564	*R1* = 0.0895, *wR2* = 0.1997
R indices (all data)	*R1* = 0.2105, *wR2* = 0.2916	*R1* = 0.1293, *wR2* = 0.2251
Largest diff. peak and hole	0.481 and -0.492 e.Å^{-3}	1.182 and -0.674 e.Å^{-3}

Chapter 3 Synthesis, Characterisation and Reactivity of Tribenzyl Chromium *tris*(Tetrahydrofuran)

3.1 Introduction

In the past few decades a large amount of effort has been made in order to synthesise alkyl and aryl chromium complexes.[135] The first fully characterised triaryl chromium (III) complex, triphenyl chromium *tris*(tetrahydrofuran), was synthesised for the first time in 1957 by Zeiss. [136] The preparation was carried out at low temperature by adding three equivalents of phenylmagnesium bromide to chromium trichloride in THF.

3.1
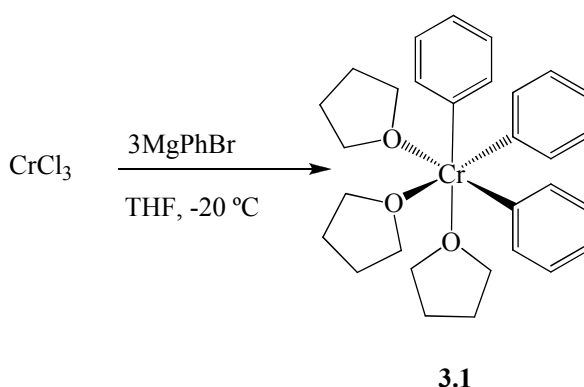
Scheme 3.1: Synthesis of triphenylchromium tris(tetrahydrofuran) by Zeiss.

This complex was isolated as very air and thermally sensitive blood red crystals. This complex loses tetrahydrofuran when it is heated at atmospheric pressure, also under vacuum at room temperature and by washing with diethyl ether. The resulting product is a black unidentified solid.

The structure of complex **3.1** was elucidated by crystallographic techniques in 1983 by Bau. [137] This complex adopts an octahedral geometry with three σ-bonded phenyl ligands in *fac* configuration and three THF molecules bonded through the oxygen atom occupying the remaining positions. It is interesting that the six ligands are arranged in three mutually perpendicular planes: each opposing pair of Ph and THF ligands are approximately coplanar and are perpendicular to the other two Ph/THF planes.

The Cr-C bond lengths [2.060 (10) Å] are significantly shorter than the Cr-O bonds [2.225(10) Å], probably due to the presence of π-back-bonding provided by the soft phenyl ligands as opposed to the lack of such interactions for the hard THF ligands.

The synthesis of trialkyl chromium complexes is believed to be significantly more difficult than the triaryl chromium complexes, due to the weaker Cr-(sp^3)C bond

compared to Cr-C(sp^2). As a consequence the synthesis and characterisation of trialkylchromium complexes has been unsuccessful and no examples have been reported to date.

There are only a few examples in which alkylcomplexes have been synthesised and characterised. For example, the synthesis of dichloromethyl chromium complex by reaction of CrCl$_3$ with methylmagnesium chloride in THF was reported briefly for the first time by Kurras. [138]

Other example of methyl chromium complexes containing lithium have been also reported [139] as well as the synthesis of alkylcyclopentadienyl dinitrosyl chromium CpCr(NO)$_2$R, (R= CH$_3$, C$_2$H$_5$). [140]

Nishimura [141] and co-workers reported for the first time a method to synthesise alkylchromium dichloride complexes by reaction of CrCl$_3$THF$_3$ with an excess of an organoaluminium compound (AlR$_3$ or AlR$_2$OEt, R= CH$_3$, C$_2$H$_5$, n-C$_3$H$_7$ and i-C$_4$H$_9$) as shown in Scheme 3.2.

These complexes act as a Ziegler-type initiator in the polymerisation of ethylene under mild conditions. The catalytic activities, as well as the thermal stability, decreased the in order: methyl>ethyl>propyl>isobutyl. The preparation of these complexes is accompanied by the formation of CrCl$_2$ and evolution of gas (methane, ethane, propane or butane) as a consequence of the partial decomposition of the monoalkyl chromium complexes.

3.2　　　　　**3.3**
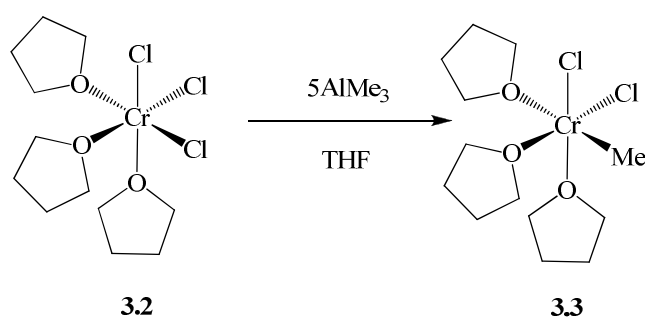
Scheme 3.2: Synthesis of dichloromethyl chromium *tris*(tetrahydrofuran) by Nishimura.

There are some examples of the preparation of dialkyl chromium complexes by reaction of CrCl$_3$(THF)$_3$ with Grignard reagents, [142] but the separation of these complexes from the magnesium salts was reported to be difficult.

The first trialkylchromium complex is reported now in this thesis. Tribenzyl chromium *tris*(tetrahydrofuran) has been characterised by single crystal X-ray diffraction and the synthesis is described in detail in this chapter. The reactivity of this interesting complex has also been tested by using a wide range of ligands in order to substitute the THF molecules and the results are also described in detail below.

3.2 Results and Discussion

The synthesis of trialkyl and triaryl chromium complexes has been an important topic in organometallic research for the past decades as discussed above. These complexes tend to be difficult to isolate. In the first place the separation of the desired complex from the side products of the reaction (Mg or Al salts) is reported to be very difficult and impossible in some cases. Another difficulty is that they are extremely sensitive to air and moisture, with the additional inconvenience of being also thermally unstable and contain coordinating solvent molecules which are labile under vacuum.

Tribenzyl chromium *tris*(tetrahydrofuran) **3.4** shown in Scheme 3.3 below has been synthesised by reaction at low temperature of Cr(acac)$_3$ in THF with slight excess of freshly prepared dibenzyl magnesium solution in ether. Complex **3.4** can be crystallised at -30 ℃ from the reaction mixture if the THF and ether are in the right ratio (see experimental details) to give orange needles. The greater yield is obtained by dissolving Cr(acac)$_3$ (0.24g) in 5 mL of THF and using 15mL of dibenzylmagnesium (0.07 M) in diethyl ether. Any attempt of scaling up the reaction was unsuccessful until the point that any crystals were isolated with 1.00 g of Cr(acac)$_3$ dissolved in different amounts of THF after a week at -30 ℃.

Since complex **3.4** is extremely thermally unstable it was not possible to weigh accurately the mass produced during the reaction and after the crystallisation of this compound. Therefore in the reactions described below amounts of **3.4** were estimated and ligands were used in excess.

3.4
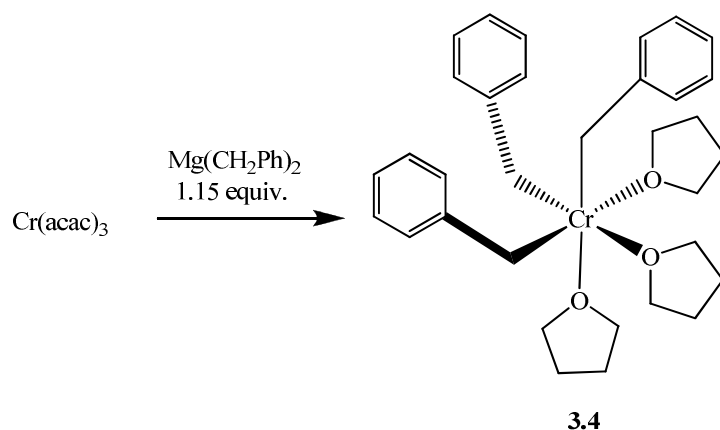
Scheme 3.3: Synthesis of the new Cr(III) trialkyl complex **3.4**.

The structure of complex **3.4** shown in Figure 3.1 was elucidated by crystallographic techniques. Due to its thermal instability crystal selection and data collection were

carried out at low temperatures. It adopts a distorted octahedral geometry with *fac* benzyl groups. The three THF molecules are bonded through the oxygen atom in the remaining octahedral positions. The Cr-C bond distances [2.142(6) Å, 2.138(6) Å and 2.144(6) Å] are very similar, within the measured estimated standard deviations, and they are within the observed range in the literature for Cr-C σ-bonds. [76(a), 115,119] The C-Cr bonds are significantly longer than in the analogue $Cr(Ph)_3(THF)_3$ **3.1**, a fact that corroborates that σ-Cr-C(sp^3) bonds are weaker than σ-Cr-C(sp^2) bonds.

THF groups showed disorder in the structure. The Cr-O distances [2.206(4) Å, 2.191(4) Å and 2.225(4) Å] are within the expected value for Cr-O(THF) bond lengths reported in the literature for THF groups in *trans* to Cr-C σ-bonds [143] and they compare well with the Cr-O distances for **3.1**. The Cr-O bond lengths for **3.4** are longer than in Cr(III) cations reported in the literature [119] and cations **2.18** and **2.20** described in chapter 2. This may be due to the fact that **3.4** is a neutral complex and also for the *trans* effect produced by the benzyl groups.

Cr-C-C bond angles [120.5(4)°, 117.5(4)° and 119.2(4)°] are similar to the corresponding bond angles for dibenzyl chromium compound **2.19** [120.43(4)° and 114.88(4)°] described in chapter 2.

The fact that complex **3.4** has *fac* orientation of the labile THF groups makes the complex a potentially good starting material for the synthesis of other Cr complex by substitution of the THF molecules.

Bond Distances (Å)	
Cr(1)-C(1)	2.142(6)
Cr(1)-C(8)	2.138(6)
Cr(1)-C(15)	2.144(6)
Cr(1)-O(1)	2.206(4)
Cr(1)-O(2)	2.191(4)
Cr(1)-O(3)	2.225(4)
Angles (°)	
C(1)-Cr(1)-C(8)	89.7(2)
C(1)-Cr(1)-O(2)	94.3(2)
C(1)-Cr(1)-C(15)	88.2(2)
Cr(1)-C(1)-C(2)	120.5(4)
Cr(1)-C(8)-C(9)	117.5(4)
Cr(1)-C(15)-C(16)	119.2(4)
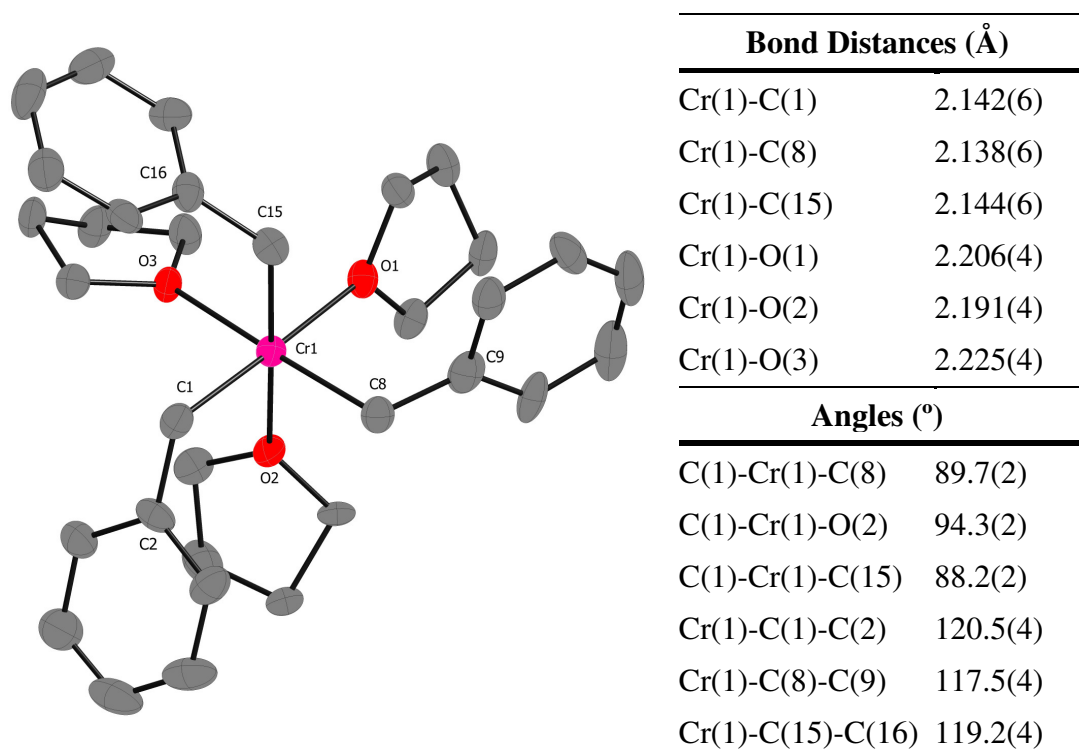
Figure 3.1: CrystalMaker representation of complex **3.4**. Thermal ellipsoids at 50% probability. Hydrogen atoms have been omitted for clarity. Only one disordered THF is shown (O2). Selected bond lengths (Å) and angles (deg) with estimated standard deviations on the right of the diagram.

The reactivity of complex **3.4** has been studied and it is described in detail bellow:

Attempts to react imidazolium salt **2.1** with **3.4** in THF in order to synthesise the dibenzyl chromium complex **2.19** were made. It was thought that the ligand would be deprotonated in at least one position (C2-imidazolium proton or/and 5-membered indenyl ring) by the tribenzyl chromium complex **3.4** with the subsequent formation of toluene. However no reaction was observed on stirring the mixture first at low temperature and then at room temperature and the imidazolium salt was recovered unreacted as is shown in Scheme 3.4.
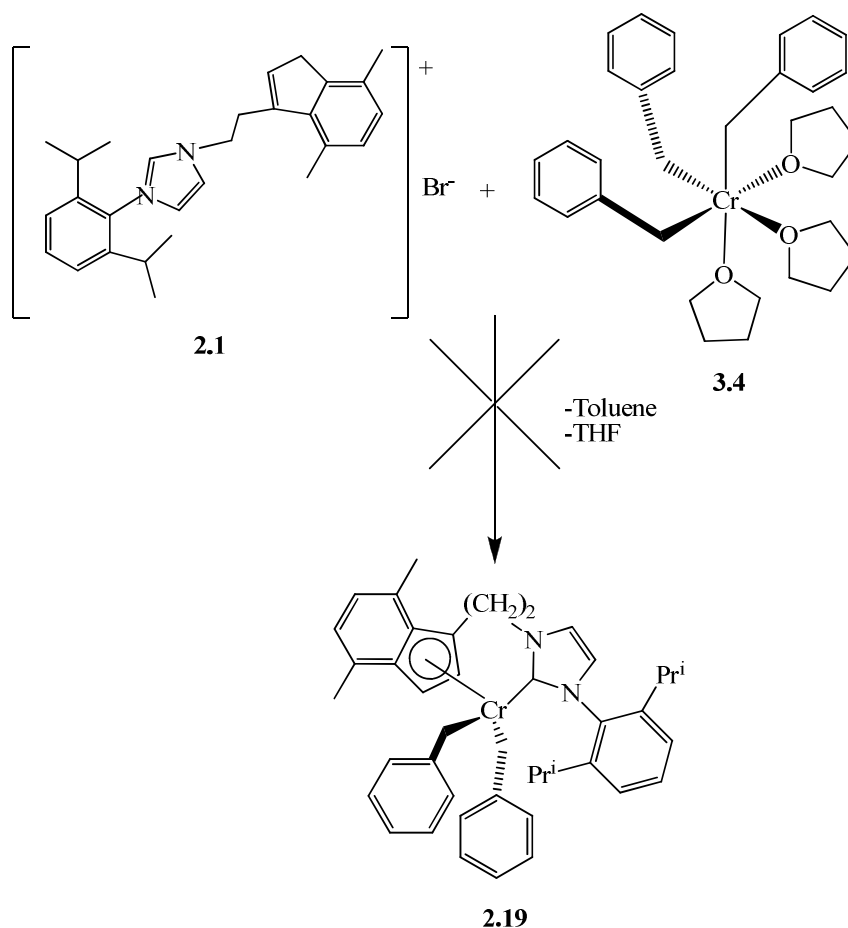
Scheme 3.4: Attempted synthesis of **2.19** by reaction of the imidazolium salt **2.1** with tribenzyl chromium **3.4**. Note: Complex **2.19** was synthesised by reaction of the dichloride chromium complex **2.11** with dibenzylmagnesium (see chapter 2).

Macrocyclic ligands were thought to be suitable ligands to replace the THF molecules in **3.4,** providing extra stability of the organometallic species based on the macrocycle effect. Therefore tribenzyl chromium **3.4** was reacted with excess of TACN in THF to form complex **3.5**.
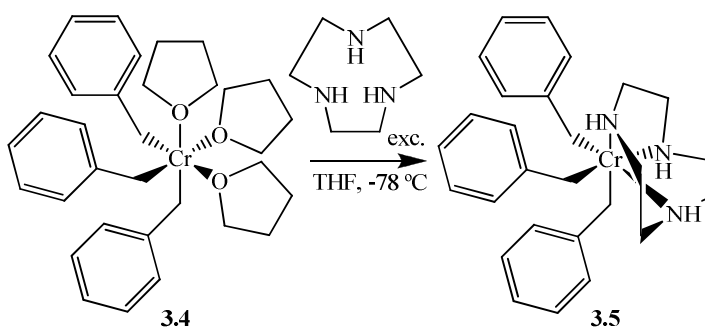
Scheme 3.5: Synthesis of complex **3.5**.

Complex **3.5** is more thermally stable than the starting material **3.4**. Therefore, it was possible to handle it at room temperature for short periods of time. It is soluble in DCM and THF, and insoluble in petrol, diethyl ether and toluene. Cooling a concentrated solution of **3.4** in THF gave red crystals which were characterised by using single crystal X-ray diffraction techniques. A CrystalMaker representation of **3.4** is shown in Figure 3.2. It adopts a distorted octahedral geometry with the benzyl groups occupying *fac* positions and the TACN molecule occupying the remaining sites in the complex.

The Cr-C bond distances [2.145(3) Å, 2.145(3) Å and 2.150(3) Å] are very similar, within the measured estimated standard deviations, and they are in the observed range in the literature for Cr-C σ-bonds. [76(a), 115, 119] The Cr-N bond lengths [2.567(2) Å, 2.167(2) Å and 2.171(2) Å] are considerable longer than other azo-macrocycles Cr(III) complexes reported in the literature. [144] This may be due to the fact of the *trans* influence offered by the benzyl groups and the neutral nature of complex **3.5**. Cr(1)-N(1) distance might be especially large due to steric factors.

Bond Distances (Å)	
Cr(1)-C(21)	2.145(3)
Cr(1)-C(14)	2.145(3)
Cr(1)-C(7)	2.150(3)
Cr(1)-N(1)	2.567(2)
Cr(1)-N(2)	2.167(2)
Cr(1)-N(3)	2.171(2)
Angles (º)	
C(7)-Cr(1)-C(14)	91.76(11)
C(7)-Cr(1)-N(2)	92.37(10)
C(7)-Cr(1)-C(21)	93.71(11)
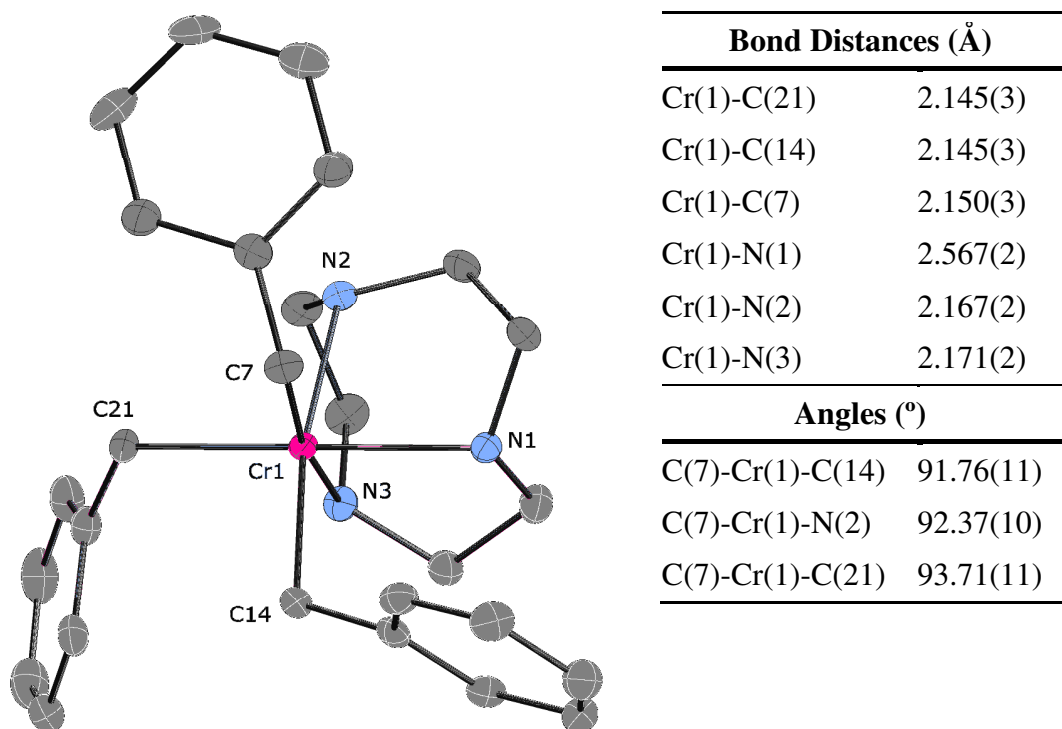
Figure 3.2: CrystalMaker representation of complex **3.5**. Thermal ellipsoids at 50% probability. Hydrogen atoms have been omitted for clarity. Selected bond lengths (Å) and angles (deg) with estimated standard deviations on the right of the diagram.

The synthesis of the complex below was attempted by the reaction of **3.4** with excess of the macrocycle shown in Scheme 3.6. The reaction was carried out in THF at low temperature but no reaction was observed. The reaction mixture was kept over a week at -30 ℃ and no colour change was observed. Therefore it was stirred at room temperature overnight. In an attempt at crystallising any formed product, the brown reaction mixture, which did not show any colour change, was layered with petrol and kept at -30 ℃. Uncharacterisable material was obtained after a week.
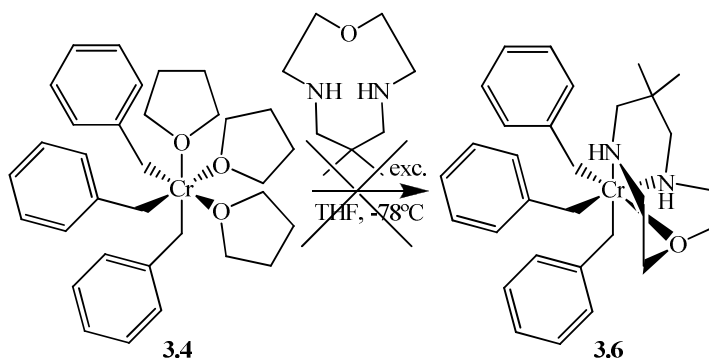
Scheme 3.6: Attempted synthesis of complex **3.6**.

NHCs were also thought to be suitable for the substitution of THF molecules in **3.4**. The reaction of this complex with 1,3-diisopropyl- imidazol-2-ylidene gave the Cr(II) complex **3.7** shown in Scheme 3.7.
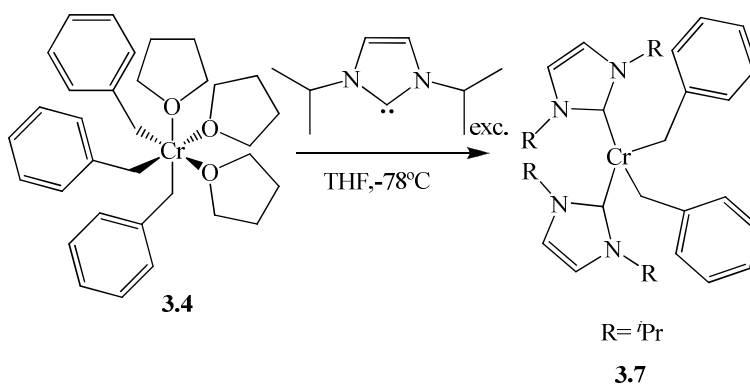
Scheme 3.7: Synthesis of Cr(II) complex **3.7**.

This complex has solubility in toluene, limited solubility in THF and it is insoluble in diethyl ether and petrol.

In this reaction the THF molecules in complex **3.7** are substituted by the carbene molecules, but the Cr(III) is reduced also to Cr(II). The mechanism why this occurs is unknown and attempts have been made to isolate any intermediate were not successful. It is possible that alkylimidazolium formation takes place to give a Cr(I)

complex which is oxidised to Cr(II) by Cr(benzyl)$_3$(THF)$_3$ **3.4**. Alkyl imidazolium elimination has been observed with other alkyl derivatives of late transition metals. [145]

Complex **3.7** is isolated as fine orange crystals after crystallisation at low temperature in the reaction mixture with excess of the free carbene in solution. This compound is extremely air sensitive and the crystals decompose quickly when they are isolated from the reaction mixture and washed with cold petrol. This fact suggests an on-off mechanism of the carbene ligand in complex **3.7** in solution, which is in agreement with the observed lability of Cr(II) species.

A CrystalMaker representation of **3.7** is shown in Figure 3.3. It adopts a distorted *cis* square planar geometry [C(19A)-Cr(1)-C(1)= 91.52(9)º, C(19A)-Cr(1)-C(4)= 159.94(11)º, C(1)-Cr(1)-C(4)= 90.76(6)º]. The two benzyl groups are pointing in opposite directions, their ring planes are almost perpendicular to each other and they are also perpendicular with the corresponding NHC ligand in *trans* position. This arrangement is the most efficient to minimise steric interactions.

Cr-C(NHC) bond lengths [2.1667(16) Å and 2.1626(15) Å] are slightly longer than in Cr(II) complex **2.21** reported in chapter 2, which may be due to the *trans* influence exerted by the benzyl groups, which is quite important for square planar complexes.

 Cr-C(benzyl) distances [2.152(3) Å and 2.1850(16) Å] are slightly longer that for benzyl Cr(III) complexes **3.4** and **3.6** reported above in this chapter and they are also longer than in the *cis*-Cr(II)(Mes)$_2$(THF)$_2$ reported in the literature [Cr-C(Mes) = 2.083(11) Å]. [146] This might be due, to the *trans* influence, as it is been discussed above, and also for the different oxidation state.

NHC ligand, 1, 3-diisopropyl-4,5 dimethylimidazol-2-ylidene, was used for the synthesis of Ni(NHC)$_2$(Me)$_2$ complex reported by Danopoulos [147] and also resulted in the formation of the *cis* distorted square planar product.
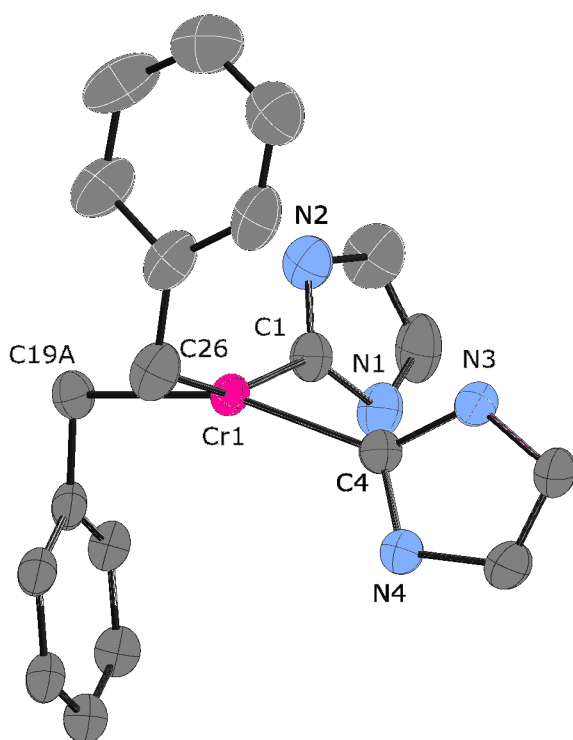
Bond Distances (Å)	
Cr(1)-C(19A)	2.152(3)
Cr(1)-C(26)	2.1850(16)
Cr(1)-C(1)	2.1667(16)
Cr(1)-C(4)	2.1626(15)
Angles (º)	
C(19A)-Cr(1)-C(1)	91.52(9)
C(19A)-Cr(1)-C(4)	159.94(11)
C(1)-Cr(1)-C(4)	90.76(6)

Figure 3.3: CrystalMaker representation of complex **3.7**. Thermal ellipsoids at 50% probability. Hydrogen atoms and isopropyl groups on N1, N2, N3 and N4 have been omitted for clarity. Selected bond lengths (Å) and angles (deg) with estimated standard deviations on the right of the diagram.

Attempted reactions with NHC pincer ligands shown in Scheme 3.8 below with complex **3.4** were carried out in THF at low temperature. A solution of an estimated excess of the pincer ligand in THF was added to solutions of **3.4** in the same solvent at -78 ºC. The solutions turned blood red and they were kept at -30 ºC for a few days.

Attempts at crystallisation were made by removal of the volatile components under reduced pressure, washing the residue with petrol, to eliminate the excess of ligand and dissolving the residue in fresh carefully dried THF. These solutions were layered with petrol and kept at -30 ºC but no X-ray quality crystals were obtained.
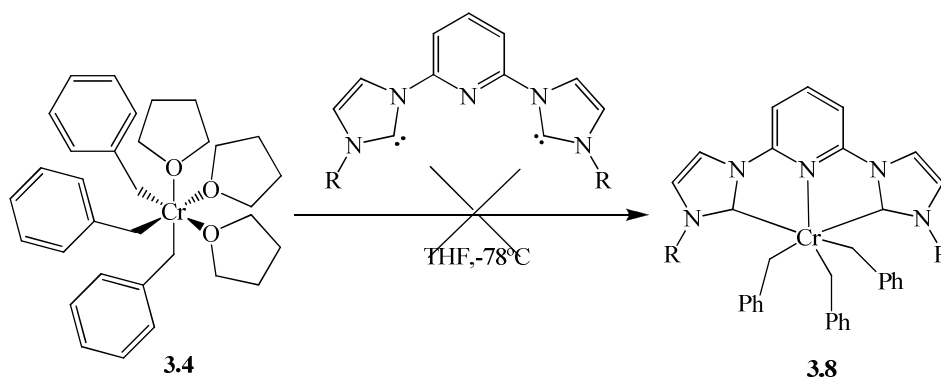
Scheme 3.8: Attempted reaction of **3.4** with pincer NHCs; R= DiPP, Mes, ^{t}Bu.

Several phosphine ligands were reacted with complex **3.4** as is shown in Scheme 3.9 below. Solutions of phosphine ligands shown below were added to solutions of **3.4** in the same solvent at -78 ºC. No colour change was observed after the addition in any of the cases. They were kept at -30 ºC for a few days but no reaction was observed.

The reaction mixture of **3.4** with trimethylphosphine was concentrated under reduced pressure to give small orange crystals, which were identified by single crystal X-ray diffraction as the staring material, complex **3.4**. Attempts at crystallisation of the other two reaction mixtures were made but no crystals were isolated. Therefore it is thought that no reaction took place with any of the phosphine ligands below and complex **3.4** under these reaction conditions.
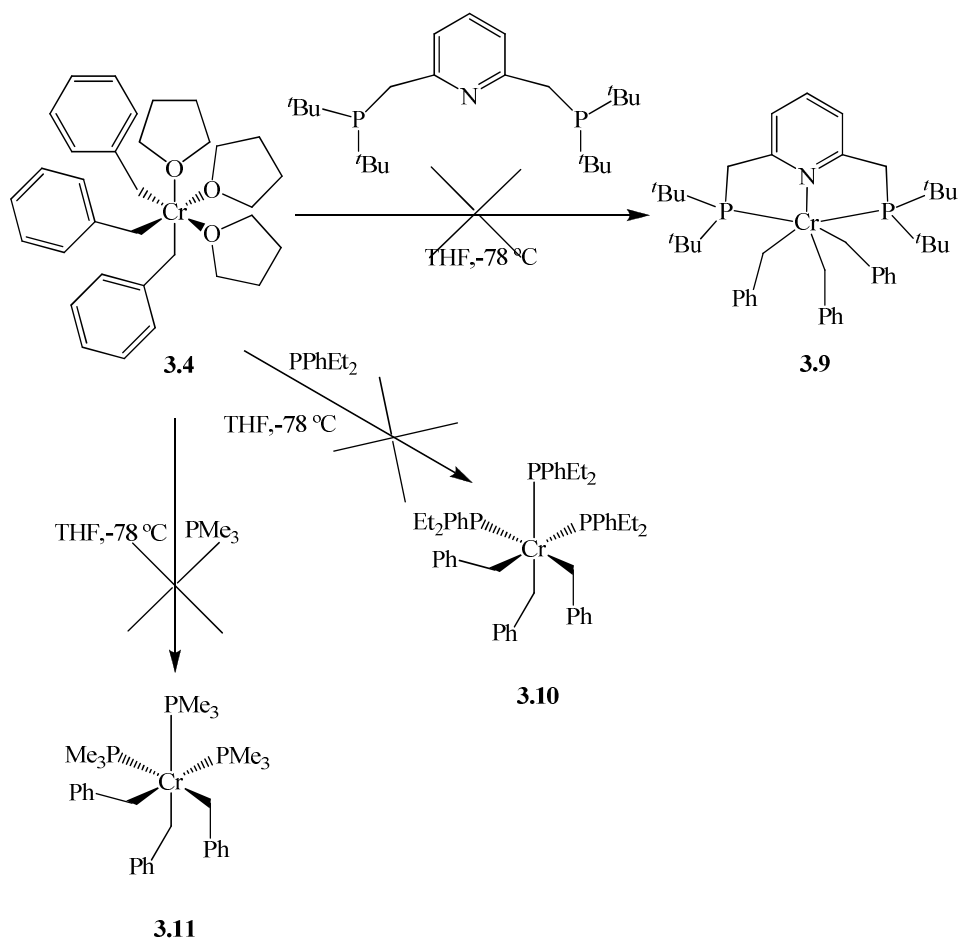
Scheme 3.9: Attempted reactions of complex **3.4** with different phosphine ligands.

Complex **3.4** was reacted with NO in order to obtain the Cr compound **3.12** shown in Scheme 3.10. A THF solution of **3.4** at -78 °C was saturated with NO. No colour changes were observed after stirring the reaction mixture at room temperature for 30 min. Attempt at crystallisation was made by concentrating the reaction mixture and layering the solution with petrol; the mixture was kept at -30 °C for 1 week to afford an uncharacterisable pale solid.
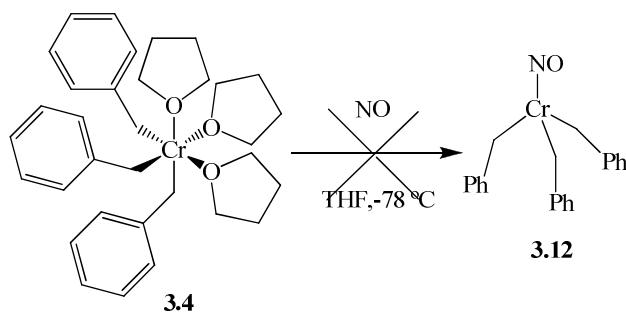
Scheme 3.10: Attempted synthesis of **3.12**.

121

Oxidation of complex **3.4** to the Cr(V) compound **3.13** was attempted by reaction of **3.4** with Mes-N$_3$ as is shown in Scheme 3.11 below. Two drops of the azide were added to a cold solution of **3.4** in THF. No reaction was observed and attempts at crystallisation were made in THF and THF/petrol at low temperature.
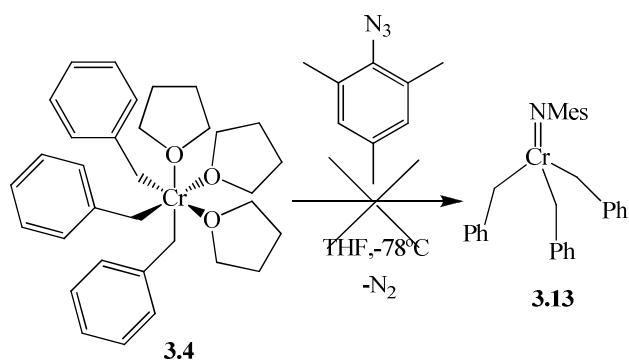
Scheme 3.11: Attempted synthesis of Cr(IV) compound **3.13**.

3.3 Conclusions

The first trialkyl chromium(III) compound, tribenzyl chromium *tris*(tetrahydrofuran) **3.4**, has been synthesised and characterised by X-ray crystallographic techniques. This complex is extremely air and moisture sensitive and decomposes quickly at room temperature in absence of the mother liquor. However, tribenzyl chromium *tris*(tetrahydrofuran) is thought to be an interesting metal precursor in which the THF molecules can be substituted by other ligands such a NHCs and phosphines.

Complex **3.4** adopts a *fac* conformation, which makes it suitable to be used with bidentate or tridentate chelating ligands to give more stable species. The synthesis of complex **3.5** is an example in which a TACN molecule has replaced three THF ligands and is acting as a tridentate chelating ligand. Complex **3.5** does not decompose at room temperature in the absence of solvent and it is stable in DCM solution for a short period of time (<1day).

The reaction of **3.4** with 1,3-diisolpropylimidazol- 2-yildene gave surprisingly the Cr(II) complex **3.7**. A mechanism in which alkyl imidazolium elimination gives a Cr(I) complex, which is oxidised by **3.4** to give **3.7** has been proposed. However, there are no reported examples of this chemical behaviour with chromium and any attempt to isolate intermediates resulted in decomposition of the reaction mixture.

Despite many attempts have been made in order to isolate new complexes by substitution of the THF ligands in complex **3.4** with several NHCs and macrocyclic ligands, only complexes **3.5** and **3.7** were isolated and characterised. This may be due to the fact that complex **3.4** is extremely sensitive, therefore difficult to handle, as well as the products of these reactions are thought to be.

Complex **3.4** showed no reactivity towards phosphine ligands and other small oxidising molecules such us nitrogen monoxide and mesitylazide.

3.4 Experimental

3.4.1 General Methods

Elemental analysis was carried out by the London Metropolitan University microanalytical laboratory. All manipulations were performed under nitrogen in a Braun glovebox or using standard Schlenk techniques under argon, unless stated otherwise. Solvents were dried using standard methods and distilled under nitrogen prior to use and they were also cooled down prior use in dry ice-acetone bath. The light petroleum used throughout had a bp of 40-60 °C. Starting materials were purchased from Aldrich: $Cr(acac)_3$, TACN; or prepared according to literature procedures: dibenzyl magnesium ether solution, [148] 1,3-diisolpropylimidazol, 2-yildene. [149] Data for X-ray crystallography is included at the end of this chapter.

3.4.2 Synthesis of Chromium Complexes

Tribenzyl chromium *tris*(tetrahydrofuran), 3.4
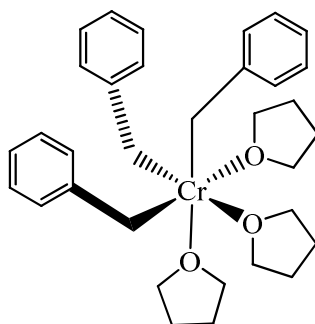
To a stirred solution of $Cr(acac)_3$ (0.24 g, 0.7 mmol) in THF (5 mL) at -40 ºC a solution of freshly made dibenzylmagnesium in ether (15 mL, 0.07M) was added dropwise over a period of 5 min. On completion of the addition the purple suspension was stirred at this temperature for 4h, the solution turned into orange brown. It was stored at -25 ºC for two weeks to afford extremely thermally unstable large brown-orange crystals, which were washed with cold petrol (2x 5mL). This compound was characterised by single crystal X-ray diffraction. Drying under vacuum was avoided due to decomposition of the compound under reduced pressure. Attempts to weigh the complex in the glove box were made but it decomposes quickly at room temperature.

Cr(Bz)₃(TACN), 3.5
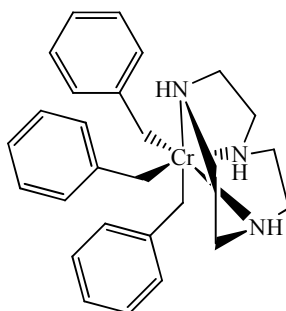
To a cold solution of Cr(CH₂Ph)₃(THF)₃ ~ (0.80g, 1.4 mmol) in THF (20 mL, -78 °C) a solution of TACN (0.25g, 1.9 mmol) in diethyl ether (30 mL) was added *via* cannula at the same temperature. The mixture that turned into blood red was stirred at room temperature for 3 h and kept at -30°C overnight. Volatile components were removed under reduced pressure and the red residue extracted with cold dichloromethane and filtered through Celite. Dichloromethane was removed under reduced pressure and the residue was washed with cold petrol (-78 ºC) and dried under vacuum to give the analytically pure product as blood-red solid. Yield: 0.40 g, 63%.

Elemental Analysis: Calculated (%): C, 71.84; H, 7.72; N, 9.31. Found (%): C, 71.69; H, 7.25; N, 9.29.

The red solid was dissolved in THF (5 mL) and kept at 5°C to afford red X-ray quality crystals.

***cis*-Dibenzyl chromium *bis*(1, 3-diisopropylimidazol-2-ylindene), 3.7**
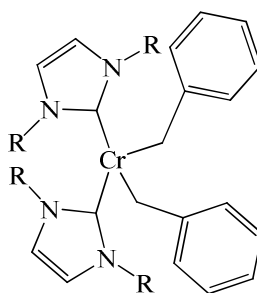
R= ^*i*Pr

To a cold solution of Cr(CH₂Ph)₃THF₃ ~ (0.25g, 0.5 mmol) in THF (3 mL, -78 °C) was added a solution of 1, 3-diisopropylimidazol-2-ylindene in toluene (3 mL, 0.28M). The solution turned into blood red and it was kept at -30 °C overnight to afford thermally unstable dark orange crystals. This complex was characterised by single crystal X-ray diffraction.

3.4.3 Crystallographic Parameters for Compounds in this Chapter

Table 3.1: Crystallographic parameters for complexes **3.4** and **3.5**.

Identification code	**3.4**	**3.5**
Empirical formula	$C_{33}H_{45}CrO_3$	$C_{108}H_{144}Cr_4N_{12}$
Formula weight	541.69	1818.35
Temperature	120(2) K	120(2) K
Wavelength	0.71073 Å	0.71073 Å
Crystal system	Monoclinic	Orthorhombic
Space group	C_c	$Pna2_1$
Unit cell dimensions	a = 17.1273(7) Å	a = 22.4869(10) Å
	$\alpha = 90°$	$\alpha = 90°$
	b = 20.6239(9) Å	b = 7.6737(4) Å
	$\beta = 91.595(2)°$	$\beta = 90°$
	c = 8.1996(3) Å	c = 13.4837(5) Å
	$\gamma = 90°$	$\gamma = 90°$
Volume	2895.2(2) Å³	2326.72(18) Å³
Z	4	1
Density (calculated)	1.243 Mg/m³	1.298 Mg/m³
Absorption coefficient	0.426 mm⁻¹	0.511 mm⁻¹
$F(000)$	1164	972
Crystal size	0.14 x 0.08 x 0.04 mm³	0.23 x 0.20 x 0.05 mm³
Theta range for data collection	3.17 to 27.63°	3.05 to 27.55°
Index ranges	-22<=h<=22	-29<=h<=28
	-26<=k<=25	-9<=k<=9
	-10<=l<=10	-17<=l<=17
Reflections collected	13584	14367
Independent reflections	6324 [$R(int)$ = 0.0726]	4906 [$R(int)$ = 0.0333]
Completeness to theta = 27.63°	98.5 %	99.3 %
Absorption correction	Semi-empirical from equivalents	Semi-empirical from equivalents
Max. and min. transmission	0.9832 and 0.9427	0.9749 and 0.8915
Refinement method	Full-matrix least-squares on F^2	Full-matrix least-squares on F^2
Data / restraints / parameters	6324 / 8 / 353	4906 / 1 / 281
Goodness-of-fit on F^2	1.126	1.123
Final R indices [I>2sigma(I)]	$R1$ = 0.0779, $wR2$ = 0.1558	$R1$ = 0.0389, $wR2$ = 0.0904
R indices (all data)	$R1$ = 0.1317, $wR2$ = 0.1818	$R1$ = 0.0417, $wR2$ = 0.0920
Absolute structure parameter	0.21(4)	0.55(2)
Largest diff. peak and hole	0.428 and -0.405 e.Å⁻³	0.481 and -0.347 e.Å⁻³

Table 3.2: Crystallographic parameters for complex **3.7**.

Identification code	**3.7**
Empirical formula	$C_{36}H_{54}CrN_4O$
Formula weight	610.83
Temperature	120(2) K
Wavelength	0.71073 Å
Crystal system	Triclinic
Space group	*P-1*
Unit cell dimensions	a = 10.4254(4) Å
	α = 81.140(2)°
	b = 10.6281(4) Å
	β = 85.553(2)°
	c = 16.0874(6) Å
	γ = 88.504(2)°
Volume	1755.77(11) Å^3
Z	2
Density (calculated)	1.155 Mg/m^3
Absorption coefficient	0.358 mm^{-1}
F(000)	660
Crystal size	0.20 x 0.18 x 0.15 mm^3
Theta range for data collection	2.97 to 25.03°
Index ranges	-12<=*h*<=12
	-12<=*k*<=12
	-19<=*l*<=19
Reflections collected	29819
Independent reflections	6188 [*R(int)* = 0.0642]
Completeness to theta = 25.03°	99.6 %
Max. and min. transmission	0.9483 and 0.9319
Refinement method	Full-matrix least-squares on *F^2*
Data / restraints / parameters	6188 / 428 / 520
Goodness-of-fit on *F^2*	1.098
Final *R* indices [I>2sigma(I)]	*R1* = 0.0747, *wR2* = 0.1712
R indices (all data)	*R1* = 0.1000, *wR2* = 0.1894
Largest diff. peak and hole	0.719 and -0.431 e.Å^{-3}

Chapter 4

N, N'-*bis*(2, 6-Isopropylphenyl) Amidine/Amidinate-Functionalised *N*-Heterocyclic Carbene Complexes

4.1 Introduction

4.1.1 Amidine and Amidinate Ligands

Amidine ligands were reported for the first time by Sanger in 1973, together with the synthesis of *N,N,N' - tris*(trimethylsilyl)benzamidine.[150] Amidinates are a wide group of ligands in which the original amidine has been deprotonated to form the anionic species, and are isostructural and isoelectronic with carboxylates. The two ends can be equivalent nitrogen donor atoms, in which the N atoms bear the same substituents, leading to symmetrical amidinates, or inequivalent with different substituents leading to nonsymmetrical ligands. A generic representation of amidine and amidinate species is shown in Figure 4.1.

4.1   **4.2**
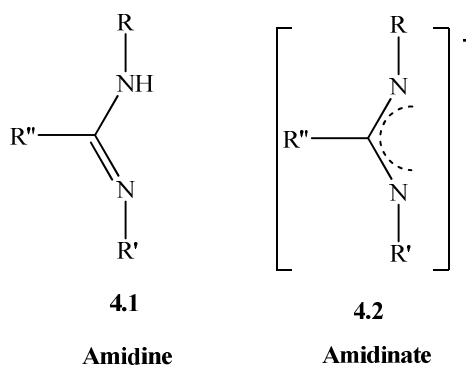
Amidine   **Amidinate**

Figure 4.1: Generic representation of amidine and amidinate ligands.

The coordination chemistry of amidine and amidinate ligands is well established.[151] Amidinate ligands usually bind to the metal center through both nitrogen atoms in a bidentate fashion contributing 6 electrons and are therefore analogous to cyclopentadienyl ligands. Complexes bearing these ligands have received attention as non-metallocene complexes which perform as single-site olefin polymerization initiators in presence of MAO.[88]

Other relevant ligands, isoelectronic with amidinate species, are guanidinate and amidato ligands, these anionic species are represented in Figure 4.2.

4.3

Guanidinate

4.4
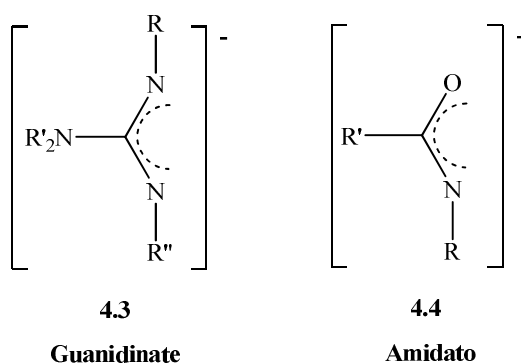
Amidato

Figure 4.2: Generic representation of guanidinate and amidato ligands.

N-amidato-containing systems have been studied due to their role as models for the interactions between metal centers and proteins. [152] The electronic and steric properties of *N*-substituted guanidinate anions, [RNC(NR′$_2$)NR″]⁻, can be easily tuned in order to form complexes with versatile coordination abilities. [153]

4.1.2 Amidinate Complexes in Catalysis

Titanium and zirconium benzamidinate complexes have shown potential in olefin polymerisation catalysis as has been briefly mentioned in chapter 1. [88] However these organometallic species have shown generally lower activities than the traditional metallocene systems Cp$_2$MR$_2$ (R= Halide or Alkyl). The zirconium *N,N'-bis*(trimethylsilyl)benzamidinate complexes shown in Figure 4.3 were studied and compared to the well-known cyclopentadienyl systems. [88(a)]

R= SiMe$_3$
R'= CH$_3$ **4.5** or
H **4.6**
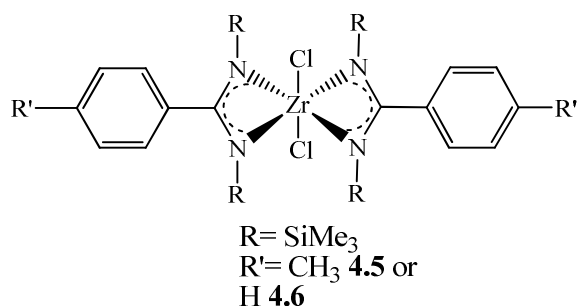
Figure 4.3: *bis*(Benzamidinate) Zr complexes by Eisen.

Interestingly, the activity and the molecular weight of the polymer obtained with early metal benzamidinate complexes increased as the MAO/complex ratios decreased. This behaviour is opposite to that observed with cyclopentadienyl early transition metal systems.

Eisen explained the difference in the catalytic performance between amidinate and metallocene catalysts based on the sterics around the metal centre. He suggested that the two bulky SiMe$_3$ groups on the amidinate ligand hinder the approach of the ethylene molecule to the metal centre, making therefore more difficult the initial insertion step. Therefore electronic and steric hindrance of the ligands on the metal centre plays a very important role in the catalytic performance of the complexes bearing amidinate ligands.

bis-(Alkylamidinate) complexes of group 4 were reported by Richeson. [154] This synthesis was motivated by the possibility of exploring the effects of important steric and electronic modifications in the nitrogen and carbon bridging groups with respect to the well-studied *bis*(benzamidinate) complexes above.

R= CH$_3$, M= Ti, **4.7** Zr, **4.8** Hf **4.9**
R= ^{t}Bu, M= Zr **4.10**
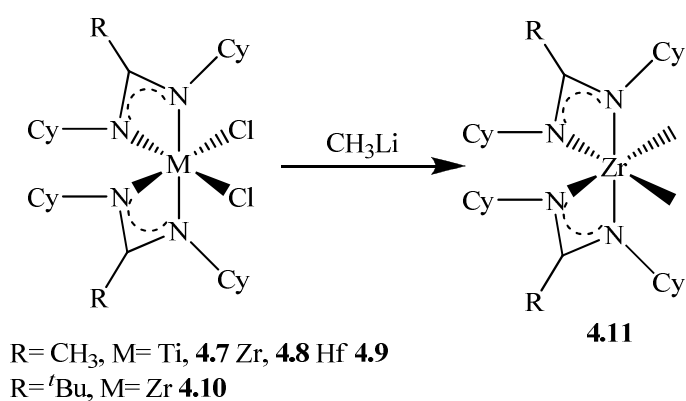
Scheme 4.1: *bis*(Alkylamidinate) complexes of group 4 by Richeson.

The olefin polymerisation catalysts were generated from complexes **4.7-4.11** by using MAO as cocatalyst. The most active species were the dichloride zirconium species and a small improvement of *Mw* was observed as the Al:Zr ratio decreased; this result is similar to that observed for *bis*(benzamidinate) Zr complexes **4.5** and **4.6** shown in Figure 4.3 above.

Zirconium complex **4.8** showed better activity than the analogous Ti and Hf complexes and the same trend as both metallocene and *bis*(benzamidinate) systems. Although the activities are comparable to *bis*(benzamidinate) systems they are significantly less active than those of the metallocene systems. [155]

In this chapter the synthesis and characterisation of the first *bis*(DiPP-amidinate) functionalised NHC ligand is reported. The potassium salt of this ligand 3-(2.6-diisopropylphenyl)-1-[2-N, N'-*bis*(2,6 diisopropylphenylamidinate)ethyl]imidazol-2-

ylidene potassium (L'K) has been isolated by double deprotonation of the imidazolium chloride precursor (L'H$_2$Cl) with KN(SiMe$_3$)$_2$. It has proved to be an excellent compound to incorporate the ligand L' to a wide range of transition metal precursors offering versatile coordination modes depending on the metal.

The first early transition metal abnormal carbene has also been isolated and fully characterised. Crabtree was the first to observe "abnormal" C-5 metalation of the NHC ring in bidentate picolyl and pyridyl-NHC dihydrides of iridium(III), prepared by metalation of imidazolium salts with IrH$_5$(PPh$_3$)$_2$. [156]

Danopoulos reported iron complexes with C-2 and C-5 metalated carbenes on the same metal. [157]

The imidazolium chloride precursor (L'H$_2$Cl), is also suitable to form silver carbene complexes useful in transmetallation reactions.

The different electronic character of the anionic amidinate group and the neutral N-hetorocyclic carbene donor leads to versatile coordination chemistry; tridentate, bidentate and monodentate coordination modes are conceivable which might have implications to catalysis. All these possible coordination modes are represented in Figure 4.4.

A monometallic or bimetallic bridging coordination mode forming polymeric structures might be also possible, as well as discrete bimetallic complexes.

L'K

Bidentate mode

- Imine monodentate
- NHC monodentate
  - Normal NHC monodentate
  - Abnormal NHC monodentate
- K^2-imine-NHC
  - K^2-imine normal NHC
  - K^2-imine abnormal NHC
- Iminoyl monodentate
- K^2-Iminoyl-NHC
  - K^2-iminoyl-normal NHC
  - K^2-iminoyl-abnormal NHC
- K^2-amidinate

Tridentate mode

- K^3-amidinate-normal NHC
- K^3-amidinate-abnormal NHC
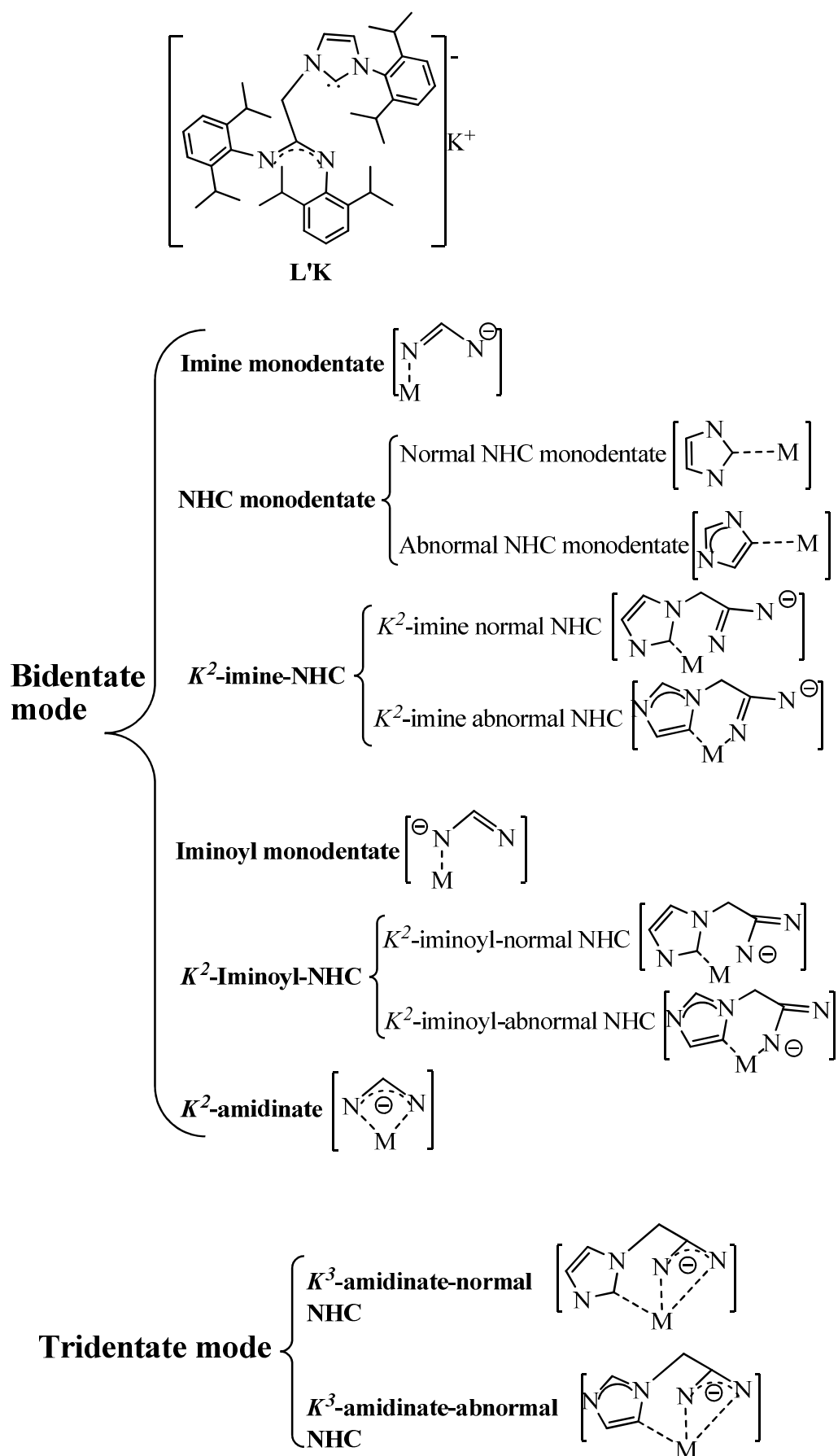
Figure 4.4: Possible coordination modes of ligand L'.

4.2 Results and Discussion

4.2.1 *bis*(DiPP-Amidinate)-Functionalised NHC Ligand Synthesis

Imidazolium Chloride Pro-Ligand

The imidazolium salt pro-ligand **4.13** was synthesised by heating in an ampoule under partial vacumm 2-chloro-*N, N'-bis*(2,6-diisopropylphenyl)acetamidine **4.12** and 2,6-diisopropylphenylimidazol **2.4** for 4 days.
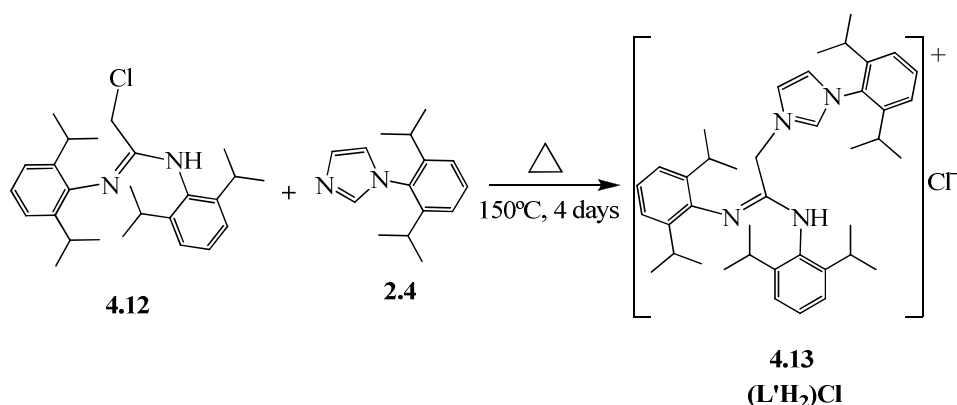
Scheme 4.2: Synthesis of imidazolium salt chloride **4.13**.

The product **4.13** was dried azeotropically in toluene after purification by crystallisation from DCM/Ether.

The ^{1}H-NMR spectrum of **4.13** in CDCl$_3$ is complicated and clearly showed the presence of two different isomers in an approximately 2:3 ratio. This mixture probably corresponds to the coexistence of the Z and E isomers in solution. The existence of the two isomers with the corresponding tautomers was reported for the starting material **4.12**, [158] however it is not obvious from the spectroscopic information which isomers or tautomers are present in solution.

The ^{1}H-NMR spectrum in CDCl$_3$ showed two peaks in the imidazolium proton region as well as two peaks for the methylene protons of the bridge that correspond to the different Z and E isomers. The DiPP groups are non-equivalent and they appear as three septets (C*H*(CH$_3$)$_2$) and six doublets (CH(C*H*$_3$)$_2$) for each isomer.

The ^{13}C-NMR(Dept 135) spectrum in CDCl$_3$ showed also two peaks corresponding to the methylene bridge groups (C*H*$_2$) of the isomers Z and E.

However the ^{1}H-NMR and ^{13}C-NMR spectra in d^6-DMSO are simplified in comparison with the spectra in CDCl$_3$. The peaks that correspond to the Z and E isomers converge to give an average signal. Therefore the higher polarity of DMSO might favour the interconversion between Z and E isomers in solution. Another possibility is that compound **4.13** is not stable in DMSO; therefore the NNR signals corresponded to a mixture of the starting materials **4.12** and **2.4**.

The structure of imidazolium chloride **4.13** (isomer Z) has been elucidated by crystallographic techniques and a CrystalMaker representation as well as bond distances and angles are shown in Figure 4.5. Steric interactions of the isopropyl groups might be the reason why the isomer Z has crystallised instead of the E isomer.

The three planes that contain the phenyl groups are perpendicular to each other in order to minimise steric interactions.

Bond Distances (Å)	
N1-C13	1.322(5)
N2-C13	1.334(5)
N2-C16	1.466(4)
C16-C17	1.521(5)
C17-N3	1.366(5)
C17-N4	1.273(5)
C13-H13	0.9500
N3-H1	0.857(10)
Angles (º)	
N2-C13.N1	108.6(3)
N3-C17-N4	121.4(3)
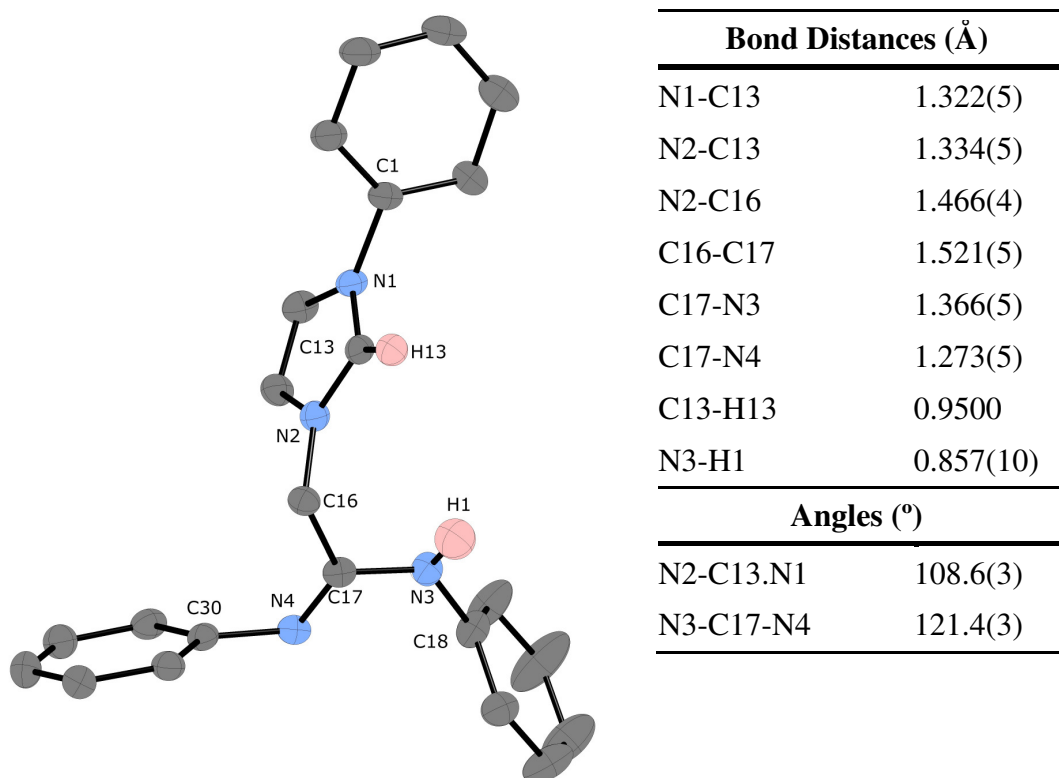
Figure 4.5: CrystalMaker representation of the imidazolium cation counterpart of pre-ligand **4.13**. Thermal ellipsoids at 50% probability. Hydrogen atoms, except N-H and imidazolium-H, isopropyl substituents in positions 2 and 6 on the phenyl groups and chloride anions have been omitted for clarity. Selected bond lengths (Å) and angles (deg) with estimated standard deviations on the right of the diagram.

Deprotonation and Double deprotonation of the Imidazolium Chloride Ligand 4.13

The reaction of imidazolium chloride **4.13** with one equivalent of $KN(SiMe_3)_2$ in benzene gave the neutral compound **4.14** after filtration of the solution through Celite and removal of the volatile components under reduced pressure. Compound **4.14**, shown in Scheme 4.3, was isolated as a light yellow air- and moisture-sensitive yellow powder and it was characterised by spectroscopic techniques.

The ^{1}H-NMR spectrum in d^6-benzene showed some broadness and it was considerably simplified with respect to the spectrum in $CDCl_3$ of the starting material **4.13**. It may be due to the fast interconversion between the Z and E isomers in solution, giving an average signal for the two isomers.

The neutral compound **4.14** would be suitable as monodentate ligand in reactions with different metal precursors. However, as it has been explained above, the synthesis of new metal complexes bearing asymmetric chelating ligands is of great interest for this project due to the fact that they might show interesting properties in catalysis.

In order to obtain a tridentate chelating ligand the neutral ligand **4.14** was submitted to a second deprotonation with another equivalent of $KN(SiMe_3)_2$ in benzene to give the potassium salt **4.15** in good yield (Scheme 4.3 below). The air and moisture sensitive white solid was isolated on a frit, washed with benzene and petrol and dried under reduced pressure.
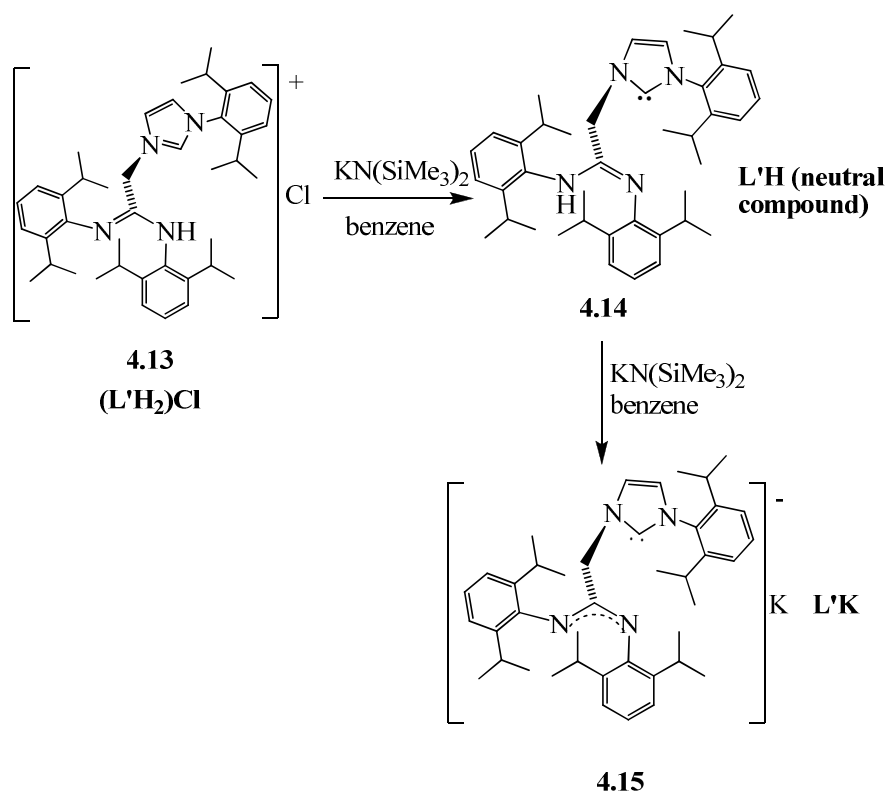
Scheme 4.3: Synthesis of the potassium salt **4.15**.

Potassium salt **4.15** was characterised by analytical and spectroscopic methods and crystallised from THF/petrol. Its ^{1}H-NMR spectrum in d^5-pyridine showed some broadness, as well as the spectrum of the neutral ligand **2.14**. The protons of the DiPP substituents are all no-equivalent and appear at different shifts. The carbene carbon signal can be observed in the ^{13}C{H}-NMR spectrum at 214.6 ppm.

The synthesis of the potassium salt **4.15**, as it has been described above, involves the isolation of the neutral carbene ligand **4.14**. However in order to scale up the synthesis of **4.15** and make the whole process more efficient, the isolation of the neutral ligand is not necessary. The potassium salt **4.15** can be obtained by two consecutive deprotonation steps with KN(SiMe$_3$)$_2$ in benzene. In order to improve the yield of the second deprotonation and to obtain the potassium salt analytically pure the benzene solution must be filtrated through Celite to remove the potassium chloride.

The structure of **4.15** was determined by crystallographic techniques. It comprises polymeric "zig-zag" chains with potassium atoms and bridging NHC units as it is shown in Figure 4.6 below.
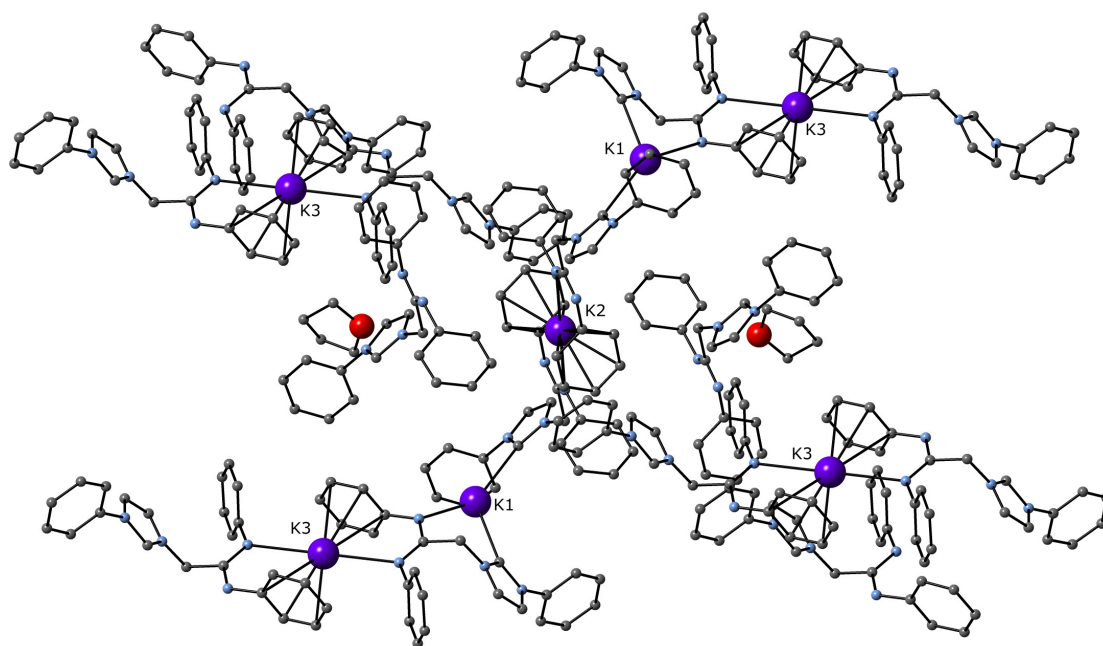
Figure 4.6: CrystalMaker representation of potassium salt **4.15**. Ball and stick model. Hydrogen atoms and isopropyl groups in positions 2 and 6 on the phenyl groups have been omitted for clarity.

There are two types of alternating repeating units in which the potassium atoms have three different coordination spheres. The unit represented in Figure 4.7 below shows the environments of K(1) and K(3). K(1) is coordinated to only one nitrogen atom of the amidinate group and to two different carbene atoms corresponding to two different ligand molecules C(3) and C(53). The coordination between K(1) and C(3) is shown in Figure 4.8.

K(3) is flanked by two phenyl groups, and amid two nitrogen atoms corresponding to two different amidinate groups, only one nitrogen atom of each amidinate group is coordinated to the potassium atom K(3). Carbon atoms C(83) and C(84) are the closest atoms of the phenyl groups to K(3) [K(3)-C(83)= 3.276(3)Å and K(3)-C(84)= 3.146(2) Å]; therefore both phenyl rings form a distorted "sandwich structure" with the potassium atom K(3) in between.

Bond Distances (Å)	
K(1)-C(53)	2.862(3)
K(1)-N(5)	2.803(2)
K(3)-C(83)	3.276(3)
K(3)-C(84)	3.146(2)
K(3)-N(6)	2.946(2)
C(40)-N(5)	1.328(3)
C(40)-N(6)	1.327(3)
Angles (°)	
N(6)-K(3)-N(6)	180.0
C(83)-K(3)-C(83)	180.0
C(53)-K(1)-N(5)	76.94(7)
N(5)-K(1)-C(3)	147.02(7)
C(53)-K(1)-C(3)	127.30(7)
N(5)-C(40)-N(6)	125.9(2)
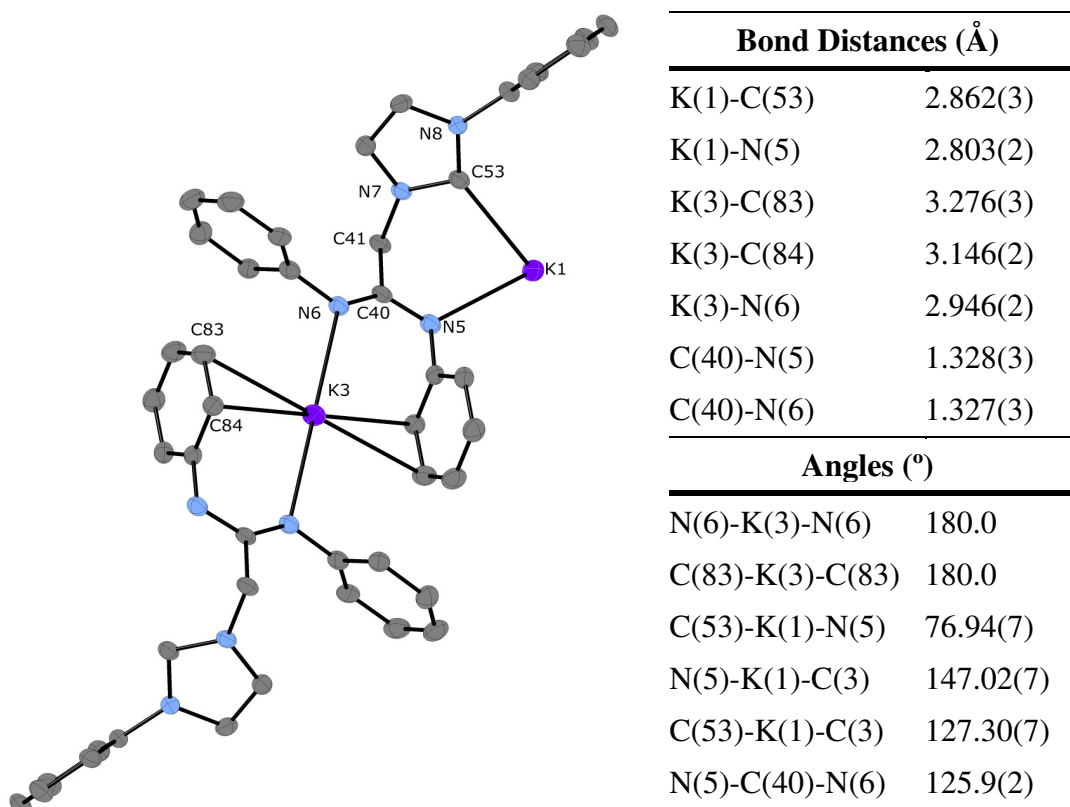
Figure 4.7: CrystalMaker representation of potassium salt **4.15**. Thermal ellipsoids at 50% probability. Hydrogen atoms and isopropyl substituents in positions 2 and 6 on the phenyl groups have been omitted for clarity. Selected bond lengths (Å) and angles (deg) with estimated standard deviations on the right of the diagram.

The coordination sphere of K(2) in shown in Figure 4.8. K(2) is flanked by two phenyl groups in one direction and amid two amidinate groups in the perpendicular plane, although only one nitrogen atom of each amidinate group is coordinated to the potassium atom K(2). The distances between K(2) and all the carbon atoms of the phenyl rings are similar. Therefore the "sandwich structure" given by the phenyl rings in this case is less distorted than for the K(3) atom discussed above. K-C(NHC) bond distances [2.953(3)Å and 2.862(3)Å] are comparable with the fluorenyl-functionalised NHC potassium salt reported by Danopoulos [94] and shorter than other examples reported previously (3.048Å). [159]

Bond Distances (Å)	
K(2)-N(2)	3.035(2)
K(2)-C(30)	3.307(2)
K(2)-C(31)	3.331
K(2)-C(32)	3.279(2)
K(2)-C(33)	3.256(2)
K(2)-C(34)	3.248(2)
K(2)-C(35)	3.260(2)
K(1)-C(3)	2.953(3)
Angles (º)	
C(53)-K(1)-C(3)	127.30(7)
N(2)-K(2)-N(2)	180.00(7)
N(1)-C(1)-N(2)	126.0(2)
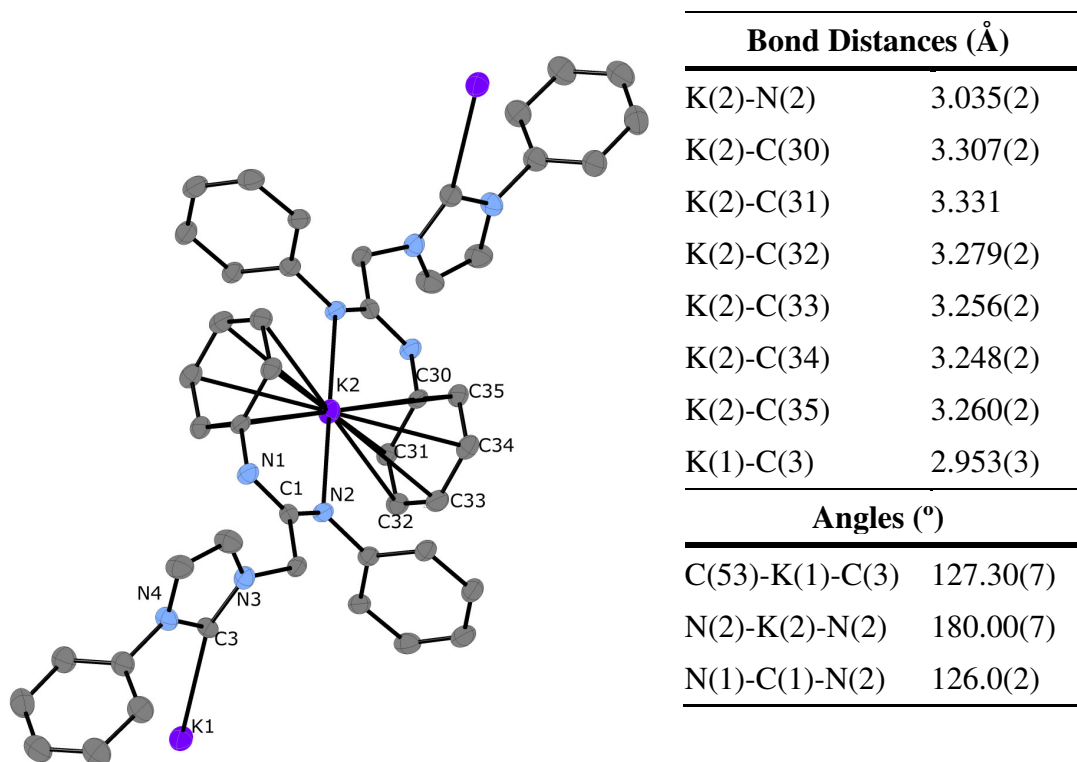
Figure 4.8: CrystalMaker representation of potassium salt **4.15**. Thermal ellipsoids at 50% probability. Hydrogen atoms and isopropyl substituents in positions 2 and 6 on the phenyl groups have been omitted for clarity. Selected bond lengths (Å) and angles (deg) with estimated standard deviations on the right of the diagram.

4.2.2 *bis*(DiPP-Amidinate)-Functionalised NHC Early Transition Metal Complexes

Amidinate titanium and zirconium complexes have been studied as catalyst in the polymerisation of ethylene and they have often been compared with the well-known metallocene catalyst systems as it has been discussed above. [88]

In this chapter the synthesis of the first *bis*-N,N'(DiPP-amidinate)-functionalised NHC ligand **4.15** has been reported and its reactivity towards different metal precursors is discussed in detail below.

bis(DiPP-Amidinate)-Functionalised NHC Titanium Complexes

The reaction of the potassium salt **4.15** with the metal precursor Ti(N^{t}Bu)Cl$_2$Py$_3$ gave in good yield the complex **4.16** shown in Scheme 4.4.
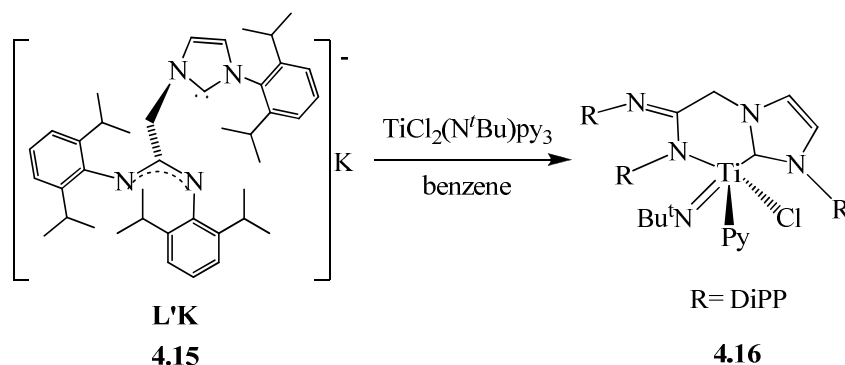
Scheme 4.4: Synthesis of Ti(IV) complex **4.16**.

Complex **4.16** was obtained analytically pure after filtration of the benzene solution through Celite, removal of the volatile components under reduced pressure, washing with petrol and dried under vacuum. The product was characterised by analytical and spectroscopic techniques.

The low molecular symmetry of the titanium complex **4.16** was highlighted by the ^{1}H-NMR spectrum. Although the spectrum shows some broadness it is clear that the methyl groups of the isopropyl substituents and the protons of the methylene bridge (CH_2) appear as diastereotopic. The carbene carbon NHC signal in the ^{13}C{H} NMR spectrum was observed at 192.0 ppm, slightly shielded relative to the potassium salt **4.15** (214.6 ppm).

X-ray quality crystals of **4.16** were obtained from toluene/petrol. CrystalMaker representation of the molecule is shown in Figure 4.9 below.

In 1984 Adisson defined parameter "τ" to differentiate square pyramidal or trigonal bypyramidal geometries of 5 coordinated metal complexes. The geometry of the majority of the 5 coordinate complexes lays between the idealised square-pyramidal (τ = 0) and the trigonal-bipyramidal (τ = 1) geometries. (τ = α - β) where α and β are the largest and second largest angles, respectively, around the central atom. [160]

Complex **4.16** adopts distorted trigonal bipyramidal geometry (τ = 0.58), in which the equatorial positions are occupied by Cl(1), N(3) and N(5) and the axial positions by C(1) and N(4). The Ti-C(NHC) bond length [2.2441(15) Å] is slightly longer than for the indenyl- functionalised Ti(IV) NHC imido complexes **2.8** and **2.9** discussed in chapter 2 above. Complexes **2.8** and **2.9** do not experience *trans* influence due to the fact that the ligands do not have any other ligand in *trans* position, since they have tetrahedral geometry. However the *trans* influence exerted by the pyridine ligand in

143

trans position to the NHC group is noticeable for this geometry in complex **4.16**. The Ti-C(NHC) for **4.16** is also slightly shorter than some carbene imido Ti(IV) complexes reported in the literature with the same geometry [2.290(6) Å and 2.297(3) Å]. [113]

The Ti=N(imido) bond distance for **4.16** [1.7002(14) Å] is similar to the corresponding distance found for complexes **2.8** and **2.9** [1.705(3) Å and 1.703(3) Å] discussed in chapter 2 and similar to the bond length for the starting material Ti(=N^{t}Bu)Cl$_2$Py$_3$ [1.705(3) Å] and other imido compounds such as Ti(=NPh)Cl$_2$Py$_3$ [1.714(2) Å] and Ti(=Np-Tol)Cl$_2$Py$_3$ [1.705(4) Å]. [114] The *tert*-butyl imido group is deviating slightly from linearity Ti(1)-N(3)-C(47) = 177.80(12)º although this deviation is less pronounced than in complexes **2.8** and **2.9** described above in chapter 2.

The difference between the endocyclic angle N(2)-C(1)- Ti(1) and exocyclic angle N(1)-C(1)-Ti(1) is 25°. This large distortion value is possible due to the strain imposed by the one carbon atom bridging functionality in complex **4.16**, and it may be the reason why the amidinate substituent is not acting as a bidentate ligand.

The difference between the bond distances C(17)-N(5) and C(17)-N(6) [0.067 Å] indicates that ligand L' is acting as a κ^2-iminoyl- normal NHC ligand. This coordination mode is represented in Figure 4.4.

The Ti(1)-N(5) bond length [2.1014(13) Å] is considerable longer than Ti-imido bond distances discussed above but shorter than Ti-py bond length [2.2730(13) Å]. This agrees with the formal charge on the nitrogen atom in the amidinate group.

The Ti-Cl and Ti-N(py) bond lengths are similar to the corresponding values of other Ti(IV) complexes reported in the literature and to the corresponding bond lengths for the starting material Ti(=N^{t}Bu)Cl$_2$Py$_3$, Ti-N(py) [2.247(3) *cis* Å and 2.450(3) *trans* Å] and Ti-Cl [2.432(1) Å and 2.436(1) Å]. [114]

Bond Distances (Å)	
Ti(1)-C(1)	2.2441(15)
Ti(1)-N(5)	2.1014(13)
Ti(1)-Cl(1)	2.3444(5)
Ti(1)-N(3)	1.7002(14)
Ti(1)-N(4)	2.2730(13)
C(17)-N(5)	1.3632(19)
C(17)-N(6)	1.296(2)
Angles (º)	
Ti(1)-N(3)-C(47)	177.80(12)
N(5)-Ti(1)-Cl(1)	136.03(3)
C(1)-Ti(1)-N(4)	171.15(5)
N(1)-C(1)-Ti(1)	140.41(11)
N(2)-C(1)-Ti(1)	115.49(10)
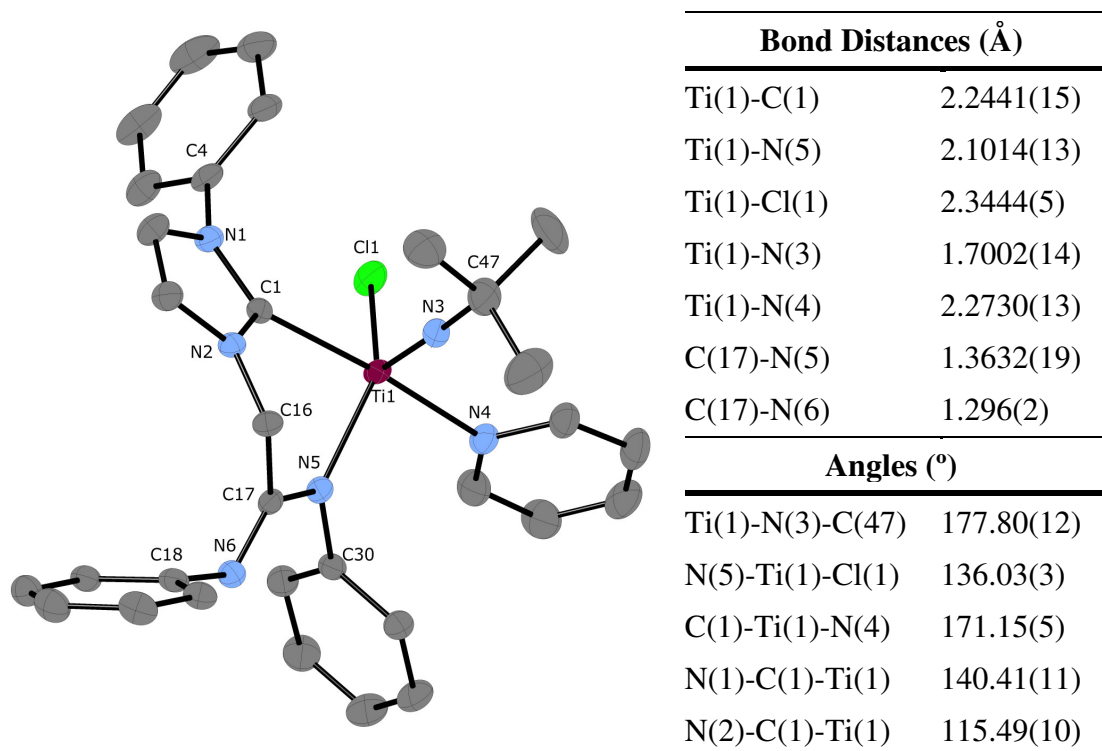
Figure 4.9: CrystalMaker representation of Ti complex **4.16**. Thermal ellipsoids at 50% probability. Hydrogen atoms and isopropyl substituents in positions 2 and 6 on the phenyl groups have been omitted for clarity. Selected bond lengths (Å) and angles (deg) with estimated standard deviations on the right of the diagram.

The reaction of the potassium salt **4.15** and the metal precursor $TiCl_2(NMe_2)_2$ gave the complex **4.17** shown in Scheme 4.5 below in good yield.
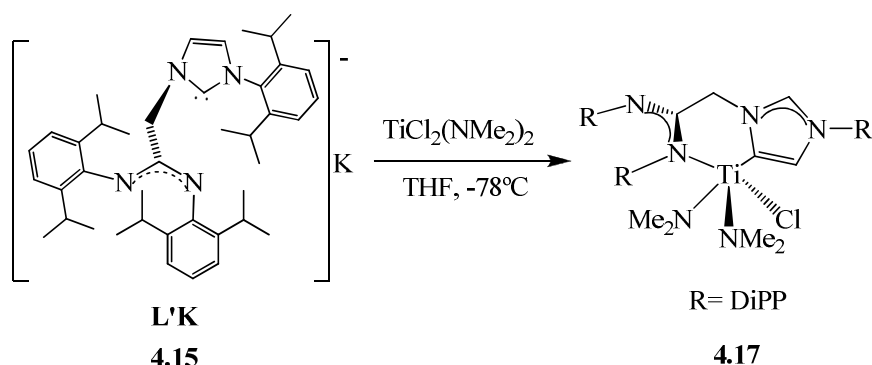
Scheme 4.5: Synthesis of Ti(IV) complex **4.17**.

The product **4.17** was isolated as a deep orange air-moisture sensitive powder after extraction of the residue in toluene, filtration through Celite, removal of the volatile components under reduced pressure and washing with petrol. This compound was

characterised by spectroscopy and analytical techniques. X-ray quality crystals were obtained from toluene/petrol.

The low molecular symmetry of the titanium complex **4.16** was shown in the ^{1}H-NMR spectrum. The methyl groups of the isopropyl substituents and the protons of the methylene bridge (CH_2) appear as diastereotopic. The signal corresponding to the protons of the NHC ring were observed slightly shielded 6.12 ppm and 6.05 ppm, which is in agreement with the abnormal carbene bonding structure given by single crystal X-ray diffraction techniques. A CrystalMaker representation is shown below in Figure 4.10.

Complex **4.17** adopts distorted square-pyramidal geometry (τ = 0.18), N(6) in the apical position and Cl(2), N(5), N(4) and C(2) in the base of the pyramid. Surprisingly the crystal structure shows that the titanium atom is coordinated to C5 instead the C2 of the N-heterocyclic ring. Abnormal carbenes have been mainly observed in late transition metals,[161] as it has been discussed above in the introduction of this chapter, therefore complex **4.17** is the first titanium abnormal NHC complex reported to date.

The Ti-C(NHC) bond length [2.189(11) Å] is significantly shorter than in the other Ti(IV) complexes reported above **4.16**, **2.8** and **2.9**, 2.2441(15) Å, 2.227(4) Å, 2.226(2) Å respectively due to the fact that abnormal carbenes are better σ-donors than regular NHC ligands.

Ti(1)-N(4) bond length [2.061(9) Å] is in the same range than the corresponding bond for **4.16** above [2.1014(13) Å]. The difference between the bond distances C(17)-N(4) and C(17)-N(3) [0.074 Å] indicates that the coordinating mode for ligand L' is κ^2-iminoyl- abnormal NHC mode which is represented in Figure 4.4 above.

The difference between the endocyclic N(2)-C(2)- Ti(1) and exocyclic angle C(3)-C(2)-Ti(1) is 21°. Therefore the strain imposed by the methylene group between the amidinate and the NHC functionalities is easily noticeable as was the case in complex **4.16** above.

Bond Distances (Å)	
Ti(1)-C(2)	2.189(11)
Ti(1)-N(4)	2.061(9)
Ti(1)-N(5)	1.919(8)
Ti(1)-N(6)	1.854(9)
Ti(1)-Cl(1)	2.378(3)
C(17)-N(3)	1.295(12)
C(17)-N(4)	1.369(12)
Angles (º)	
N(2)-C(2)-Ti(1)	117.4(9)
C(3)-C(2)-Ti(1)	138.8(9)
C(2)-Ti(1)N(5)	157.5(9)
N(4)-Ti(1)-Cl(1)	146.8(3)
Cl(1)-Ti(1)-N(5)	88.4(3)
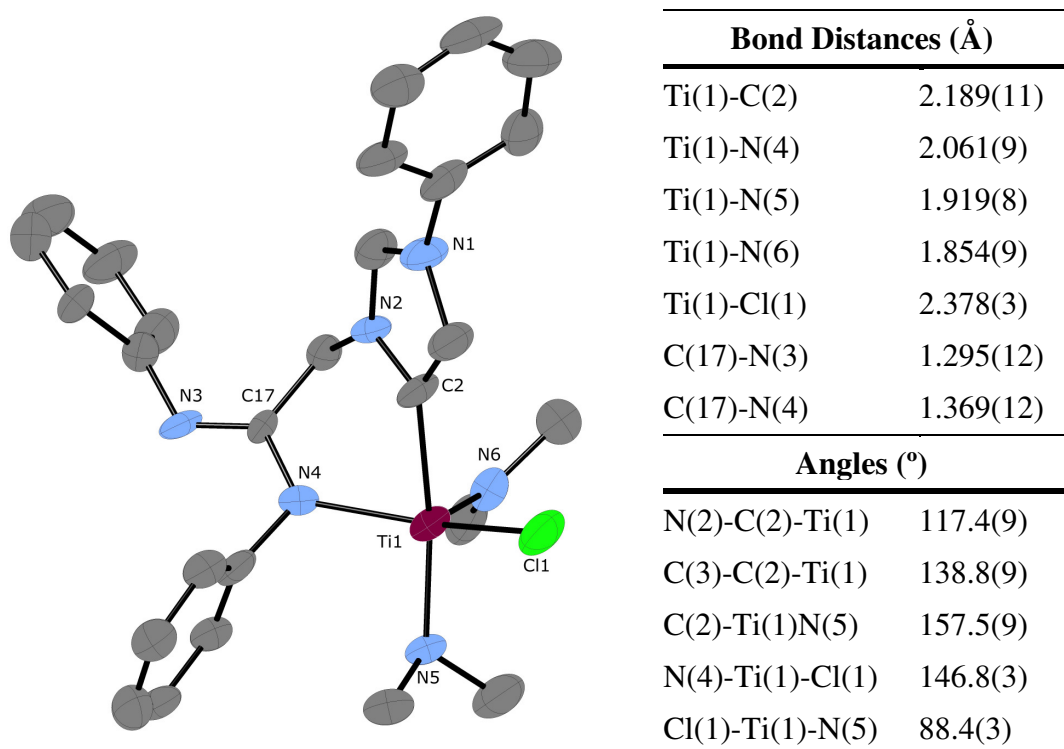
Figure 4.10: CrystalMaker representation of Ti complex **4.17**. Thermal ellipsoids at 50% probability. Hydrogen atoms and isopropyl substituents in positions 2 and 6 on the phenyl groups have been omitted for clarity. Selected bond lengths (Å) and angles (deg) with estimated standard deviations on the right of the diagram.

A proposed mechanism for the formation of the "abnormal carbene" is shown in Scheme 4.6. A proton exchange must take place at some point in the reaction due to the fact that potassium salt **4.15** showed a regular carbene-potassium bond through C2 of the N-heterocyclic ring.

147
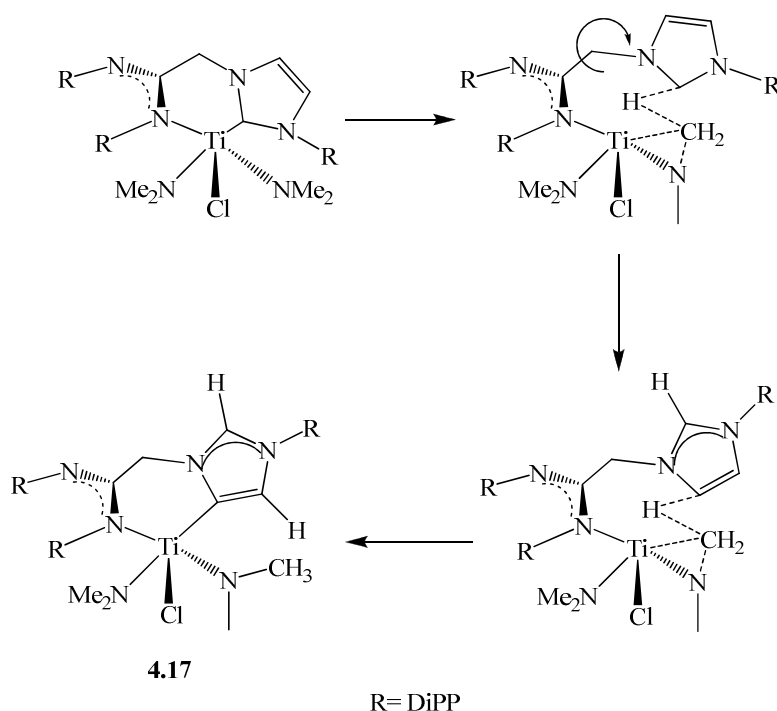
Scheme 4.6: Proposed mechanism for the conversion of the normal carbene into the "abnormal" carbene for complex **4.17**.

bis(DiPP-Amidinate)-Functionalised NHC Zirconium Complexes

When potassium salt **4.15** is reacted with $ZrCl_2(NMe_2)_2(THF)_2$ complex **4.18** showed in Scheme 4.7 is obtained in good yield (51 %).
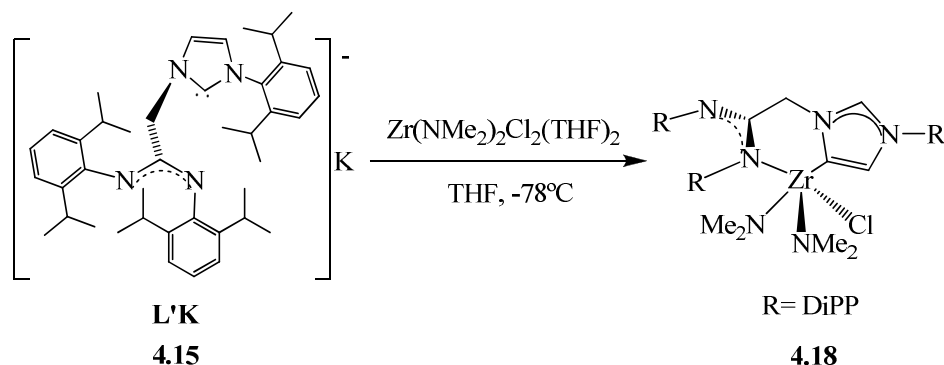
Scheme 4.7: Synthesis of Zr(IV) complex **4.18**.

Petrol was added to the reaction mixture in THF in order to precipitate the potassium chloride. The solution is filtered through Celite and dried under vacuum. The residue was washed with petrol and dried under reduced pressure to give the analytically pure product, which was characterised by spectroscopic and analytical techniques. The ^{1}H-NMR spectrum was quite similar to the spectrum of the titanium analogue **4.17**. The methyl groups of the isopropyl substituents appear as diastereotopic. The signal

corresponding to the protons of the NHC ring were observed significantly shielded 6.07 ppm and 5.55 ppm, which is in agreement with the abnormal carbene bonding structure observed in titanium complex **4.17** above. However this fact could not be confirmed by X-ray crystallography techniques since attempts to crystallise this compound in different solvent systems (THF, toluene/ petrol) several times were unsuccessful.

The carbene carbon signal in the ^{13}C-{H}-NMR spectrum was observed at 190.8 ppm, slightly shielded relative to the potassium salt **4.15** (214.6 ppm).

In order to study alkyl complexes with the new amidinate-functionalised NHC ligand, the metal precursor ZrBz$_4$ was reacted with the imidazolium chloride **4.13** in toluene at -78 ºC to give the tribenzyl zirconium complex **4.19** shown in Scheme 4.8 below along with other unidentified side products of the reaction.
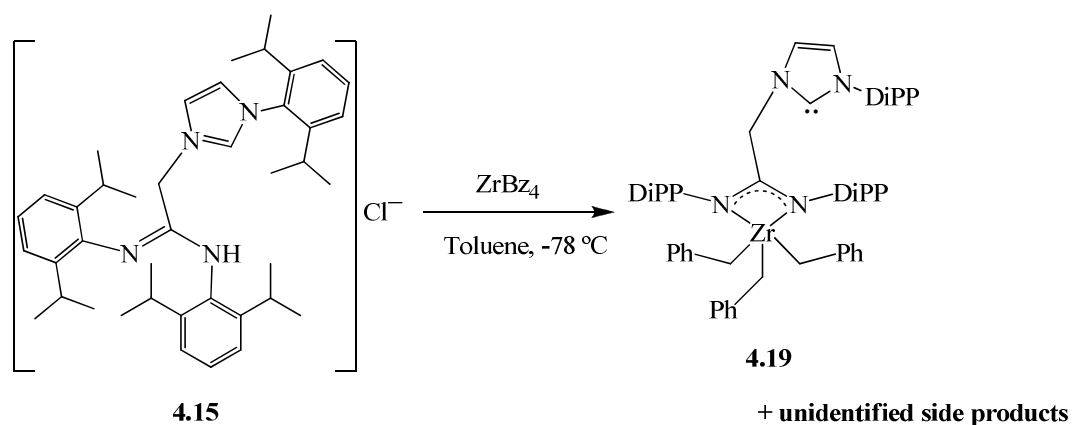
Scheme 4.8: Synthesis of the tribenzyl Zr(IV) complex **4.19**.

It was thought that by the metal precursor ZrBz$_4$ could deprotonate one or two positions of the imidazolium salt **4.13** with the production of toluene as a driving thermodynamic force for this reaction. Complex **4.19** was isolated by crystallisation in diethyl ether at low temperature (-25 ºC) after extracting the residue of the reaction with this solvent, filtration through Celite and concentration of the ether solution under reduced pressure. The yellow crystals were characterised by single crystal X-ray diffraction techniques and a CrystalMaker diagram is shown in Figure 4.11. ^{1}H-NMR spectroscopy in benzene showed a very complicated spectrum probably due to the co-existence of more than one compound in solution.

The crystal structure showed that both amidine and the NHC ring positions have been deprotonated. Due to stoichiometric reasons there would be other side products in the

reaction such as ZrClBz$_3$, a possible mechanism for this reaction is shown in Scheme 4.9 below.
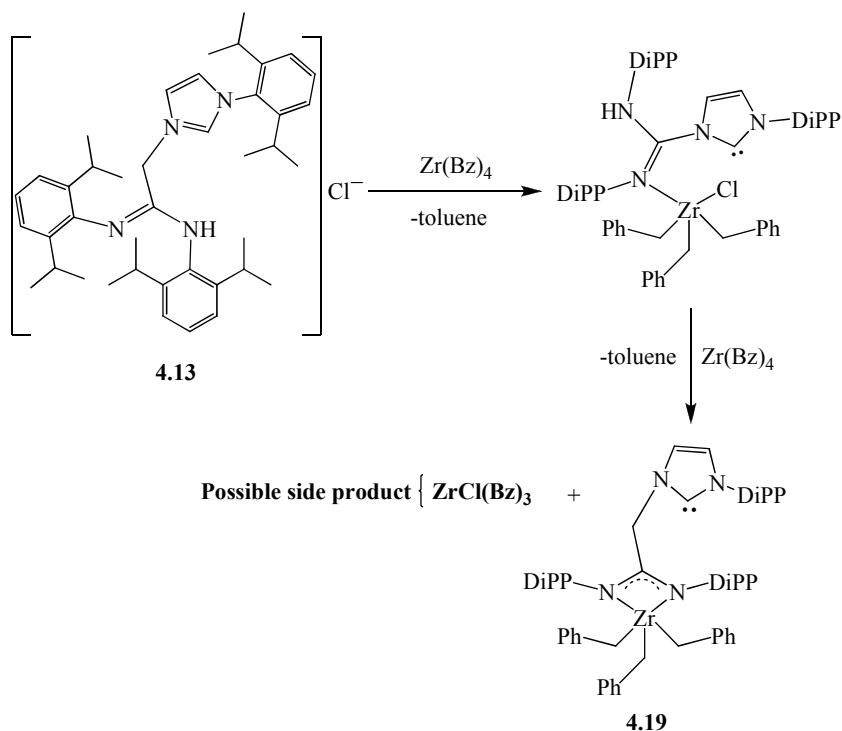
Scheme 4.9: Proposed mechanism for the reaction of ZrBz$_4$ with the imidazolium chloride **4.13**.

Complex **4.19** adopts distorted square-pyramidal geometry ($\tau = 0.31$), C(49) is situated in the apical position and C(42), C(56), N(2) and N(3) in the base of the pyramid [torsion angle C(42)-C(56)-N(2)-N(3) = 33.6º]. The amidinate substituent is acting as bidentate ligand and the NHC ring is dangling. The Zr-N distances [2.189(5) Å and 2.151(5) Å] are slightly shorter than for other amidinate Zr complexes reported in the literature[155] [Zr(1)-N(1)= 2.238(5) Å, Zr(1)-N(2)= 2.204(5) Å]. The Zr-benzyl distances [2.331(5) Å, 2.304(6) Å and 2.277(6) Å] are similar to those of other benzyl Zr(IV) complexes reported in the literature [2.296(4) Å]. [162]

Bond Distances (Å)	
N(3)-Zr(1)	2.189(5)
N(4)-Zr(1)	2.151(5)
N(1)-C(13)	1.356(8)
N(2)-C(13)	1.339(7)
Zr(1)-C(42)	2.331(5)
Zr(1)-C(49)	2.304(6)
Zr(1)-C(56)	2.277(6)
Angles (º)	
C(42)-Zr(1)-N(4)	142.5(2)
C(49)-Zr(1)-C(56)	124.1(3)
C(1)-N(1)-C(13)	128.6(5)
C(13)-N(2)-C(16)	133.8(5)
N(3)-C(17)-N(4)	104.6(5)
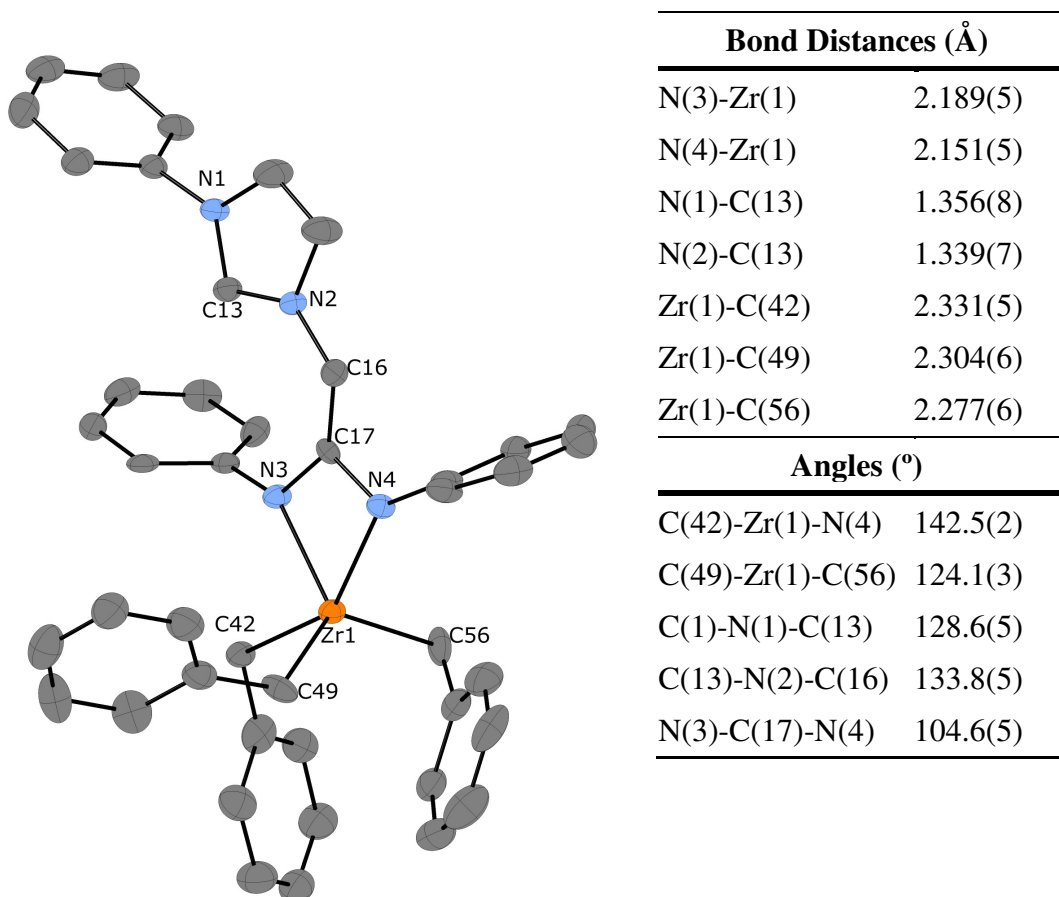
Figure 4.11: CrystalMaker representation of Zr(IV) complex **4.19**. Thermal ellipsoids at 50% probability. Hydrogen atoms and isopropyl substituents in positions 2 and 6 on the phenyl groups have been omitted for clarity. Selected bond lengths (Å) and angles (deg) with estimated standard deviations on the right of the diagram.

bis(DiPP-Amidinate)-Functionalised NHC Chromium Complexes

The reaction of the potassium salt **4.15** with the chromium precursor $CrCl_3(THF)_3$ gave the complex **4.20** showed in Scheme 4.10 below in good yield.
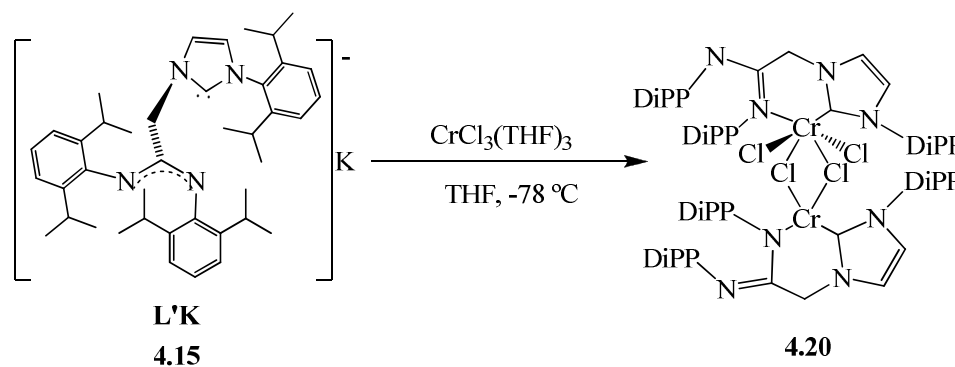
Scheme 4.10: Synthesis of complex **4.20**.

Complex **4.20** was obtained analytically pure by extraction of the reaction residue in toluene, filtration through Celite and removal of the volatile components under reduced pressure. Crystals were obtained from THF/ether and they were characterised by single crystal diffraction techniques.

A CrystalMaker diagram is shown in Figure 4.12 below. The Cr(III) metal precursor was comproportionated during the reaction with the potassium salt **4.15** to give a bimetallic complex **4.20** with two different coordination spheres around the two chromium atoms. The chromium oxidation states are Cr(II) for the square planar and Cr(IV) for the octahedral geometry.

Complex **4.20** showed a distorted octahedral geometry around Cr(1). The amidinate functionalised-NHC ligand L' is coordinated by the carbene carbon atom and just one nitrogen atom of the amidinate substituent. C(17)-N(3) bond distance is slightly longer than C(17)-N(4), which indicates that the coordination mode for L' is κ^2-imine-normal NHC around the Cr(IV) atom (see Figure 4.4). The remaining positions are occupied by chlorides, two of which are bridging chlorides which are also coordinated to Cr(2).

Distorted *cis*-square planar geometry is observed around Cr(2) [C(51)-Cl(3)-Cl(2)-N(8) = 6.8°], as in other NHC Cr(II) complexes such as complex **3.7** described in chapter 2. The Cr-NHC bond lengths [2.093(4) Å, 2.120(4) Å] are in the observed range for other NHC chromium complexes reported in the literature. [116] They are also similar to the corresponding distances for Cr(II) **2.21** and Cr(III) **2.11** chloride complexes [2.085(4) Å and 2.154(2) Å respectively] reported above in chapter 2.

The Cr-Cl bond lengths are also comparable with the same distances for indenyl functionalised NHC complex **2.11** [2.2436(6) Å, 2.3074(6) Å] described in chapter 2 above. However Cr-Cl bond lengths observed in complex **4.20** for the chloride atoms in *trans* position to the carbene ligand are slightly longer than for the tetrahedral complexes **2.11** and **2.12**, as a consequence of strong the *trans* influence exerted by the NHC ligand. This *trans* influence is more important for square planar than for octahedral complexes, [2.6311(17) Å and 2.4126(15) Å respectively].

C(67)-N(8) bond distance is slightly longer than C(67)-N(7), which indicates that the coordination mode for L' is κ^2-iminoyl-normal NHC around the Cr(II) atom (see Figure 4.4 above).

The Cr-N bond length [Cr(2)(square planar)-N(8)= 2.050(3) Å] is very similar to amidinate Cr(III) complex reported in the literature [163] [2.0364(13) Å, 2.0620(13) Å, 2.0395(14) Å and 2.0450(14) Å]; however Cr(1)(octahedral)-N(4)= 2.124(3) Å is slightly longer than amidinate complexes in the literature due to its imine-chromium coordination mode character of the amidinate functionality.

The difference between the exocyclic and endocyclic angles is the result of the strain imposed by the bridge tethered functionality, and it is significantly most important for square planar than for octahedral geometries (23.4º and 16.1º, respectively).
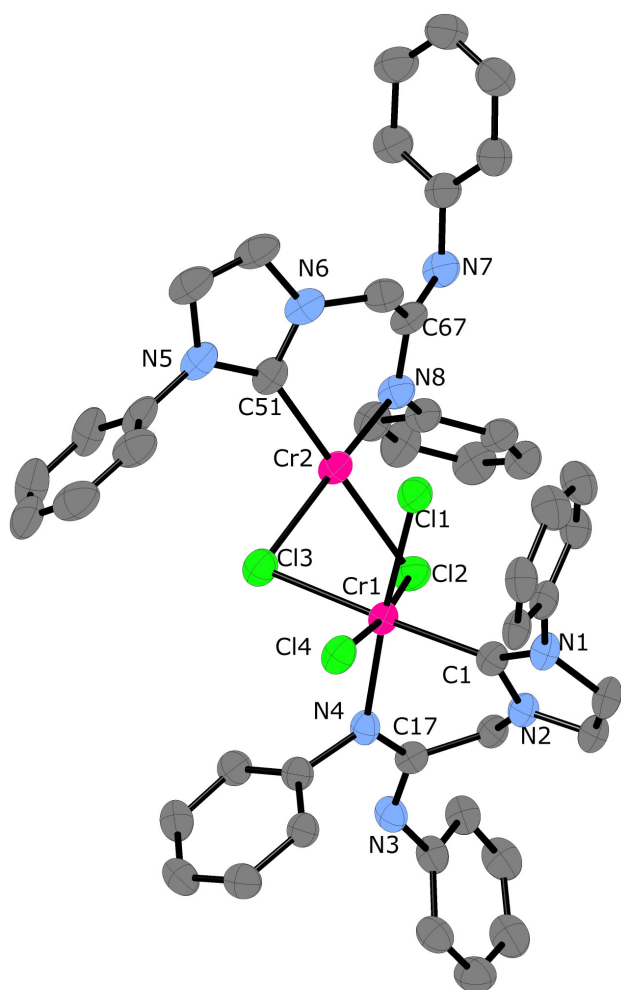
Bond Distances (Å)	
Cr(1)-Cl(1)	2.3500(17)
Cr(1)-Cl(2)	2.3996(16)
Cr(1)-Cl(3)	2.4126(15)
Cr(1)-Cl(4)	2.2645(15)
N(8)-C(67)	1.340(5)
N(7)-C(67)	1.292(5)
Cr(1)-C(1)	2.093(4)
Cr(1)-N(4)	2.124(3)
Cr(2)-Cl(2)	2.6311(17)
Cr(2)-Cl(3)	2.3824(15)
Cr(2)-C(51)	2.120(4)
Cr(2)-N(8)	2.050(3)
C(17)-N(3)	1.342(5)
C(17)-N(4)	1.308(5)
Angles (º)	
Cl(1)-Cr(1)-N(4)	172.72(9)
C(1)-Cr(1)-Cl(3)	176.66(10)
Cr(1)-C(1)-N(1)	136.0(3)
Cr(1)-C(1)-N(2)	119.9(3)
Cl(3)-Cr(2)-N(8)	169.29(10)
N(5)-C(51)-Cr(2)	140.2(3)
N(6)-C(51)-Cr(2)	116.8(3)

Figure 4.12: CrystalMaker representation of Cr complex **4.20**. Thermal ellipsoids at 50% probability. Hydrogen atoms and isopropyl substituents in positions 2 and 6 on the phenyl groups have been omitted for clarity. Selected bond lengths (Å) and angles (deg) with estimated standard deviations on the right of the diagram.

The reaction of the metal precursor $Cr(Me)Cl_2(THF)_3$ with the potassium salt **4.15** at low temperature in THF gave the complex **4.21** shown in Scheme 4.11 below in good yield.

L'K
4.15

R= DiPP

4.21
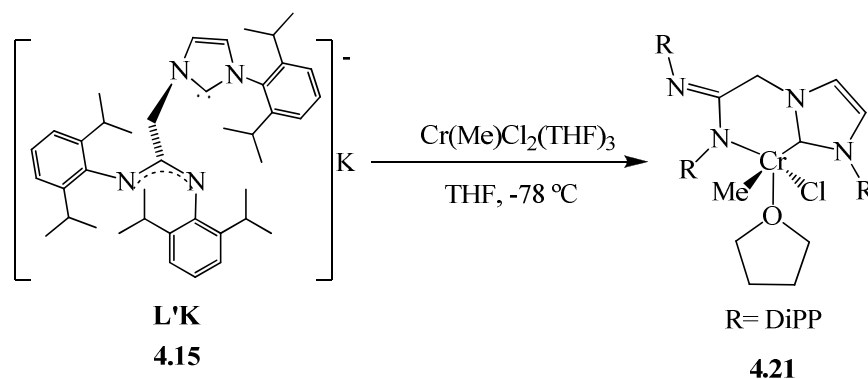
Scheme 4.11: Synthesis of Cr(III) complex **4.21**.

Complex **4.21** was obtained analytically pure by extraction of the reaction residue in diethyl ether, filtration through Celite and removal of the volatile components under reduced pressure. Crystals were obtained from ether/petrol and they were characterised by single crystal diffraction techniques.

A CrystalMaker diagram is shown in Figure 4.13 below. Complex **4.21** adopts distorted square-pyramidal geometry ($\tau = 0.42$), C(51) occupies the apical position and C(1), N(1), O(1A) and Cl(2) form the base of the pyramid in which the torsion angle is 21.3°. The Cr-C(NHC) bond length [2.107(3) Å] is similar to the corresponding bonds for complexes **2.11** and **2.12** [2.089(4) Å and 2.154(2) Å respectively] discussed in chapter 2 above, and it is in the same range than NHC Cr(III) reported in the literature. [116] The Cr(1)-O(THF) bond length [2.131(2) Å] is longer than the corresponding distances for chromium cations **2.18** and **2.20** [2.070(2) Å and 2.060(6) Å respectively] but slightly shorter than the bond lengths observed in the trialkyl chromium complex **3.4** [2.206(4) Å, 2.191(4) Å and 2.225(4) Å]. The Cr-Cl bond length [2.3064(9) Å] is similar to the indenyl-functionalised methyl chromium complex **2.15** [2.287(2) Å] reported in chapter two above; however the Cr-Me distance [2.055(3) Å] is slightly shorter than for the corresponding bond in complex **2.15** [2.150(6) Å]. The Cr-N distance is within the observed range for amidinate Cr(III) complexes in the literature. [163] C(30)-N(3) is longer than C(30)-N(4) which indicates that ligand L' is acting as κ^2-iminoyl-normal NHC ligand (Figure 4.4 above).

The difference between the exocyclic [N(1)-C(1)-Cr(1)] and endocyclic [N(2)-C(1)-Cr(1)] angles is 18.8° which indicates that the strain produced by the bridged

155

functionality inhibits this ligand of acting a tridentate ligand, as well as in the titanium complexes **4.16** and **4.17** described above.

Bond Distances (Å)	
Cr(1)-C(1)	2.107(3)
Cr(1)-C(51)	2.055(3)
Cr(1)-Cl(2)	2.3064(9)
Cr(1)-O(1A)	2.131(2)
Cr(1)-N(3)	2.030(2)
N(3)-C(30)	1.370(4)
N(4)-C(30)	1.290(4)
Angles (º)	
C(1)-Cr(1)-O(1A)	177.86(10)
Cl(2)-Cr(1)-N(3)	152.81(8)
N(2)-C(1)-Cr(1)	119.0(2)
N(1)-C(1)-Cr(1)	137.8(2)

Figure 4.13: CrystalMaker representation of Cr complex **4.21**. Thermal ellipsoids at 50% probability. Hydrogen atoms and isopropyl substituents in positions 2 and 6 on the phenyl groups have been omitted for clarity. Selected bond lengths (Å) and angles (deg) with estimated standard deviations on the right of the diagram.

A brief exploration to Cr(II) chemistry using the new amidinate-functionalised NHC ligand was made. Reaction of $CrCl_2$ with the potassium salt **4.15** in cold THF gave complex **4.22**, the proposed structure for this complex is shown in Scheme 4.12. An analytically pure indigo blue powder was isolated by extraction the reaction residue in diethyl ether, filtration through Celite and removal of the volatile components under reduced pressure. However attempts at crystallisation from different solvents (THF/petrol, ether and toluene) were unsuccessful.
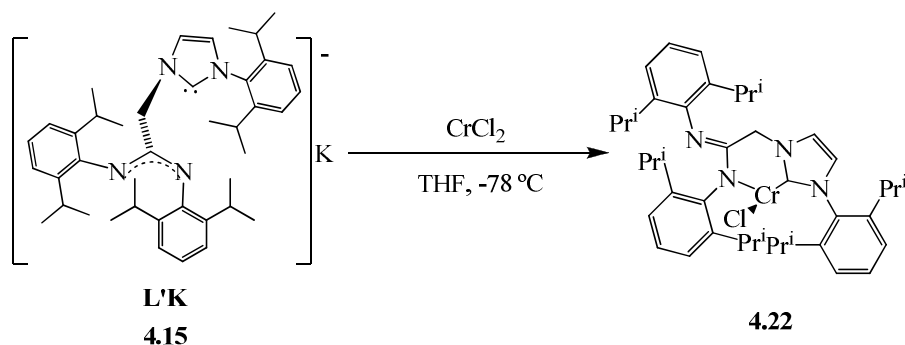
Scheme 4.12: proposed structure for Cr(II) complex **4.22**.

4.2.3 *bis*(DiPP-Amidine/Amidinate)-Functionalised NHC Late Transition Metal Complexes

bis-(DiPP-Amidine)-Functionalised NHC Silver Complex

Silver NHC complexes are useful in transmetallation reactions, as it has been discussed in the first chapter, especially with late transition metals. Complex **4.23** was obtained by refluxing imidazolium chloride **4.13** and silver oxide in 1, 2-dichloroethane as it is shown in Scheme 4.13 below.
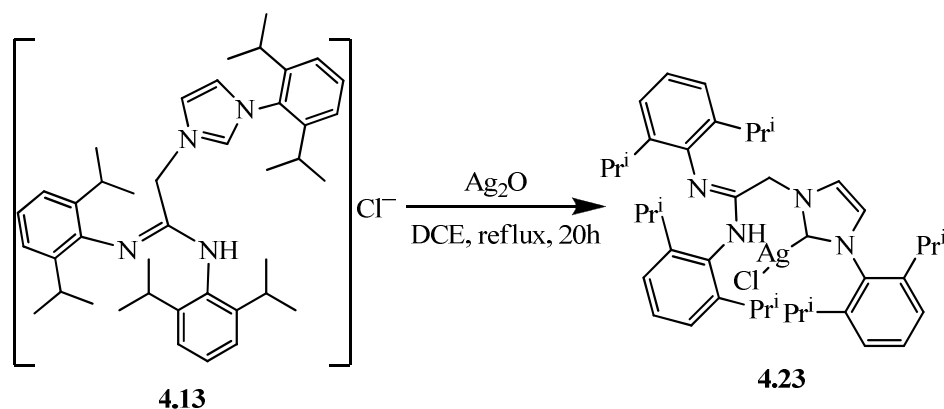
Scheme 4.13: Synthesis of silver complex **4.23**.

Silver complex **4.23** was crystallised from DCM/diethyl ether and characterised by analytical and spectroscopic methods. Its ^{1}H-NMR spectrum was more simplified than the spectrum for the starting material **4.13** in which a mixture of Z/E isomers was evident. The isopropyl substituents appeared as diastereotopic giving six doublets (CH(C*H*$_3$)$_2$) and three septets (C*H*(CH$_3$)$_2$).

The structure of **4.23** was elucidated by single crystal X-ray crystallographic techniques and a CrystalMaker diagram is shown in Figure 4.14. It has linear geometry around the silver atom C(13)-Ag(1)-Cl(1) = 178.49(18)° and the planes

defined by the phenyl rings are almost perpendicular to each other, in order to minimise steric interactions between the isopropyl substituents.

The Ag-C(NHC) [2.076(5) Å] is similar to other NHC silver complex reported in the literature [2.090(5) Å and 2.090(6) Å] [164]

Bond Distances (Å)	
Ag(1)-C(13)	2.076(5)
Ag(1)-Cl(1)	2.3174(16)
N(1)-C(13)	1.346(7)
N(2)-C(13)	1.356(7)
N(3)-C(17)	1.371(7)
N(4)-C(17)	1.275(7)
Angles (º)	
C(13)-Ag(1)-Cl(1)	178.49(18)
N(4)-C(17)-N(3)	126.8(6)
N(1)-C(13)-Ag(1)	125.9(4)
N(2)-C(13)-Ag(1)	129.5(4)
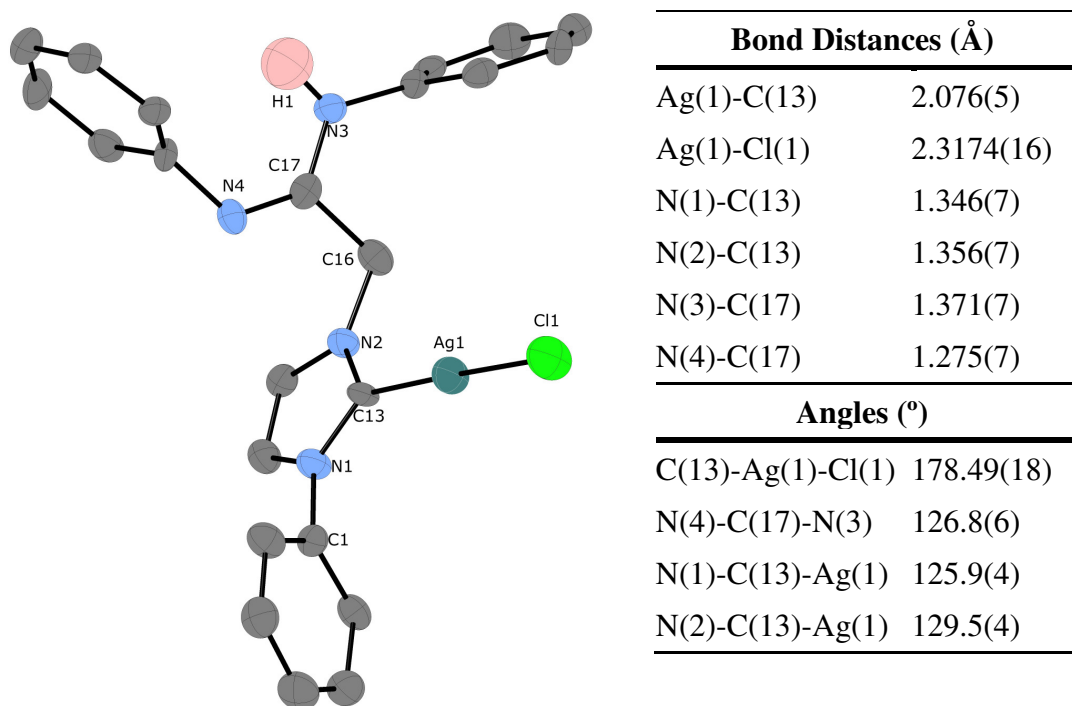
Figure 4.14: CrystalMaker representation of Ag complex **4.23**. Thermal ellipsoids at 50% probability. Hydrogen atoms, except the amidine hydrogen atom, and isopropyl substituents in positions 2 and 6 on the phenyl groups have been omitted for clarity. Selected bond lengths (Å) and angles (deg) with estimated standard deviations on the right of the diagram.

bis(DiPP-Amidinate)-Functionalised NHC Rhodium and Iridium Complexes

The reaction of the metal precursor [RhCl(COD)]$_2$ with silver complex **4.23** gave the Rh complex **4.24** shown in Scheme 4.14 in good yield.
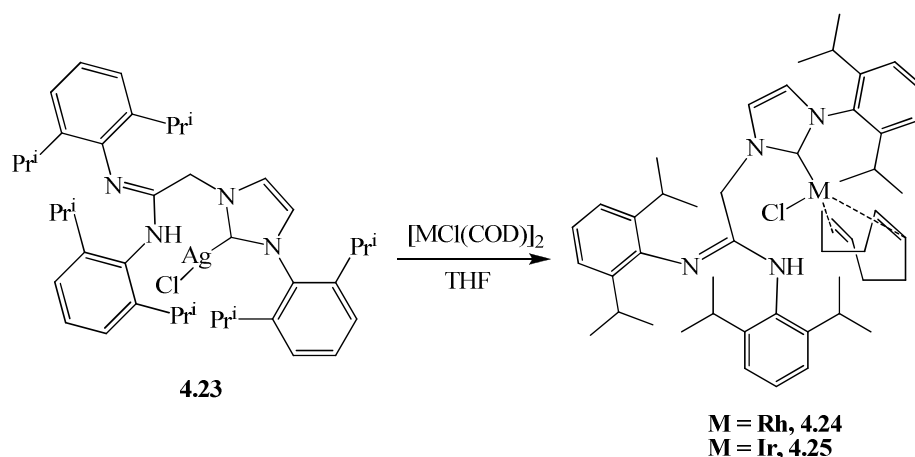
Scheme 4.14: Synthesis of Rh(I) and Ir(I) complexes **4.24** and **4.25** by transmetallation reaction from the silver complex **4.23**.

Complex **4.24** was isolated as an analytically pure bright yellow powder by extraction of the reaction mixture residue with diethyl ether, AgCl precipitate was allowed to settle and the solution was decanted with a cannula and dried under vacuum. Complex **4.24** was characterised by analytical and spectroscopic techniques.

Complex **4.24** is highly asymmetric and this is reflected in its complicated ^{1}H-NMR spectrum. The methyl groups of the isopropyl substituents are diastereotopic and they appear as twelve doublets. The two methylene protons (CH_2) of the bridge and the twelve protons of the COD ligand are inequivalent, as well as the six methylene protons of the isopropyl substituents CH(CH$_3$)$_2$).

The carbene carbon signal was observed at 184.6 ppm in the ^{13}C-{H}-NMR spectrum, significantly more shielded than in the potassium salt **4.15** and the titanium and zirconium complexes with this ligand reported above in this chapter.

Complex **4.24** was crystallised by slowly cooling a concentrated diethyl ether solution to -30 ℃ and its structure was elucidated by crystallographic techniques. A CrystalMaker representation is shown in Figure 4.15. It adopts a *cis*-square planar geometry, as can be seen in the values of the angles below in Figure 4.15, with the central points between C(42) and C(43) and between C(46) and C(47) occupying two positions.

The Rh-C(NHC) bond length [2.035(9) Å] is very similar to other NHC rhodium complexes in the literature [2.032(4) Å] as well as the Rh-Cl distance [2.396(6) Å]. [165]

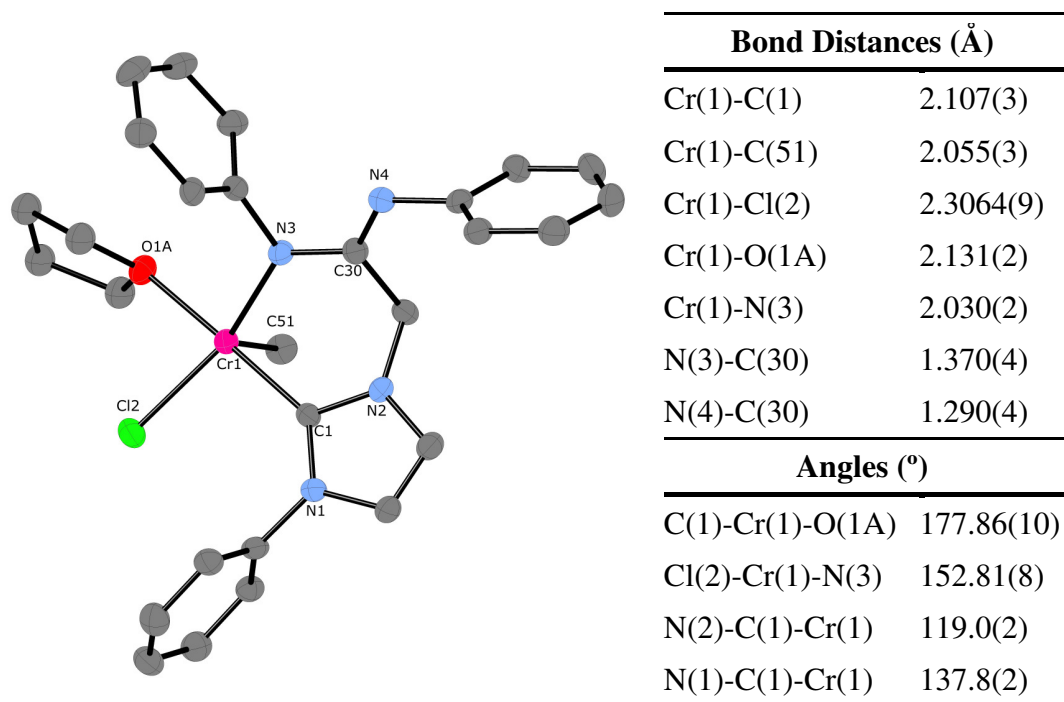| Bond Distances (Å)	
C(13)-Rh(1)	2.035(9)
C(13)-N(1)	1.375(11)
C(13)-N(2)	1.353(11)
C(46)-Rh(1)	2.113(10)
C(47)-Rh(1)	2.120(9)
C(42)-Rh(1)	2.180(9)
C(43)-Rh(1)	2.224(9)
Cl(1)-Rh(1)	2.378(3)
Angles (º)	
C(13)-Rh(1)-C(46)	92.6(4)
C(13)-Rh(1)-C(47)	95.9(4)
C(13)-Rh(1)-Cl(1)	87.6(3)
N(2)-C(13)-Rh(1)	126.5(6)
N(1)-C(13)-Rh(1)	129.6(6)

Figure 4.15: CrystalMaker representation of Rh complex **4.24**. Thermal ellipsoids at 50% probability. Hydrogen atoms, except the amidine proton, and isopropyl substituents in positions 2 and 6 on the phenyl groups have been omitted for clarity. Selected bond lengths (Å) and angles (deg) with estimated standard deviations on the right of the diagram.

The iridium analogue to the rhodium complex **4.25** was synthesised and crystallised using the same methods as those employed for complex **4.24**. However the diffraction produced by the crystals of complex **4.25** was not strong enough, therefore no crystallographic data were collected.

The ^{1}H-NMR spectrum of **4.25** is very similar to the rhodium analogue **4.24**. The methyl groups of the isopropyl substituents, the two methylene protons (CH_2) of the bridge, the twelve protons of the COD ligand and the six methylene protons of the isopropyl substituents CH(CH$_3$)$_2$) appeared as diastereotopic. The carbene carbon signal was observed at 181.2 ppm in the ^{13}C-{H}-NMR spectrum, significantly more shielded than in the potassium salt **4.15** and the titanium and zirconium complexes with this ligand disused above in this chapter.

The chloride atom of complex **4.24** can be abstracted by reaction with NaBAr$_4$ (Ar= 3,5-CF$_3$C$_6$H$_3$) in DCM to give the rhodium cation **4.26** showed in Scheme 4.15 below.

4.24   **4.26**
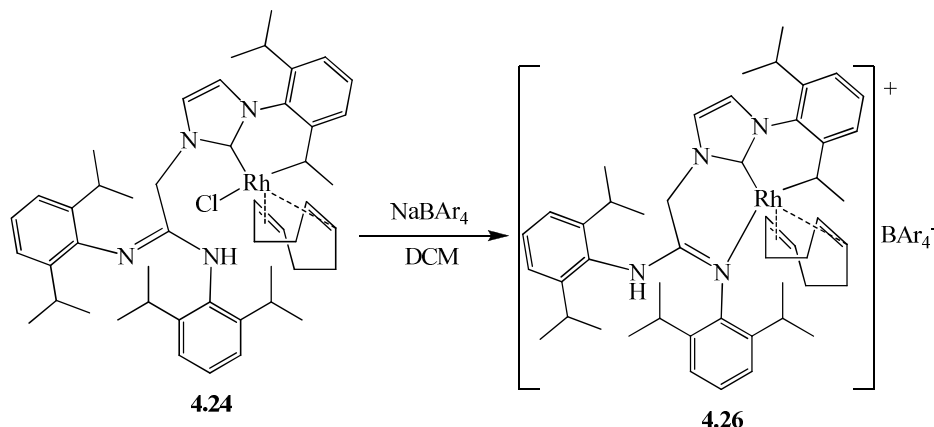
Scheme 4.15: Synthesis of Rh(I) cation **4.26**.

The DCM solution was stirred for 20 hours and filtered through Celite in order to remove the NaCl. The clear solution was dried under reduced pressure to give complex **4.26** as an analytically pure yellow powder which was crystallised from DCM/petrol.

The structure was elucidated by crystallographic techniques and a CrystalMaker representation is shown in Figure 4.16 below. It adopts *cis*-square planar geometry, as the rhodium starting material **4.24**, with the central points between C(42) and C(43) and between C(46) and C(47) occupying two positions. Since the chloride atom has been abstracted in order to form the cation **4.26**, N(3) from the amidine group has coordinated to the rhodium, therefore the amidine-functionalised NHC ligand is acting as a bidentate κ^2-imine-normal NHC ligand.

The difference between the exocyclic and endocyclic angle is 22.2°, this large distortion value is in agreement with the strain imposed by the bridged functionality. However the difference between these two angles in the starting material **4.24** is only 3.1°, due to the fact that the amidinate functionality is dangling in this complex.

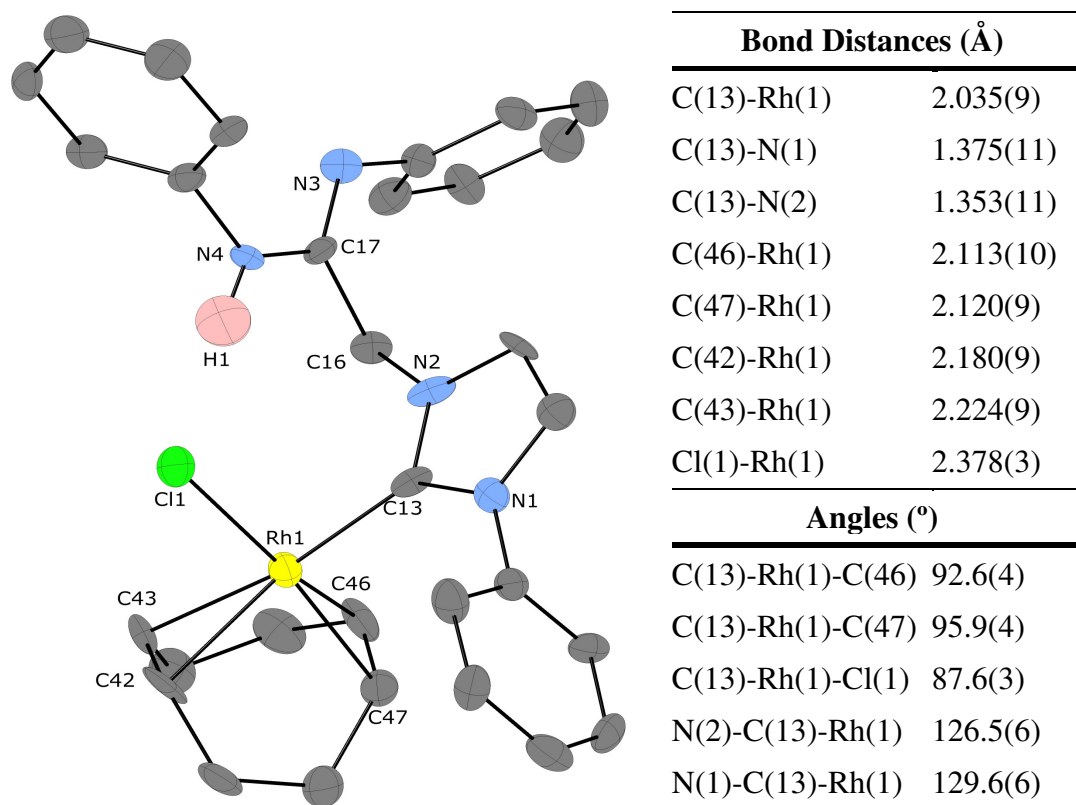| Bond Distances (Å)	
C(13)-Rh(1)	2.069(4)
C(13)-N(1)	1.382(5)
C(13)-N(2)	1.362(5)
C(42)-Rh(1)	2.135(4)
C(43)-Rh(1)	2.130(4)
C(46)-Rh(1)	2.209(4)
C(47)-Rh(1)	2.156(4)
Angles (º)	
N(2)-C(13)-Rh(1)	117.4(3)
N(1)-C(13)-Rh(1)	139.6(3)
C(13)-Rh(1)-N(3)	88.25(15)
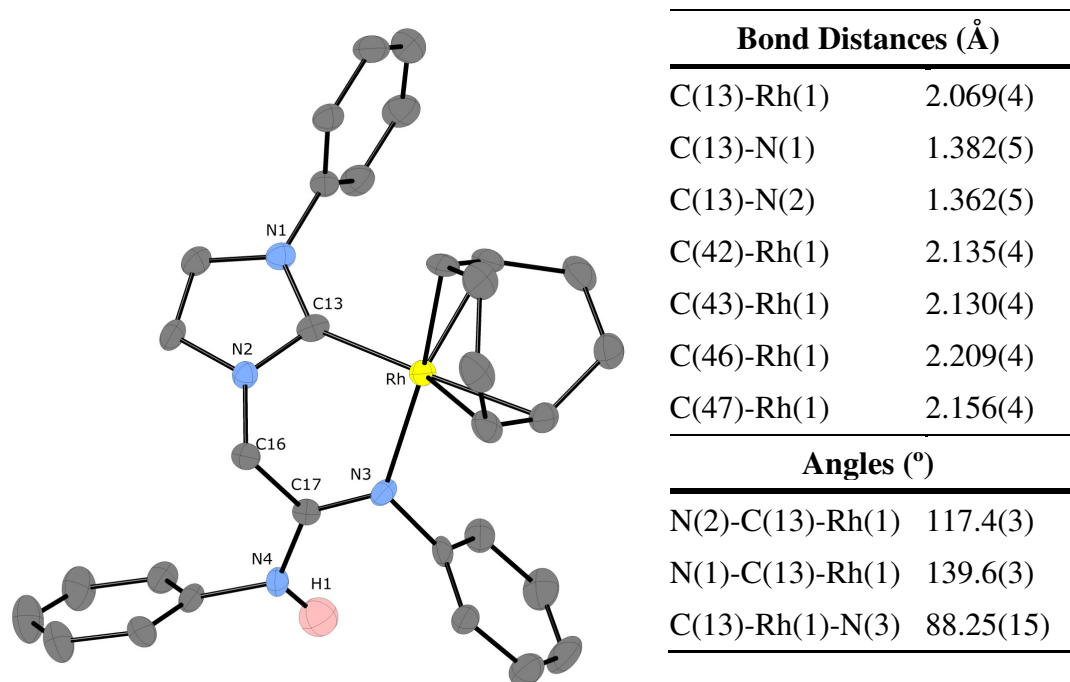
Figure 4.16: CrystalMaker representation of the cationic Rh complex **4.26**. Thermal ellipsoids at 50% probability. Hydrogen atoms, except the amidine proton, isopropyl substituents in positions 2 and 6 on the phenyl groups and anion have been omitted for clarity. Selected bond lengths (Å) and angles (deg) with estimated standard deviations on the right of the diagram.

4.3 Conclusions

The synthesis and characterisation of the first amidinate-functionalised NHC ligand **L'** has been reported in this chapter. The different electronic character of the anionic amidinate group and the neutral N-hetorocyclic carbene donor leads to versatile coordination chemistry, which may have implications in the catalytic performance of these species.

The new potassium salt **L'K** was obtained by double deprotonation of the imidazolium chloride **(L'H$_2$)Cl** with KN(SiMe$_3$)$_2$. The potassium salt **L'K** is suitable to introduce the amidinate-functionalised NHC ligand **L'** to different chloride metal precursors, liberating KCl as driving force for the reaction.

Ligand **L'** acts a as bidentate ligand with early transition metals as titanium, zirconium and chromium. In these complexes the carbene carbon and one of the nitrogen atoms of the amidinate group are coordinate to the metal in bidentate fashion (κ^2-iminoyl- normal NHC or κ^2-iminoyl- abnormal NHC coordination modes). The structure of these metal complexes has been elucidated by diffraction techniques and the difference between exocyclic and endocyclic angles have confirmed that ligand **L'** is prevented of acting as tridentate ligand due to the strain imposed by the methylene group between the NHC and amidinate functionalities.

Zirconium benzyl complexes are also suitable to deprotonate the imidazolium chloride **(L'H$_2$)Cl** to give amidinate-functionalised NHC complexes; the formation of toluene may be the driving force for this reaction to take place. The reaction of **(L'H$_2$)Cl** with tetrabenzyl zirconium gave the tribenzylamidinate zirconium complex, in this complex the amidinate group is coordinated in bidentate fashion to the metal and the NHC functionality is dangling (κ^2-amidinate coordination mode). Steric integrations produced by the bulky benzyl ligands might be the reason why **L'** presented this particular coordination mode in this case.

The imidazolium chloride **(L'H$_2$)Cl** is also suitable to form NHC silver complexes. The *N*-heterocyclic ring was deprotonated in the reaction with Ag$_2$O to give the NHC silver complex in which the amidine is non-coordinated. This silver complex is suitable for transmetallation reactions with rhodium and iridium metal precursors [M(COD)Cl]$_2$ to give NHC complexes with dangling amidine functionality. The chloride atom can be abstracted from these species by reaction with NaBAr$_4$ (Ar =

3,5-CF$_3$C$_6$H$_3$) to give the cation species in which the amidine- functionalised NHC ligand is acting as a bidentate ligand in a κ^2- imine- normal NHC fashion, in order to cover the electronic vacancy left by the chloride.

4.4 Experimental

4.4.1 General Methods for Synthesis of Ligands and Complexes

Elemental analyses were carried out by the London Metropolitan University microanalytical laboratory. All manipulations were performed under nitrogen in a Braun glovebox or using standard Schlenk techniques, unless stated otherwise. Solvents were dried using standard methods and distilled under nitrogen prior to use. The light petroleum used throughout had a bp of 40-60 °C. The starting materials were prepared according to literature procedures: 2-Chloro- -*bis*(2,6-diisopropylphenyl)acetimidamide. [158] NMR data were recorded on Bruker AV 300 and DPX-400 spectrometers, operating *N, N'* at 300 and 400 MHz (1H), respectively. The spectra were referenced internally using the signal from the residual protio-solvent (^{1}H) or the signals of the solvent (^{13}C). Data for X-ray crystallography is included at the end of this chapter.

4.4.2 Pro-Ligand Synthesis Imidazolium Salt Precursor

2-Chloro-*N, N'*-*bis*(2,6-diisopropylphenyl)acetamidine, 4.12
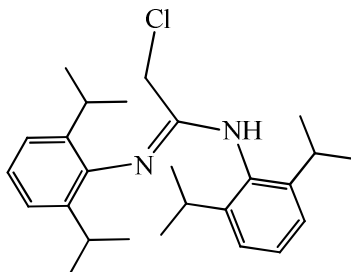
PCl$_5$ (28.53g, 0.137 mmol) was dissolved in dry benzene (75 mL) by heating. When the solution had cooled down 2-chloro-N-(2, 6-diisopropylphenyl)acetamide (31.72g, 0.025mmol) was added. The mixture was heated at reflux until gas evolution ceased. After cooling 2, 6-diisopropylaniline (22g, 0.125 mol) in benzene (75 mL) was added and the reaction mixture was refluxed for 20 h. A white precipitate appeared after cooling which was washed with petrol. To liberate the free base the solid was dissolved in ethanol (250 mL) and treated with aqueous ammonia (25%, 6x 60 mL).The solid was collected by filtration, recrystallised from ethanol and dried under reduced pressure to give small white crystals.

^{1}H-NMR(CDCl$_3$, 300 MHz): (mixture of E/Z isomers) 7.28-6.88 (6H, m, H-aromatic); 6.11 (0.6H, s, NH), 5.35(0.4H, s, NH); 3.96(1.2H, s, CH$_2$Cl); 3.89 (0.8, s,

CH$_2$Cl); 3.25(1.2H, sept, J= 7.5 Hz, CH(CH$_3$)$_2$); 3.09(2H, sept, J= 7.5 Hz,

CH(CH$_3$)$_2$); 2.81 (0.8H, sept, J= 7.5 Hz, CH(CH$_3$)$_2$); 1.20-0.91 (24H, m, CH(CH_3)$_2$)

^{13}C-NMR(CDCl$_3$, 75 MHz): 151.7; 150.7; 147.2; 147.0; 143.8; 139.2; 138.9; 132.8;

132. 2; 128.9; 128.2; 123.9; 123.8; 123.3; 123.1; 123.0; 40.8(-CH$_2$-); 39.3(-CH$_2$-);

28.7; 28.3; 28.2; 27.7; 25.3; 24.3; 23.8; 23.7; 22.8; 22.4.

M. S. (ES$^+$): 415.6 (M+H)$^+$; 413.5 (M+H)$^+$

3-(2.6-diisopropylphenyl)-1-[*N, N'-bis*(2,6-diisopropylphenyl)acetamidyl]
imidazolium chloride, 4.13
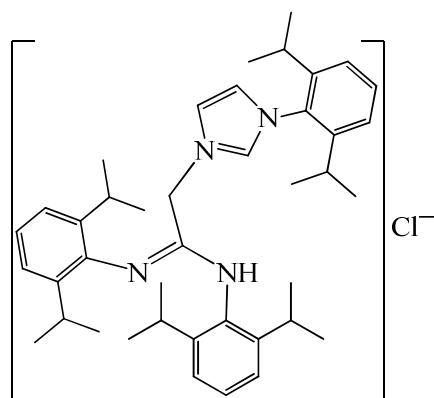
(L'H$_2$)Cl

2-Chloro-N, N'-bis(2,6-diisopropylphenyl)acetimidamide (20g, 50 mmol) and 2,6-
diisopropylphenylimidazol (12.56g, 55 mmol) were heated under partial vacuum at
150 ºC for 4 days. The resulting material was dissolved in the minimum amount of
DCM and triturated with diethyl ether to give a white solid which was dried
azeotropically in toluene. It was finally washed with dry diethyl ether, dried under
vacuum and stored in the glove-box. Yield: 19.69 g, 65%. The product can be
crystallized by layering with diethyl ether a very concentrated DCM solution.

^{1}H-NMR(CDCl$_3$, 300 MHz): (mixture of E/Z isomers) 10.95 (0.4H, s, imidazolium-
H); 10.91 (0.6H, s, imidazolium-H); 9.69 (0.4H, s, N-H); 7.50 (0.4H, t, J= 6Hz,
aromatic-H); 7.40 (0.6H, t, J= 6Hz, aromatic-H); 7.30-6.90 (8H, m, aromatic-H and
0.8H NHC-backbone); 6.90 (0.6H, s, NHC-backbone); 6.05 (0.6H, s, NHC-
backbone); 5.53 (0.6H, s, N-H); 5.49 (0.8, s, CH_2); 5.49 (1.2, s, CH_2); 3.30-3.11 (2H,
m, CH(CH$_3$)$_2$); 2.95 (1.2H, two overlapped sept, J= 6.5Hz, CH(CH$_3$)$_2$); 2.81 (0.8H,
sept, J= 6.5Hz, CH(CH$_3$)$_2$); 2.35 (1.2H, sept, J= 6.5Hz, CH(CH$_3$)$_2$); 2.15 (0.8H, sept,
J= 6.5Hz, CH(CH$_3$)$_2$); 1.40, 1.35, 1.30, 1.15, 1.10, 1.00 and 0.90 (36H, d (some are
overlapping), J= 6.5Hz, CH(CH_3)).

¹³C-{H}-NMR (CDCl₃, 300 MHz):148.7; 147.2; 146.6; 145.6; 145.1; 142.3; 142.0; 139.5; 139.0; 138.7; 133.4; 132.1; 131.7; 130.8; 130.4; 130.1; 129.5; 127.6; 124.8; 124.5; 124.3; 124.1; 123.9; 123.2; 123.2; 123.0; 122.9; 122.7; 65.8; 49.6(-CH₂-); 46.1(-CH₂-); 29.0; 28.7; 28.6; 28.5; 28.3; 25.8; 25.0; 24.5; 24.4; 24.3; 24.1; 24.0; 23.3; 22.3; 22.2; 21.8; 15.3.

^{1}H-NMR(d^{6}-DMSO, 300 MHz): 9.62 (1H, s, imidazolium-H); 8.11 (1H, s, NHC-backbone); 7.77 (1H, s, NHC-backbone); 7.70-6.95 (9H, m, aromatic-H); 4.70 (2H, s, CH_2); 3.25 (2H, sept, J= 7.5Hz, CH(CH₃)₂); 2.95 (2H, sept, J= 7.5Hz, CH(CH₃)₂); 2.30 (2H, sept, J= 7.5Hz, CH(CH₃)₂); 1.38 (6H, d, J= 7 Hz, CH(CH_3)₂),; 1.33 (6H, d, J =7 Hz, CH(CH_3)₂); 1.20-0.90 (24H, m, CH(CH₃)₂).

^{13}C-{H}-NMR($d6$-DMSO, 75 MHz): 147.4; 146.9; 145.1; 142.9; 139.9; 137.9; 132.5; 131.4; 130.5; 128.5; 124.3; 123.7; 122.7; 122.6; 49.6(CH₂); 27.8; 27.7; 24.4; ; 23.9; 23.5; 22.9; 22.4.

M. S. (ES⁺): 607.7 (M-Cl)⁺; 606.7 (M-Cl)⁺; 605.7 (M-Cl)⁺

4.4.3 Double Deprotonation of the Imidazolium Salt Precursor

3-(2.6-diisopropylphenyl)-1-[*N, N'-bis*(2,6-diisopropylphenyl)acetamidyl] imidazol-2-ylidene, 4.14
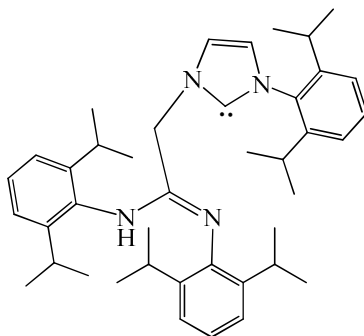
3-(2.6-Diisopropylphenyl)-1-[N, N'-*bis*(2,6-diisopropylphenyl)acetamidyl] imidazolium chloride (1.88g, 3 mmol) was combined with KN(SiMe₃)₂ (0.60 g, 3 mmol) in benzene (20 mL) and the yellow suspension was stirred overnight. The precipitated KBr was removed by filtration thought Celite and the solution pumped to dryness. The yellow solid was submitted for NMR spectroscopy in d^{6}-benzene.

^{1}H-NMR (d^{6}-benzene, 300 MHz): 8.05(1H, broad s, N-H); 7.20-6.85(9H, m, H-aromatic); 6.20(2H, d, J= 6.5Hz, NHC-backbone); 4.45(2H, s, -CH₂-); 3.50(2H, sept,

J= 7.5Hz, CH(CH$_3$)$_2$); 3.25(2H, sept, J= 7.5Hz, CH(CH$_3$)$_2$); 2.65(2H, sept, J= 7.5Hz, CH(CH$_3$)$_2$); 1.35-0.8(36H, m, CH(CH_3)$_2$)

^{13}C-{H}-NMR(d^6-benzene, 75 MHz): 217.0 (NHC-C:); 150.9; 145.7; 145.1; 144.3; 137.7; 136.8; 133.1; 127.8; 122.5; 122.0; 121.8; 120.9; 119.0; 48.4 (-CH$_2$-); 27.7; 26.9; 26.8; 23.0; 22.9; 22.8; 22.4; 21.6.

3-(2.6-diisopropylphenyl)-1-[2-*N, N'bis*(2,6-diisopropylphenylamidinate)ethyl]imidazol-2-ylidenepotassium, 4.15
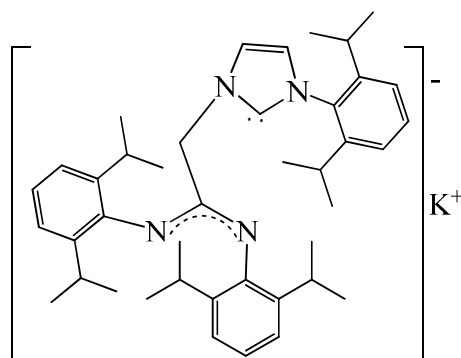
L'K

3-(2.6-Diisopropylphenyl)-1-[N, N'-*bis*(2,6-diisopropylphenyl)acetamidyl] imidazolium chloride (1.88g, 3 mmol) was combined with 1 eq. of KN(SiMe$_3$)$_2$ (0.60 g, 3 mmol) in benzene (20 mL) and the yellow suspension was stirred overnight. The precipitated KCl was removed by filtration thought Celite and the solution of the neutral ligand was subjected to a second deprotonation with another equivalent of KN(SiMe$_3$)$_2$ (0.60 g, 3 mmol) in benzene (20 mL). The orange suspension was stirred overnight. The precipitated product was isolated on a frit washed with benzene (2mL) and petrol (10 mL) and dried under vacuum. Yield: 1.15 g, 61%. The product can be crystallized by layering a very concentrated THF solution with petrol (3/10mL).

Elemental Analysis: Calculated (%): C, 76.18; H, 8.73; N 8.88. Found (%): C,76.09; H, 8.67; N, 8.95

^{1}H-NMR (d^5-pyridine, 300 MHz): 7.45-7.00 (11H, m, aromatic-H and NHC carbene backbone); 4.95 (2H, s, CH_2); 3.76 (4H, m, CH(CH$_3$)$_2$); 2.91(2H, m, CH(CH$_3$)$_2$); 1.35-0.89 (36H, m, CH(CH_3)$_2$)

^{13}C-{H}-NMR(d^5-pyridine, 75 MHz): 214.6 (NHC); 165.1; 156.8; 156.3; 147.3; 142.4; 140.1; 138.4; 129.2; 122.7; 121.2; 119.98; 53.71; 51.37; 28.7; 28.5; 25.4; 25.0; 24.8; 24.4; 24.1

4.4.4 Titanium Complexes and Zirconium Complexes

Ti (L')(N^{t}Bu)(py)Cl, κ^2-iminoyl-normal NHC coordination mode, 4.16
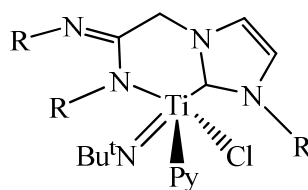
R= DiPP

A suspension of L'K (0.25g, 0.38 mmol) in benzene (15mL) was added to a solution of Ti(N^{t}Bu)Cl$_2$Py$_3$ (0.16g, 0.38 mmol) in the same solvent (15mL) at room temperature. The orange solution was stirred for 3 hours and filtered through Celite. Benzene was removed under reduced pressure and the orange residue was washed with petrol (3x 5 mL) and dried under vacuum to give the analytically pure product. Yield: 0.150 g, 52%. The product can be crystallized by layering a concentrated solution of toluene with petrol.

Elemental Analysis: Calculated (%): C, 71.30; H, 8.45 ; N, 9.24 . Found (%): C, 71.26; H, 8.53; N, 9.15

^{1}H-NMR (d^6-benzene, 300 MHz): 8.08-7.90 (2H, m, py); 7.29-6.91 (9H, m, C-H aromatic); 6.55 (1H, broad t, py); 6.25 (2H, broad t, py); 6.20 (1H, s, NHC back-bond); 5.70 (1H, s, NHC back-bond); 5.00-4.91 (1H, m, C*H*$_2$); 3.95-3.83 (1H, m, C*H*$_2$); 3.55-3.33 (3H, m, C*H*(CH$_3$)$_2$); 3.25-3.12 (1H, m, C*H*(CH$_3$)$_2$); 3.00-2.40 (1H, m, C*H*(CH$_3$)$_2$); 2.50-2.36 (1H, m, C*H*(CH$_3$)$_2$); 1.60 (3H, d, *J*= 6.5 Hz, CH(C*H*$_3$)$_2$); 1.47 (3H, d, *J*= 6.5 Hz, CH(C*H*$_3$)$_2$); 1.35 (3H, d, *J*= 6.5 Hz, CH(C*H*$_3$)$_2$); 1.27-0-80 (36H, m, NC(C*H*$_3$)$_3$ and CH(C*H*$_3$)$_2$ overlapped).

^{13}C{H}-NMR (d^6-benzene, 75 MHz): 192.0 (NHC- carbene); 156.4; 149.7; 147.0; 145.7; 145.1; 144.7; 144.3; 144.1; 143.4; 143.0; 140.0; 138.2; 138.0; 137.7; 136.9; 136.4; 135.7; 133.2; 130.4; 124.2; 123.8; 123.1; 122.5; 122.4; 122.2; 122.0; 121.9; 121.6; 121.4; 121.1; 120.9; 120.5; 120.2; 118.9; 70.6; 64.5; 50.3; 48.5; 33.6; 32.4; 30.6; 30.5; 29.8; 27.8; 27.3; 27.1; 26.9; 26.8; 26.7; 26.2; 26.1; 25.9; 25.5; 25.2; 25.0; 24.7; 24.2; 24.1; 23.6.

Ti (L')(NMe₂)₂Cl, κ^2-iminoyl-abnormal NHC coordination mode, 4.17
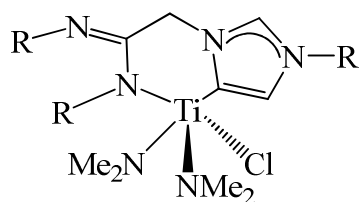
R= DiPP

A solution L'K (0.25g, 0.38 mmol) in THF (15mL) was added to a solution of Ti(NMe₂)₂Cl₂ (0.08g, 0.38 mmol) in the same solvent (15mL) at -78 °C. The orange solution was stirred overnight and volatile components were removed under reduced pressure. The residue was extracted with toluene (40 mL) and filtered through Celite. Toluene was removed under reduced pressure and the orange residue was washed with petrol (3x 5 mL) and dried under vacuum to give the analytically pure product. Yield: 0.160 g, 54%. The product can be crystallized by slow diffusion of petrol in a concentrated toluene solution.

Elemental Analysis: Calculated (%): C, 69.74; H, 8.65; N, 10.85. Found (%): C, 69.68; H, 8.55; N, 10.76.

^{1}H-NMR (d^6-benzene, 300 MHz): 7.30-6.65(9H, m, C-H aromatic); 6.12(1H, s, NHC-back-bone); 6.05(1H, s, NHC-back-bone); 5.45(1H, s, CH_2); 4.35(1H, s, CH_2); 4.05-3.85(4H, m, CH(CH₃)₂); 3.53(2H, s, N(CH_3)₂); 3.35(10H, s, N(CH_3)₂); 1.65(2H, sept, J= 6Hz, CH(CH₃)₂); 1.55(6H, d, J= 7.5Hz, CH(CH_3)₂); 1.45(6H, d, J= 7.5Hz, CH(CH_3)₂); 1.35(6H, d, J= 7.5Hz, CH(CH_3)₂); 1.05(6H, d, J= 7.5Hz, CH(CH_3)₂); 0.78(6H, d, J= 7.5Hz, CH(CH_3)₂); 0.61(6H, d, J= 7.5Hz, CH(CH_3)₂).

^{13}C-NMR (d^6-benzene, 75 MHz): 164.7; 161.3; 148.0; 147.4; 147.1; 146.3; 145.8; 145.5; 145.3; 145.2; 144.1; 143.5; 139.1; 131.5; 131.2; 130.9; 130.7; 130.4; 126.2; 124.8; 124.3; 124.2; 123.8; 123.6; 123.5; 122.7; 122.5; 122.3; 121.4; 120.9; 120.4; 73.7; 72.8; 48.2; 46.3; 29.13; 28.7; 28.5; 28.3; 28.1; 27.8; 26.0; 25.8; 25.8; 25.2; 24.8; 24.5; 24.4; 24.1; 23.8; 23.6; 23.0; 22.7.

4.4.5 Zirconium Complexes

Zr(L')(NMe$_2$)$_2$Cl, κ^2-iminoyl- abnormal NHC coordination mode, 4.18
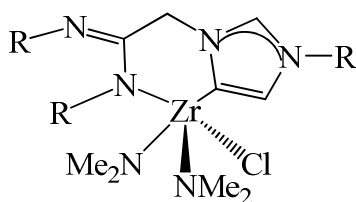
R= DiPP

A solution of L'K (0.30g, 0.47 mmol) in THF (15mL) was added to a solution of Zr(NMe$_2$)$_2$Cl$_2$(THF)$_2$ (0.18g, 0.47mmol) in the same solvent (15mL) at -78 ºC. The bright yellow solution was stirred overnight at room temperature. Petroleum ether (10 mL) was added to precipitate any KCl remaining in solution and it was filtered through Celite. The frit was washed with toluene (10mL) and diethyl ether (10mL). Volatile components were removed under reduced pressure and the residue was washed with petroleum ether (3x 5mL) and dried under vacuum to give the analytically pure product. Yield: 0.20 g, 51%. Attempts to crystallize the product by layering concentrated solutions of THF and toluene with petrol were made and resulted unsuccessful.

Elemental Analysis: Calculated (%): C, 66.04; H, 8.19; N, 10.27. Found (%): C, 65.95; H, 8.28; N, 10.20.

^{1}H-NMR (d^6-benzene, 300 MHz): 7.22-6.97(9H, m, C-H aromatic); 6.07(1H, s, NHC back-bone); 5.55(1H, s, NHC back-bone); 4.70(2H, s, C*H*$_2$); 3.27 (2H, sept, *J*= 7.5Hz, C*H*(CH$_3$)$_2$); 3.16-3.09 (4H, m, C*H*(CH$_3$)$_2$); 2. 92 (2H, s, N(C*H*$_3$)$_2$); 2. 87 (1H, s, N(C*H*$_3$)$_2$); 2. 74 (9H, s, N(C*H*$_3$)$_2$); 1.60 (3H, d, *J*= 7.5Hz, CH(C*H*$_3$)$_2$); 1.41 (6H, d, *J*= 7.5Hz, CH(C*H*$_3$)$_2$); 1.28 (9H, d, *J*= 7.5Hz, CH(C*H*$_3$)$_2$); 1.08 (6H, d, *J*= 7.5Hz, CH(C*H*$_3$)$_2$); 1.05 (6H, d, *J*= 7.5Hz, CH(C*H*$_3$)$_2$); 0.88 (6H, d, *J*= 7.5Hz, CH(C*H*$_3$)$_2$).

^{13}C-NMR (d^6-benzene, 75 MHz): 190.8(NHC carbene); 156.7; 155.2; 145.6; 144.0; 143.3; 142.2; 138.6; 135.9; 129.9; 128.7; 127.9; 124.5; 122.7; 122.6; 122.3; 122.2; 122.1; 121.3; 119.5; 119.4; 118.5; 73.7; 50.0; 48.7; 43.9; 42.9; 40.7; 40.6; 39.3; 28.6; 27.2; 26.4; 24.0; 23.8; 22.5; 21.4; 21.9; 21.0; 19.4.

Zr(L')(Bz)₃, κ^2-amidinate coordination mode, 4.19
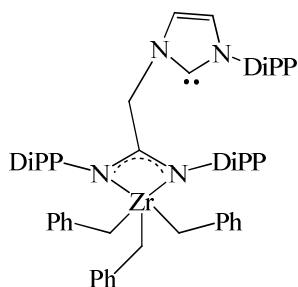
A suspension of the imidazolium salt 3-(2.6-diisopropylphenyl)-1-[N, N'-*bis*(2,6-diisopropylphenyl)acetamidyl] imidazolium chloride in toluene (15mL) was added at -78 ºC to a solution of tetrabenzylzirconium (0.20g, 0.44 mmol) in the same solvent (15mL) at the same temperature. The orange mixture was stirred at room temperature overnight. In this time the suspension became a solution due to the formation of the product. Toluene was removed under reduced pressure and the orange residue extracted with diethyl ether and filtered through Celite. Volatile components were removed under reduced pressure and the solid was washed with petrol. The solid was crystallised by cooling a very concentrated diethyl ether solution at -25 ºC overnight.

4.4.6 Chromium Complexes

Cr(L')(CH₃)Cl(THF), κ^2-iminoyl-normal NHC coordination mode, 4.21

R = DiPP
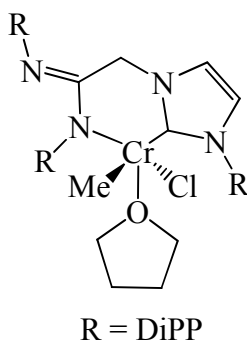
A solution of L'K (0.30g, 0.47mmol) in THF (30mL) at -78 ºC was added to a solution of CrCl₂Me(THF)₃ in the same solvent (20mL) at the same temperature. The solution was let reach room temperature and stirred for 1 hour. During this time the solution tuned from light green to purple. THF was removed under vacuum and the residue extracted with diethyl ether and filtered through Celite. Volatile components were removed under reduced pressure to give the analytically pure product. Yield: 0.190 g, 58%. The product can be crystallized by slow diffusion of petrol in a concentrated diethyl ether solution.

Elemental Analysis: (without THF molecule) Calculated (%): C, 71.44; H, 8.22; N, 7.94. Found (%): C, 71.33; H, 8.17; N, 7.83.

[Cr(L')Cl$_2$]$_2$, κ^2-iminoyl-normal NHC coordination mode for Cr(II) and κ^2-imine-normal NHC coordination mode for Cr(IV), 4.20
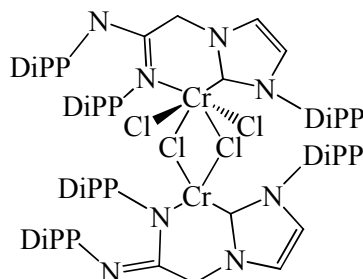
A solution of L'K (1.00g, 1.56 mmol) in THF (20mL) at -78 ºC was added to a solution of CrCl$_3$THF$_3$ in the same solvent (20mL) at the same temperature. The solution was let reach room temperature and stirred overnight. During this time the solution tuned from purple to brown. THF was removed under vacuum and the residue extracted with toluene and filtered through Celite. Volatile components were removed under reduced pressure to give the analytically pure product in quantitative yield. Yield: 1.10 g, 97%. The product can be crystallized by slow diffusion of ether in a concentrated THF solution.

Elemental Analysis: Calculated (%): C, 67.76; H, 7.57; N, 7.71. Found (%): C, 67.78; H, 7.64; N, 7.81.

Cr(L')Cl, κ^2-iminoyl-normal NHC coordination mode, 4.22
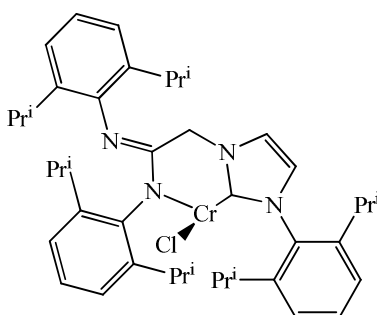
A solution of L'K (0.3, 0.47 mmol) in THF (20mL) at -78 ºC was added to a suspension of CrCl$_2$ in the same solvent (20mL) at the same temperature. The solution was allowed to reach room temperature and stirred for 1 hour. During this time the solution tuned from yellow to indigo. It was kept at -30 ºC overnight. THF was removed under vacuum and the residue extracted with diethyl ether and filtered

through Celite. Volatile components were removed under reduced pressure to give the analytically pure product. Yield: 0.12 g, 36%.

Attempts of crystallisation in different solvents (THF/petrol, ether and toluene) were unsuccessful.

Elemental Analysis: Calculated (%): C, 71.25; H, 7.97; N, 8.11. Found (%): C, 71.15; H, 8.02; N, 8.10.

4.4.7 Late Transition Metal Complexes. Silver, Rhodium and Iridium Complexes

Ag(L'H)Cl, normal NHC monodentate coordination mode, dangling amidine, 4.23
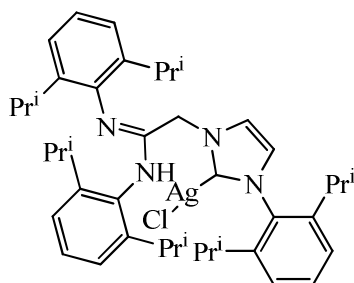
Ag_2O (0.54g, 2.3 mmol) was added to a solution of 3-(2.6-diisopropylphenyl)-1-[N, N'-*bis*(2,6 diisopropylphenyl)acetamidyl] imidazolium chloride (1,00g, 1.5 mmol) in 1,2-dichloroethane (50mL). The mixture was heated at reflux for 20 hours. It was allowed to cool and the black suspension was isolated by filtration through Celite to remove the unreacted Ag_2O. Volatile components were removed under reduced pressure and the residue was dissolved in the minimal amount of DCM (5mL) and precipitate with diethyl ether (20mL). The solid was isolated as white needles which were washed with diethyl ether (3x15mL) and dried under vacuum. Yield: 0.40 g, 53%.

Elemental Analysis: Calculated (%): C, 65.56; H, 7.43; N, 8.05. Found (%): C, 65.89; H, 7.76; N, 8.49.

^{1}H-NMR (CDCl$_3$, 300 MHz): 7.35(1H, t, *J*=9Hz, C-H aromatic); 7.20(1H, t, *J*=9Hz, C-H aromatic); 7.19-7.09(7H, m, C-H aromatic); 7.00(1H, dd, *J*=6Hz, NHC-backbone); 6.88(1H, dd, *J*=3Hz, NHC-backbone); 5.46(1H, s, N-H); 4.69(2H, s, CH$_2$-bridge); 3.20(2H, sept, *J*= 6Hz, C*H*(CH$_3$)$_2$); 2.98(2H, sept, *J*= 6Hz, C*H*(CH$_3$)$_2$); 2.37(2H, sept, *J*= 6Hz, C*H*(CH$_3$)$_2$); 1.39(6H, d, J= 6Hz, CH(C*H$_3$*)$_2$); 1.29(6H, d, J=

6Hz, CH(CH_3)$_2$); 1.08(6H, d, J= 6Hz, CH(CH_3)$_2$); 1.03(6H, d, J= 6Hz, CH(CH_3)$_2$); 1.02(6H, d, J= 6Hz, CH(CH_3)$_2$); 0.96(6H, d, J= 6Hz, CH(CH_3)$_2$).

^{13}C-NMR(CDCl$_3$, 75 MHz): 148.8; 147.1; 145.8; 142.9; 138.6; 134.7; 131.2; 130.4; 129.4; 124.3; 124.2; 123.1; 122.2; 122.1; 52.0; 35.1; 28.8; 28.6; 28.1; 24.8; 24.5; 24.3; 24.2; 23.6; 21.7.

Rh (L'H)(COD)Cl, normal NHC monodentate coordination mode, dangling amidine, 4.24
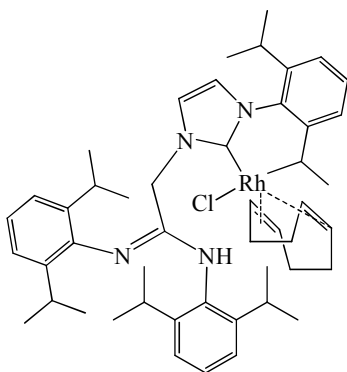
A solution of Ag (L'H)Cl (0.21g, 0.28 mmol) in THF (20mL) was added *via* cannula to a solution of [RhCODCl]$_2$ (0.07g, 14.2 mmol) in the same solvent at room temperature. After 30 min of the mixture a white precipitate came out (AgCl). The yellow suspension was stirred at room temperature overnight. THF was removed under reduced pressure and the residue dissolved in diethyl ether. The white precipitate (AgCl) was allowed to settle on the bottom of the schlenk and the solution decanted *via* cannula. Volatile components were removed under reduced pressure to give the analytically pure product as a yellow microcrystalline solid. Yield: 0.15g, 81%. The solid was crystallized by slow cooling to -25 ℃ of a very concentrated solution in diethyl ether.

Elemental Analysis: Calculated (%): C, 69.05; H, 8.10; N, 6.57. Found (%): C, 69.05; H, 8.08; N, 6.53.

^{1}H-NMR (C$_6$D$_6$, 300 MHz): 8.88(1H, s, N-H); 7.20-7.00(9H, m, H aromatic); 6.95(1H, d, *J*= 3Hz, NHC-backbone); 6.89(1H, d, *J*= 6Hz, COD); 6.87(1H, d, *J*= 6Hz, COD); 6.20 (1H, d, *J*= 18Hz, COD), 6.26 (1H, d, *J*= 3Hz, NHC-backbone); 5.25-5.15 (1H, m, CH_2); 5.04-4.96 (1H, m, CH_2); 4.88 (1H, d, *J*= 18Hz, COD); 3.79 (1H, sept, *J*= 6Hz, CH(CH$_3$)$_2$); 3.60 (1H, sept, *J*= 6Hz, CH(CH$_3$)$_2$); 3.45 (1H, sept, *J*= 6Hz, CH(CH$_3$)$_2$); 3.31 (1H, sept, *J*= 6Hz, CH(CH$_3$)$_2$); 3.08(1H, broad t, COD);

2.92 (1H, broad t, COD); 2.20-2.05 (2H, m, C*H*(CH$_3$)$_2$); 2.00-1.95 (2H, m, COD), 1.80-1.61 (4H, m, COD); 1.51 (6H, two overlapped d, *J*= 6Hz, CH(C*H$_3$*)$_2$); 1.45 (3H, d, *J*= 6Hz, CH(C*H$_3$*)$_2$); 1.35 (3H, d, *J*= 6Hz, CH(C*H$_3$*)$_2$); 1.30 (6H, two overlapped d, *J*= 6Hz, CH(C*H$_3$*)$_2$); 1.18 (3H, d, *J*= 6Hz, CH(C*H$_3$*)$_2$); 1.00 (6H, two overlapped d, *J*= 6Hz, CH(C*H$_3$*)$_2$); 0.98 (3H, d, *J*= 6Hz, CH(C*H$_3$*)$_2$); 0.82 (3H, d, *J*= 6Hz, CH(C*H$_3$*)$_2$); 0.75 (3H, d, *J*= 6Hz, CH(C*H$_3$*)$_2$).

^{13}C-{H}-NMR(C$_6$D$_6$, 75 MHz): 184.6(NHC); 184.6(NHC); 150.2; 147.2; 145.5; 143.9; 143.8; 138.5; 137.4; 134.1; 133.0; 128.9; 123.1; 122.7; 121.9; 121.22; 118.11; 97.2; 97.1; 96.8; 96.7; 77.2; 77.0; 66.7; 66.5; 66.3; 47.7; 32.8; 30.4; 28.0; 27.9; 27.8; 27.2; 27.0; 24.5; 22.7; 22.6; 22.1; 21.3; 19.8.

M.S. (ES$^+$): 817.4 (M-Cl)$^+$, 816.4 (M-Cl)$^+$, 815.4 (M-Cl)$^+$

[Rh(L'H)(COD)]$^+$[BAr$_4$]$^-$, κ^2-imine-normal NHC coordination mode, 4.26
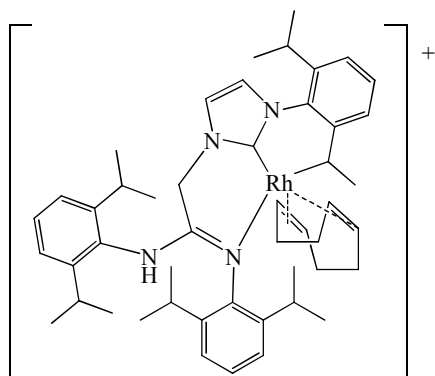
A solution of Na(BAr)$_4$ (Ar= 3,5-CF$_3$C$_6$H$_3$) (72 mg, 0.082 mmol) in DCM (20 mL) was added to a solution of Rh(L'H)(COD)Cl (70 mg, 0.082 mmol) in the same solvent (20 mL) at room temperature. The orange solution was stirred for 20 hours and filtered through Celite. Volatile components were removed *in vacuo* to give a light orange solid. The solid can be crystallised by layering a concentrated DCM solution with petrol. Yield: 105mg, 82%.

Elemental Analysis: Calculated (%): C, 55.83; H, 4.33; N, 3.57. Found (%): C, 55.25; H, 5.63; N, 3.45.

Ir (L'H)(COD)Cl, normal NHC monodentate coordination mode, dangling amidine, 4.25
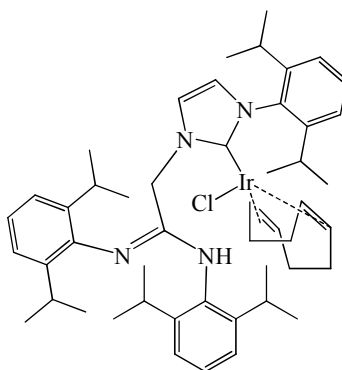
A solution of Ag(L'H)Cl (0.14g, 0.19 mmol) in THF (20mL) was added *via* cannula to a solution of [Ir(COD)Cl]$_2$ (0.06g, 0.09 mmol) in the same solvent at room temperature. After 30 min of the mixture a white precipitate came out (AgCl). The yellow suspension was stirred at room temperature overnight. THF was removed under reduced pressure and the residue dissolved in diethyl ether. The white precipitate (AgCl) was allowed to settle on the bottom of the schlenk and the solution decanted *via* cannula. Volatile components were removed under reduced pressure to give the analytically pure product as a yellow microcrystalline solid. Yield: 0.09g, 47%. The solid was crystallized by slow cooling of a very concentrated solution in diethyl ether.

Elemental Analysis: Calculated (%): C, 62.57; H, 7.24; N, 5.96. Found (%): C, 62.46; H, 7.16; N, 5.85.

^{1}H-NMR (C$_6$D$_6$, 400 MHz): 8.57 (1H, s, N-H); 7.31-7.15 (9H, m, H aromatic); 7.10 (1H, d, *J*= 4.5Hz, NHC backbone); 7.00 (2H, dd, *J*= 7.5Hz, COD); 6.63 (1H, d, *J*= 14.0Hz, COD); 6.30 (1H, d, *J*= 4.5Hz, NHC backbone); 4.80 (1H, d, *J*= 14.0Hz, COD); 5.05-5.00(1H, m, C*H*$_2$); 4.89-4.82 (1H, m, C*H*$_2$); 4.00-3.95 (1H, m, COD); 3.85 (1H, sept, *J*= 6.5Hz, C*H*(CH$_3$)$_2$); 3.65-3.50 (2H, m, C*H*(CH$_3$)$_2$); 3.41 (1H, sept, *J*= 6.5Hz, C*H*(CH$_3$)$_2$); 3.20-3.05(1H, m, COD); 2.99-2.81 (2H, m, COD); 2.19-2.10 (2H, m, COD); 1.99 (1H, sept, *J*= 6.5Hz, C*H*(CH$_3$)$_2$); 1.85 (1H, d, *J*= 6Hz, COD); 1.72 (1H, d, *J*= 6Hz, COD); 1.65-0.95 (36H, overlapped doublets, CH(C*H*$_3$)$_2$).

^{13}C-{H}-NMR (C$_6$D$_6$, 75MHz):181.2 (NHC); 150.4; 149.7; 147.1; 147.0; 143.9; 143.6; 138.4; 137.8; 133.8; 132.8; 128.9; 123.0; 122.7; 121.9; 121.3; 118.0; 84.1;

83.9; 83.4; 80.6; 50.9; 50.3; 50.2; 48.6; 47.5; 36.0; 33.3; 31.5; 29.9; 28.1; 27.9; 27.3; 27.2; 26.9; 22.2; 22.0; 21.3; 20.5; 19.8.

4.4.8 Crystallographic Parameters for Compounds in this Chapter

Table 4.1: Crystallographic parameters for compounds **4.13** and **4.15**.

Identification code	**4.13**	**4.15**
Empirical formula	$C_{41}H_{57}ClN_4$	$C_{43}H_{59}KN_4O_{0.5}$
Formula weight	640.50	679.04
Temperature	120(2) K	120(2) K
Wavelength	0.71073 Å	0.71073 Å
Crystal system	Monoclinic	Triclinic
Space group	*Cc*	*P-1*
Unit cell dimensions	a = 22.5237(3) Å	a = 13.80520(10) Å
	α= 90°	α= 90.5980(10)°
	b = 12.7743(2) Å	b = 14.34640(10) Å
	β= 102.6610(10)°	β= 94.8700(10)°
	c = 16.6305(2) Å	c = 20.6098(2) Å
	γ= 90°	γ= 95.8140(10)°
Volume	4668.65(11) Å³	4045.47(6) Å³
Z	4	4
Density (calculated)	1.167 Mg/m³	1.115 Mg/m³
Absorption coefficient	0.371 mm⁻¹	0.166 mm⁻¹
F(000)	1740	1472
Crystal size	0.25 x 0.20 x 0.10 mm³	0.2 x 0.17 x 0.16 mm³
Theta range for data collection	2.95 to 27.53°	3.06 to 27.48°
Index ranges	-29<=*h*<=29	-17<=*h*<=17
	-16<=*k*<=16	-18<=*k*<=18
	-21<=*l*<=21	-26<=*l*<=26
Reflections collected	50959	83379
Independent reflections	5357 [R*(int)* = 0.0537]	18419 [R*(int)* = 0.0565]
Completeness to theta = 27.53°	99.6 %	99.3 %
Absorption correction	Semi-empirical from equivalents	Semi-empirical from equivalents
Max. and min. transmission	0.9608 and 0.9119	0.9804 and 0.9576
Refinement method	Full-matrix least-squares on F^2	Full-matrix least-squares on F^2
Data / restraints / parameters	5357 / 3 / 503	18419 / 5 / 901
Goodness-of-fit on F^2	1.045	1.080
Final *R* indices [I>2sigma(I)]	*R1* = 0.0546, *wR2* = 0.1387	*R1* = 0.0721, *wR2* = 0.1516
R indices (all data)	*R1* = 0.0615, *wR2* = 0.1439	*R1* = 0.1080, *wR2* = 0.1739
Absolute structure parameter	0.08(7)	0.637 and -0.590 e.Å⁻³
Largest diff. peak and hole	1.098 and -0.585 e.Å⁻³	C43 H59 K N4 O0.50

Table 4.2: Crystallographic parameters for complexes **4.16** and **4.17**.

Identification code	**4.16**	**4.17**
Empirical formula	$C_{50}H_{69}Cl\,N_6Ti$	$C_{135}H_{201}Cl_3N_{18}Ti_3$
Formula weight	837.46	2326.19
Temperature	120(2) K	120(2) K
Wavelength	0.71073 Å	0.71073 Å
Crystal system	Triclinic	Trigonal
Space group	*P -1*	*R -3*
Unit cell dimensions	a = 11.271 Å	a = 37.015(5) Å
	α = 103.30°	α = 90.000(5)°
	b = 12.033 Å	b = 37.015(5) Å
	β = 92.33°	β = 90.000(5)°
	c = 19.627 Å	c = 23.193(5) Å
	γ = 109.50°	γ = 120.000(5)°
Volume	2421.8 Å^3	27520(8) Å^3
Z	2	6
Density (calculated)	1.148 Mg/m^3	0.842 Mg/m^3
Absorption coefficient	0.270 mm^{-1}	0.210 mm^{-1}
F(000)	900	7524
Crystal size	0.14 x 0.14 x 0.14 mm^3	0.13 x 0.13 x 0.10 mm^3
Theta range for data collection	3.05 to 27.57°	3.09 to 17.50°
Index ranges	-14<=*h*<=14	-30<=*h*<=31
	-15<=*k*<=15	-31<=*k*<=31
	-25<=*l*<=25	-19<=*l*<=19
Reflections collected	48275	30138
Independent reflections	11129 [*R(int)* = 0.0419]	3855 [*R(int)* = 0.0996]
Completeness to theta = 27.57°	99.2 %	99.2 %
Absorption correction	Semi-empirical from equivalents	Semi-empirical from equivalents
Max. and min. transmission	0.9631 and 0.8881	0.9793 and 0.6230
Refinement method	Full-matrix least-squares on F^2	Full-matrix least-squares on F^2
Data / restraints / parameters	11129 / 0 / 538	3855 / 0 / 494
Goodness-of-fit on F^2	1.056	1.069
Final R indices [I>2sigma(I)]	*R1* = 0.0440, *wR2* = 0.0942	*R1* = 0.0941, *wR2* = 0.2652
R indices (all data)	*R1* = 0.0562, *wR2* = 0.1017	*R1* = 0.1319, *wR2* = 0.2975
Largest diff. peak and hole	0.275 and -0.308 e.Å^{-3}	1.055 and -0.346 e.Å^{-3}

Table 4.3: Crystallographic parameters for complexes **4.19** and **4.20**.

Identification code	**4.19**	**4.20**
Empirical formula	$C_{62}H_{76}N_4Zr$	$C_{88}H_{126}Cl_8Cr_2N_8O$
Formula weight	968.49	1699.57
Temperature	120(2) K	120(2) K
Wavelength	0.71073 Å	0.6889 Å
Crystal system	Monoclinic	Monoclinic
Space group	*P21/c*	*P21/c*
Unit cell dimensions	a = 14.8303(4) Å	a = 14.433(10) Å
	$\alpha = 90°$	$\alpha = 90°$
	b = 17.3255(4) Å	b = 21.648(15) Å
	$\beta = 101.1760(10)°$	$\beta = 97.642(7)°$
	c = 21.7198(6) Å	c = 29.447(19) Å
	$\gamma = 90°$	$\gamma = 90°$
Volume	5474.9(2) Å^3	9119(11) Å^3
Z	4	4
Density (calculated)	1.175 Mg/m^3	1.238 Mg/m^3
Absorption coefficient	0.242 mm^{-1}	0.520 mm^{-1}
F(000)	2064	3608
Crystal size	0.38 x 0.08 x 0.01 mm^3	0.10 x 0.10 x 0.08 mm^3
Theta range for data collection	2.99 to 25.03°	2.86 to 24.21°
Index ranges	-17<=h<=17	-17<=h<=17
	-20<=k<=20	-25<=k<=25
	-25<=l<=25	-34<=l<=27
Reflections collected	96492	71778
Independent reflections	9644 [R(int) = 0.2922]	15908 [R(int) = 0.0908]
Completeness to theta = 25.03°	99.8 %	98.8 %
Absorption correction	Semi-empirical from equivalents	Semi-empirical from equivalents
Max. and min. transmission	0.9956 and 0.9137	0.9596 and 0.9498
Refinement method	Full-matrix least-squares on F^2	Full-matrix least-squares on F^2
Data / restraints / parameters	9644 / 0 / 616	15908 / 1206 / 970
Goodness-of-fit on F^2	1.189	1.026
Final R indices [I>2sigma(I)]	*R1* = 0.1163, *wR2* = 0.1622	*R1* = 0.0670, *wR2* = 0.1778
R indices (all data)	*R1* = 0.1775, *wR2* = 0.1797	*R1* = 0.1224, *wR2* = 0.2097
Largest diff. peak and hole	0.636 and -0.512 e.Å^{-3}	0.870 and -1.133 e.Å^{-3}

Table 4.4: Crystallographic parameters for complexes **4.21** and **4.23**.

Identification code	**4.21**	**4.23**
Empirical formula	$C_{46}H_{66}ClCrN_4O$	$C_{41}H_{56}Ag\,ClN_4$
Formula weight	778.48	748.22
Temperature	153(2) K	120(2) K
Wavelength	0.71073 Å	0.71073 Å
Crystal system	Orthorhombic	Triclinic
Space group	$P2_12_12_1$	$P\text{-}1$
Unit cell dimensions	a = 14.4973(4) Å	a = 10.2894(7) Å
	$\alpha = 90°$	$\alpha = 80.103(4)°$
	b = 16.0212(4) Å	b = 12.4817(13) Å
	$\beta = 90°$	$\beta = 86.108(5)°$
	c = 18.7006(4) Å	c = 16.3801(17) Å
	$\gamma = 90°$	$\gamma = 74.035(5)°$
Volume	4343.48(19) Å^3	1992.0(3) Å^3
Z	4	2
Density (calculated)	1.190 Mg/m^3	1.247 Mg/m^3
Absorption coefficient	0.363 mm^{-1}	0.605 mm^{-1}
$F(000)$	1676	788
Crystal size	0.15 x 0.15 x 0.02 mm^3	0.26 x 0.06 x 0.06 mm^3
Theta range for data collection	3.01 to 27.64°	2.44 to 27.80°
Index ranges	-18<=h<=18	-13<=h<=13
	-17<=k<=20	-15<=k<=15
	-23<=l<=24	-20<=l<=20
Reflections collected	30195	39376
Independent reflections	9596 [R(int) = 0.0569]	8364 [R(int) = 0.2321]
Completeness to theta = 27.50°	99.2 %	88.5 %
Max. and min. transmission	0.9928 and 0.9476	0.9646 and 0.8586
Refinement method	Full-matrix least-squares on F^2	Full-matrix least-squares on F^2
Data / restraints / parameters	9596 / 6 / 487	8364 / 1 / 441
Goodness-of-fit on F^2	1.075	0.937
Final R indices [I>2sigma(I)]	$R1 = 0.0520$, $wR2 = 0.0962$	$R1 = 0.0702$, $wR2 = 0.1191$
R indices (all data)	$R1 = 0.0752$, wR2 = 0.1069	$R1 = 0.2433$, wR2 = 0.1637
Absolute structure parameter	0.13(2)	
Largest diff. peak and hole	0.301 and -0.332 e.Å^{-3}	0.545 and -0.728 e.Å^{-3}

Table 4.5: Crystallographic parameters for complexes **4.24** and **4.25**.

Identification code	**4.24**	**2.26**
Empirical formula	$C_{53}H_{78}Cl\ N_4ORh$	$C_{81}H_{80}BF_{24}N_4Rh$
Formula weight	925.55	1679.21
Temperature	120(2) K	120(2) K
Wavelength	0.8914 Å	0.71073 Å
Crystal system	Monoclinic	Triclinic
Space group	*P2$_1$/n*	*P-1*
Unit cell dimensions	a = 11.950(2) Å	a = 13.4793(4) Å
	$\alpha = 90°$	$\alpha = 81.071(2)°$
	b = 35.000(7) Å	b = 16.1623(4) Å
	$\beta = 110.53(3)°$	$\beta = 89.3780(10)°$
	c = 12.940(3) Å	c = 19.3716(5) Å
	$\gamma = 90°$	$\gamma = 76.8710(10)°$
Volume	5068.4(18) Å^3	4058.81(19) Å^3
Z	4	2
Density (calculated)	1.213 Mg/m^3	1.374 Mg/m^3
Absorption coefficient	0.429 mm^{-1}	0.310 mm^{-1}
F(000)	1976	1720
Crystal size	0.12 x 0.02 x 0.01 mm^3	0.30 x 0.08 x 0.04 mm^3
Theta range for data collection	2.87 to 21.97°	2.92 to 25.03°
Index ranges	-10<=*h*<=12	-16<=*h*<=16
	-36<=*k*<=36	-19<=*k*<=19,
	-13<=*l*<=10	-23<=*l*<=23
Reflections collected	14100	78405
Independent reflections	6068 [*R(int)* = 0.1200]	14293 [*R(int)* = 0.1154]
Completeness to theta = 21.97°	98.0 %	99.8 %
Absorption correction	Semi-empirical from equivalents	Semi-empirical from equivalents
Max. and min. transmission	0.9957 and 0.9503	0.9677 and 0.9127
Refinement method	Full-matrix least-squares on *F^2*	Full-matrix least-squares on *F^2*
Data / restraints / parameters	6068 / 8 / 559	14293 / 1 / 1042
Goodness-of-fit on F^2	0.955	1.039
Final *R* indices [I>2sigma(I)]	*R1* = 0.0764, *wR2* = 0.1623	*R1* = 0.0679, *wR2* = 0.1296
R indices (all data)	*R1* = 0.1392, *wR2* = 0.1935	*R1* = 0.1064, *wR2* = 0.1436
Largest diff. peak and hole	1.247 and -1.038 e.Å^{-3}	0.744 and -0.597 e.Å^{-3}

References

1 Arduengo, A. J.; Diaz, H. V. R.; Harlow, R.; Kline, M. *J. Am. Chem. Soc*. **1992**, 114, 5530.

2 Schuster, G. B. *Adv. Phys. Org. Chem*. **1986**, 22, 311.

3 Gleiter, R.; Hoffmann, R. *J. Am. Chem. Soc.* **1968**, 90, 1475.

4 (a) Harrison, J. F. *J. Am. Chem. Soc*. **1971**, 93, 4112; (b) Harrison, J. F.; Liedtke, C. R.; Liebman, J. F. *J. Am. Chem. Soc*. **1979**, 101, 7162.

5 Hoffmann, R.; Zeiss, G. D.; Van Dine, G. W. *J. Am. Chem. Soc*. **1968**, 90, 1485.

6 Baird, N. C.; Taylor, K. F. *J. Am. Chem. Soc*. **1978**, 100, 1333.

7 Gilbert, B. C.; Griller, D.; Nazran, A. S. *J. Org. Chem*. **1985**, 50, 4738.

8 Tomioka, H.; Hattori, M.; Hirai, K.; Murata, S. *J. Am. Chem. Soc*. **1996**, 118, 8723.

9 Fischer, E. O.; Massbol, A. *Angew. Chem., Int. Ed. Engl*. **1964**, 76, 580.

10 Schrock, R. R. *J. Am. Chem. Soc*. **1974**, 96, 6796.

11 Alder, R. W.; Allen, P. R. and Williams, S. J. *J. Chem. Soc., Chem. Commun.* **1995**, 1267.

12 Breslow, R. *Chemistry and Industry*, **1957**, 26, 893.

13 Breslow, R. *J. Am. Chem. Soc.* **1957**, 79, 1762.

14 (a) Wanzlick, H. W.; Kleiner, H. J. *Angew. Chem*. **1961**, 73, 493; (b) Wanzlick, H. W. *Angew. Chem., Int. Ed. Engl*. **1962**, 1, 75; (c) Wanzlick, H. W.; Esser, F.; Kleiner, H. J. *Chem. Ber*. **1963**, 96, 1208.

15 (a) Wanzlick, H. W.; Schonherr, H. *J. Liebigs Ann. Chem*. **1970**, 731, 176; (b) Schonherr, H. J.; Wanzlick, H. W. *Chem. Ber*. **1970**, 103, 1037.

16 Arduengo, A. J.; Harlow, R. L. and Kline, M. *J. Am. Chem. Soc.* **1991**, 113, 361.

17 Arduengo, A. J.; Dias, H. V. R.; Harlow, R. L. and Kline. M. *J. Am. Chem. Soc.* **1992**, 114, 5530.

18 Arduengo, A. J.; Goerlich J. R.; Marshall, W. J. *J. Am. Chem. Soc.* **1995**, 117, 11027.

19 (a) Denk, M. K.; Thadani, A.; Hatano, K.; Lough, A. J. *Angew. Chem., Int. Ed. Engl.* **1997**, 36, 2607; (b) Alder, R. W.; Blake, M. E.; Bortolotti, C.; Bufali, S.; Butts, C. P.; Lineham, E.; Oliva, J. M.; Orpen, A. G.; Quayle, M. J. *J. Chem. Soc.*, *Chem. Commun.* **1999**, 241; (c) Kuhn, N.; Kratz, T. *Synthesis,* **1993**, 561; (d) Enders, D.; Breuer, K.; Raabe, G.; Runsink, J. Teles, J. H.; Melder, J. P.; Ebel, K.; Brode, S. *Angew. Chem., Int. Ed. Engl.* **1995**, 34, 1021; (e) Arduengo, A. J.; Goerlich, J. R.; Marshall, W. *J. Liebigs Ann. Chem.* **1997**, 365; (f) Alder, R. W.; Allen, P. R.; Murray, M.; Orpen, G. *Angew. Chem., Int. Ed. Engl.* **1996,** 35, 1121; (g) Alder, R. W.; Buts, C. P.; Orpen, A. G. *J. Am. Chem. Soc.* **1998**, 120, 11562.

20 Lehmann, J. F.; Urquhart, S. G.; Ennis, L. E.; Hitchcock, A. P.; Hatano, K.; Gupta, S.; Denk, M. K. *Organometallics*, **1999**, 18, 1862.

21 Alder, R. W.; Allen, P. R.; Murray, M. and Orpen, A. G. *Angew. Chem., Int. Ed. Engl.* **1996**, 35, 1121.

22 Arduengo, A. J.; Davidson, F.; Dias, H. V. R.; Goerlich, J. R.; Khasnis, D.; Marshall, W. J.; Prakasha, T. K. *J. Am. Chem. Soc.* **1997**, 119, 12742.

23 Herrmann, W. A.; Kocher, Ch.; Goossen, L. J.; Artus, G. R. J. *Chem. Eur. J.* **1996**, 2, 1627.

24 Herrmann, W.A.; Elison, M.; Fischer, J.; Köcher, C.; Artus, G. R. J. *Chem. Eur. J.,* **1996**, 2, 772.

25 Douthwaite, R. E.; Haussinger, K.; Green, M. L. H.; Silcock, P. J.; Gomes, P. T.; Martins, A. M.; Danopoulos, A. A. *Organometallics*, **1999**, 18, 4584.

26 Bildstien, B.; Malaun, M.; Kopacka, H.; Ongania, K.H.; Wurst, K. *J. Organomet. Chem.* **1999**, 572, 177.

27 Kuhn, N.; Kratz, T. *Synthesis,* **1993**, 561.

28 Scholl, M.; Ding, S.; Lee, C. W.; Grubbs, R. H. *Org. Lett*. **1999**, 1, 953.

29 Herrmann, W.A.; Goossen, L. J.; Artus, G. R. J.; Köcher, C. *Organometallics*, **1997**, 16, 2472.

30 Herrmann, W. A.; Gerstberger, G.; Spiegler, M. *Organometallics*, **1997**, 16, 2209.

31 Ofele, K., *J. Organomet. Chem*. **1968**, 12, 42.

32 Herrmann, W. A.; Elison, M.; Fischer, J.; Köcher, C.; Artus, G. R. J. *Angew. Chem., Int. Ed. Engl*. **1995**, 34, 2371.

33 Herrmann, W. A.; Elison, M.; Fischer, J.; Köcher,C.; Artus, G. R. J. *Chem. Eur.J.,* **1996**, 2, 772.

34 Herrmann, W. A. And Schwarz, J. *Organometallics*, **1999**, 18, 4082.

35 Lappert, M. F. *J. Organomet. Chem*. **1988**, 358, 185.

36 H. M. J. Wang, I. J. B. Lin, *Organometallics*, **1998**, 17, 972.

37 Ku, R. Z.; Huang, J. C.; Cho, J. Y.; Klang, F. M.; Reddy, K. R.; Chen, Y. C.; Lee,K. J.; Lee, J./ .; Lee, G. H.; Peng, S./ .; Liu, S. T. *Organometallics,* **1999**, 18, 2145.

38 Liu, S. T.; Hsieh, T. Y.; Lee, G. H.; Peng, S. M. *Organometallics,* **1998**, 17, 993.

39 Papini, G.; Bandoli, G.; Dolmella, A.; Lobbia, G. G. ; Pellei, M.; Santini, C.;

   Inorg. Chem. Comm. **2008**, 11, 1103.

40 R. H: Crabtree, *J. Organom. Chem*. **2005,** 690, 5451.

41 Heck, R. F.; *Org. React.* **1982**, **27**, 345.

42 Meijere, A.; Meyer, F. E. . *Angew. Chem. Int. Ed. Engl*. **1994***,* 33, 2379.

43 Sonogashira, K.; Tohda, Y.; Hagihara, N. *Tetrahedron Letters*, **1975**, 16, 50, 4467.

44 Chinchilla, R.; Nájera, C. *Chem. Rev*. **2007**, 107, 3, 874.

45 Kotha, S.; Lahiri, K.; Kashinath, D. *Tetrahedron*, **2002**, 48, 9633

46 Barder, E.; Walker, S. D.; Martinelli, J. R. and Buchwald, S. L. *J. Am. Chem. Soc*.

   2005, 127, 4685.

47 Whitcombe, N. J.; Kuok, K.; Hii and Gibson, S. E. *Tetrahedron*, **2001**, 45, 7449.

48 Herrmann, W. A.; Bohm, V. P. W.; Reisinger, C. P. *J. Organomet. Chem.* **1999**,

   576, 23.

49 Weskamp, T.; Bohm, V. P. W.; Herrmann, W. A.; *J. Organomet. Chem.* **2001**,

   585, 348.

50 Mc Guinness, D. S.; Cavell, K. J. *Organometallics*, **2000**, 19, 741.

51 King, A. O.; Okukado, N. and Negisi, E. *J. Chem. Soc. Chem. Comm.*, **1977**, 683.

52 Peris, E.; Loch, J. A.; Mata, J.; Crabtree, R. H. *Chem. Commun*. **2001**, 210.

53 Scholl, M.; Ding, S.; Lee, C. W.; Grubbs, R. H. *Org. Lett.* **1999**, 1, 953.

54 Chatterjee, A. K.; Morgan, J. P.; Scholl, M.; Grubbs, R. H. *J. Am. Chem. Soc*.

   2000, 122, 3783.

55 Vieille-Petit, L.; Luan, X.; Gatti, M.; Blumetritt, S.; Linden, A.; Clavier, H.; Nolan, S.; Dorta, R. *Chem. Comm*. **2009**, 3783

56 Gardiner, M. G.; Herrmann, W. A.; Reisinger, C. P.; Spiegler, M. *J. Organomet. Chem.,* **2001**, 635.

57 Arnold, P. L.; Mungur, S. A.; Blake, A. J.; Wilson, C. *Angew. Chem., Int. Ed. Engl*. **2003**, 42, 598.

58 Aihara, H.; Matuso, T.; Kawaguchi, H. *Chem. Commun*. **2003**, 2204.

59 McGuinness, D. S.; Vernon, C.; Gibson and Jonathan W. Steed, ; *Organometallics*. **2004**, 23, 6288.

60 Pugh, D.; Wright, J. A.; Freeman, S.; Danopoulos, A. A. *Dalton Trans*., **2006**, 775.

61 Pugh, D.; Danopoulos, A. A. *Coord. Chem. Rev*.; **2006**, 251, 610.

62 Kealy, T, J and Pauson, P.L, *Nature,* **1951**, 168 , 1039.

63 Wilkinson, G; Rosenblum, M; Whiting, M. C.; Woodward, R. B.; *J. Am. Chem. Soc*., **1952**, 74, 2125.

64 Fischer, E. O; Pfab, W, *Z. Naturforsch*, **1952**, B7, 377.

65 Dunitz, J.; Orgel, L.; Rich, A.; *Acta Crystallographica*, **1956**, 9, 373.

66 Laszlo, P.; Hoffmann, R.; *Angew. Chem. Int. Ed*.; **2000**, 39, 123.

67 "Press Release: The Nobel Prize in Chemistry 1973". *The Royal Swedish Academy of Sciences*. **1973**.

68 Paulson, P. L.; Wilkinson, G. *J. Am. Chem. Soc*. **1954**, 76, 2024.

69 White, C.; Mawby, R.J.; Hart-Davis, A. J. *Inorg. Chim. Acta*, **1970**, 4, 261.

70 Basolo, F. *Coord. Chem. Rev*. **1982**, 43, 7.

71 Rerek, M. E.; Ji, L. N.; Basolo, F. *J. Chem. Soc. Chem. Commun*. **1983**, 1208.

72 Rerek, M. E. and Basolo, F. *J. Am. Chem. Soc.* **1984**, 106, 5908.

73 Veiros, L. F. *Organometallics,* **2000**, 19, 3127.

74 Calhorda, M. J.; Roma, C. C. and Veiros, L. F. *Chem. Eur. J.* **2002**, 8, 868.

75 Hart-Davis, A.J.; Mawby, R.J. *J. Chem. Society,* **1969**, 2403.

76 (a)Dohring, A.; Gohre, J.; Jolly, P. W.; Kryger, B.; Rust, J.; Verhovnik, G. P. J.
Organometallics, **2000**, 19, 388; (b) Jensen, V. R.; Angermund, K.; Jolly, P. W.;
Børve, K. J. *Organometallics,* **2000**, 19, 403.

77 Dohring, A.; Jensen, V. R.; Jolly, P. W.; Thiel, W. And Weber, J. C.
Organometallics, **2001**, 20, 2234.

78 Komon, Z. J. A.; Diamond, G. M.; Leclerc, M. K.; Murphy, V.; Okazaki, M. and
Bazan, G. C. *J. Am. Chem. Soc.,* **2002**, 124, 15280.

79 Kuwabara, J.; Takeuchi, D.; Osakada, K. *Chem. Comm*. **2006**, 3815.

80 (a) Gibson, V. C.; Spitzmesser, S. K. *Chem. Rev*. **2003**, 103, 283. (b) Coates, G.
W.; Hustad,P. D.; Reinartz, S. *Angew. Chem., Int. Ed.* **2002**, 41, 2236.

81 Rix, F.; Brookhart, M. *J. Am. Chem. Soc*. **1995**, 117, 1137; (b) Peuckert, M.; Keim,
W. *Organometallics*, **1983,** 2, 594; (c) Wilke, G. *Angew. Chem., Int. Ed. Engl.*
1988, 27,185; (d) Mohring, V. M.; Fink, G. *Angew. Chem., Int. Ed. Engl.* **1985**,
24, 1001.

82 Johnson, L. K.; Killian, C. K.; Brookhart, M.; *J. Am. Chem. Soc*. **1995**, 117, 6414.

83 US 5,866,663 "Process of Polymerizing Olefins," Samuel David Arthur, Alison
Margaret Anne Bennett, Maurice S. Brookhart, Edward Bryan Coughlin, Jerald
Feldman, Steven Dale Ittel, Lynda Kaye Johnson, Christopher Moore Killian;
Kristina Ann Kreutzer, Elizabeth Forrester McCord, Stephan James McLain,

Anju Parthasarathy, Lin Wang, Zhen-Yu Yang; February 2, **1999**. WO 9623010 A2 960801.

84 Britovsek, G. J. P.; Gibson, V.; Kimberley, B. S.; Maddox, P. J.; McTavish, S. J.; Solan, G. A.; White, A. J. P.; Williams, D. *J. Chem. Commun.* **1998**, 7, 849.

85 Small, B. L.; Brookhart, M.; Bennett, A. M. A. *J. Am. Chem. Soc.* **1998**, 120, 16, 4049.

86 Ittel, S. D.; Johnson, L.K. and Brookhart, M. *Chem. Rev.* **2000**, 100, 1169.

87 Small, B. L. and Brookhart, M. *J. Am. Chem. Soc.* **1998**, 120, 7143.

88 (a)Herskovics-Korine, D. And Eisen; M.S. *J. Organomet. Chem.* **1995**, 503, 307; (b) Flores, J.C.; Chien, J.C.W; Rausch, M. D. *Organometallics*, **1995**, 14, 1827; (c) Averbuj, C.; Tish, E.; Eisen, M.S. *J. Am. Chem. Soc.* **1998**, 120, 8640; (d) Littke, A.; Sleiman, N.; Bensiman, C.; Richeson, D. S.; Yap, G.P.A.;. Brown, S. J. *Organometallics*, **1998**, 17, 446; (e) Volkis, V.; Shmulison, M.; Averbuj, C.; Lisovskii, A.; Edelmann, F.T.; Eisen, M.S. *Organometallics*, **1998**, 17, 3155; (f) Gomez, R.; Green, H. M. L.; Haggitt, J. L.; *J. Chem. Soc., Dalton Trans.*, **1996**, 6, 939.

89 Wang, C.; Friedrich, S.; Younkin, T. R.; Li, R. T.; Grubbs, R. H.; Bansleben, D. A.M.; Day, W.; *Organometallics*, **1998**, 17, 3149.

90 US 6,174,975, "Polymerization of Olefins," Lynda Kaye Johnson; Alison Margaret Anne Bennett, Lin Wang, Anju Parthasarathy, Elisabeth Hauptman, Robert D. Simpson, Jerald Feldman, Edward Bryan Coughlin, and Steven Dale Ittel. January 16, **200l**.

91 Matsui, S.; Tohi, Y.; Mitani, M.; Saito, J.; Makio, H.; Tanaka, H.; Nitabaru, M.; Nakano, T.; Fujita, T. *Chem. Lett.*, **1999**, 1065.

92 Niehues, M.; Erker, G.; Kehr, G.; Schwab, P.; Frolich, R. *Organometallics*, **2002**, 21, 2905.

93 Liddle, S. T.; Edworthy, I. S.; Arnold, P. L. *Chem. Soc. Rev*. **2007**, 36, 1732.

94 Downing, S. P.; Danopoulos A. A. *Organometallics,* **2006**, 25, 1337.

95 Downing, S. P.; Conde-Guadaño, S.; Pugh, D.; Danopoulos, A. A.; Bellabarba, R. M.; Hanton, M.;Smith, D. and. Tooze, R. P. *Organometallics*, **2007**, 26, 3762.

96Sun, H.; Hu, D.; Wang, Y.; Shen, Q.; Zhang, Y. *J. Organom. Chem*. **2007**, 692, 903.

97 Costa, A. P.; Viciano, M.; Sanaú, M.; Merino, S.; Tejeda, J.; Peris, E. and Royo, B. *Organometallics*, **2008**, 27, 1305.

98 Kandepi,V. V. K. M.; Costa, A. P.; Peris, E. and Royo, B. *Organometallics*, **2009**, 28, 4544.

99 Wu, F.; Dioumaev, V. K.; Szalda, D. J.; Hanson, J.; Bullock, R, M. *Organometallics,* **2007**, 26, 5079.

100 Faller, J. W.; Anderson, A. S.; Jakubowski, A. *J. Organomet. Chem.* **1971**, 27, 47.

101 Dixon, J. T.; Green, M. J.; Hess, F. M. and Morgan, D. H. *J. Organom. Chem,* **2004**, 689, 3641.

102 Britovsek, G. J. P.; Gibson, V. C. and Wass, D. F.; *Angew. Chem. Int. Ed*., **1999**, 38, 428.

103 (a) Alpha Olefins (02/03-4), PERP Report, Nexant Chem Systems; (b) W.K. Reagan, EP 0417477 (Phillips Petroleum Company),March 20, **1991**.

104 (a) McGuinness, D. S.; Wasserscheid, P.; Keim, W.; Morgan, D.; Dixon, J. T.; Bollmann, A.; Maumela, H.; Hess, F. and Englert, U.; *J. Am. Chem. Soc.*, **2003**, 125, 5272; (b) McGuinness, D. S.; Wasserscheid, P.; Keim, W.; Dixon, J. T.; Grove, J. J. C.; Hu, C.; Englert, U. *Chem. Commun.* **2003**, 334.

105 (a) Carter, A.; Cohen, S. A.; Cooley, N. A.; Murphy, A.; Scutt, J.; Wass, D. F. *Chem. Commun.* **2002**, 858; (b) Agapie, T.; Schofer, S. L.; Labinger, J. A.; Bercaw, J. E. *J. Am. Chem. Soc.* **2004**, 126, 1304.

106 (a) Carter, A.; Cohen, S. A.; Cooley, N. A.; Murphy, A.; Scutt, J.; Wass, D. F. *Chem. Commun.* **2002**, 858; (b) Wu, F.-J. U.S. Patent 5,811,618, **1998**.

107 Arteaga-Muller, R.; Tsurugi, H.; Saito, T.; Yanagawa, M.; Oda, S. and Mashima, K. *J. Am. Chem. Soc.*, **2009**, 131, 5370.

108 (a) Bollmann, A.; Blann, K.; Dixon, J.T.; Hess, F.M.; Killian, E.; Maumela, H.; McGuinness, D.S.; Morgan, D.H.; Nevelling, A.; Otto, S.; Overett, M.; Slawin, A. M. Z.; Wasserscheid, P.; Kuhlmann, S. *J. Am. Chem. Soc.*, **2004**, 126 , 14712; (b) Blann, K.; Bollmann, A.; Dixon, J.T.; Neveling, A.; Morgan, D.H.; Maumela, H.; Killian, E.; Hess, F.; Otto, S.; Pepler, L.; Mahomed, H.A.; Overett, M. J.; Green, M. WO 2004,056,478, to Sasol Technology; (c) Blann, K.; Bollmann, A.; Dixon, J.T.; Neveling, A.; Morgan, D.H.; Maumela, H.; Killian, E.; Hess, F.; Otto, S.; Pepler, L.; Mahomed, H. A.; Overett, M. J. WO 2004,056,479, to Sasol Technology; (d) Overett, M. J.; Blann, K.; Bollmann, A.; Dixon, J. T.; Haasbroek, D.; Killian, E.; Maumela, H.; McGuinness, D.S.; Morgan, D.H. *J. Am. Chem. Soc.* **2005,** 127, 10723; (e) Walsh, R.; Morgan, D. H.; Bollmann, A.; Dixon, J. T. *Appl. Catal. A Gen.* **2006**, 306, 184; (f)

Kuhlmann, S.; Dixon, J.T.; Haumann, M.; Morgan, D.H.; Ofili, J.; Spuhl, O.; Taccardi, N.; Wasserscheid, P. *Adv. Synth. Catal*., **2006**, 348, 1200; (g) Blann, K.; Bollmann, A.; Dixon, J.T.; Morgan, D.H.; Killian, E.; Overett, M.J.; Walsh, R. N. WO 2005,123,633, to Sasol Technology; (h) WO 2005,123,884, to Sasol Technology; (i) Overett, M. J.; Blann, K.; Bollmann, A.; Dixon, J. T.; Hess, F.M.; Killian, E.; Maumela, H.; Morgan, D. H.; Neveling, A.; Otto, S. *Chem. Commun*., **2005**, 622.

109 Manyik, R. M.; Walker, W. E.; Wilson, T. P.; *J. Catal*., **1977**, 47, 197.

110 (a) McGuinness, D.S.; Overett, M. J.; Tooze, R.P.; Blann, K.; Dixon, J. T.; Slawin, A. M. Z. *Organometallics,* **2007**, 26, 1108; (b) Rucklidge, A. J.; McGuinness, D.S.; Tooze, R.P.; Slawin, A. M. Z.; Pelletier, J. D. A.; Hanton, M. J.; Webb, P. B. *Organometallics*, **2007**, 26, 2782.

111 Martinez-Carrera, S.; *Acta Cryst.,***1966**, 20, 783.

112 (a) Alder, R. W.; Allen, P. R.; Williams, S. J. *Chem. Commun*. **1995**, 1267; (b) Bordwell, F. G.; Bausch, M. J. *J. Am. Chem. Soc*. **1983**, 105, 6188.

113 Lorber, C. and Vendier, L. *Organometallics*, **2008**, 27, 2774.

114 Blake, A. J.; Collier, P. E.; Dunn, S. C.; Li, W. S.; Mountford, P.; Shishkin, A. V.; *Dalton Trans***. 1997**, 1549.

115 Enders, M.; Fernandez, P.; Mihan, S.; Pritzkow, H.; *J. Organom. Chem*, **2003**, 687, 125.

116 (a) Voges, M. H.; Rømming, C.; Tilset, M. *Organometallics,* **1999**, 18, 529; (b) McGuinness, D. S.; Gibson, V. C.; Wass, D. F.; Steed, J. W. *J. Am. Chem.*

Soc. **2003**, 125, 12716; (c) Abernethy, C. D.; Clyburne, J. A. C.; Cowley, A. H.; Jones, R. A. *J. Am. Chem. Soc.* **1999**, 121, 2329.

117 Clark, A. *Catal. Rev*. **1969**, 3, 145.

118 (a) Karol, F. J.; Karapinka, G. L.; Wu, C.; Dow, A. W.; Johnson, R. N.; Carrick, W. L. *J. Polym. Sci. Part A,* **1972**, 10, 2621; (b) Karol, F. J.; Brown, G. L.; Davison, J. M. *J. Polym Sci., Polym. Chem. Ed*. **1973**, 11, 413.

119 Thomas, B. J.; Noh, S.; Schulte, G. K.; Sendlinger, S. C. and Theopold, K. H. *J. Am. Chem. Soc*. **1991**, 113, 893.

120 Kreisel, K. A.; Yap, G. P. A. and Theopold, K. H. *Organometallics*, **2006**, 25, 19, 4675.

121 Heinemann, O.; Jolly, P. W.; Kruger, C. and Verhovnik, G. P. J. *Organometallics*, **1996**, 15, 5462.

122 Urushiyama, A.; Nomura, T. and Nakahara M.; *Bull. Chem. Soc. Jap.* **1970**, 43, 3971.

123 McConnell, A. C.; Pogorzelec, P. J.; Slawin, A. M. Z. Williams, G. L.; Elliot, P. I.; Haynes, A.; Marr, A. C.; Cole-Hamillton, D. J.; *Dalton Trans*. **2006**, 91.

124 Vagedes, D.; Erker, G.; Fröhlich, R.; *J. Organomet. Chem*. **2002**, 641, 148.

125 Leusen, D.; Beetstra, D. J.; Hessen, B. and Teuben. J. H. *Organometallics*, **2000**, 19, 4084.

126 Deppener, M.; Burger, R.; Alt, H. G. *J. Organomet. Chem*. **2004**, 689, 1194.

127 Erker, G.; Psiorz, C.; Frohlich, R.; Grehl, M.; Krueger, C.; Noe, R.; Nolte, M. *Tetrahedron*, **1995**, 15, 4348.

128 Johnson, A. L. US Patent 3,637,731, **1972.**

129 Chung, F. M.; Westland A. D. *Can J. Chem*. **1969**, 47, 195.

130 Dunn, S. C.; Mountford, P.; Robson, D. A. *J. Chem. Soc., Dalton Trans.* **1997**, 293.

131 H. H. Zeiss, W. Herwig, *J. Org. Chem.* **1958**, 23, 1404.

132 Nishimura, K.; Kuribayashi, H.; Yamamoto, A.; Ikeda, S.; J. Organomet. Chem., 1972, 37, 317.

133 Wagner, B.O.; Hammond, G.; J. Organomet. Chem., 1975, 85, 1.

134 Brookhart, M.; Grant, B.and Volpe, A. F. Jr.; Organometallics; 1992, 11, 3920.

135 (a) Tsutsui, M. and Zeiss, H. H. *J. Amer. Chem. Soc*. **1959**, 81, 8090. (b) Metlesics, W. and Zeiss, H. H. *J. Amer. Chem. Soc*. **1959**, 1, 4117. (c) Metlesin, W.; Wheatley, P. J. and Zeiss, H. H. *J. Amer. Chem. Soc*. **1962**, 84, 2327. (d) Sneeden, R. P. A. and Zeiss, H. H. *J. Organometal. Chem.* **1968**, 13, 369. (e) Sneeden, R. P. A. and Zeiss, H. H. *J. Organometal. Chem.* **1968**, 13, 377. (f) Sneeden, R. P. A. and Zeiss H. H. *J. Organometal. Chem.* **1968**, 15, 139. (g) Michman, M. and Zeiss, H. H. *J. Organometal. Chem.* **1968**, 13, 23. (h) Sneeden, R. P. A. and Zeiss, H. H. *J. Organometal. Chem.* **1969**, 16, 449. (i) Sneeden, R. P. A. and Zeiss, H. H. *J. Organometal. Chem.* **1969,** 19, 93. (j) Sneeden, R. P. A. and Zeiss, H. H. *Angew. Chem.* **1968,** 80, 1029. (k) Light, J. R. C. and Zeiss, H. H. *J. Organometal. Chem.* **1970**, 21, 391. (l) Light, J. R C. and Zeiss, H. H. *J. Organometal. Chem.* **1970**, 21, 517. (m) Sneeden, R. P. A. and Zeiss, H. H. *J. Organometal. Chem.* **1970**, 22, 713. (n) Sneeden, R. P. A. and Zeiss, H. H. *J. Organometal. Chem.* **1971,** 26, 101. (o) Sneeden, R. P. A. and Zeiss, H. H. *J. Organometal. Chem.* **1971,** 27, 89. (p) Kochi, J. K. and Powers, J. W. *J. Amer. Chem. Soc*., **1970**, 92, 137.

136 Zeiss, H. H. and Tsutsui, *J. Amer. Chem. Soc.* **1957**, 79, 3062.

137 Khan, S. I. and Bau, R. *Organometallics*, **1983**, 2, 1896.

138 Kurras, E.; Monarsber. *Dt. Akad. Wiss*. **1963**, 5, 378.

139 Kurras, E. and Otto, J. *J. Organometal. Chem*. **1965**, 4, 114.

140 Wilkinson, G. and Piper, T. S. *J. Inorg. Nuccl. Chem*. **1956**, 3, 104.

141 Nishimura, K.; Kuribayashi, H.; Yamamoto, A.; Ikeda, S. *J. Organom. Chem*, **1972**, 37, 317.

142 Arakawa, T.; Zasshi, K. K. *J. Ind. Chem. Jap*. **1960**, 70, 132.

143 Collman, J. P.; Morrow, J. C.; Roper, W. R.; Ulkii, D. *J. Am. Chem. Soc*, **1966**, 4287.

144 Bernhardt, P.V.; Comba, P.; Curtis, N. F.; Hambley, T. W.; Lawrance, G. A.; Maeder, M.; Siriwardena, A. *Inorg. Chem*, **1990**, 29, 3208

145 Cavell, K. J. And McGuinness, D. S. *Coord. Chem. Rev*. **2004**, 248, 671

146 Edema, J. J. H. and Gambarotta, S. *J. Organomet. Chem*. **1990**, 389, 47.

147 Danopoulos, A. A. and Pugh, D. *Dalton Trans*. **2008**, 30.

148 Wagner, B. O.; Hammond, G.; *J. Organomet. Chem*. **1975**, 85, 1.

149 Kuhn, N. and Kratz, T. *Synthesis*, **1993**, 561.

150 Sanger, A. R. *Inorg. Nucl. Chem. Lett*. **1973***, 9,* 351.

151 (a) Edelmann, F. T. *Top. Curr. Chem*. **1996,** 179, 113. (b) Kilner, M.; Baker, J. *Coord. Chem. Rev*. **1994**, 133, 219. (c) Edelmann, F. T. *Coord. Chem. Rev*. **1994**, 137, 40. (d) Hagadorn, J. R.; Arnold, J. *Organometallics*, **1998**, 17, 1355. (e) Hagadorn, J. R.; Arnold, J. *J. Chem. Soc., Dalton Trans*. **1997**, 3087. (f) Hagadorn, J. R.; Arnold, J. *J. Am. Chem. Soc*. **1996**, 118, 893. (g) Hagadorn, J. R.; Arnold, J. *Organometallic,* **1994**, 13, 4670.

152 Sigel, H.; Martin, R. B. *Chem. Rev.* **1982**, 82, 385.

153 (a) Bailey, P. J.; Pace, S. *Coord. Chem. Rev*. **2001**, 214, 91. (b) Foley, S. R.; Yap, G. P. A.; Richeson, D. S. *Inorg. Chem.* **2002**, 41, 4149. (c) Coles, M. P.; Hitchcock, P. B. *J. Chem. Soc., Dalton Trans*. **2001**, 1169. (d) Mullins, S. M.; Duncan, A. P.; Bergman, R. G.; Arnold, *J. Inorg. Chem.* **2001**, 40, 6952. (f) Okamoto, S.; Livinghouse, T. *Organometallics*, **2000**, 19, 1449.

154 Littke, A.; Sleiman, N.; Bensimon, C.; Richeson, D. S. *Organometallics*, **1998**, 17, 446.

155 Herskovics-Korine, D.; Eisen, M. *J. Organomet. Chem.* **1995**, 503, 307.

156 (a) Gründemann, S.; Kovacevic, A.; Albrecht, M.; Faller, J. W.; Crabtree, R. H. *J. Am. Chem. Soc.* **2002**, 124, 10473. (b) Kovasevic, A.; Gründemann, S.; Miecznikowski, J. R.; Clot, E.; Eisenstein, O.; Crabtree, R. H. *Chem. Commun*. **2002**, 2580.

157 Danopoulos, A., A.; Tsoureas, N.;Wright, J. A.; Light, M. E. *Organometallics,* **2004**, 23, 166.

158 Boere, R. T.; Klassen, V.; Wolmershäuser, G. *J. Chem. Dalton. Trans*., **1998**, 4147.

159 Arnold, P. L.; Rodden, M.; Wilson, C. *Chem Commun*. **2005**, 13, 1743.

160 Addison, a. W. and Rao, T. N. *J. Chem. Soc. Dalton Trans*. **1984**, 1349.

161 Arnold, P.L. and Pearson, S. *Coord. Chem. Rev*. **2007**, 251, 596.

162 Groysman, S.; Goldberg, I.; Kol, M.; Genizi, E.; Goldschmidt, Z. *Inorg. Chim. Act*. **2003**, 345, 137.

163 Dykerman, B. A.; Smith, J. J.; McCarvill, E. M; Gallant, A. J.; Doiron, N. D.;

Wagner, B. D.; Jenkins, H. A.; Patrick, B. O.; Smith, K. M. *J. Organomet.*

Chem.; **2007**, 3183.

164 Edworthy, I. S.; Rodden, M.; Mungur, S. A.; Davis, K. M.; Blake, A. J.; Wilson,

C.; Schröder, M.; Arnold, P. L. *J. Organomet. Chem.* **2005**, 690, 5710.

165 Chen, A. C.; Ren, L.; Decken, A.; Crudden, C. M. *Organometallics,* **2000**, 19,

3359.